Imperial College London

National Heart and Lung Institute

Vascular Science Department

Neutrophil biophysical properties and the impact of hypoxia in ANCA Associated Vasculitis

Noelle Pisacano

Supervisors: Dr. Katharine Mary Lodge, Dr. Maria Prendecki, Dr. Andrew Cowburn

Thesis submitted to Imperial College London for the degree of Doctor of Philosophy (PhD)

Statement of Originality

I, Noelle Pisacano, confirm that the work presented in this thesis is my own. I have indicated where work has been derived from other sources at necessary places in this thesis.

Copyright Declaration

The copyright of this thesis rests with the author. Unless otherwise indicated, its contents are licensed under a Creative Commons Attribution-Non. Commercial 4.0 International Licence (CC BY-NC). Under this licence, you may copy and redistribute the material in any medium or format. You may also create and distribute modified versions of the work. This is on the condition that: you credit the author and do not use it, or any derivative works, for a commercial purpose. When reusing or sharing this work, ensure you make the licence terms clear to others by naming the licence and linking to the licence text. Where a work has been adapted, you should indicate that the work has been changed and describe those changes. Please seek permission from the copyright holder for uses of this work that are not included in this licence or permitted under UK Copyright Law.

Για τη μεγάλη μου αδερφή. Always c

Acknowledgements

I would firstly like to thank the National Heart and Lung Institute (NHLI) for providing me funding, which allowed me to carry out this research.

I would like to thank the patients who consented to donating blood for this work, and Dr. Amrita Dhutia who helped recruit this cohort. I would also like to thank all the healthy controls who repeatedly donated blood, particularly at Vascular Sciences, and the clinicians who kindly bled volunteers for me, Dr. Andrew Porter, Dr. Adam Hartley, and Dr. Kavita Gulati. I could not have completed this PhD without all of you.

I am grateful to the Cowburn group. I would like to specifically thank my supervisors, Dr. Maria Prendecki and Dr. Katharine Lodge, for their efforts, particularly with editing this thesis.

I would especially like to thank those who were there from the start of my time in the lab during my MSc in the JCM group and continued to help and support me throughout my PhD – Dr. Charis Pericleous and Dr. Robert Maughan. Special thanks to Dr. Andrew Porter as well for his assistance in and out of the lab.

I would like to thank Stephen Rothery of FILM for all his efforts, even during the early bird confocal sessions. As for other members of Vascular Sciences, I would like to thank Dr. Daniela Pirri and Dr. Koralia Paschalaki for their insight. I would also like to thank Dr. Joseph Boyle for always taking the time to explain things to me. I would like to thank Dr. Kelly De Coteau for her input. Special thanks to my mentor Professor Cecilia Johansson as well.

I would particularly like to thank the PhD Bay. To those who were students when I first began my PhD and now have their doctorates, and to those who are still there, on their way to finishing theirs. I value your honest opinions, feedback, and simply having peers to talk to.

Last, but not least, I will somehow keep this short. I would like to thank again Dr. Charis Pericleous for yesterday, today, and tomorrow, as of course I will need you then. I would not be here nor who I am without you.

Abstract

The anti-neutrophil cytoplasm antibody (ANCA) associated vasculitides (AAV) are a group of systemic autoimmune diseases characterised by inflammation of small blood vessels and the presence of circulating ANCA. Neutrophils are central to disease pathogenesis; they are target of the autoantibody, ANCA, and contribute to vascular damage. Cell deformability has a marked impact on trafficking of neutrophils through microvasculature and neutrophil-endothelial interactions. Inflamed vasculature is characteristically hypoxic, a stimulus which enhances neutrophil secretion and delays apoptosis. The aim of this study was to investigate morpho-rheological phenotype of neutrophils from patients with AAV, and how this may contribute to endothelial injury in hypoxic environments.

A novel technique, Real Time-Deformability Cytometry (RT-DC), was used to identify mechanical cell signatures. Results presented identified a distinct morpho-rheological phenotype of neutrophils in patients with active AAV, compared to those in remission and healthy controls (HC), with changes in cell size, deformation, and elasticity. In keeping with this, *in vitro* stimulation of neutrophils with MPO- or PR3-ANCA IgG leads to decreased deformability of cells in comparison to HC-IgG stimulated cells. MPO- and PR3-ANCA promote NETosis and actin polymerisation; both mechanisms are reduced under physiological venous oxygen tension (5% O_2) but are enhanced under pathological hypoxia (1% O_2). MPO- or PR3-ANCA stimulation and hypoxia synergise to impact neutrophil-endothelial cell interactions, demonstrated by changes in adhesion protein secretion levels and neutrophil transendothelial migration through glomerular endothelial cells in co-culture.

In conclusion, ANCA- and hypoxia-induced morpho-rheological changes in neutrophils may influence cell trafficking through microvasculature and potential for neutrophil-mediated endothelial injury, thus contributing to the pathogenesis of AAV. It is possible distinct biophysical properties of neutrophils in patients with aAAV promote endothelial injury. Collectively these findings indicate biomechanical phenotyping can identify pro-inflammatory neutrophils with increased endothelial damage capacity in active vasculitis, with implications for diagnosis and guiding response to treatment.

List of Figures

Figure 1. Neutrophil extravasation, interactions, and pathogen killing mechanisms 39
Figure 2. Neutrophil ANCA pathogenesis 54
Figure 3. Real-time deformability cytometry 75
Figure 4. IgG purified from patients with AAV displays typical cANCA and pANCA of binding to ethanol washed neutrophils 95
Figure 5. Anti-MPO ELISA 96
Figure 6. RT-DC gating 99
Figure 7. Actin polymerisation quantification macro steps 107
Figure 8. Whole blood neutrophils in sodium citrate have lowest deformability 114
Figure 9. Isolation methods do not alter neutrophil mechanophenotype 116
Figure 10. Time post-venepuncture does not alter neutrophil mechanophenotype 118
Figure 11. Neutrophil deformability is not altered by media calcium concentration 120
Figure 12. Low-dose TNF priming does not alter neutrophil deformability 122
Figure 13. ANCA induced IL-8 secretion 125
Figure 14. Increased NET production in ANCA simulated neutrophils 127
Figure 15. MPO-ANCA stimulation decreases neutrophil deformability over time 129
Figure 16. No difference between MPO- or PR3-ANCA stimulation on isolated neutrophil deformability 131
Figure 17. MPO-ANCA promotes IL-8 secretion in serum following whole blood stimulation 133
Figure 18. Neutrophil deformability decreases in whole blood stimulated with MPO-ANCA 135
Figure 19. MPO/PR3-ANCA stimulation promotes actin polymerisation in HC neutrophils 137
Figure 20. MPO/PR3-ANCA promotes actin polymerisation in HC stimulated neutrophils 139
Figure 21. No change in parameters of untreated neutrophils with cytoskeletal inhibitors 142
Figure 22. Inhibitors of cytoskeletal remodelling inhibit MPO/PR3-ANCA promotion of actin polymerisation in HC stimulated neutrophils 144
Figure 23. Cytochalasin D best inhibits ANCA promotion of actin polymerisation 145
Figure 24. No change in deformability in untreated neutrophils treated with Cytochalasin B/D 147
Figure 25. No change in deformability in ANCA stimulated neutrophils treated with Cytochalasin B or D 149
Figure 26. Inhibitors do not influence ANCA stimulated neutrophil protein secretion levels 151
Figure 27. Transcriptomic analysis of untreated versus MPO-ANCA stimulated neutrophils 155
Figure 28. Transcriptomic analysis of untreated versus PR3-ANCA stimulated neutrophils 157
Figure 29. Oxygen tension alters whole blood neutrophil mechanophenotype 169
Figure 30. Oxygen tension alters isolated neutrophil deformability 171
Figure 31. Oxygen tension alters neutrophil deformability in whole blood stimulated with ANCA 173
Figure 32. 5% O_2 alters neutrophil deformability in whole blood stimulated with ANCA 175

Figure 33. Hypoxia alters neutrophil deformability in whole blood stimulated with ANCA 177
Figure 34. 5% O_2 decreases the effect of ANCA on isolated neutrophil deformability . 179
Figure 35. 1% O_2 decreases the effect of ANCA on isolated neutrophil deformability . 181
Figure 36. Oxygen tension influences actin polymerisation in neutrophils..... 184
Figure 37. Oxygen tension influences neutrophil actin polymerisation 186
Figure 38. Oxygen tension alters ANCA induced actin polymerisation in HC stimulated neutrophils 190
Figure 39. 5% O_2 influences actin polymerisation in MPO-ANCA stimulated neutrophils 191
Figure 40. 1% O_2 influences actin polymerisation in ANCA stimulated neutrophils 192
Figure 41. No change in parameters at 5% O_2 with actin polymerisation inhibitors..... 194
Figure 42. ANCA promotion of actin polymerisation in HC is inhibited by Cytochalasin B at 1% O_2..... 196
Figure 43. Cytochalasin B best inhibits ANCA promotion of actin polymerisation under hypoxia 197
Figure 44. Hypoxia alters MPO-ANCA stimulated neutrophil IL-8 secretion..... .208
Figure 45. Oxygen tension alters MPO-ANCA stimulated whole blood neutrophil IL-8 secretion..... 210
Figure 46. Oxygen tension alters ANCA induced NET production 212
Figure 47. 5% O_2 influences gEC protein secretion levels when treated with ANCA SN 215
Figure 48. 1% O_2 influences gEC protein secretion levels when treated with ANCA SN 217
Figure 49. Increased IL-8, ICAM-1, and VCAM-1 levels in ANCA stimulated co-culture 220
Figure 50. Increased migration in neutrophils stimulated with ANCA IgG at 1% O_2 ... 223
Figure 51. ANCA IgG promotes neutrophil migration through gEC, and hypoxia enhances this effect 225
Figure 52. Differential expression analysis of 1% O_2 untreated v MPO-ANCA v PR3-ANCA..... 231
Figure 53. Enrichment ratio of 1% O_2 untreated v MPO-ANCA v PR3-ANCA 232
Figure 54. Biomechanical phenotype of neutrophils is altered in AAV..... 246
Figure 55. Decreased neutrophil deformability significantly correlates with BVAS 249
Figure 56. Decreased neutrophil deformability in patients with renal and lung disease 250
Figure 57. Decreased deformability in AAV is a myeloid phenotype..... 252
Figure 58. Increased actin capping in AAV neutrophils at baseline..... 254
Figure 59. Baseline actin polymerisation is increased in aAAV 255
Figure 60. Increase in actin polymerisation in MPO/PR3-ANCA stimulated AAV neutrophils 258
Figure 61. Increase in actin polymerisation in ANCA stimulated AAV neutrophils 259
Figure 62. Oxygen tension influences actin polymerisation in HC and AAV neutrophils 261
Figure 63. Oxygen tension influences HC and AAV neutrophil actin polymerisation .. 262
Figure 64. 5% O_2 increases actin polymerisation in AAV ANCA stimulated neutrophils 265
Figure 65. Hypoxia increases actin polymerisation in AAV ANCA stimulated neutrophils 267
Figure 66. Increase in actin polymerisation in ANCA stimulated AAV neutrophils at 5% O_2..... 269

Figure 67. Increase in actin polymerisation in ANCA stimulated AAV neutrophils under hypoxia 270
Figure 68. Increased IL-8, ICAM-1, and VCAM-1 secretion in AAV 272
Figure 69. aAAV SN promote gEC secretion of IL-8 and VCAM-1 at 21% and 5% O_2 274
Figure 70. gEC protein secretion levels when treated with aAAV SN are similar in 21% and 1% O_2 276
Figure 71. Top DE genes express greatest fold change in aAAV 278
Figure 72. Transcriptomic analysis of healthy control versus active AAV 282
Figure 73. Transcriptomic analysis healthy control versus remission AAV 285
Figure 74. Transcriptomic analysis of remission AAV versus active AAV 288

List of Tables

Table 1. 2022 ACR/EULAR classification criteria for AAV 51
Table 2. 2022 EULAR treatment criteria for AAV (MPA/GPA) 52
Table 3. Designed primers– Synthesis scale at 25 nmol 80
Table 4. Cells and media 82
Table 5. Other tissue culture reagents 82
Table 6. Reagents for Percoll Density Gradient 83
Table 7. Reagents for Immunomagnetic negative selection 83
Table 8. Reagents for cytospins 83
Table 9. Reagents for protein purification 84
Table 10. Reagents for assays 84
Table 11. Reagents for MPO binding assay 84
Table 12. Reagents for IL-8 85
Table 13. Reagents for ICAM-1 85
Table 14. Reagents for VCAM-1 85
Table 15. Reagents for RT-DC 86
Table 16. Reagents for Immunofluorescence 86
Table 17. Reagents for RNA isolation 86
Table 18. Reagents for cDNA synthesis and RT-qPCR 87
Table 19. Reagents for protein quantification 87
Table 20. Stimulation conditions 104
Table 21. Cytoskeletal inhibitors 141
Table 22. Top upregulated and downregulated significant DE in 21% O_2 untreated v MPO-ANCA 154
Table 23. Top upregulated and downregulated significant DE in 21% O_2 untreated v PR3-ANCA 156
Table 24. Summary of stimulation conditions in comparison to untreated neutrophil deformability 182
Table 25. Top upregulated and downregulated significant DE in 1% O_2 untreated v MPO-ANCA 229
Table 26. Top upregulated and downregulated significant DE in 21% O_2 untreated v PR3-ANCA 230
Table 27. Characteristics of patients included in study 244
Table 28. Characteristics of patients included in RNA-seq 279
Table 29. Top upregulated and downregulated significant DE in HC v aAAV 281

Table 30. Top upregulated and downregulated significant DE in HC v rAAV 284
Table 31. Top upregulated and downregulated significant DE in rAAV v aAAV..... 287

Publications and Presentations

Publications

Prendecki, M., Gulati, K., **Pisacano, N.**, Pinheiro, D., Bhatt, T., Mawhin, M., Toulza, F., Masuda, E., Cowburn, A., Lodge, K., Tam, F., Roufosse, C., Pusey, C., McAdoo, S. Syk Activation in Circulating and Tissue Innate Immune Cells in Antineutrophil Cytoplasmic Antibody-Associated Vasculitis. *Arthritis Rheumatol*. 2023;75(1):84-97.

Conference Presentations

Pisacano, N., Dhutia, A., Rothery, S., McAdoo, S., Guck, J., Pusey, C., Chilvers, E., Cowburn, A., Lodge, K., Prendecki, M. Hypoxia and MPO-ANCA IgG Induced Biophysical Changes in Neutrophils May Promote Endothelial Injury in ANCA Associated Vasculitis. Annals of the Rheumatic Diseases. 2023;82(261-262). EULAR Presentation – Poster Tour

Pisacano, N., McAdoo, S., Guck, J., Pusey, C., Chilvers, E., Cowburn, A., Lodge, K., Prendecki, M. Biomechanical Phenotype of Circulating Neutrophils is Altered in ANCA Associated Vasculitis. Rheumatol. 2022;62(2). BSR poster presentation

Pisacano, N., McAdoo, S., Guck, J., Pusey, C., Chilvers, E., Cowburn, A., Lodge, K., Prendecki, M. Biomechanical Phenotype of Circulating Neutrophils is Altered in ANCA Associated Vasculitis. Arthritis Rheumatol. 2022;74(9). ACR poster presentation

Pisacano, N., McAdoo, S., Guck, J., Pusey, C., Chilvers, E., Cowburn, A., Lodge, K., Prendecki, M. Biomechanical Phenotype of Circulating Neutrophils is Altered in ANCA Associated Vasculitis. Arthritis Rheumatol. 2022;74(9. ANCA workshop poster presentation

Abbreviations

aAAV	active antineutrophil cytoplasm antibody associated vasculitis
AAV	Anti-neutrophil cytoplasm antibody associated vasculitis
AFM	atomic force microscopy
AI	autoimmune
ANCA	anti-neutrophil cytoplasm antibody
APC	antigen presenting cell
ARD	autoimmune rheumatic disease
ARP	actin related protein
ATP	adenosine triphosphate
AZA	azathioprine
BAFF	B cell activating factor
BB	Binding buffer
BCA	bicinchoninic acid
β-mercap	2-Mercaptoethanol
BSA	Bovine Serum Albumin
BVAS	Birmingham Vasculitis Activity Score
β2M	Beta-2 microglobulin
cANCA	cytoplasmic anti-neutrophil cytoplasm antibody
CD	cluster of differentiation
cDNA	complementary DNA
C5a	Complement component 5a
C5aR1	complement C5a receptor 1
CO_2	carbon dioxide
COPD	chronic obstructive pulmonary disease
CR	complement receptor
CRP	C-reactive protein
CYC	cyclophosphamide
DAH	diffuse alveolar haemorrhage
DAPI	4'-6-diamidino-2-phenylindole
dH_2O	distilled water
ddH_2O	double distilled water

DMARD	disease-modifying antirheumatic drugs
DPBS	Dulbecco’s Phosphate-Buffered Saline
dsDNA	double stranded DNA
DVT	deep vein thrombosis
EB	Elution buffer
EC	Endothelial cell
ECM	extracellular matrix
EDTA	Ethylenediaminetetraacetic acid
EGPA	eosinophilic granulomatosis with polyangiitis
ELISA	enzyme-linked immunosorbent assay
ENT	ear nose throat
ERK	extracellular-signal-regulated kinase
Fab	fragment antigen-binding
F-actin	Filamentous actin
FasL	Fas ligand
FBS	foetal bovine serum
FcR	Fc receptors
FCS	foetal calf serum
FIH	Factor-inhibiting hypoxia-inducible factor
FMF	Familial Mediterranean fever
fMLP	formyl-methionyl-leucyl-phenylalanine
FPR2	N-formyl peptide receptor 2
G-actin	globular actin
GBM	glomerular base membrane
GF	growth factor
GLUT1	glucose transporter 1
GM-CSF	granulocyte/macrophage colony-stimulating factor
GN	glomerulonephritis
GPA	Granulomatosis with polyangiitis
GSDMD	Gasdermin D
GTP	guanosine triphosphate
GWAS	Genome Wide Association Studies
h	hour
HAEC	Human Aortic Endothelial Cell

HBSS	Hank's Balanced Salt Solution
HC	healthy control
HDAC	histone deacetylase
HDG	high-density granulocyte
HIF	hypoxia-inducible factor
HLA	human leukocyte antigen
HRP	horseradish peroxidase
H3Cit	citrullinated histone H3
DPBS	Dubecco's Phosphate-Buffered Saline
GN	glomerulonephritis
GPA	granulomatosis with polyangiitis
ICAM-1	intercellular adhesion molecule 1
IgG	immunoglobulin G
IFN	interferon
IF	immunofluorescence
Ig	immunoglobulin
IL	interleukin
ILD	Interstitial lung disease
IMDM	Iscove's Modified Dulbecco's Media
LAMP-2	lysosome-associated membrane protein-2
LDG	low-density granulocyte
LFA-1	lymphocyte function-associated antigen 1
LPS	lipopolysaccharide
mAb	monoclonal antibody
Mac-1	macrophage-1 antigen
MAPK	mitogen-activated protein kinase
Mcl-1	myeloid cell leukaemia-1
MDS	myelodysplastic syndrome
MEK	ERK kinase
MFI	mean fluorescence intensity
MHC	major histocompatibility complex
MMF	mycophenolate mofetil
mmHg	millimetre of mercury
MMP	matrix metalloproteinase

MPA	microscopic polyangiitis
MPO	Myelopeeroxidase
mRNA	messenger RNA
mTOR	mammalian target of rapamycin
NADPH	nicotinamide adenine dinucleotide phosphate
NB	Neutralisation buffer
NE	neutrophil elastase
NET	Neutrophil extracellular trap
NK	natural killer
NF-κB	Nuclear factor kappa-light-chain-enhancer of activated B cells
ns	non-significant
NSP	neutrophil serine proteases
O_2	oxygen
OD	optical density
P	passage
pAb	primary antibody
PAD4	Peptidyl arginine deiminase 4
pANCA	perinuclear anti-neutrophil cytoplasm antibody
PBMC	peripheral blood mononuclear cell
PBS	phosphate-buffered saline
PBST	phosphate-buffered saline Tween
PHD	prolyl hydroxylase
PI	Propodium Iodide
PI3K	phosphatidylinositol-3-kinase
PKC	protein kinase C
PLEX	plasma exchange
PMA	phorbol 12-myristate 13-acetate
PMN	polymorphonuclear leukocytes
PR3	proteinase 3
PS	phosphatidylserine
qPCR	quantitative polymerase chain reaction
rAAV	remission anti-neutrophil cytoplasm antibody associated vasculitis
RIPA buffer	radioimmunoprecipitation assay buffer
RIPK	receptor-interacting serine/threonine-protein kinase 1

ROS	reactive oxygen species
RPGN	rapidly progressive glomerulonephritis
RPMI	Roswell Park Memorial Institute medium
RT	room temperature
RT-DC	real time deformability cytometry
RTX	rituximab
sAb	secondary antibody
SD	standard deviation
SEM	standard error of mean
SLE	systemic lupus erythematosus
SN	supernatant
SPECT	single-photon emission computerised tomography
SSc	Systemic sclerosis
SVV	small vessel vasculitis
Syk	spleen tyrosine kinase
TEM	transendothelial migration
TF	tissue factor
TFPI	tissue factor pathway inhibitor
T_h	T helper cell
TLR	toll-like receptor
TMA	thrombotic microangiopathies
TMB	3,3',5,5'-Tetramethylbenzidine
TNF	tumour necrosis factor
TNFR	tumour necrosis factor receptor
tPA	tissue plasminogen activator
tPE	therapeutic plasma exchange
TRAF	TNFR associated factor
VCAM-1	vascular cell adhesion molecule 1
VEGF	vascular endothelial growth factor
WAS	Wiskott-Aldrich syndrome
WBC	white blood cell
WRC	WAVE regulatory complex
3D	3-dimensional

Table of Contents

Acknowledgements……..….4
Abstract…….5
List of Figures…….……...6
List of Tables……..……...8
Publications and Presentations…….10
Abbreviations……...11
Table of Contents…….16

1. Chapter 1 – Introduction 22
1.1. Neutrophils 23
1.2. Neutrophil mechanisms 26
1.2.1. Priming 26
1.2.3. Degranulation 27
1.2.4. ROS and phagocytosis 28
1.2.5. NETosis 29
1.2.10. Cytokine release 34
1.2.11. Recruitment 35
1.2.11. Neutrophil/endothelial interactions 36
1.2.12. Resolution of inflammation 37
1.3. Neutrophil actin cytoskeleton 40
1.3.3. Neutrophil deformability 42
1.3.5. Role of actin in neutrophil function 43
1.3.6. Pharmacological modulators of actin 44
1.3.8. Actin disruption 46
1.4. Autoimmunity: breakdown of tolerance 47
1.5. Anti-neutrophil Cytoplasm Antibody Associated Vasculitis (AAV) 48
1.5.2. Diagnosis and clinical features 49
1.5.3. Pathogenicity of ANCA 53
1.5.5. ANCA induced activation of neutrophils 56
1.5.8. LDGs 58
1.6. Neutrophil recruitment and endothelial injury 59
1.7. Complement in AAV 63
1.8. B Cells in AAV 64
1.9. T Cells in AAV 65
1.10. Hypoxia 66
1.10.1. Hypoxia and oxygen tensions 66

1.10.3. Neutrophil function 67
1.11. Biomechanics 73
1.11.1. Previous techniques for biomechanics 73
1.11.2. Development of RT-DC 74
1.11.3. RT-DC in cell type/disease 76
1.12. Hypothesis and Aims 77
1.12.1. Hypothesis 77
1.12.2. Aims of the study 77
2. Chapter 2 – Materials and Methods 78
2.1. Materials 79
2.1.1. Tissue culture 82
2.1.2. Neutrophil Isolation 83
2.1.3. Cytospin 83
2.1.4. ANCA protein purification 84
2.1.5. Recombinant proteins & inhibitors 84
2.1.6. ELISA 84
2.1.7. RT-DC 86
2.1.8. Immunofluorescence 86
2.1.9. mRNA quantification 86
2.1.10. Protein analysis 87
2.2. Methods 88
2.2.1. Patients and Controls 88
2.2.1.1. Study approvals 88
2.2.1.2. Inclusion criteria 88
2.2.2. Tissue culture 88
2.2.2.1. Neutrophil and PBMC isolation 88
2.2.2.2. Isolation of human neutrophils – Percoll density gradient 88
2.2.2.3. Assessing neutrophil purity – Kwikdiff staining 89
2.2.2.4. Isolation of human neutrophils – Negative immunomagnetic selection 90
2.2.2.5. Isolation of LDGs from patients with aAAV 91
2.2.2.6. gEC 91
2.2.3. Purification and dialysis of IgG 92
2.2.3.1. IgG purification 92
2.2.3.2. IgG concentration and dialysis 93
2.2.4. *In vitro* treatment with human IgG, neutrophil SN, and neutrophils 93
2.2.4.1. Neutrophil stimulation 93
2.2.5. MPO binding – immunofluorescence 94
2.2.6. Anti-MPO ELISA 96
2.2.7. Hypoxic equilibration – Whitley H35 Hypoxystation 97
2.2.8. Mechanophenotyping - RT-DC 98
2.2.9. Measuring gene expression levels 100
2.2.9.1. RNA extraction stimulation – neutrophils 100

2.2.9.4. cDNA synthesis 102
2.2.9.5. RT-qPCR 102
2.2.10. Measuring protein secretion levels in neutrophils and gEC – ELISA 103
2.2.10.1. Neutrophil and gEC activation analysis 103
2.2.11. Experiments for neutrophil trans-endothelial migration 104
2.2.11.1. Neutrophil endothelial trans-well migration assay 104
2.2.12. Immunofluorescence 105
2.2.12.1. Co-culture trans-well monolayer assessment 105
2.2.12.2. Visualisation of actin polymerisation and quantification 106
2.2.12.3. Visualisation of NET formation 108
2.2.13. Statistical analysis 108

3. Chapter 3 – Characterising the biomechanical phenotype of neutrophils following stimulation with ANCA IgG 110

3.1. Introduction 111

3.2. Optimisation of RT-DC 113
3.2.1. Whole blood neutrophils in sodium citrate have lower deformability than EDTA 113
3.2.2. Isolation methods do not alter neutrophil mechanophenotype 115
3.2.3. Time post-venepuncture does not alter neutrophil mechanophenotype 117
3.2.4. Neutrophil deformability is not altered by cell culture media calcium concentration 119
3.2.5. Low dose TNF priming does not alter neutrophil deformability 121

3.3. Neutrophil pathogenic responses following stimulation with ANCA 123
3.3.1. MPO- and PR3-ANCA increases neutrophil IL-8 secretion 123
3.3.2. Increased NET production in ANCA stimulated neutrophils 126

3.4. Effect of ANCA on neutrophil mechanophenotype 128
3.4.1. MPO-ANCA stimulation decreases neutrophil deformability over time 128
3.4.2. No difference between MPO- or PR3-ANCA stimulation on isolated neutrophil deformability 130

3.5. Whole blood treatment with ANCA 132
3.5.1. Increased IL-8 secretion in whole blood treated with MPO-ANCA 132
3.5.2. Neutrophil deformability decreases in whole blood stimulated with MPO-ANCA 134

3.6. Increase in actin polymerisation in MPO/PR3-ANCA stimulated neutrophils 136
3.6.1. MPO/PR3-ANCA promotes actin polymerisation in HC stimulated neutrophils 136

3.7. Effect of inhibitors of cytoskeletal remodelling on ANCA mediated neutrophil actin polymerisation 140
3.7.1. Cytochalasin D best inhibits ANCA induced actin polymerisation 140
3.7.2. No change in deformability in ANCA stimulated neutrophils treated with Cytochalasin B or D 146

3.7.3. Inhibitors of actin polymerisation do not influence ANCA stimulated neutrophil protein secretion levels 150
3.8.1. Identification of a gene signature comparing 21% untreated neutrophils to 21% MPO-ANCA or PR3-ANCA stimulated neutrophils 152
3.9. Discussion 158
4. Chapter 4 – The effect of hypoxia on neutrophil biomechanics following stimulation with ANCA IgG 165
4.1. Introduction 166
4.2. Oxygen tensions 168
4.2.1. Oxygen tension alters whole blood neutrophil mechanophenotype 168
4.3. Oxygen tension alters isolated neutrophil deformability 170
4.4. The effect of oxygen tension on ANCA stimulated neutrophil deformability 172
4.4.1. Oxygen tension alters neutrophil deformability in whole blood stimulated with ANCA IgG 172
4.4.2. Hypoxia decreases the effect of ANCA on isolated neutrophil deformability 178
4.5. Effect of hypoxia and ANCA on actin cytoskeleton 183
4.5.1. Oxygen tension influences neutrophil actin polymerisation 183
4.6. Oxygen tension influences actin polymerisation in neutrophils stimulated with ANCA 187
4.7. Effect of inhibitors on ANCA mediated neutrophil response 193
4.7.1. Cytochalasin B best inhibits ANCA induced actin polymerisation under hypoxia 193
4.8. Discussion 198
5. Chapter 5 – The effect of hypoxia on ANCA induced functional responses 203
5.1. Introduction 204
5.2. Impact of hypoxia on ANCA induced pathogenic neutrophil responses 206
5.2.1. Hypoxia alters MPO-ANCA induced neutrophil IL-8 secretion 206
5.2.2. Whole blood ANCA stimulation IL-8 production 209
5.3. Effect of oxygen tension on ANCA induced NETosis 211
5.3.1. NET production in ANCA stimulated neutrophils is enhanced at 1% O_2 and diminished at 5% O_2 211
5.4. Effect of ANCA and hypoxia on protein secretion levels from neutrophil and gEC 213
5.4.1. Oxygen tension influences gEC protein secretion levels following treatment with neutrophil-conditioned SNs 213
5.4.2. Increased IL-8, ICAM-1, and VCAM-1 secretion following co-culture of gEC and ANCA stimulated neutrophils 218

5.5. ANCA IgG and hypoxia promote neutrophil trans-endothelial migration through gEC 221
5.5.1. gEC form confluent monolayers under pathological hypoxia 224
5.6. RNA-Sequencing of neutrophils in 1% O_2; untreated v MPO-ANCA v PR3-ANCA stimulation 226
5.6.1. Identification of a gene signature comparing 21% O_2 untreated neutrophils to 1% O_2 untreated neutrophils 226
5.6.2. Identification of a gene signature comparing 1% untreated neutrophils to 1% MPO- or PR3-ANCA stimulated neutrophils 226
5.7. Discussion 233
6. Chapter 6 – AAV 241
6.1. Introduction 242
6.2. AAV 244
6.2.1. Biomechanical phenotype of neutrophils in whole blood is altered in AAV 245
6.2.2. Disease correlations 247
6.2.2.1. Disease severity (BVAS) correlates with neutrophil deformability 247
6.2.2.2. ANCA specificity does not influence neutrophil deformability 247
6.2.2.3. Steroids do not alter neutrophil deformability 247
6.2.2.4. Association between clinical phenotype and neutrophil deformability 248
6.3. Increased elasticity in AAV is a myeloid phenotype 251
6.4. Actin polymerisation is altered in neutrophils from patients with AAV 253
6.4.1. Untreated HC v Untreated AAV 253
6.4.2. Increase in actin polymerisation in MPO/PR3-ANCA stimulated AAV neutrophils at 21% O_2 256
6.4.3. Hypoxia increases actin polymerisation in AAV neutrophils 260
6.4.4. Hypoxia increases actin polymerisation in AAV ANCA stimulated neutrophils 263
6.5. Protein secretion levels 271
6.5.1. Increased IL-8, ICAM-1, and VCAM-1 secretion in aAAV 271
6.5.2. Effect of hypoxia on co-cultured neutrophil and gEC protein secretion 273
6.5.2.1. Hypoxia influences gEC protein secretion levels when treated with AAV SN 273
6.6. Optimising isolation of RNA isolation and gene expression analysis from aAAV neutrophils 277
6.7. RNA Sequencing – Age match HC v rAAV v aAAV 279
6.7.1. Identification of a gene signature comparing aAAV to age matched HC 280
6.7.2. Identification of a gene signature comparing rAAV to age match HC 283
6.7.3. Identification of a gene signature comparing aAAV to rAAV 286
6.8. Discussion 289

7. Chapter 7 – Concluding remarks 298

7.1. Discussion and Future work 299

7.1.1. Active AAV neutrophils have altered biophysical phenotype 299

7.1.2. ANCA stimulation leads to altered biophysical phenotype and changes in actin, which associates with EC injury 300

7.2. Conclusions 309

1. Chapter 1 – Introduction

1.1. Neutrophils

In humans, neutrophils are the most abundant cell type in the peripheral blood and large numbers are produced in the bone marrow daily (1). Generated in the bone marrow from myeloid precursors, neutrophils undergo a process of development called granulopoiesis beginning as myeloblast, then maturing through a promyelocyte, myelocyte, metamyelocyte, and band cell, to a polymorphonuclear segmented cell (2). In health, immature neutrophils mature in the bone marrow for 4-6 days, before being released into the blood where they remain for several hours, and arguably up to approximately 5 days, although this timescale is still under debate (1,3–5). In tissue, neutrophils are typically expected to have a lifespan of 1-2 days (6). During different stages of maturation, four types of bactericidal granules are formed in the neutrophil cytoplasm: i) primary or azurophilic (containing myeloperoxidase (MPO), proteinase 3 (PR3), cathepsin, and neutrophil elastase (NE)) (7–9), ii) secondary (containing lactoferrin) (10–12), iii) tertiary (containing matrix metalloproteinase 9 (MMP9)) (13,14), and iv) secretory vesicles, but this is not a complete list of prepackaged proteins. Neutrophils are defined as granulocytes due to the presence of these cytoplasmic granules and are characteristically polymorphonuclear, with a multi-lobed nucleus. These properties may contribute to neutrophils deformable capabilities in the vasculature and endothelial cell (EC) junctions, which will be discussed further in section 1.3.3. (15,16).

1.1.1. Programmed functions

The key function of neutrophils is to kill pathogens upon activation; their main effector functions and mechanisms include phagocytosis, degranulation, and neutrophil extracellular trap (NET) formation. Phagocytosis is the process of engulfing bacteria into a vacuole, called the phagosome, for destruction (17). Degranulation is the process whereby neutrophil granule contents are assembled for movement intracellularly to eliminate pathogens within the

neutrophil phagosome or are released extracellularly to kill external pathogens (18,19). The respiratory, or oxidative, burst occurs because of increased oxygen consumption leading to increased production of reactive oxygen species (ROS), modulated through Nicotinamide adenine dinucleotide phosphate (NADPH), oxidase activity, an enzyme complex which produces superoxide anion (O_2^-) (20). For neutrophils to carry out these key responses, they must undergo a two-step activation process, a mechanism implemented to prevent inapt stimulation in the circulation (21). This includes an initial phase of "priming", allowing the neutrophil to enter a pre-activated state, before a secondary activating stimulus triggers the neutrophil to enter its fully activated, cytotoxic state (22,23). Once activated, dependent upon the circumstances of stimulation, neutrophils employ the appropriate programmed mechanism to perpetuate or resolve the state of acute inflammation or clear up a site of infection (24).

Neutrophils are highly plastic cells which exhibit manifold phenotypic and functional signatures contributing to innate and adaptive immune responses (25). Neutrophils can alter their functional status in response to immuno-modulating signals or change physical shape (26) to navigate through narrowed constrictions of the capillary beds. In the innate immune response, neutrophils have a key role in dampening acute inflammatory response through cytokine release in addition to having a pro-inflammatory function; while in adaptive immunity, neutrophils are involved in contributing to chronic inflammation (27–29). Neutrophil's role in inflammation and interaction with other immune cells will be discussed further in sections 1.2.12. and 1.2.13.

1.1.2. Functional responses in disease

The role of neutrophils in health involves carrying out pathogen killing mechanisms for immune defence, including degranulation, phagocytosis, and NETosis. Of these many

mechanisms acting as immune system defence strategies, the processes can be disrupted in disease, potentially enhancing pathogenic responses, and leading to 'bystander' tissue injury (30). Additionally, neutrophils contribute to regulating inflammation and produce cytokines, such as interleukin-8 (IL-8), which modulate the immune response (31,32). Although neutrophils are highly effective at pathogen elimination and immune surveillance, excessive or dysregulated neutrophil activation can be harmful and cause damage to host tissue. In autoimmune disease, whereby the host improperly recognises self-antigens as foreign, over-activation of neutrophil effector functions is commonly found. Disease progression in autoimmunity can consequentially result from dysregulation of main effector functions in aberrantly activated neutrophils.

1.2. Neutrophil mechanisms

1.2.1. Priming

Neutrophil priming is a pre-activation state regulating neutrophil responses, which enables a more robust response to a secondary activating stimulus (21). Neutrophils undergo a state of priming following exposure to several different agents including tumour necrosis factor (TNF), granulocyte macrophage-colony stimulating factor (GM-CSF), IL-8 and lipopolysaccharide (LPS) (31,33). While the exact priming mechanism depends on the activation agent, common downstream pathways can be activated as reviewed in Futosi et. al 2013 (34). Neutrophils employ various signalling pathways via activation of different receptors, dependent on which effector response is required. For example, multiple signalling pathways are activated after TNF priming, including phosphoinositide 3-kinase (PI3K), nuclear factor kappa-light-chain-enhancer B (NF-κB), p38, and extracellular signal-regulated kinases (ERK) 1/2, which can consequentially result in tissue injury (34,36). Once primed, neutrophils become more adhesive and shed L-selectin, a process regulating several neutrophil mechanisms including recruitment, signalling, adhesion, and migration (37). When neutrophils are quiescent, they secrete little or no granule contents or ROS but upon activation, both granule cargo and ROS can be released extracellularly which results in tissue injury. This process will be further discussed in section 1.2.4. The function of the healthy lung includes de-priming neutrophils, thus returning them to a quiescent state. This mechanism may fail in inflammation and in disease, inadvertently releasing primed neutrophils, and therefore increasing circulating neutrophil activation (38).

1.2.2. Morphological changes

In addition to enhancing pathogen-killing mechanisms, priming also alters the morphology of neutrophils. Neutrophils initially undergo a transient phase of cell shrinkage and stiffening once primed, then undergo expansion once activated (39–41). This change in cell size is

accompanied by corresponding changes in cell deformation with smaller cells having low deformability (stiffer) followed by a sequential increase in deformation (softer) when cell size increases (41,42). Cell stiffening during neutrophil priming may hinder their ability to transit through blood vessels, leading to accumulation particularly in the microvasculature such as pulmonary vessels, and potentially contributing to acute lung injury (43). Neutrophils primed *ex vivo* and re-injected become trapped in the lungs (38) and healthy volunteers inhaling LPS have delayed neutrophil transit through the lungs as a result, with similar findings in patients with chronic obstructive pulmonary disease (COPD) in the absence of LPS (44). Retention of neutrophils in the microvasculature has the potential to increase neutrophil-endothelial interactions, particularly in the lung as seen in the disease setting of COPD (45). The lung can therefore act as a reservoir for mature neutrophils, harbouring primed neutrophils in the pulmonary circulation before de-priming and release into the peripheral circulation (38,40). One of the roles of the lung is to deprime neutrophils as a safety mechanism to prevent primed neutrophils from circulating; this is thought to be due to repeated mechanical constriction as they pass through the lung vessels and has been displayed in microfluidic devices using a series of constrictions to mimic this (46). This mechanism can be faulty in the lung in inflammatory disease state, resulting in premature release of primed neutrophils from the lung due to a failure of de-priming (40). Priming agents are present in circulation, therefore at sites of inflammation, neutrophils can also participate in this cycle of priming, de-priming, and re-priming spontaneously, outside of the lung, displaying their flexible capabilities (40,46). Primed neutrophils are also described to be found systemically in patients with trauma or sepsis (47–50). While priming promotes neutrophil retention in the lung only in disease states, the lung's capability to de-prime neutrophils may modulate local and systemic neutrophil responses (40).

1.2.3. Degranulation

A main pathogen-killing mechanism of neutrophils is the coordinated release of proteolytic granule contents (51,52). Upon stimulation, granules are directed to translocate within the cytoplasm and can either fuse with the phagosome or with the plasma membrane, depending on the stimulus and strength of the activation signal. Receptors, such as Fc-gamma (Fcγ) (53), complement receptor 3 (CR3), and formyl peptide receptor 2 (FPR2), in the neutrophil cell membrane, once activated, signal to the cytoplasm to secrete granule contents (54–56). Degranulation, or exocytosis, of preformed granule release first occurs with granule recruitment (57), and is dependent on calcium signalling (55). Azurophil granules contain the most potent cytotoxic proteins, such as NE, as well as MPO and PR3, and require the strongest stimulus for degranulation. Their main role is to fuse with the phagosome to kill pathogens (16) and they are only released extracellularly when additional excess stimulation occurs, or when an extracellular pathogen is too large to fully engulf, such as fungal hyphae (58,59). Granule fusion with the plasma membrane may allow primed neutrophils to present antigens, or to express granule proteins at the cell surface, including MPO and PR3 (60). Natural inhibitors of MPO and PR3 after degranulation, ceruloplasmin (MPO) and Alpha1-antitrypsin (PR3) (61,62), can limit the exposure of MPO and PR3 to the healthy immune system (63). In pro-inflammatory disease states, immune cell activation stimulates the release of proinflammatory cytokines promoting neutrophil priming, degranulation, and MPO and PR3 cell surface expression (64), which is typically an appropriate response to control pathogens. If neutrophils are aberrantly or excessively activated in circulation, this may lead to vascular damage, frequently found in autoimmune rheumatic diseases (ARDs) (65).

1.2.4. ROS and phagocytosis

Neutrophils can respond to infection by engulfing pathogens into the phagosome (66), an intracellular compartment capable of degrading fungus and bacteria once fused with neutrophil

granules. NADPH-dependent killing mechanisms occur through degranulation, NET formation, or generation of ROS, and can eliminate pathogens and microorganisms (67,68). NADPH oxidase recruitment to the phagosomal membrane can lead to granule activation, and result in oxidative or respiratory burst within these phagosomes once fused. The release of ROS through respiratory burst is a pathogen killing mechanism neutrophils can carry out once primed (20), and opsonisation, or engulfment, of pathogens occurs (69). Although pathogen killing requires phagosomal ROS, which is generated through NADPH oxidase activation as a main source, tissue injury can result from extracellular ROS release. If ROS is released extracellularly, activation of granular proteases occurs, including NE, which can promote formation of NETs (70). While these mechanisms are programmed as anti-microbial responses, excess ROS production, degranulation, and overproduction of NETs, can contribute to endothelial and tissue damage (71).

1.2.5. NETosis

NETosis is a unique type of neutrophil cell death whereby the cells' granule contents are expelled into the extracellular space in mesh structures, called NETs. NETs are formed in net-like structures comprising double-stranded DNA (dsDNA), citrullinated histone peptides (e.g. citrullinated histone 3 (H3Cit)), and granule derived antimicrobial peptides such as MPO and PR3 (71). The best studied pathways for the generation of NETosis are those linked to NADPH oxidase. A variety of stimuli such as PMA, bacteria, immune complexes, or crystals lead to activation of protein kinase C (PKC) and Ras/Raf/mitogen-activated protein kinase (MAPK)-extracellular signal-related kinase/extracellular signal-regulated kinase (Ras-Raf-MEK-ERK) pathways (72). This leads to intracellular ROS production via NADPH oxidase, the release of neutrophil granule components intracellularly, the migration of these proteases to the nucleus and chromatin decondensation through histone modification (64,72–76). DNA is then expelled

through the disrupted plasma membrane. NETs trap foreign bodies such as bacteria (77), removing them from the circulation, as one of the neutrophil's anti-microbial defence mechanisms (78).

1.2.6. Types of NETosis

There are thought to be two types of NETosis, either classical, that occurs by ROS dependent pathways as described above, which results in programmed cell death, or vital, whereby neutrophils are speculated to remain viable and functional, although vital NETosis remains controversial. Viable NET formation is thought to occur through either ROS-independent mechanism, which rely on nuclear NET formation (79), or ROS-dependent NET formation, that relies on mitochondrial NET formation (80). In non-lytic nuclear chromatin release, the neutrophil is thought to then survive without a nucleus and be capable of phagocytosis, but it is questionable whether this is possible (79). Although, it is unclear how rupture of the mitochondrial membrane may occur (80), in vital NETosis, NETs may therefore have a proinflammatory effect rather than bacterial killing effect (82). NET pathways are also thought to be linked to autophagy, a process by which intracellular degradation occurs facilitating protein and organelle turnover (83). Due to the complicated mechanisms and multiple pathways involved in autophagy, how ROS and NETosis impact on this process are not completely understood. Although there is speculation that mitochondrial ROS provides the link between ROS and autophagy, by contributing to NADPH oxidase activation and NET induction being mitochondrial ROS (84), which results in inflammation and the release of mitochondrial DNA. Yet, some studies have shown autophagy and NETosis may not be linked (85). Alternative pathways for NADPH oxidase independent NETosis have been identified through a mechanism of calcium influx with NETosis occurring in response to calcium ionophores (86). Neutrophils may have low numbers of mitochondria (87,88) in comparison to

other leucocytes, but nonetheless thesis mechanisms are thought to contribute to programmed cell death.

1.2.7. Regulators of NETosis

While ROS contributes to autophagy (89), and the amount of intracellular ROS can regulate whether NETosis will occur after autophagy (90,91), the role of ROS in NETosis is still controversial. In some settings, NETs are thought to be calcium dependent (92,93). NE role in NETosis is cleaving histones, which definitively contributes to chromatin decondensation (75). Prompted by ROS and MPO, NE is translocated to the neutrophil cellular membrane once released from neutrophil granules where it then activates breakdown, or proteolysis, of neutrophil proteins (114). In turn, these mechanisms regulate neutrophils undergoing NET formation, and additionally promote actin cytoskeleton disassembly (64,75). Previous studies have shown NET formation is also dependent on cell lysis induced by multiprotein complexes such as Gasdermin D (GSDMD), a protein involved in key processes in controlling membrane permeability (94). Yet, recent developments have shown agonist induced NET formation independent of GSDMD can occur and does not result in cell lysis, in addition to these NETs forming from viable neutrophils through inflammasome activation (95).

Peptidyl arginine deiminase 4 (PAD4) is described in many studies to be essential to NET formation, by converting arginine to citrulline in histone proteins. Some studies suggest that auto-citrullination of PAD4 decreases its capability to interact with histone deacetylase (HDAC) (96) and hyper-citrullination of PAD4 induces chromatin decondensation. As a result, chromatin unfolding occurs, which promotes NET formation, particularly when PAD4 is overexpressed. PAD4 is a calcium dependent enzyme and some *in vitro* studies have suggested that for activity it requires intracellular calcium levels between 10^{-8}-10^{-6} molar, far higher than

found in normal homeostasis but which may be present following cell damage (97), but PAD4 citrullination is also proven to be calcium dependent (98,99). There is conflicting evidence as to whether PAD4 is ROS dependent or not with some studies suggesting it is downstream of NADPH, but others suggesting calcium can activate PAD4 independent of ROS (100, 101).

Influx of intracellular calcium and calcium ionophores have been shown to contribute to NETosis progression through regulation of actin disassembly (102,103). Time lapse microscopy has confirmed the role of actin cytoskeleton disassembly in allowing for NETosis to begin (104). Upon the usage of pharmacological agents (105,106) or through genetic defects (107), inhibiting actin assembly has also confirmed actin involvement and the importance of the cytoskeleton in NET formation (108). For NE to be translocated to the cell surface (64), neutrophil cytoskeletal rearrangements and endomembrane disassembly needs to occur. This is another mechanism displaying the important of actin in NET formation as NE is necessary for histone hydrolysis, in turn facilitating chromatin decondensation (75).

1.2.8. NETosis and Cell death pathways

NETosis differs from apoptosis and pyroptosis as the apoptotic mechanism prevents the release of neutrophil histotoxic contents, and the pyroptotic mechanism retains DNA during cell lysis (109). Receptor-interacting protein kinase (RIPK1/3)/Mixed lineage kinase domain-like pseudokinase (MLKL)-dependent necroptosis, PI3K (110), or PAD4 dependency (98,99,111), and complement activation (112) have all been identified in pathways involved in NETosis. Necroptosis is a form of neutrophil programmed cell death, with features of both apoptosis and necrosis but without the typical morphological features of apoptosis such as membrane blebbing. RIPK1 activates RIPK3/MLK1-dependent necroptotic death, leading to downstream PAD4 activation for promotion of chromatin decondensation, and expulsion of NETs is

presumed to occur. Currently, more is known about PAD4's involvement in this pathway in murine neutrophils than human neutrophils cellular mechanisms, and human and murine neutrophils significantly differ as reviewed in Nauseef et. al 2022 (113).

1.2.9. NETs in auto-immune and auto-inflammatory diseases

While neutrophils are responsible for eliminating pathogens intra- and extracellularly through phagocytosis, degranulation, and NET formation, many ARDs promote an increase in these neutrophil pathogen killing mechanisms with a consequence being inadvertent host tissue damage (115,117). Based on the stimulus, neutrophils will release NETs when in their activated state, comprising different components (116).

There have been studies characterising NETs in several ARDs, including Familial Mediterranean Fever (FMF), a neutrophil and NETosis dependent, heritable autoinflammatory disorder (118). During FMF attacks, an influx of neutrophils are recruited to sites of tissue injury, resulting in NET release. *In vitro* experimentation showed these NETs to be decorated with IL-1β, identifying a potential source of IL-1β production in FMF. Additionally, neutrophils from patients with remission FMF are not responsive to induced NET production *in vitro* (118). Anti-IL-1β is a treatment strategy used to dampen inflammation in FMF (83).

Autoantigens have been found within NETs, including in SLE (119,120), and therefore are presented to the microenvironment once neutrophils undergo NETosis. An archetype of autoimmunity is a defective clearance mechanism of apoptotic cells; therefore, autoantigens remain within the circulation, continuously perpetuating autoimmunity. Autoantibodies in SLE are directed towards self-antigens, including immunogenic complexes made up of antimicrobial peptides and DNA from neutrophils. Patients with SLE develop autoantibodies

against the immunogenic complexes found in NETs (121,122). pDC are then activated by the immunogenic complex components from NET production, exposing autoantigens, in turn activating B cells to facilitate autoantibody production, and thereby perpetuating autoimmunity in SLE (123).

NETs and neutrophils have also been shown to play a critical role in venous thromboembolism (VTE) *in vivo* (124), including due to tissue factor (TF) being found within released NETs and subsequent TF dependent activation of the coagulation cascade (90,125). This mechanism may also be present in AAV, as there is evidence for neutrophils from patients with AAV displaying increased TF expression from release of NETs and microparticles decorated with TF (126). NETs in AAV will be discussed further in sections 1.5.6. and 1.6.1.

1.2.10. Cytokine release

Historically, neutrophil cytokine production was thought to be limited to IL-8 (127). This has been challenged in many studies and are now widely accepted to make a range of chemokines/cytokines (128). Neutrophils are proven to express or secrete numerous cytokines (129): of the proinflammatory, immunoregulatory or anti-inflammatory families; C-C, or C-X-C chemokines; TNF-superfamily members; colony-stimulating, angiogenic or fibrogenic factors (117,130–132); and other cytokines that do not fall within these categories. The vast range of cytokines produced by neutrophils, either constitutively or once activated, indicates their involvement in many different physiological and pathological processes. It is generally accepted that neutrophils make less cytokine than monocyte or macrophages (117), but *in vivo*, cells numbers may compensate for low absolute levels released by each cell as reviewed in Altan et. al 2019 (133). Therefore, this emphasises the importance of purity in cell isolation preparations for accurate results.

Upon activation, neutrophils can release pro-inflammatory cytokines, such as IL-8, through myeloid differentiation primary response 88 (MyD88)-dependent pathways, nuclear factor kappa-light-chain enhancer of activated B cells (NF-κB) upregulation, and MAPK activation (134). LPS can also trigger activation of this pathway through toll-like receptor 4 (TLR4) (135,136), and neutrophils may be capable of responding to even extremely low doses of LPS exposure (137). Chemokines, such as IL-8, act as chemoattractants for neutrophils and other immune cells to sites of injury, leading to a positive amplification loop (138–140). Molecular mechanisms that underpin the promotion of the production and secretion of some cytokines are well established, but expression of other cytokines and pathways for their production and release are still ill-defined and controversy remains.

1.2.11. Recruitment

Neutrophils are recruited by chemoattractants, such as IL-8, which signal a need for an influx of neutrophils at the site of infection, inflammation, or vascular damage (141,142), are recruited in the microvasculature for protection against infection, but in disease neutrophils can also be recruited to tissue (143,144). Inflammatory mediators stimulate neutrophil recruitment, leading to neutrophil tethering, rolling, adhesion, crawling along blood vessel walls, and finally transmigration through the endothelium to become extravasated into the surrounding tissue (145). This classical description of neutrophil recruitment has been derived mainly from studies of post capillary venules. Mechanisms in other vascular beds or tissues may not be the same (146). Neutrophils enter their rolling state upon interaction with an activated endothelium, through interactions between receptors expressed on neutrophils (P-selectin glycoprotein ligand (PSGL-1) and CD44)(147) and selectins on ECs (P- and E-selectin) (148,149). Once rolling, upregulation of integrins on neutrophils occurs (24), particularly lymphocyte function-associated antigen 1 (LFA-1) and macrophage-1 antigen (Mac-1). Chemokines such as IL-8

then further activate neutrophils leading to conformational change of integrins and eventually β2-integrin mediated neutrophil arrest, promoting binding with adhesion molecules (43,150), such as intracellular adhesion molecule-1 (ICAM-1), expressed by the endothelium (151). Adherent neutrophils then crawl along vessel walls to sites where chemokine dependent extravasation occurs (152). Integrin binding to ICAM-1 is vital for cell-cell adhesion and transendothelial migration (TEM) to occur; this mechanism has also been shown in adherent neutrophils with endothelial VCAM-1 (153,154).

1.2.11. Neutrophil/endothelial interactions

Primed neutrophils entrapped within the microvasculature are in direct contact with the endothelium as the diameter of capillaries is approximately 10 μm (155). Activated EC express receptors for immune cells to bind, promoting leucocyte release of chemokines, such as IL-8, and other cytokines, which encourages immune cell infiltration (156). Proinflammatory cytokines promote upregulation of adhesion molecules, including ICAM-1 and P-selectin, which are expressed by the endothelium, allowing neutrophil-endothelial interaction to occur (157,158). Rolling, adhesion, and TEM are facilitated through increased interaction and retention of neutrophils at the endothelium. When neutrophils are activated, β2-integrins, required for cell adhesion particularly to EC (ICAM-1), migrate to the cell surface. However, in the pulmonary capillaries, β2 integrin-independent neutrophil recruitment and accumulation has been shown, with the suggestion that deformability plays a role here (159,160). Gelatinase, within the tertiary granules, can digest extracellular matrix (ECM), aiding in TEM. Due to upregulation of cytokine production (161) and neutrophil degranulation, increasing neutrophil transmigration to resident tissues occurs, leading to tissue damage, and decreased neutrophil clearance, which in turn can result in unresolved, chronic inflammation (**Fig 1**).

1.2.12. Resolution of inflammation

Resolution of inflammation relies on the effective 'switching off' of the neutrophil, promotion of apoptosis, and the successful clearance of these cells (162–164). Once physiological function has been fulfilled at the tissue level, such as destruction of invading organisms, neutrophils undergo spontaneous apoptosis, which occurs to preserve neutrophil membrane integrity and prevent uncontrolled release of toxic cell contents (165,166). Apoptotic cell death allows for the controlled removal of cells in an immunosuppressive manner, predominantly by macrophages (efferocytosis). Exposure of phosphatidylserine (PS) residues during apoptosis on the apoptotic neutrophil membrane allows for greater recognition by macrophages, thereby enhancing clearance of the cells (165,167).

1.2.13. Inflammation

If neutrophil clearance does not follow apoptosis, secondary necrosis can occur, leading to exacerbated inflammation (168–170). This creates a self-fuelling inflammatory amplification loop. Activated neutrophils promote continuous inflammation and begin to leave the circulation, leading to further tissue inflammation. Damaged cells may not be cleared properly due to deficiency in clearance proteins, such as annexin-A1 or PS (171).When clearance proteins are not expressed, opsonisation of apoptotic cells by macrophages does not occur, leaving apoptotic cells and their internal proteins in the presence of the immune system; if released, these proteins may also be taken up by EC (172). As a result, uptake of antigens (apoptotic cells' cytoplasmic, nuclear, and cell membranous proteins) by B cells functioning as antigen presenting cells (APC), can contribute to disrupted immune tolerance, and the development of ARDs as reviewed in Oleinika 2019 (173).

While apoptotic neutrophils are typically functionally quiescent, increased TNF, which may be present in disease states, can alter this phenotype (165). TNF has a dual effect on neutrophil survival: early apoptosis is extrinsic, typified by TNF triggering whereby this pathway through binding of the death receptor, tumour necrosis factor receptor (TNFR1) (174), whereas delayed apoptosis is intrinsic, and inhibited by TNF. In early, intrinsic apoptotic pathways, anti-apoptotic factors are not present, resulting in permeabilisation of the mitochondrial membrane and cytochrome C, a protein responsible for apoptosome assembly promotion, being released into the neutrophil cytoplasm (165). A stressor or stimulus, such as DNA damage or ischaemia, activates the intrinsic pathway to promote apoptosis (175). In late, extrinsic apoptosis, pathways include Fas/Fas ligand (FasL), NF-κB and survival proteins, including myeloid cell leukaemia-1 (Mcl-1) and TNFR associated factor 1/2 (TRAF1/2) (176).

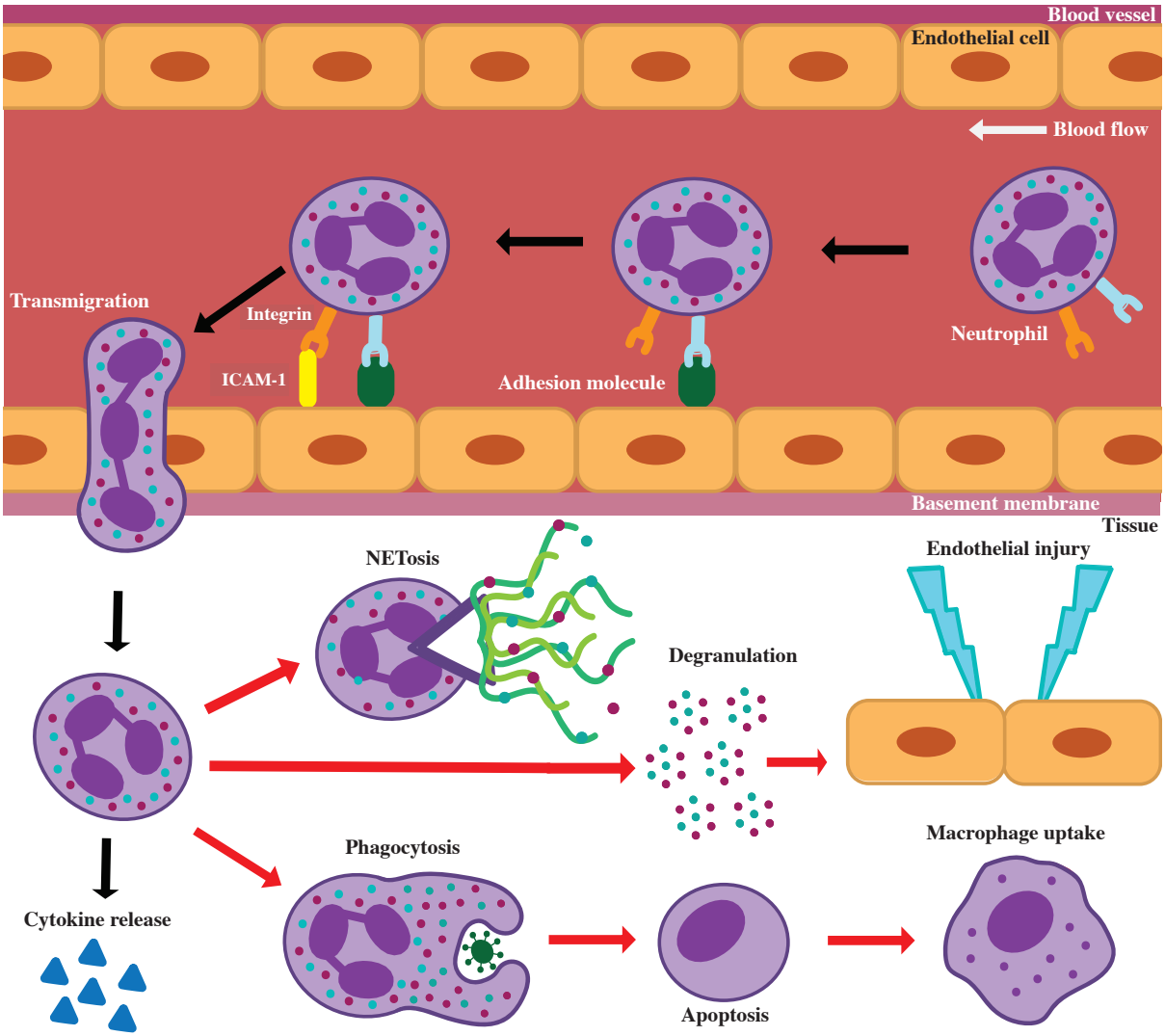


Figure 1. Neutrophil extravasation, interactions, and pathogen killing mechanisms
Circulating neutrophils bind to cell adhesion molecules (I/VCAM-1 and selectins) expressed by the endothelium and are captured through receptors/ligands on their cell surface. Neutrophils enter a rolling state as integrin (β1/β2) binding follows, allowing neutrophils to enter an arrested state on the endothelium. Chemoattractants recruit neutrophils to undergo TEM, where the neutrophil will deform to fit through endothelial junctions. Neutrophils sustain cytokine production and secretion, while later resorting to other pathogen killing mechanisms in response to infection, including phagocytosis, degranulation and NETosis. Extracellular release of granule contents through exocytosis or NETosis can lead to further endothelial or tissue damage. Apoptotic neutrophils are cleared by macrophages to resolve inflammation.

1.3. Neutrophil actin cytoskeleton

The cytoskeleton is made up of three proteins: intermediate filaments, actin filaments and microtubules. Intermediate filaments are fibrous proteins, affording cellular resistance and mechanical strength against shear stress (review in Hermann et. al 2016,175). Actin filaments are protein filaments contributing to cell shape and motility (178). Microtubules are proteins responsible for intracellular transport or positioning of membrane-enclosed organelles (179). Myosin is a motor protein involved in converting adenosine triphosphate (ATP) to ADP, (180) and plays a key role in cellular motility through actin-myosin interactions. While these proteins have integral, individual roles in cell integrity and function, they cannot act on their own.

1.3.1. Actin

Actin is a protein found in majority of eukaryotic cell types and can be found in different states, including globular (G)-actin, the monomeric form, and filamentous (F)-actin, the polymerised form (181). G-actin performs as a reservoir for actin monomers (182), which are constituents for F-actin in forming the actin cytoskeleton of cells. Actin polymerisation is the process by which the binding sites of actin monomers capable of induction, or G-actin, at the positively charged, or barbed end of actin, act as a substrate for binding to other monomers, to form F-actin filaments (183,184). Many cell processes, including cell signalling, locomotion, junction formation, and division involve actin, particularly due to its binding properties, polarity, and the potential for reversing actin polymerisation.

1.3.2. Neutrophil actin cytoskeleton

Typically, as cells mature or differentiate, this couples with changes in cellular mechanical properties, including an increase in cytoskeletal proteins (185,186). This is not observed in neutrophils (187,188) but instead, upregulation of expression of cytoskeletal proteins occurs

only once cells are degraded. Thus, as neutrophils undergo apoptosis, the cytoskeleton changes (189). Neutrophils are small in diameter, typically ranging between 7-11 μm in size, allowing them to pass through small vessels particularly due to their deformable properties (190). Due to neutrophils role *in vivo* as infection monitoring cells, mature neutrophils are required to transit through vessels or deform and migrate through vessel walls (191,192). There are several factors which may contribute to a neutrophil's high deformability. Changes in neutrophil size are sodium/hydrogen exchanger dependent and this may contribute. The distinct structure of the mature neutrophil multilobulated nucleus and decreased expression of vimentin, a cytoskeletal intermediate filament protein also contributes (193). Actin remodelling can be triggered through environmental signalling and is necessary for neutrophil motility; this process occurs through remodelling of microfilaments, thereby reorganising the cytoskeleton, and in some cases, the cellular membrane (194,195).

Pseuodpodia formation, a process by which neutrophils travel and carry out phagocytosis, extends the cellular membrane and occurs due to actin polymerisation, promoting membranous tension of the cell (196). These extensions of pseudopods alter neutrophil function, motility, and deformability (197,198). Pseudopodia pathways (199) include involvement from the WASP family verprolin homologous protein (WAVE) regulatory complex (WRC), the actin related protein 2/3 (Arp 2/3) complex, the Rho/Rac pathway, and PI3K. WRC is essential for cell protrusion and cell migration as WRC links Rho-subfamily guanosine triphosphate (GTPase) signalling to activate one of the three major actin nucleation factors, the Arp2/3 complex (200–203). The Rho/Rac pathway includes a set of Ras-related GTP-binding proteins, controlling polymerised actin and its spatial pattern in the cell (204). GTPases, including Cell division control protein 42 (Cdc42), are part of the Rho-subfamily, and regulate neutrophil rearrangement of the cytoskeleton and recruitment to sites of infection (205,206). Protrusion

formation, or lamellipodia, are stimulated by Rac-subfamily proteins (207). Once activated and actin nucleation occurs beneath the plasma membrane, the Arp2/3 complex promotes forcing lamellopodia through the cell leading edge (208). Neutrophil activation can therefore lead to deformation and pseudopod formation allowing them to perform TEM (45,209). Microtubule dynamics also contributes to neutrophil deformability along with the neutrophil's actin network to maximise their migratory capabilities (188,198,210).

1.3.3. Neutrophil deformability

In vitro experiments on isolated neutrophils have shown that after priming, neutrophils undergo a phase of shrinkage and stiffening (41,42). Once exposed to a secondary stimulus, neutrophils enter an activated state resulting in a second phase of morphology change with an increase in cell size. This change in size typically results in an increase in neutrophil deformability, i.e. the cell becomes softer (22,40,211,212). Previous studies using a range of neutrophil priming agents, have shown it is possible to identify morphorheological changes as early as 1 minute after stimulation with formyl-methionyl-leucyl-phenylalanine (fMLP) (41). Neutrophils can endure extreme cellular deformation by going through three phases: initiation, deformation, and remodelling. This allows neutrophils to carry out locomotion and processes such as TEM (213). This is said to be due to their deformable multi-lobulated nucleus (214), nuclear envelope (215), and cytoskeleton (216), which jointly contribute to the deformability of neutrophils. Biophysical cellular and nuclear properties of neutrophils have been measured *in vitro*, in high resolution imaging (217), utilising lattice light sheet microscopy (218), 3-D modelling of inflammation-on-a-chip (219), microfluidics in whole blood (220), and mechanical deformation using an optical stretcher and a mimetic chip (46). These experiments identified neutrophils can undergo transient deformation in the absence of priming or activation (209,221). There is evidence for actin-related primary immunodeficiencies altering neutrophil

cytoskeletal function, and mutations in Wiskott-Alrich syndrome (WAS) gene, influencing neutrophil adhesion, migration, and cell-cell interactions (222). Moreover, actin remodelling and immune dysregulation is linked in immunological disorders as reviewed in Papa et. al 2020 (223). More genetic defects targeting neutrophil morphology and rheology therefore need to be studied to fully characterise the impact of modulating the cytoskeleton.

1.3.4. Neutrophil mechanophenotyping in RT-DC

Recent work analysing cell mechanics has identified mechanical changes in fMLP-treated neutrophils, identifying a phase of initial stiffening followed by a phase of expansion and softening (41). Priming-induced neutrophil stiffness may therefore hinder cell transit through blood vessels, leading to accumulation of cells at sites of injury, amplifying the inflammatory response. Chemoattracts, including IL-8, enhance neutrophil deformation, potentially linking neutrophil TEM to biomechanical properties (224). Primed neutrophils have delayed transit through the lung as evidenced by studies using radiolabelled transferrin in neutrophils (225). Transferrin is a glycoprotein contributing to iron transport in blood plasma and can be taken up by permeable blood vessels in tumours, allowing for non-invasive quantitative measurement using single-photon emission computed tomography (SPECT) (225).

1.3.5. Role of actin in neutrophil function

Dynamic actin remodelling in neutrophils is necessary to support their motile functions, but the cytoskeleton is also important for neutrophils retaining their structural integrity. Differentiation of progenitor cells leads to changes in mechanical properties whereby immature cells are stiff and resistant to deformation, and mature neutrophils are highly deformable (192,226,227). There is also a cytoskeletal signature of neutrophil activation, as more deformable neutrophils typify an activated state, while primed cells tend to be stiffer

(41,216,228). In some disease states such as sepsis or inflammatory conditions, neutrophils are released prematurely from the bone marrow due to overactivation of the immune system and depletion of the mature neutrophil population. This neutrophil population exhibits increased stiffness suggesting they may be primed (229). The retention of primed and/or stimulated neutrophils in the lung microvasculature is hypothesised to result from their decreased deformability. Immature neutrophils released due to emergency granulopoesis, or following increased generation from progenitors are also retained in the lung microvasculature (230). As this population has increased migratory capabilities from the tissue into lymphatic vessels, these neutrophils may not be the same population as those found trapped in the lung (231,232), but this remains to be determined.

Neutrophils sequestered in the lung undergo actin cytoskeletal changes and this may account for sequestration to a greater degree than changes in adhesion molecules or neutrophil-platelet interactions (45). Actin polymerisation has also been shown to occur at an early point following activation *in vitro* with stimuli such as fMLP or PAF (233,234). *In vivo*, this may allow for change in neutrophil cell shape to engulf an organism (235,236). Following initial rearrangement of the actin cytoskeleton, a pseudopod extension is then formed to make a phagosomal cup for phagocytosis (237,238) and translocation of granules thereafter occurs along microtubules to destroy the ingested pathogen. These processes both rely on calcium as a regulator, displaying the importance of calcium signalling in neutrophil programmed mechanisms (239–241).

1.3.6. Pharmacological modulators of actin

Many inhibitors of actin polymerisation in non-muscle cells are well established and are capable of inhibiting actin polymerisation at specific phases of polymerisation process (242–

244). Actin polymerisation entails three phases: nucleation, elongation, and a steady state (245). Firstly, three actin monomers form a complex, making up an actin nucleus. Next, this complex rapidly binds to the positive, barbed end of the filament promoting elongation of the actin filaments. Finally, capping of the pointed ends of filaments occurs, allowing for the filament dynamics to achieve equilibrium, or steady state (245). For the cell, this means further signalling pathways are activated and cytoskeletal rearrangement can occur (246).

1.3.7. Inhibition of actin polymerisation

Cytochalasins are a group of metabolites originating from fungi (247,248). Cytochalasins bind to the positively charged end of F-actin, disrupting polymerisation by inhibiting monomers intended for actin filament binding (249). Although not physiological compounds in humans, cytochalasins are useful experimentally to understand the role of actin dynamics (250). Cytochalasin B blocks monomer addition to the fast-growing end of the actin polymer (251). Cytochalasin D increases F-actin content, therefore increasing actin-filament ends for binding sites forming filamentous aggregates and disrupting organisation (252). *In vitro*, cytochalasin D can decrease TNF-priming induced formin-dependent cytoskeletal reorganisation, and neutrophil adhesion (253), but does not alter integrin-mediated neutrophil rolling or immobilisation. Functionally, cytochalasin D has been shown to inhibit phagocytosis, and enhances fMLP-mediated degranulation but NET production is preserved (55,77). Cytochalasin B also increases fMLP-dependent degranulation (254).

Inhibitors of actin/myosin interaction can also be used to modulate the cell cytoskeleton. Blebbistatin is a small molecule inhibitor capable of inhibiting class II myosins and ATP activity through blocking myosin head binding to ATP (255). This promotes actin polymerisation more so than monomers once bound to ADP (255). Paraaminoblebbistatin is a

derivative of blebbistatin, and although it has weaker inhibitory capabilities than blebbistatin, its advantageous experimental properties include being non-fluorescent and photostable (256). Additionally, *in vitro*, cytochalasin D and blebbistatin have been shown to decrease NET formation, which is linked to cytoskeletal changes (257). The individual inhibitory properties of cytochalasins and blebbistatins on actin polymerisation allows for usage as research tools.

1.3.8. Actin disruption

Once actin dysfunction in neutrophils occurs, not only are their locomotive and deformable capabilities altered, but other effector functions as well. The neutrophil actin cytoskeleton regulates granule, and therefore granule contents, exposure to the plasma membrane (55). Granule contents such as NE are also linked to the degradation of F-actin by arresting the function of F-actin, and F-actin disruption is linked to increased ROS production as discussed in section 1.2.4. (258). Once NE is released and undergoes activation, it binds to actin, leading to actin degradation, allowing for NE entry into the nucleus (259). As described above, inhibition of actin dynamics using cytochalasins have proven that other neutrophil functions, such as rolling and adhesion, are modulated by their cytoskeleton (260). Actin microfilament disruption by cytochalasin D has been shown to alter L-selectin shedding, resulting in increased membranous L-selectin clustering, and altered neutrophil tethers, containing actin filaments (261). More studies are still required regarding how the cytoskeleton contributes to neutrophil responses under different shear stress and pressure gradients, such as in neutrophil extravasation.

1.4. Autoimmunity: breakdown of tolerance

When a foreign antigen is recognised by the body, an immune response is stimulated as a defence mechanism against this antigen. Under normal circumstances, the immune system resets the function of autoreactive B and T cells via two self-tolerance processes, central and peripheral tolerance. Central, or maintenance tolerance is a mechanism controlling tolerance to self-antigens, while peripheral tolerance mediates anergy and activation induced cell death. Autoreactive cells are removed or edited through three key mechanisms: clonal deletion, clonal anergy, and receptor editing. When these self-tolerance processes fail, a breakdown of tolerance occurs, and, if uncontrolled, leads to autoimmune disease (262). A key biological mechanistic process leading to breakdown of tolerance, is molecular mimicry, where self and foreign antigens share similar sequence and structure, causing the persistent stimulation of autoreactive B and T cells (263). After an initial loss of tolerance, activation of the humoral immune response through T-helper (Th) cell activation occurs and autoantibodies are produced by autoreactive B cells, or plasma cells against self-antigens. Once formed, autoantibodies bind and interact with Fc receptors and through autoantigens, engaging downstream adaptors while upregulating production of inflammatory cytokines. In turn, dependent upon disease pathogenesis, immune complex deposition on organs may occur, leading to detrimental systemic effects (264). Immunologic memory follows, repeating this cycle upon exposure to the autoantigen, leading to indefinite flare ups and continuous autoimmune disease activity. This is the central mechanism (265) by which several systemic autoimmune diseases develop, including AAV.

1.5. Anti-neutrophil Cytoplasm Antibody Associated Vasculitis (AAV)

The anti-neutrophil cytoplasm antibody (ANCA) associated vasculitides (AAV) are a group of systemic autoimmune diseases characterised by inflammation of microvasculature and comprising three clinical phenotypes: microscopic polyangiitis (MPA), granulomatosis with polyangiitis (GPA), and eosinophilic granulomatosis with polyangiitis (EGPA) (266). Neutrophils are a main contributor to disease pathogenesis of AAV as they mediate vascular and endothelial damage (267), in addition to being the main target of the autoantibody, ANCA.

1.5.1. Clinical phenotypes

MPA and GPA are classified based on clinical and histological features. MPA is typically associated with ANCA directed against MPO (in around 60% of cases). Patients may have predominant kidney involvement and there is absence of granulomas (266). There may be pulmonary capillaritis and diffuse alveolar haemorrhage (DAH) (266). Patients with GPA more commonly have PR3-ANCA positivity (in 75% of cases). The hallmark of disease is necrotising granulomatous inflammation (268) often involving the upper and lower respiratory tracts. There may also be involvement of extravascular tissues (269,270). Relapse is more common in patients with PR3-AAV, particularly in those with persistent antibody positivity (271). EGPA is AAV with eosinophil involvement, associated with asthma and blood eosinophilia. EGPA may be associated with ANCA positivity, and patients may have vasculitic features (266). EGPA is somewhat distinct from GPA and MPA with differing pathogenesis, clinical features, and genetic associations. My thesis focusses on patients with MPA and GPA, as such EGPA is not discussed in detail here. Genome Wide Association Studies (GWAS) in AAV have reported GPA and MPA to be genetically distinct but there was greater distinction seen between those who are MPO-ANCA and PR3-ANCA positive. In large GWAS studies,

anti-PR3 AAV was associated with variants in *HLA-DP, PRTN3*, and *SERPINA1* (Alpha1-antitrypsin, a circulating inhibitor of PR3). Anti-MPO AAV was mainly associated with HLA-DQ polymorphisms (272,273). There is also evidence for a shared genetic risk between MPO- and PR3-AAV as PTPN22 variants were common in AAV (272,274).

There are also many reported environmental associations with AAV. Infection can trigger disease relapse, potentially via mechanisms of molecular mimicry (275). In some patients an atypical ANCA, anti-human lysosome-associated membrane protein-2 (anti-LAMP-2) antibody can be identified which has 100% sequence homology with FimH a bacterial protein (276,277). This finding has not been confirmed in all studies. In one study, patients with PR3-AAV were shown to have circulating antibodies to both PR3 and anti-sense complementary PR3 peptides suggesting the initial immune response may be against an anti-sense peptide; this leads to development of anti-idiotype antibodies which can recognise both complementary PR3 and PR3 (278). There are numerous other environmental risk factors that have been identified including seasonality, geoepidemiological factors such as UV exposure, drugs, heavy metals, and silica (279–281) as reviewed in Scott 2020 (282) .

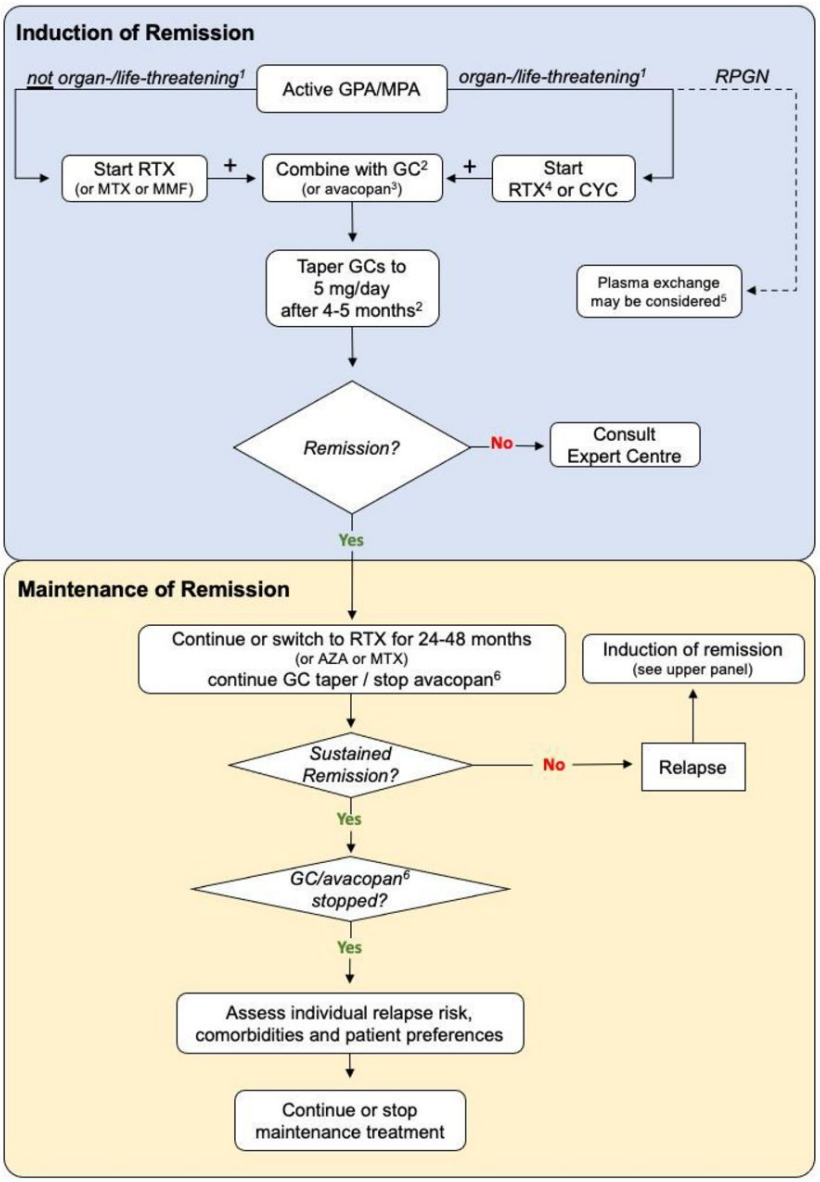
1.5.2. Diagnosis and clinical features

Multiple organ systems and tissues can be affected in AAV with the lung and kidney commonly involved. AAV is often associated with life threatening clinical manifestations such as rapidly progressive glomerulonephritis (RPGN) (classified as a decrease in GFR by at least 50% due to crescent formation in the glomerulus) and pulmonary haemorrhage (283). Other organ systems involved can include the skin, joints, ear/nose/throat (ENT), peripheral and central nervous systems, gut, or eyes (**Table 1**). Patients are usually positive for ANCA, but a negative ANCA titre does not rule out AAV in the context of a clinical or histological diagnosis. Patients

may have elevation of c-reactive protein (CRP) and erythrocyte sedimentation rate (ESR) indicating systemic inflammation. CRP, synthesised in the liver, elevates in response to IL-6 secretion and is used as a non-specific marker of inflammation in whole blood. ESR measures the sedimentation rate of red blood cells in anticoagulated whole blood and is also used as a measurement of inflammation. ANCA can be detected using indirect immunofluorescence (IF) or specific ELISA. On IF of ethanol washed neutrophils typical patterns of ANCA staining are seen for MPO (perinuclear) or PR3 (cytoplasmic) (284). Disease activity can be measured using Birmingham Vasculitis Activity Score (BVAS), which evaluates nine organ systems, as well as defining patients' response to therapy and status of remission (285). Current treatment strategies for AAV are summarised in **Table 2**.

Two entry requirements			
A clinical diagnosis of small- or medium-vessel vasculitis has been made and other medical conditions mimicking vasculitis should be excluded			
Variables	Disease classification		
At the time of the first classification	GPA	MPA	EGPA
Clinical criteria			
Nasal passage involvement	+3	-3	
Cartilaginous involvement	+2		
Conductive or sensorineural hearing loss	+1		
Obstructive airway disease			+3
Nasal polyp			+3
Mononeuritis multiplex			+1
Laboratory criteria			
PR3-ANCA (or C-ANCA) positivity	+5	-1	-3
MPO-ANCA (or P-ANCA) positivity	-1	+6	
Serum eosinophil ³ 1000/uL	-4	-4	+5
Haematuria			-1
Histological criteria			
Granuloma, granulomatous inflammation, or giant cells	+2		
Pauci-immune GN	+1	+3	
Extravascular eosinophilic-predominant inflammation			+2
Radiological criteria			
Pulmonary nodules, mass, or cavitation or chest imaging	+2		
Fibrosis or ILD on chest imaging		+3	
Nasal/paranasal sinusitis or mastoiditis on imaging	+1		
The cut-off of total scores for the classification	³5	³5	³6

Table 1. 2022 ACR/EULAR classification criteria for AAV



Mechanisms of action	
Glucocorticoids (Methylprednisolone/Prednisone)	Decrease inflammation through inhibition of vasodilation, vascular permeability, and leucocyte recruitment
Rituximab (RTX)	Biological therapy, anti CD20 monoclonal antibody, targets B cells, leads to B cell depletion
Avacopan	Inhibits C5aR interaction with C5a, blocks neutrophil activation/migration mediated by C5a
Plasma exchange (PLEX)	Filters plasma and removes circulating pathogenic antibodies, replaces with fresh plasma/fluid consisting of albumin solutions
Disease modifying anti-rheumatic drugs (DMARDs) - Decrease disease effects of overactive immune system	
Cyclophosphamide (CYC):	Blocks DNA synthesis, kills immune cells through programmed cell death
Methotrexate (MTX):	Inhibits cellular folate metabolism and decreases nucleic acid synthesis
Azathioprine (AZA):	Inhibits purine synthesis, modulates B and T cell apoptosis
Mycophenolate Mofetil (MMF):	Selectively inhibits the S phase of the cell cycle/DNA synthesis, halts B and T cell proliferation

Table 2. 2022 EULAR treatment criteria for AAV (MPA/GPA) (286)

1.5.3. Pathogenicity of ANCA

ANCA, an autoantibody of usually immunoglobulin G (IgG) isotypes, are produced in patients with AAV. After an initial loss of tolerance, activation of the humoral immune response through T_h cell activation occurs and ANCA are produced by plasma cells. Circulating ANCA are directed towards MPO and PR3, found in neutrophil cytoplasm granules and the lysosomes of monocytes (287,288). Translocation of MPO and PR3 to the neutrophil cellular membrane occurs during inflammation, exposing the autoantigens for ANCA to readily bind (**Fig 2**). There is evidence of a pathogenic role for ANCA from *in vitro* (289–293), *in vivo* (294–297), and clinical studies (298–300). *In vitro* ANCA directly bind to and activate neutrophils (60,63) and monocytes (301) leading to cytokine production, degranulation, and generation of neutrophil extracellular traps (NETosis). *In vivo* ANCA can be used in passive transfer models of mouse AAV (294,302,303) in which mice develop crescentic GN and pulmonary haemorrhage, even in the absence of a cellular immune response (304,305).

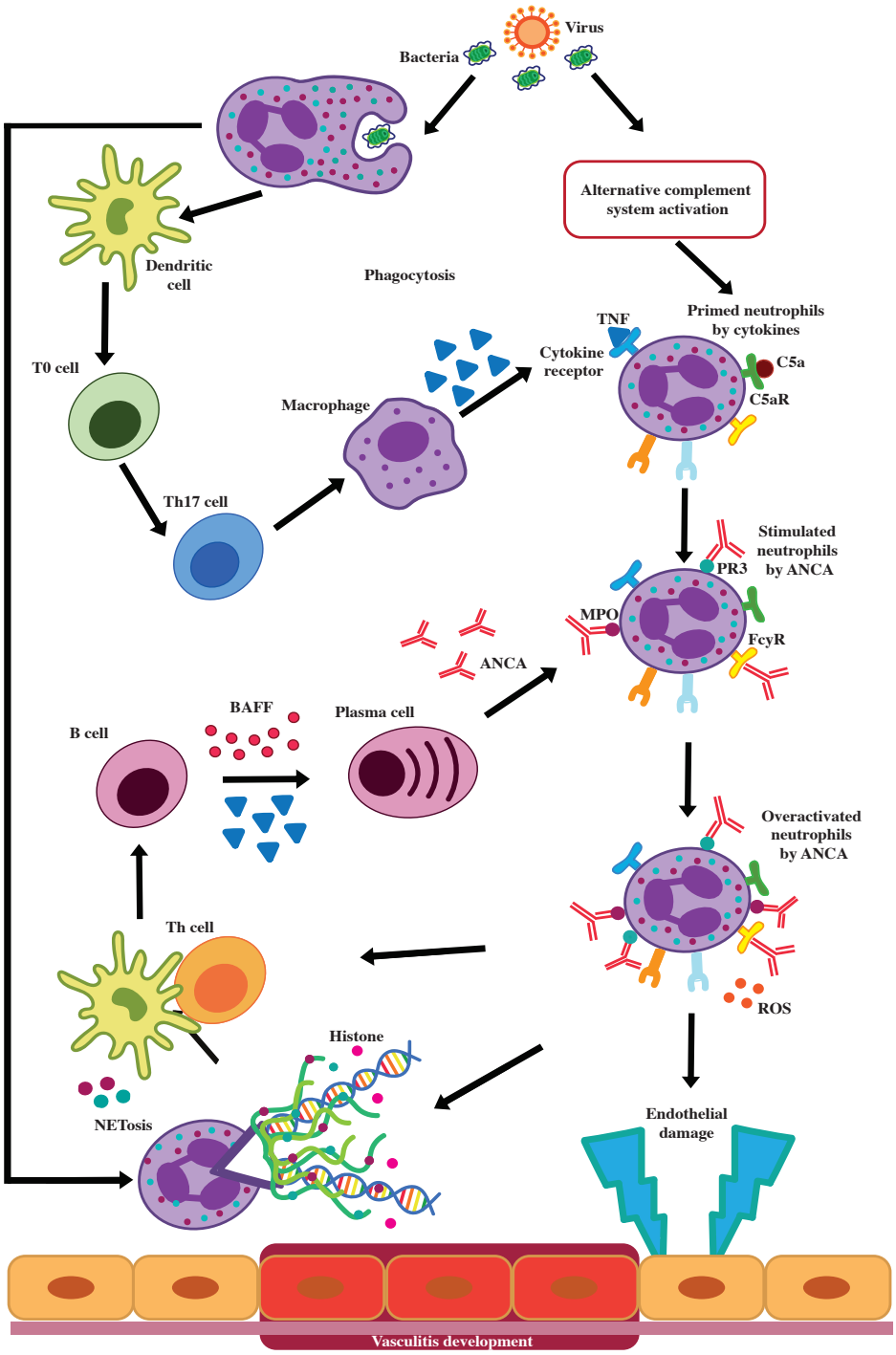


Figure 2. Neutrophil ANCA pathogenesis

Infectious agents are either phagocytosed by neutrophils or the alternative complement pathway is activated. Neutrophils will simultaneously undergo NETosis. Antigens derived from infectious agents are presented to T0 cells by dendritic cells. T0 cells differentiate into T_h17 cells and stimulate cytokine production by macrophages. Cytokines, including TNF, and C5a binding both prime neutrophils. MPO and PR3 antigens are released from the neutrophils which underwent NETosis, and antigens are presented to T_h cells by dendritic cells. B cells are stimulated by cytokines, including BAFF produced by neutrophils. Plasma cells produce ANCA and bind to neutrophil Fcγ receptor or MPO and PR3 expressed by TNF/C5a primed neutrophil on their cell surface. Increased activation of neutrophils occurs due to continuous ANCA production by plasma cells, ROS generation, and increased NET formation. Endothelial damage occurs, and vasculitis develops.

1.5.4. Disease activity

In patients there is significant evidence for the pathogenicity of ANCA. Levels of ANCA may correlate with disease activity, and therapeutic strategies such as removing autoantibodies with therapeutic plasma exchange (TPE) or depleting B cells with rituximab (RTX) are used as treatments (274). However, this relationship is complex with several lines of evidence to suggest that not all ANCA are pathogenic. ANCA can be identified in healthy people, and ANCA can persist in remission, or recur without relapse (306). IgG subclass may be important in contributing to this, as there is evidence IgG3-ANCA induce the most pathogenic responses *in vitro*. However, there are conflicting results in clinical AAV with one study identifying no correlation between IgG3 ANCA titre and relapse (307–309). There is also evidence that ANCA binding via both fragment antigen-binding (F(ab)) and Fc receptor (FcR) are important. One study identified that ANCA F(ab) were able to bind to ANCA antigens, but this did not result in neutrophil activation (310). Cross-linked F(ab) fragments, or $F(ab')_2$ ANCA fragments can both bind to cells and stimulate ROS and cytokine production, although studies vary as to whether this is the same or lower magnitude than responses induced by intact ANCA (290,308,311,312).There is evidence from *in vitro* studies for the importance of ANCA binding to FcγRIIa (CD32A) (308). ANCA also binds to FcγRIIIb (CD16b), which is expressed at much higher levels on neutrophils than CD32A, although this role is more controversial. FcR polymorphisms may be another explanation for conflicting results relating to the pathogenicity of ANCA *in vitro* and *in vivo* (311,313). Epitope specificity may also play a role. In healthy individuals with natural anti-MPO antibodies, differences in MPO epitope specificity were identified in comparison to patients with AAV. Epitope mapping showed that out of the 25 anti-MPO autoantibody epitopes, 12 were only found in patients with active AAV (aAAV) (300).

1.5.5. ANCA induced activation of neutrophils

Neutrophil priming can be achieved using low dose TNF, GM-CSF, or complement component 5a (C5a) (314), which induces increased expression of ANCA antigens on the neutrophil cell surface. Increased MPO and PR3 expression on the cell surface of neutrophils therefore facilitates interactions between the antigens and ANCA. Studies have described variable efficiency levels in activating neutrophils *in vitro,* more so when using ANCA isolated from patients with active disease to activate neutrophils in comparison to using ANCA isolated from patients in remission (60). This may be due to different epitope specificities of ANCA IgG from patients with aAAV than those from patients in remission. Similarly, neutrophils from patients with aAAV, both in whole blood and once isolated, may reflect a different phenotype as they respond to stimuli more robustly than HC neutrophils incubated with the same stimuli (296).

1.5.6. Activated neutrophil responses

Activation by ANCA IgG results in neutrophil adhesion and transmigration through the vascular endothelium, pro-inflammatory cytokine release, and stimulation of neutrophil pathogen-killing mechanisms (ROS generation, degranulation, and NET formation). Activation of intracellular signalling pathways occurs downstream of ANCA activation, including spleen tyrosine kinase (SYK), MAPK, and PI3K (315,316). There are several studies suggesting a role for ANCA induced NETosis in the pathogenesis of AAV. ANCA stimulation leads to NET production *in vitro*, and NETs have also been observed in kidney biopsies from patients with small vessel vasculitis (SVV) (317). NETs cause tissue injury in AAV both through release of enzymes and particularly extracellular histones, which contribute to inducing EC apoptosis and vascular damage (318). PAD4-mediated histone citrullination can lead to NET formation, and one study has identified that overactivation of PAD4 following

ANCA stimulation of neutrophils can lead to increased NET formation, resulting in vascular leakage and thrombosis. Therefore, inhibiting NETs via PAD4 may be a therapeutic option in AAV (319,320).

Danger signals exposed during NET release may also promote breakdown of tolerance and the inflammatory response (321). ANCA antigens was proven transferred by NETs to myeloid dendritic cells in an *in vivo* mouse model, displaying another method whereby ANCA production is promoted (321). Excess neutrophils, named emergency granulopoesis, may be released in circulation, including immature neutrophils (322). This can lead to accumulation of neutrophils or the inability to dampen inflammation, as well as compromising infection control due to dysregulated neutrophil pathogen killing mechanisms, ultimately causing disease flares and tissue damage (323).

1.5.7. Overactivation of neutrophil programmed mechanisms

Degranulation also occurs upon ANCA activation of neutrophils, resulting in neutrophil serine proteases (NSP) (PR3, cathepsins) and MPO release. NSP such as cathepsins and PR3 have been shown to contribute to the pathogenesis of AAV, independent of their role as ANCA antigens. NSP release following ANCA activation of monocytes can lead to EC injury (324), play a role in NETosis, and drive cytokine release (325,326) studies have also identified cytokine release, including IL-8, in response to ANCA stimulation *in vitro* (327). IL-8 has also been identified to have increased expressed at the protein and mRNA level in monocytes in AAV glomerulonephritis (GN) (328).

1.5.8. LDGs

It is increasingly recognised that neutrophils are heterogeneous and can be separated into low- and high-density granulocyte fractions (LDG and HDG, respectively) (218). LDGs were first identified in cancer and have subsequently been identified in SLE and other inflammatory conditions (329,330). The origin and function of LDGs is yet to be fully defined. Some, but not all LDG may be derived from the immature neutrophil population as some, but not all LDG exhibit a similar cell surface phenotype to immature cells with absent or low CD10 expression (331). However, in some cases, as is described in SLE, LDG often display a mature phenotype and therefore the subset may themselves be heterogenous (332). In lupus, studies suggest LDGs have a pro-inflammatory phenotype with increased ability to produce ROS and undergo NETosis (333). Increasing numbers of SLE LDG are associated with increased vascular inflammation, and atherosclerosis independent of typical cardiovascular risk factors (334,335). In AAV, the number of LDG correlates with disease activity (336,337), but mechanisms underlying their production and phenotype, and their contribution to disease pathology, are yet to be fully understood. Whether LDGs arise after the onset of acute vasculitis, in response to systemic inflammation signals, or if they act as drivers or initiators of endothelial injury also remains to be determined. It is hypothesised that a subpopulation of LDGs are immaturely released from the bone marrow during acute granulopoiesis (338), contributing to pernicious disease progression, predominantly in autoimmune disease.

1.6. Neutrophil recruitment and endothelial injury

Characteristically, primed neutrophils are recruited to the endothelium, transmigrate, and kill pathogens at sites of infection, but activated neutrophils can also accumulate on the vascular endothelium resulting in inflammation and destruction of the vasculature (330), as occurring in vasculitis. In AAV, neutrophil adhesion to the endothelium is promoted through increased ICAM-1 and integrins (339). It has been shown *in vitro* that ANCA stimulation activates pathways in neutrophils that simulate contact with an activated and inflamed endothelium (340). Intracellular calcium increases, which promotes activation of integrins and endothelial adhesion (339). ANCA stimulation is therefore capable of converting neutrophils from the rolling to adhesive state, while also promoting migration through the vascular bed (310). Neutrophils from PR3-ANCA positive AAV patients have an increased proportion of CD177+ neutrophils, which results in increased PR3 presentation at the neutrophil cellular membrane (341). CD177 interacts with platelet endothelial cell adhesion molecule (PECAM-1) to regulate neutrophil TEM (590). Patients with MPO-ANCA positive AAV also displayed this phenotype, but this was not significant in comparison to HC (341–343). Once vascular damage has occurred this can then lead to an increase in neutrophil TEM allowing neutrophils to pass through the vessel wall more easily, and exiting into the tissue causing further damage, and resulting in chronic inflammation.

Neutrophil trapping has been shown in the renal glomeruli, as these vascular beds display increased adhesion factors and are more susceptible in ANCA-associated disease; this intravascular trapping may be due to ANCA induced decrease in neutrophil deformability (327,342). Injury is more prominent in the pulmonary than the glomerular microvasculature, potentially due to having a lower pressure system in the lung contributing to altering neutrophil mechanophenotype (344). Additionally, adhesion is independent of neutrophil trapping in

selectin-independent neutrophil sequestration (159,345). ICAM-1 and β2 integrins interactions promote neutrophil diapedesis (346), leading to increased microvascular permeability, enhanced by ROS production, and causes neutrophil induced EC damage.

1.6.1. Thrombosis in AAV

In AAV, fibrinolysis, whereby the protein fibrin involved in blood clotting is broken down, is delayed. Plasminogen, which binds to fibrin and tissue plasminogen activator (tPA) after fibrin clot formation, was identified as an autoantigen in PR3-ANCA (347). Antibodies purified from patients with PR3-ANCA inhibited decreased conversion of plasminogen to plasmin, an enzyme which degrades fibrin clots, and presence of this antibody correlated with predisposition to thrombotic events (347). Coagulation factors impaired by ANCA include prothrombin, and tissue factor-expressing microparticles released by activated neutrophils, in turn increased thrombogenicity (347,348). Clinical studies have also identified increased thrombosis risk in AAV (349). These changes in coagulation factors have been shown to be upregulated when neutrophils are primed by C5a, which also increases NET production, and therefore tissue factor expression (350,351).

One of the triggering factors of deep vein thrombosis (DVT) is the disturbance of blood flow. Platelet recruitment to the vessel wall is also required for DVT to occur and this is mediated through von Willebrand Factor (VWF) (352). VWF is a multimeric glycoprotein, which carries the coagulation co-factor, Factor VIII. Specifically, the VWF A1 domain interacts with platelets (353), promoting recruitment and adhesion to VWF, and thereafter thrombosis. Once blood is perfused over intact NETs, NET-bound VWF activates platelets, in addition to exposed histones inducing platelet aggregation, and clot formation then occurs (354). In *in vivo* flow-disturbance modelling, VWF-platelet interaction is proven pathogenic (352). Although *in*

vivo, fibrin generation and platelet accumulation diminished, in addition to decreased TF when neutrophil binding to the vessel wall is inhibited (352). *In vivo* modelling has proven neutrophil-endothelial interaction is crucial for platelet accumulation and adhesion thereby initiating thrombus formation at the site of vessel injury (125).

Individual NET components, such as histones or DNA, can interact with factors of the coagulation cascade, including NE inhibiting TF pathway inhibitor (TFPI), and histones promoting thrombin generation independent (355) and dependent (355) of platelet mechanisms. In AAV, NETs released expressed TF, therefore exposing other initiators of thromboinflammation to the vessel's surroundings (126). Yet, some studies have shown that human intact NETs do not cause as much damage as their individual components; *in vitro* human intact NETs did not directly initiate or amplify coagulation, potentially due to their large scaffolding and histone-histone/-DNA complex interactions (356).

Markers of NETs have been detected in plasma from patients with thrombotic disease such as DVT (357,358) and acute thrombotic microangiopathies (TMAs), a group of microvascular thrombotic diseases (359). Patients with TMAs also displayed decreased DNase-I in plasma, which is required for the degradation of NETs, and has also been found in patients with SLE (72). In mice with sepsis induced neutrophilia, when DNase-I, and DNAseI-like 3 were present in the circulation, NET degradation occurred (360). Once both DNAses were absent *in vivo*, NETs released within the vasculature formed clots and led to blood vessel occlusion during neutrophilia and septicaemia (360). *In vivo* it has been shown that DNase-I inhibits thrombus formation initially after injury, but this effect may be independent of NET formation (361). This effect was shown in a NETosis independent laser induced injury model in which DNase-I treatment, inhibited neutrophil accumulation, secretion of NE, and platelet thrombus

formation (361). In addition to DNAse-I reducing NET formation and DVT frequency, NETs have been identified in thrombi in pathological specimens from a mouse model of DVT. This study also identified a critical role for PAD-4 mediated histone modification in the same context (362).

The alternative complement pathway has been shown to be activated by NETs, in several studies, in turn resulting in neutrophil induced EC damage (291,318,363). Overall, these mechanisms may also contribute to increased thrombosis in AAV. In AAV, necrosis occurs in the vessel walls whereby plasma components leak into the perivasculature tissue, promoting the hypercoagulable state found in AAV as reviewed in Al-Hussain et. al & Brilland et. al (364,365). Endothelial damage can also occur from oxidative stress caused by neutrophils activated by ANCA (366), in addition to releasing prothrombotic factors facilitating thrombus formation.

1.6.2. Endothelial interactions

Some studies have shown that MPO and PR3, released from neutrophils, can bind to EC in the inflammatory environment (367). Circulating ANCA may be able to bind to these ANCA antigens on the endothelium with some studies suggesting this can lead to enhanced endothelial injury (170,368). There is speculation that atypical, non-MPO, non-PR3 ANCA are capable of binding to the endothelium. However, these antibodies are relatively rare and further research is necessary before this theory is confirmed. Neutrophils accumulate within the vessel wall through multiple mechanisms, and this ultimately leads to neutrophil cell death. It is possible that distinct biophysical properties of neutrophils in patients with aAAV, which may occur in response to direct ANCA stimulation, contributes to endothelial injury, due to increased neutrophil retention.

1.7. Complement in AAV

AAV is classically a pauci-immune necrotising vasculitis with few or no immune complex deposits of immunoglobulin or complement in the vessel walls. Despite this, complement is increasingly recognised to play a role in the pathogenesis of AAV (369). Mouse models of AAV have identified a role for the alternative pathway of complement activation, with C5 deficient and factor B deficient mice protected from disease whereas C4 knockout has no effect (294,370). Further evidence for alternate complement activation in MPO-ANCA AAV is the presence of complement at sites of tissue inflammation in AAV using tissue immunofluorescence (IF) and immunohistochemistry (IHC) staining (371). Plasma levels of complement activation proteins such as C3a, C5a, and C5b-9 have been identified to be elevated in patients with ANCA-associated GN (371). Complement pathway activation leads to the formation of the protein fragment C5a which is a powerful chemoattractant for inflammatory cells, including neutrophils. Neutrophils can also undergo priming by C5a. ANCA neutrophil stimulation then results in further complement activation via the alternative pathway, leading to amplification of the inflammatory loop in AAV (370). Activated neutrophils release complement activating factors, promoting C5a production, increasing neutrophil recruitment and activation at the site of tissue or vascular injury (291,370). Additionally, formation of the C5b-9 membrane attack complex injures endothelium leading to necrosis and activation of coagulation factors (372). Therefore, targeting complement in AAV as a therapeutic mechanism has been of interest. *In vivo* work utilising complement C5a receptor (C5aR) antagonist treatment in mice with a knock in of human C5a showed that inhibiting C5aR improved the autoimmune response and renal neutrophil activation in AAV (373). Now a current therapy, the C5aR antagonist, Avacopan, is not only the first new treatment for AAV in several years but is non-inferior to steroids (373).

1.8. B Cells in AAV

B cells clearly play an important role in the pathogenesis of AAV as they produce ANCA upon differentiation to plasma cells. In addition, B cell depletion therapy with rituximab is a highly effective treatment for both induction and remission maintenance (280). Antigen presentation to naïve T_H cells results in T_{H2} cell differentiation, promoting the immune system to specifically trigger antibody production. Proliferation of B cells is promoted by T_{H2} cells and B cell activating factor (BAFF), leading to plasma cell formation from activated B cells (374). Several studies have identified alterations in B cell subsets in AAV (375,376). An increased number of B-cells, including dysfunctional B-cells with increased expression of CD38 and decreased CD5 may be present. Increased B-cell activity and number of activated B cells have also been shown to correlate with disease activity (377). Some studies have shown decreased B_{reg} (CD5+, CD24+, CD38), which skew T cell differentiation towards T_{regs} and away from T_{H1} and T_{H17} in patients with AAV. There is evidence for return of B cells after RTX treatment correlating with relapse (378). However, the phenotype of B cells which return after RTX may be important, particularly autoreactive B cells that arise post RTX therapy (375). *In vitro* studies have shown B_{reg} cells influence T cell phenotype by limiting T_{H1} differentiation and decreasing cytokine production (379,380). *In vitro* neutrophils stimulated with ANCA make BAFF and APRIL, cytokines which mediate B-cell differentiation, maturation, and survival; therefore, B cell survival is promoted in AAV (381). In clinical studies, elevated BAFF and APRIL have also been identified in aAAV (382–385).

1.9. T Cells in AAV

Abnormal T cell activity is a main contributor to break of immune tolerance. In AAV, as is the case in many ARDs, autoreactive CD4+ T or T_H cells produce activation signals for B cells to produce autoantibodies. Circulating ANCA are predominantly IgG1 and IgG4 suggesting that T cells have played a role in class switching. Additionally, T cells can be identified in renal biopsy tissue at sites of glomerular and tubulointerstitial injury (386). Aberrant T cell function in patients with AAV includes persistent T cell activation (387), and T cells mediated cytokine release contributes to neutrophil activation.

Cytokines activate T_H cells promoting cell mediated immunity, in turn driving the differentiation process of T cells into T_{H1} cells. The immune response in ANCA-associated GN is skewed towards a T_{Ht} type immune response(388), whereas T_{reg} are decreased in active disease and, T_{H2}/T_{reg} subset expansion is seen in remission (389). A higher T_{reg} count may therefore lead to early remission (390,391). *In vivo* mouse models have shown depletion of T_H or CD8 T cells are effective treatments for MPO induced vasculitis, while adoptive, or passive transfer of T cells initiates more severe AAV disease as reviewed in Sochet et. al 2020 (392).

The IL-17 axis also plays a role in the development of AAV, T_{H17} differentiation through IL-17 is promoted by MPO-ANCA activated neutrophils, resulting in IL-17 production (393). Increased IL-17 levels have been identified in serum from patients with AAV (394). While T_{H17} cells may stimulate neutrophil bacteria responses, in AAV, uncontrolled activation of T_{H17} cells occurs. This leads to increased vessel and tissue damage, specifically renal inflammation, as T_{H17} cells are found in renal tissue (395,396). However, it remains incompletely understood what drives T_{H17} expansion in AAV.

1.10. Hypoxia

1.10.1. Hypoxia and oxygen tensions

Physiological oxygen tensions range from a pO_2 of 13 kPa in main arteries, 7 kPa in arterioles, 5 kPa in venous blood, and 1.3 kPa in bone marrow (397,398). Within individual organs normal oxygen tensions may be even lower, such as in the kidney, where the pO_2 ranges from 2-7 kPa in the renal cortex down to 0.5-3 kPa in the renal medulla (399,400). Hypoxia can be defined as the delivery of an inadequate supply of oxygen to a localised area in the body or systemically (hypoxaemia) (401). Inflamed tissues and blood vessels are characteristically hypoxic (402). Hypoxia may result from increased utilisation of oxygen by recruited inflammatory cells, impaired blood flow/sluggish microcirculation, compartmentalisation of infection, and thrombosis (403–406).

1.10.2. Hypoxia sensing

Cellular adaptation to oxygen levels is coordinated by transcription factors called hypoxia inducible factors (HIF). HIF is a complex consisting of transcription factor subunits, HIF1- or 2-α, and the constitutively expressed, HIF1-β. Substrates for factors inhibiting HIF (FIH-1) are HIF1-α subunits, which allow neutrophils to sense oxygen through formed oxygen sensors (407). Neutrophils are capable of sensing hypoxia through possession of HIF1-α, FIH-1, a hydroxylase oxygen-sensing pathway, and prolyl hydroxylases (PHDs), which *in vivo* are active biological oxygen sensors (408). Regulation of the expression pattern of different HIF α subunits having nonredundant function may additionally contribute to HIF1-α oxygen sensing in neutrophil activity (409). Hydroxylases such as FIH-1 and PHDs therefore regulate HIF1α function and stabilisation (410–414). Neutrophils have HIF1-α and HIF2-α subunits, both of which can bind HIFβ separately. Although, these subunits have different roles in hypoxia adaptation (415). In normoxia, HIF α is hydroxylated by FIH and PHDs. This prevents binding

of cofactors and directs HIF α for proteasomal degradation by von-Hippel-Lindau complex. In hypoxia, this hydroxylation does not occur (416–418). This results in HIF α accumulation, translocation to the nucleus, and dimerisation with HIF β occurs to control gene transcription (419–424). Therefore, in hypoxic conditions, PHD and FIH activity is inhibited, resulting in gene transcription of HIF targets (425).

Cellular and systemic responses that are mediated by the HIF pathway under hypoxia, include angiogenesis, differentiation, metabolism, and survival (426–430). In hypoxia, cell survival is promoted through HIF1 regulation of ATP production, a process naturally reliant on oxygen consumption (431,432). HIF allows for adaptation of metabolic energy production and usage due to limited oxygen availability in hypoxic environments (407). Hypoxia can promote excessive activation of the immune host defence, and consequentially, once a foreign body is present, this may lead to collateral tissue damage for the host (433).

1.10.3. Neutrophil function

Since neutrophils are progenitors of the bone marrow, they are exposed to a hypoxic environment from the point of development (434–436). While circulating neutrophils are exposed to a range of physiological oxygen tensions (5-13kpa), they have also adapted to survive, perform, and undergo their programmed mechanisms in situations of profound pathological hypoxia in an inflamed environment. Neutrophils have the capability of sensing and responding to changes in their surrounding oxygen tensions, which alters their survival rate, secretory capabilities, and programmed pathogen killing mechanisms. Under hypoxia, overactivation of the immune response occurs, leading to heightened neutrophil responses and programmed mechanisms, but not all processes have been shown to be HIF-dependent (437).

1.10.4. Cytokine release

Activated neutrophils secrete cytokines in response to decreased blood levels of oxygen (438,439). Hypoxia promotes pro-inflammatory cytokine production in macrophages and activation in tissue through HIF2-α regulation (440). Yet *in vitro* under hypoxia, neutrophils displayed varied surface expression and secretion levels of cytokine, dependent upon the measured cytokine of interest, including IL-8 (439). Enhanced secretion of pro-inflammatory agents through hypoxia altered cytokine release is linked with delayed neutrophil apoptosis (430,441). Increased IL-8 gene expression was shown in neutrophils following binding to hypoxic endothelium (442), and upregulation of IL-8RA expression has been identified in hypoxic conditions (443),(443), indicating hypoxia can regulate levels of inflammatory cytokine release and their partnering receptors.

1.10.5. Recruitment and adhesion

Hypoxia causes an increase in integrins, neutrophil-endothelial adhesion, and TEM (444–446). Once neutrophils arrive to the sites of inflamed vasculature, increased expression of adhesion molecules on EC are present under hypoxia, therefore facilitating neutrophil adhesion (447,448). Increased ICAM-1 expression by EC under hypoxia, is comparable to that seen in a systemic inflammatory response (449,450). In a murine model of fungal infection, neutrophils lacking HIF1-α showed impaired recruitment to inflamed areas (451). Additionally, an *in vivo* murine model of neutrophil motility under hypoxia has shown HIF2-α increases neutrophil migratory capabilities to areas of inflammation and tissue (452). Increased expression of β2 integrin and CD11b was shown in whole blood leucocytes under pathological hypoxia (453). Increase of β2 integrin expression on neutrophils allows for increased binding of neutrophils to cell adhesion molecules on the endothelium (449,454,455). Increased adherence of neutrophils to EC treated with hypoxic neutrophil SNs was shown *in*

vitro in COPD, demonstrating this effect of hypoxia regulated neutrophil adherence in a disease setting (456). PI3K is upregulated in hypoxia (457), which may therefore contribute to altering neutrophil programmed functions and responses. In response to stimulus by fMLP in normoxia, PI3K influences neutrophil migration by determining which neutrophils partake in chemokinesis (458) and affects migratory accuracy, shown in neutrophils from healthy older adults and from patients with COPD (38,40). Yet, PI3K activity modulates chemokinesis dependent upon the neutrophil priming agent, and the surface neutrophils are undergoing migration through (458). Whether PI3K signalling involvement alters neutrophil chemotaxis either in a HIF-dependent or HIF-independent fashion under hypoxia is not confirmed.

1.10.6. Pathogen killing mechanisms

Hypoxia promotes neutrophil extracellular secretion of multiple histotoxic granule proteins, including NE and MPO (459). This hyperactivated state of increased neutrophil degranulation is dependent upon PI3K but does not appear to be HIF-dependent (437). Due to the lack of oxygen and promotion of autophagy under hypoxia, ROS production decreases (459), which in turn may enhance degranulation (430). While neutrophil phagocytosis is not disrupted under hypoxia, impairment of ROS production reduces neutrophil bactericidal capacity for certain pathogens, e.g. *Staphylococcus aureus* (*S. aureus*) (439). This provides a potential link between hypoxic tissue micro-environments and AAV as persistence of AAV in PR3 positive patients with ENT disease is linked with *S. aureus* nasal carriage and patients with AAV can also display decreased immune responses to *S. aureus* (460). NETosis has been shown in many studies to be a ROS-dependent mechanism, and therefore would be expected to be reduced under hypoxia, however, increased granule secretion (437,459) may counter this by promoting NET formation. Within this dichotomy, there are conflicting studies investigating the impact of hypoxia on NETosis and the effect seems to depend on whether true hypoxia or HIF

manipulation is utilised (459,461). Overall, HIF1-alpha signalling appears to increase NET production, but NETosis in true hypoxia is more variable, and may depend on the agonist. Coupled with NET formation, hypoxia also promotes vascular leakage, which could therefore drive a pathogenic and thrombotic effect (462), as found in patients with AAV.

1.10.7. Hypoxia and the cytoskeleton

The effect of hypoxia on the neutrophil cytoskeleton has been relatively unstudied. Hypoxia has been shown to alter the neutrophil actin cytoskeleton in a single study *in vitro*: neutrophils exposed to hypoxia displayed increased focal actin polymerisation, termed "actin caps". Although both jaksplakinolide and cytochalasin B affect actin polymerisation (induction and inhibition, respectively) neither agent affected hypoxic neutrophil NE release, suggesting that actin dynamics are distinct from hypoxic upregulation of neutrophil degranulation (459). Neutrophil agonists, including fMLP, also induce actin polymerisation but the functional consequences of this on programmed mechanisms in hypoxia need further investigation (459). Examining other cell types, fibroblasts displayed increased F-actin protrusions under hypoxia, while in macrophages, secretory vesicle retention occurred through actin cytoskeleton inhibition (463). HIF1-α expression has been shown to alter cytoskeletal functional changes in macrophages (464), stem cells (465), and keratinocytes (466).

1.10.8. Prolonged survival

HIF1-α dependent NF-κB activity prolongs neutrophil survival, and this pathway is mediated by cytokine release through stimulated neutrophil secretion of macrophage inflammatory protein-1β (407). Hypoxia has shown to delay constitutive neutrophil apoptosis in a HIF1 dependent manner, thus perpetuating inflammation (407,431). Hypoxic delay of neutrophil apoptosis also delays resolution of inflammation due to increased neutrophil accumulation at

sites of inflammation, and ongoing neutrophil activation (441,467). The ability of hypoxia to regulate apoptotic thresholds is mediated through NF-κB activity dependent upon HIF1-α, independent of PI3K, and sustained hypoxia exposure thereby drives neutrophil autophagy (430,468). Glucocorticoids, a therapy prescribed to patients with AAV for induction and maintenance treatment of disease, also increase NF-κB expression and have been shown in some studies to also delay neutrophil apoptosis (469). Yet, in hypoxic environments, a steroid induced decrease in apoptosis was not seen in profound hypoxia, and glucocorticoid treatment also attenuated GM-CSF-mediated neutrophil survival under hypoxia. This suggests a complex interplay of degree of hypoxia, inflammation, and therapeutic agents in regulating neutrophil apoptosis (470).

1.10.9. Hypoxia in disease pathogenesis

In health, the lung and the kidney are physiologically normoxic, while in disease states, such as aAAV, inflamed vasculature and tissue becomes increasingly more hypoxic (471). Importantly, in vivo physiological oxygen tensions are often substantially lower than atmospheric oxygen. In situations of infection and inflammation, oxygen tensions can be profoundly low, and this is deemed pathological hypoxia (472). Immune cell dysfunction in pathological hypoxia can result in detrimental effects such as inflammation, decreased blood flow and tissue ischaemia, increased oxygen consumption and poor resolution of infection. Tissue hypoxia is described at sites of vascular damage (468), such as in AAV.

Much of the work measuring evidence of hypoxia in the lung and kidney has been performed in vivo in rat and mouse models (407,473), whilst porcine in vivo modelling has been used for arterial measurements of hypoxia (474–476). However, there are increasing reports of hypoxia detected in clinical studies. Histological studies performed using pimonidazole hydrochloride

(staining tissue <1.3kPa) can measure tissue hypoxia (434), and this method has been used in irradiated human tissue (477). Hypoxia has been shown to be present in areas of atherosclerotic plaques; using vascular imaging with ^{18}F-fluoromisonidazole (FMISO). FMISO is, a nitroimidazole which in normoxia is oxidised and diffuses freely from cells; in hypoxia, reduced FMISO accumulates and can be detected using PET imaging (478). Hypoxia has shown to engender a hyper-secretory neutrophil phenotype with increased capacity for tissue damage in a pathogenic setting, such as in chronic obstructive pulmonary disease (COPD), a disease of chronic neutrophilic inflammation (456)(459). Here, supernatants from hypoxic neutrophils applied to epithelial or endothelial monolayers caused significant cell detachment and death. Additionally, hypoxia promotes fibroblast migration, dependent upon matrix metallopeptidase (MMP), in rheumatoid arthritis (RA) (479). Furthermore, patients with chronic inflammatory diseases have increased cardiovascular comorbidities even after correcting for established risk factors as reviewed in Sorriento et. al (480). Despite the capacity of hypoxia to promote neutrophil-mediated endothelial damage, no studies have been carried out investigating the effect of hypoxia on ANCA mediated neutrophil responses.

1.11. Biomechanics

1.11.1. Previous techniques for biomechanics

Dating back to the 1970s, micropipette aspiration using suction has been used to measure cellular deformation. Since then, technologies used for quantitative measurement of cellular mechanical properties have significantly advanced over time (185,481,482). The development of atomic force microscopy (AFM) allowed for measurement of elasticity of cells in suspension for the first time (483,484). In AFM, a probe applies additional forces upon individual cells and the cells' kinetic processes are recorded through generation of a detailed topographic map (485–488). Since then, further novel techniques including optical tweezers (489) and the optical stretcher (490,491) have increased our ability to measure cellular mechanical properties. Optical tweezers are a contact-free technique whereby force is applied upon a cell from momentum generated from a single beam of light, also known as a laser trap (492). The optical stretcher is a double laser beam trap, also transferring force to cells to induce contact-free deformation (493). The optical stretcher is capable of measuring cells at a rate of 1 cell per second (490,494). Although optical stretching is a non-contact study technique, it can result in neutrophil depolarisation due to continued oscillatory mechanical deformation (46). A further limitation in some of these techniques is due to immobilisation, as the cells can then become activated (46). To accurately measure neutrophil deformability, a technique is required whereby cells can be deformed in suspension, under physiological conditions. Microfluidics-based deformability cytometry introduces a high throughput method of mechanically analysing cells (495) and was advanced by Otto et al. through the introduction of real-time deformability cytometry (RT-DC) (496).

1.11.2. Development of RT-DC

RT-DC is a novel technique whereby cells in suspension (whole blood, or purified cells in buffer) flow through a microfluidic narrowed channel at a set rate while hydrodynamic force is applied, leading to reversible deformation of individual cells from shear stress and pressure gradients (**Fig 3**) (496,497). A cell tracing algorithm is applied to individual cells allowing biomechanical readout profiles to be generated from images captured. Individual cell populations are identified based on variables including cell granularity, obtained from brightness, and cross-sectional area, obtained from cell size. Morphorheological parameters (498) can be recorded using a small volume of whole blood and neutrophils can easily be differentiated from other cell types due to their unique distribution of granules and multi-lobed nuclei. RT-DC allows analysis of heterogenous populations (e.g. whole blood) and cell populations can be identified by their distinct area and brightness, while biomechanical characteristics such as size, deformability, and elasticity of individual cells can be measured (499). Using the individual cells' measured area and deformation based on channel size, flow rate, temperature, and viscosity of the sheath fluid, this technique has the capability of computing the Young's modulus, or Elastic modulus, by decoupling the other parameters of the cell such as size (500). Availability of such parameters in real-time is a prerequisite for sorting of morphorheologically distinct subpopulations, which then provides a novel opportunity for further biological analysis (499).

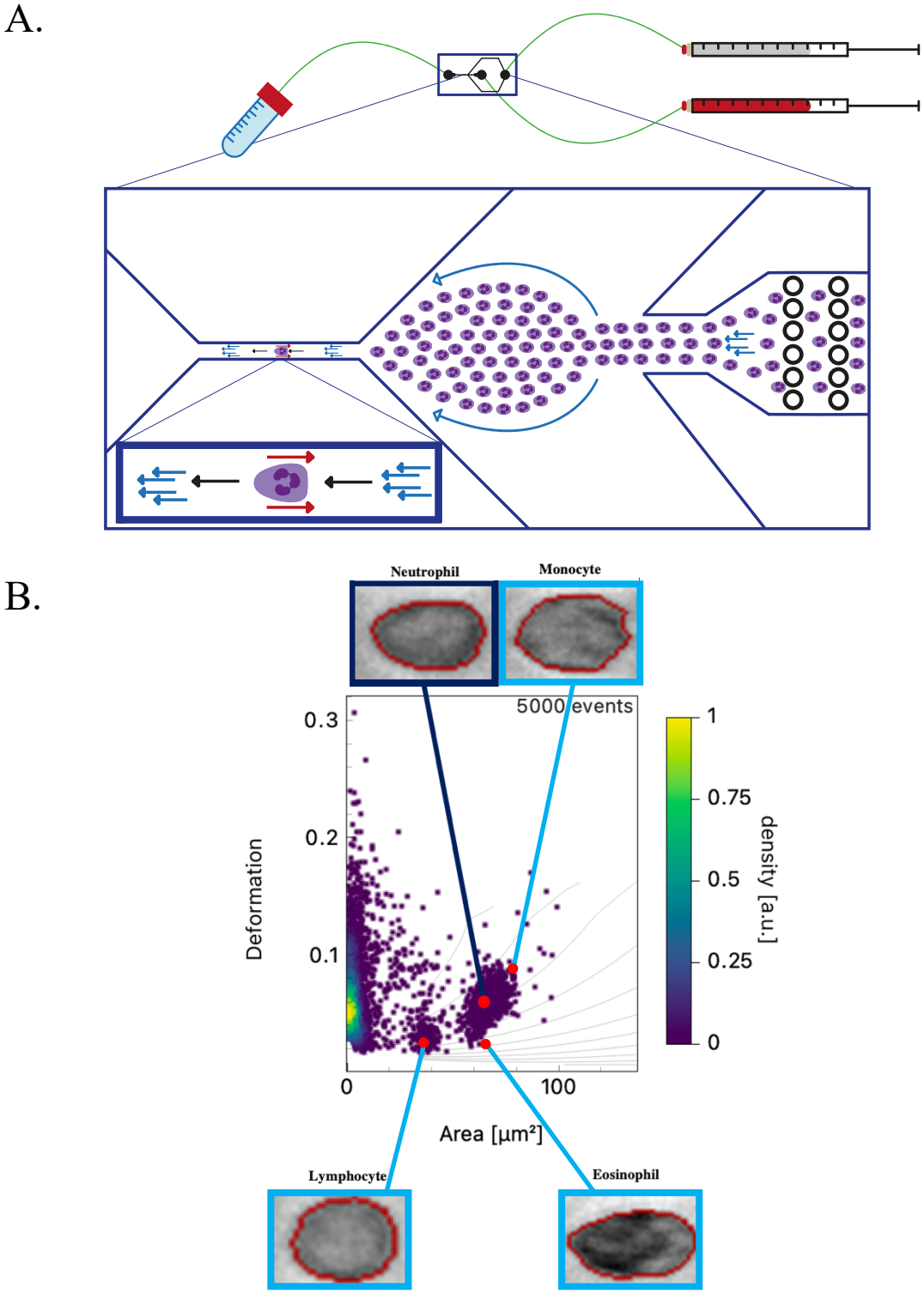


Figure 3. Real-time deformability cytometry
(A) Illustration of RT-DC setup. Sample (red) and buffer (grey) flow from syringes loaded in centre, and righthand ports of the chip. Cells undergo deformation in the narrow most part of the channel. Hydrodynamic forces applied upon each individual cell results in the cell converging, returning to its initial shape once passed through the channel, flowing into the waste channel. Individual cell still images are captured for usage towards calculated multivariate analysis of each run. Method is further detailed in section 2.2.8. (B) Plot generated in ShapeOut analysis software of a whole blood sample and images of individual cells captured within this population. Images present the difference in image recorded of each cell type.

1.11.3. RT-DC in cell type/disease

Thus far, RT-DC has displayed the capability of phenotyping neutrophils and other cells in different disease states (501). LDGs isolated from patients with SLE exhibited a phenotype of decreased deformability, and delayed transit time through a microfluidic mimetic chip, a 3-dimensional (3D) model of the pulmonary microvasculature to measure cell trafficking (218). RT-DC measurement displayed PAF, GM-CSF, or LPS primed neutrophils underwent sequential contraction and expansion, displaying priming agents stiffen neutrophils (41). Increased size and deformability were shown in neutrophils from patients with COVID-19 suggesting neutrophils were potentially activated (502). Additionally, in myelodysplastic syndrome (MDS), dysregulation of bone marrow cell morphology occurs through alterations in the actin cytoskeleton and correlates with the number of genetic mutations found in the individual MDS patients (503). RT-DC measurement identified patients with more genetic mutations with MDS correlated with a significant decrease in deformability in haemopoietic stem cells (503). Increased deformability in classical and intermediate monocytes was identified in patients with Systemic Sclerosis (SSc) and rAAV. As suggested by the authors, this reflects a monocyte specific activation phenotype in SSc as no changes in neutrophil deformability were seen (504). While deformability is the main variable of interest using RT-DC, changes of deformability may not be detected as shown in eosinophils from atopic and non-atopic donors (42). RT-DC mechanophenotyping may therefore have the capability to identify individual cellular phenotypes for diagnostic purposes in disease.

1.12. Hypothesis and Aims

1.12.1. Hypothesis

Neutrophils from patients with active AAV have a distinct morpho-rheological phenotype, which is exacerbated by hypoxia and contributes to endothelial cell injury.

1.12.2. Aims of the study

i. Characterise the morpho-rheological phenotype of ANCA-stimulated leukocytes and compare this with leukocytes from patients with AAV

ii. Investigate the effect of hypoxia on the morpho-rheological properties of ANCA-stimulated neutrophils and the impact on neutrophil-endothelial interaction

iii. Investigate the mechanism(s) by which ANCA/hypoxia influence neutrophil phenotype

2. Chapter 2 – Materials and Methods

2.1. Materials

Experimental buffers

PBS – NaCl 137 mM, KCl 2.7 mM, NA_2HPO_4 8.1 mM, KH_2PO_4 1.47 mM, pH 7.2-7.4

IgG purification

Binding buffer – 20 mM sodium phosphate, pH 7.0

Neutralising buffer – 1M Tris-HCl, pH 8.0

Elution buffer – 0.1 M glycine-HCl, pH 2.7

Neutrophil isolation

Percoll –1:10 10x PBS in Percoll

ELISA

Wash buffer – 0.05% Tween in PBS

Block buffer – 1.0% BSA in PBS

Reagent diluent – 1.0% BSA in PBS or 0.1% BSA, 0.05% Tween-20 in TBS

Staining

Permeabilisation buffer – Triton x100 0.04% (Neutrophils) or Triton x100 0.05% (gEC)

Block buffer – 1.0% BSA in PBS (Neutrophils) or 3.0% BSA in PBS (gEC)

Antibodies for IF

Immunogen	Source	Host	Concentration	Catalogue No.
Citrullinated histone H3	abcam	Rabbit	1:250	ab5103
Phalloidin	ThermoFisher	N/A	1:200	A12379
MPO	Dako	Mouse	1:100	R7209
CD15	Dako	Mouse	1:100	M3631
VE-Cadherin	Bio-techne	Goat	1:100	AF938

Secondary antibodies

Immunogen	Source	Host	Concentration	Catalogue No.
AF 555 anti-Goat IgG	Invitrogen	Donkey	1:250	A-21432
AF 568 anti-Rabbit IgG	Invitrogen	Goat	1:100	A-11011
AF 647 anti-Mouse IgG	Invitrogen	Donkey	1:250	A-31571
Anti-human IgG FITC	Sigma	Goat	1:1000	F9512-1ML

Table 3. Designed primers– Synthesis scale at 25 nmol

Primer		Oligonucleotide sequence 5' to 3'	Tm (°C)
CCL20	F	GGCGAATCAGAAGCAAGCAA	76
	R	GGATTTGCGCACACAGACAA	
CCL3	F	GCTCTCTGCAACCAGTTCTCT	72
	R	TCGCTTGGTTAGGAAGATGACA	
CCL3L1	F	AAGCCCAGTGTCATCTTCCTAA	84
	R	GGTCACACGCATGTTCCCAA	
CCL4	F	CTCCCAGCCAGCTGTGGTATTC	77
	R	CCAGGATTCACTGGGATCAGC	
CCRL2	F	CAACAGTGGTTTCTCGTGCC	74
	R	CATCTTCAGACTGCCCACTG	
CD83	F	TTGAGAGTGACAGGATGCCC	72
	R	TGTAGCCGTGCAAACTTACAA	
CXCL2	F	GAAAGCTTGTCTCAACCCCG	75
	R	TGGTCAGTTGGATTTGCCATTTT	
CXCL8	F	AGTTTTTGAAGAGGGCTGAGA	73
	R	TGCTTGAAGTTTCACTGGCATC	
CXCR2	F	GGTCAGAAGTTTCATCGTCAAGG	72
	R	TTAAATCCTGACTGGGTCGC	
F11R	F	CGAGCGGAAACTGTTGTGCC	78
	R	GCACAGGACAACTTCACAGGATTAT	
GADD45B	F	GCCCTGCAAATCCACTTCAC	74
	R	GTGTGAGGGTTCGTGACCA	
GCH1	F	GCAGCGAGGAGGATAACGAG	72
	R	TATAGCATCGTTTAGGACATCTGAG	
ID2	F	ATCCTGTCCTTGCAGGCTTC	76
	R	ACCGCTTATTCAGCCACACA	
ILA1	F	GCGTTTGAGTCAGCAAAGAAGT	76
	R	CATGGAGTGGGCCATAGCTT	
IL1B	F	TGAGCTCGCCAGTGAAATGA	78
	R	TGGAGAACACCACTTGTTGC	
ITGB2	F	CAGGGCAGACTGGTAGCAAA	80
	R	CACTCCTGAGAGAGGACGCA	

NFIL3	F	GCTCAGTCGGCAACAGGTAG	76
	R	GGGCCTCCTTCGTTATTTGC	
NF-κβ1	F	GCTTAGGAGGGAGAGCCCAC	74
	R	AGGTATGGGCCATCTGCTGT	
NLRP3	F	TGAGGCTGGCATCTGGATGAG	74
	R	TACGGGGCTATGACATTGGAC	
NR4A2	F	GTCCCTTTTGCCTGTCCAGC	74
	R	CAGCCTGTCCAATCTCCTCCTTAG	
OLR1	F	TCTTTGGATGCCAAGTTGCTG	72
	R	CCTCGGACTCTAAATAAGTGGGG	
PLAU	F	GAGCGACTCCAAACGAACTGT	75
	R	CCCTCCGAATTTTCTTTGGGC	
STAT5A	F	CTGGACTTTTCTGAAGGGGCT	78
	R	AGAATAGCCGGGGGAATGTG	
TLR1	F	GTTTTTGTGGCCAGGGTCTTC	77
	R	TAGGGGTGCCCAATATGCCT	
TNF	F	CTGCACTTTGGAGTGATCGG	79
	R	CTCAGCTTGAGGGTTTGCTACA	
TNFRSF1A	F	CTGCTGCCACTGGAACCTAC	75
	R	CACTCCCTGCAGTCCGTATC	
TRAF1	F	GGCCACCTGTTGCAACTTCTT	74
	R	TGGTGACTGAAGGCTTCCTGG	
VEGFA	F	ACAACAAATGTGAATGCAGACCA	75
	R	GAGGCTCCAGGGCATTAGAC	
WAS	F	TCAGTGAACAAGACCCCTGG	74
	R	CAGCCACTCAGTCATCCCATT	

Commercial primers – Qiagen

Primer	GeneGlobe ID
18S	QT00199367
B2M	QT00088935

2.1.1. Tissue culture

Table 4. Cells and media

Name	Source	Catalogue No.
gEC (Pooled donors)	Celprogen	36066-05
Human Glomerular Endothelial Primary Cell Culture Complete Media with Serum	Celprogen	M36066-05S
Human Glomerular Endothelial Primary Cell Culture Complete Media without Serum	Celprogen	M36066-05A
Human Glomerular Endothelial Primary Cell Culture Freezing Media	Celprogen	M36066-05FM
Human Glomerular Endothelial Primary Cell Culture Extra-cellular Expansion Matrix T25 Flasks	Celprogen	E36066-05-T25
Human Glomerular Endothelial Primary Cell Culture Extra-cellular Expansion Matrix T75 Flasks	Celprogen	E36066-05-T75
Human Glomerular Endothelial Primary Cell Culture Extra-cellular Expansion Matrix 12 Well Plates	Celprogen	E36066-05-12W
Cryovials	Starlab	E3090-6212

Table 5. Other tissue culture reagents

Name	Source	Catalogue No.
RPMI-1640 Medium	Sigma	R8758
Iscove's Modified Dulbecco's Medium	Gibco	11504556
Trypsin-EDTA solution	Sigma-Aldrich	T3924
TrypLE	Gibco	12604013
Endotoxin-free HBSS (1x)	HyClone	SH30588.01
Endotoxin-free H_2O	HyClone	SH30538.FS
Trypan Blue solution	Sigma	15250061
FCS-25	PromoCell	C-37310
MilliQ	HyClone	CDUFBI0A1
Improved Neubauer	Hawksley	AAC1000

2.1.2. Neutrophil Isolation

Table 6. Reagents for Percoll Density Gradient

Name	Source	Catalogue No.
Safety blood collection set, 21G x 19cm	Greiner	450085
Vacuette Tube 9 mL Coagulation Sodium Citrate 3.8%	Greiner bio-one	455382
Vacuette Tube 9 mL Coagulation Heparin	Greiner bio-one	455084
Vacuette Tube 9 mL K2E Coagulation K2EDTA	Greiner bio-one	455045
Dextran from Leuconostoc spp.	Merck	09184-50G-F
0.9% Sodium Chloride for Irrigation	Baxter	UKF7124
Percoll	Cytiva	17-0891-01
PBS (10X), pH 7.4 Life	Greiner bio-one	455045
Dulbecco's Phosphate Buffered Saline (-/-)	Sigma	D8537
Dulbecco's Phosphate Buffered Saline (+/+)	Sigma	D8662
Human AB serum	Sigma	H3667-20ML

Table 7. Reagents for Immunomagnetic negative selection

Name	Source	Catalogue No.
EasySep Direct Human Neutrophil Isolation Kit	StemCell	19666
EasySep Direct Isolation Cocktail	StemCell	19666C
EasySep Direct RapidSpheres	StemCell	50300
EasySep Magnet	StemCell	18000
Ethylene diaminetetraacetic acid disodium salt Dihydrate (EDTA)	Sigma	E6635-100G

2.1.3. Cytospin

Table 8. Reagents for cytospins

Name	Source	Catalogue No.
Shandon Cytoclip	ThermoScientific	59910052
Sample Chamber	ThermoScientific	A78710018
Shandon Filter Cards	ThermoScientific	5991022
Surgipath X-tra Adhesive Precleaned Micro Slides	Leica Biosystems	75809-488
Epredia Shandon Kwif-Diff Stains	ThermoScientific	10643649

2.1.4. ANCA protein purification

Table 9. Reagents for protein purification

Name	Source	Catalogue No.
HiTrap Protein G HP	Cytiva	17040501
Sodium phosphate dibasic dyhydrate	Honeywell	04272
Sodium phosphate monobasic anhydrous	Sigma-Aldrich	S-3139
Plastipak 20 mL syringe	BD	301189
Sartorius Minisart NML Syringe Filter	Fisher Scientific	11786953
Slide-A-Lyzer 10K Dialysis Cassette G2	ThermoFisher	10717975
Plastipak 1 mL glass syringe	BD	309628
Blunt Fill Needle with filter 23G x 1 ¼	BD	300700

2.1.5. Recombinant proteins & inhibitors

Table 10. Reagents for assays

Name	Source	Catalogue No.
Recombinant Human TNF-alpha	R&D	210-TA
Human IL-8	Peprotech	200-08
Cytochalasin B	Sigma	C6762-1MG
Cytochalasin D	abcam	ab143484
(-)-Blebbistatin	Bio-Techne Ltd	1760
para-amino-blebbistatin	Bio-Techne Ltd	22699
Phorbol 12-myristate 13-acetate	Bio-Techne Ltd	1201s

2.1.6. ELISA

Table 11. Reagents for MPO ELISA

Name	Source	Catalogue No.
Human Myeloperoxidase (MPO) AssayMax ELISA Kit	AssayPro	EM6501-1
Human Myeloperoxidase Microplate	AssayPro	EM6501-1
Human Myeloperoxidase Standard	AssayPro	EM6501-1
Wash Buffer Concentrate	AssayPro	WASH
MIX Diluent Concentrate	AssayPro	MIX
Chromogen Substrate	AssayPro	TMB15
Stop Solution (0.5 N HCl)	AssayPro	STOP

Biotinylated Human Myeloperoxidase Antibody SP Conjugate	AssayPro	31231-05021

Table 12. Reagents for IL-8

Name	Source	Catalogue No.
Human IL-8/CXCL8 DuoSet ELISA	R&D	DY208
Human IL-8 Capture Antibody	R&D	890804
Human IL-8 Detection Antibody	R&D	890805
Human IL-8 Standard	R&D	890806
Streptavidin-HRP	R&D	893975
Tween 20	Sigma	P1397
Assay Diluent – 0.1% BSA, 0.05% Tween-20 in TBS		
TMB Liquid Substrate System	Sigma	T0440
96 well half area microplate, flat bottomed, high binding	Greiner	6750

Table 13. Reagents for ICAM-1

Name	Source	Catalogue No.
Human ICAM-1 DuoSet ELISA	R&D	DY720
Human ICAM-1 Capture Antibody	R&D	840432
Human ICAM-1 Detection Antibody	R&D	840433
Human ICAM-1 Standard	R&D	840434
Streptavidin-HRP	R&D	893975
Assay Diluent – 1.0% BSA in PBS		

Table 14. Reagents for VCAM-1

Name	Source	Catalogue No.
Human VCAM-1/CD-106 DuoSet	R&D	DY809
Human VCAM-1 Capture Antibody	R&D	844908
Human VCAM-1 Detection Antibody	R&D	844909
Human VCAM-1 Standard	R&D	841129
Streptavidin-HRP	R&D	893411
Assay Diluent – 1.0% BSA in PBS		

2.1.7. RT-DC

Table 15. Reagents for RT-DC

Name	Source	Catalogue No.
Tubing FEP Nat 1.16 x 0.30	Cole-Parmer	1935247
P-200 Flangless Ferrule, blue EFTE, 1/16'' OD Tubing, ¼-28 Flat-Bottom	Cole-Parmer	WZ-02019-33
Flngls Sys Short 1/16 PEEK	Cole-Parmer	2047610
Adapter Female luer to ¼-28	Cole-Parmer	02014-14
Plastipak 1 mL glass syringe	BD	309628
Blunt Fill Needle with filter 18G x 1 ½ 5mM	BD	303129
CellCarrier	Zellmechanik Dresden	
CellCarrierB	Zellmechanik Dresden	
Flic20-PDMS Chip	Zellmechanik Dresden	
Plastipak 10 mL syringe	BD	305959

2.1.8. Immunofluorescence

Table 16. Reagents for Immunofluorescence

Name	Source	Catalogue No.
Normal goat serum	Abcam	ab7481
Normal horse serum blocking solution	Vector labs	S-2012-50
VectaFluor Horse Anti-Rabbit IgG	Vector labs	DI-1794-15
DyLight[R] 594 Antibody Kit, R.T.U. Mounting Medium with DAPI- Aqueous, Fluoroshield	Abcam	ab104139
Image-iT Fixative Solution	Invitrogen	FB002
Triton X100	Sigma	X100
Ibidi u-slide 8 Well High ibitreat, sterile	Ibidi	80826
96 well tissue culture treated microplate, black, microClear, with lid, sterile	Greiner	650209
Dako pen	Dako	S2002

2.1.9. mRNA quantification

Table 17. Reagents for RNA isolation

Name	Source	Catalogue No.

2-mercaptoethanol	Sigma-Aldrich	63689
RLT Lysis buffer	Qiagen	79216
RNeasy mini kit	Qiagen	74106
Nuclease-Free Water	Qiagen	129114
RNase-Free DNase Set	Qiagen	79254
Molecular Grade EtOH	Honeywell	E7023
TRIzol	Invitrogen	15596026
TE buffer	Invitrogen	12090015
Protector RNAse inhibitor 20000 U	Roche	3335399001

Table 18. Reagents for cDNA synthesis and RT-qPCR

Name	Source	Catalogue No.
10X RT buffer	ThermoFisher	4368814
25X dNTP Mix (100 mM)	ThermoFisher	4368814
10X RT Random Primers	ThermoFisher	4368814
MultiScribe Reverse Transcriptase	ThermoFisher	4368814
MicroAmp Fast Reaction Tubes (8 Tubes/Strip)	Applied Biosystems	4358293
RNA ScreenTape	Agilent Technologies	5067-5576
RNA ScreenTape Sample Buffer	Agilent Technologies	5067-5577
RNA Screen Tape Ladder	Agilent Technologies	5067-5578
QuantiTect Primer Assay	Qiagen	249900
MicroAmp Optical 384-Well Reaction Plate with Barcode	Applied Biosystems	4309849
Fast SYBR Master Mix	Applied Biosystems	4385612

2.1.10. Protein analysis

Table 19. Reagents for protein quantification

Name	Source	Catalogue No.
BCA Protein Assay Kit	Pierce/Thermo	23227
RIPA Buffer	ThermoScientific	89901
cOmplete Tablets-mini EDTA-free	Roche	04693159001
PhosSTOP Tablets	Roche	04906837001
RIPA Lysis and Extraction Buffer	ThermoScientific	89900

2.2. Methods

2.2.1. Patients and Controls

2.2.1.1. Study approvals

Blood samples and plasma exchange fluid were obtained from AAV patients and healthy volunteers under local ethics committee approval (20/WS/0181) Wales Research Ethics Service. Human renal tissue samples were obtained from patients using the Imperial College Healthcare NHS Trust Tissue Bank (Application R10015).

2.2.1.2. Inclusion criteria

The diagnosis of AAV was based upon either (i) the presence of circulating ANCA detected by indirect immunofluorescence (IIF) or antigen-specific assay, (ii) biopsy-proven pauci-immune glomerulonephritis (GN), (iii) typical clinical features of extra-renal AAV. Patients with active disease who had received steroids (oral or intravenous) prior to blood sampling were included but those who received other immunosuppression or cytotoxics were excluded. Remission was defined as a BVAS of 0 with prednisolone dose ≤7.5mg/day.

2.2.2. Tissue culture

2.2.2.1. Neutrophil and PBMC isolation

Up to 40 mLs of blood was collected by venepuncture in citrate or EDTA vacutainers from patients with AAV and healthy donors. Blood was processed promptly after venesection up to 1 hour to isolate neutrophils and peripheral blood mononuclear cells (PBMCs).

2.2.2.2. Isolation of human neutrophils – Percoll density gradient

Peripheral venous blood was collected using a 20-gauge butterfly needle into a 9 mL 3.8% sodium citrate or EDTA Vacuette (Greiner Bio-one, Stonehouse UK). Neutrophils were

isolated using dextran sedimentation and Percoll discontinuous gradient. Whole blood was diluted 2:1 with 6% Dextran (Merck, Gillingham, UK) in 0.9% NaCl (Baxter, Newbury, UK) and allowed to sediment for 30 minutes. Leucocyte enriched SN was collected and centrifuged in a 50 mL tube at 350g for 6 minutes, at 22°C with the brake and acceleration set to 9. Percoll (GE Healthcare, Buckinghamshire, UK) was made isotonic by adding 1 mL of 10xPBS (ThermoFisher, London, UK) to 9 mL Percoll and 3 layers prepared by further dilutions in 1xPBS-/- 'bottom' 81% layer, 'middle' 68% layer, and 'top' 55% layer. The cell pellet was resuspended in 55% Percoll placed in a 15 mL tube and gently underlaid with the middle and bottom layers. Gradients were centrifuged at 700g for 20 minutes, at 22°C with the brake and acceleration set to 0. The 55/68 interface contains PBMCs and 68/81 interface contains neutrophils and eosinophils, with RBCs separated, and sedimented at the bottom of the tube. Cell layers were carefully aspirated and resuspended in separate centrifuge tubes with PBS-/-. Cells were pelleted by centrifugation at 250g for 6 minutes at 22°C with the acceleration set to 5 and brake set to 9. Cells were resuspended in PBS +/+ (with Ca^{2+} and Mg^{2+}; Sigma, Poole, UK) and centrifuged again. SN was discarded and cells resuspended in 1 mL of neutrophil culture media and counted on the haemocytometer (Hawksley, Sussex, UK) with 1:1 dilution in Trypan blue (Sigma). Neutrophils were adjusted to the desired cell concentration by further dilution in neutrophil culture media.

2.2.2.3. Assessing neutrophil purity – Kwikdiff staining

Cells were re-suspended in neutrophil culture media at a concentration of $5x10^4$ cells/mL and 100 µL of cells applied to poly-L-Lysine coated slides using a cytospin centrifuge (Cytospin 2, Shandon, ThermoFisher) at 450g for 3 minutes. Slides were dried at RT for 1 hour then stained with KwikDiffTM (ThermoFisher) by immersing slides in solution 1 (methanol-fixative) for 30 seconds, solution 2 (Eosin) for 1 minute and solution 3 (Methylene blue) for 2

minutes. Slides were allowed to air dry before imaging using light microscopy to assess cytoplasmic and nuclear morphology. Neutrophils prepared in this manner were >99% neutrophils, with the major contaminating cells being eosinophils.

2.2.2.4. Isolation of human neutrophils – Negative immunomagnetic selection

This isolation method was used for RNA-Sequencing sample preparation to ensure purity of neutrophil isolation and elimination of all other cell types including eosinophils. Peripheral venous blood was collected into EDTA a 9 mL EDTA Vacuette (Greiner Bio-one) and used to isolate neutrophils using negative immunomagnetic selection (Direct neutrophil isolation kit; Stemcell, Cambridge UK) according to the manufacturer's instructions. Blood was decanted into a 50 mL tube. 100 µL 0.1M EDTA in PBS -/- was added per 10 mL blood followed by 50 µL of the isolation cocktail per mL blood. Magnetic beads were vortexed for 30 seconds and added at 50 µL/mL of blood. 50 mL tube was gently mixed by inversion and incubated at RT for 5 minutes. Cell suspension was topped up to 50 mL with 1mM EDTA in PBS -/-, again gently mixed by inversion, and placed in the magnet for 10 minutes at RT. Cell suspension was aspirated into a new 50 mL tube. Magnetic beads were vortexed, the same volume was added, tube was inverted, and left to incubate for 5 minutes at RT. Tube was placed into the magnet for 5 minutes at RT. Cell suspension was aspirated into a new 50 mL tube and placed into the magnet for 10 minutes at RT. Cell suspension was aspirated into a new 50 mL tube and topped up to 50 mL with PBS -/-. Cells were centrifuged at 335g for 5 minutes with the acceleration and brake set to 5. SN was discarded, and purified neutrophils were resuspended in neutrophil culture media for experimental usage or loaded back onto the Percoll density gradient to collect LDGs from patients with aAAV.

2.2.2.5. Isolation of LDGs from patients with aAAV

Total neutrophils were isolated using negative immunomagnetic negative selection as described in 2.2.3.4. Cells were used for Percoll discontinuous density gradient as described in 2.2.3.3. LDGs were isolated from the 55/68 top Percoll layer, while NDGs were separated into the 68/81 neutrophil layer. Cells were pelleted by centrifugation at 250g for 6 minutes at 20°C with the acceleration set to 5 and brake set to 9. Cells were resuspended in PBS +/+ and centrifuged again. SN was discarded and cells resuspended in 1 mL of Neutrophil culture media and counted on the haemocytometer with 1:1 dilution in Trypan blue (Sigma). LDGs were resuspended to $10x10^6$/mL by further dilution in neutrophil culture media.

2.2.2.6. gEC

Cryopreserved gEC from pooled donors were purchased from Celprogen at P2. Vials were gently thawed by warming in a 37°C water bath within 1-2 minutes until 90% thawed. Vial contents were transferred to a sterile 15 mL tube and pre-warmed gEC full culture media (Celprogen, York, UK) was added to the tube and resuspended. Vial was washed twice with gEC full culture media to recover any additional cells. 15 mL tube was centrifuged at 100g for 7 minutes. Media was aspirated, and cell pellet (0.9×10^6 cells) was resuspended in gEC full culture media. Cells were seeded at 10,000 cells/cm^2 on precoated 25cm^2 flasks (Celprogen) and cultured in gEC full culture media. Cells were incubated for 2-3 days at 37°C and 5% CO_2 with frequent media changes until reaching confluency.

gEC were cultured in gEC full culture media with serum, antibiotic free supplied from Celprogen, contents of serum and growth factors were not disclosed, in 25 and 75 cm^2 flasks, matrix contents were not disclosed. Cells were grown to confluency at 37°C and 5% CO_2. Once cells achieved confluency, gEC full culture media was aspirated, and cells were washed with

PBS -/-. PBS was aspirated, Trypsin-EDTA solution (Sigma) was added to cells for 3 minutes at 37°C to lift adherent cells, and neutralising media (gEC full culture media) was then added. Cells were recovered by centrifuging at 100g for 7 minutes. Pelleted cells were resuspended in gEC full culture media and live cells were counted using the haemocytometer. gEC were seeded into 75 cm^2 flasks for further passaging or seeded at 10 x 10^5 per well on 12-well plates for experimentation. gEC were used at P5 or P6 for experimentation, then frozen down in gEC freezing media (Celprogen) as subculturing allows passaging gEC up to P12. Cryovials of cells stocks were stored at -80°C for 48 hours until further long-term storage in liquid nitrogen.

2.2.3. Purification and dialysis of IgG

2.2.3.1. IgG purification

Human anti-MPO, anti-PR3 IgG were isolated from plasma exchange fluid from patients with AAV, and HC IgG isolated from serum from healthy volunteers. Samples were centrifuged at 1500g for 5 minutes at 4°C, passed through a 0.22 μm filter (ThermoFisher) and diluted 1:1 with binding buffer (20 mM phosphate, pH 7.0). Protein G columns (SLS, Nottingham, UK) used for purification have a binding capacity of approximately 25mg of human IgG to the chromatographic matrix. Columns containing 5mL protein G resin (5 mL=1 column volume/CV) stored in 20% EtOH were opened, allowing EtOH to flow through. Columns were equilibrated with 1CV binding buffer, and samples diluted 1:1 in binding buffer was added to each column at 5CV. Excess and non-specific bound protein was washed off the column with 4CV binding buffer, after which 4CV elution buffer (0.1M glycine, pH 2.7) was used to elute bound IgG into aliquots of neutralisation buffer (Tris-HCl, pH 9.0). Once completed, columns were washed with 5CV of 20% EtOH and stored in 20% EtOH at 2-8°C. To regenerate, columns were washed with binding buffer and reused for the same sample type, e.g. only MPO-AAV serum was used in one column.

2.2.3.2. IgG concentration and dialysis

IgG concentration of eluted aliquots was measured by spectrophotometry (Nanodrop, ThermoFisher). The highest concentration aliquots were pooled and dialysed overnight at 4°C using a dialysis cassette with molecular weight cut off 10,000 Daltons (ThermoFisher). Protein content was again quantified by spectrophotometry at 280 nm and samples stored at -80°C.

2.2.4. *In vitro* treatment with human IgG, neutrophil SN, and neutrophils

2.2.4.1. Neutrophil stimulation

Human neutrophils were isolated as prescribed. Isolated neutrophils were resuspended in RPMI + 10% Human AB serum (neutrophil culture media; Sigma). Cells were seeded at a concentration of 10 x 10^6 cells/mL in 1.5 mL microcentrifuge tubes (Eppendorf) and allowed to recover from isolation for 15 minutes at 37°C. Cells were primed with TNF (2ng/mL; Bio-Techne, Abingdon, UK) for 15 minutes at 37°C and stimulated with 100 µg/mL of HC IgG or MPO-/PR3-ANCA IgG for 1 hour or respective time points at 37°C. Tubes were centrifuged at 250g for 5 minutes at 22°C, SN was removed and either used immediately, or stored in aliquots at -80°C. All stimulations performed under hypoxia were equilibrated for 15 minutes prior to starting respective time courses.

2.2.4.2. Whole blood IgG treatment

Venous whole blood in EDTA from healthy volunteers was aliquoted at 1mL in microcentrifuge tubes. Whole blood was primed with TNF (2 ng/mL) for 15 minutes at 37°C. Whole blood was treated with 100 µg/mL of HC IgG or MPO-/PR3-ANCA IgG for 1 hour at 37°C. Tubes were centrifuged at 1500g for 10 minutes at 4°C, serum was removed and either used immediately, or stored in aliquots at -80°C. All stimulations performed under hypoxia were equilibrated for 15 minutes prior to starting respective time courses. When inhibitors were

used, inhibitors were diluted in neutrophil culture media and added following TNF priming as an additional 10-minute step prior to ANCA stimulation. Individual concentrations were outlined in **Table 21**.

2.2.5. MPO binding – immunofluorescence

To confirm the specificity of isolated MPO- and PR3-ANCA IgG, indirect IF was performed using ethanol washed neutrophils. MPO-ANCA IgG exhibits a perinuclear stain, whereas PR3-ANCA IgG displays a cytoplasmic stain. Neutrophils were isolated as described in 2.2.2.2. using Percoll density gradient, resuspended at $1x10^6$ cells/mL and 100 µL of cell suspension applied to microscope slides using a cytospin (ThermoFisher). Slides were fixed and permeabilised in ice-cold EtOH for 10 minutes. Slides were allowed to air dry completely and used immediately or stored at -80°C in a slide box with desiccant silica gel beads. Cells were defrosted from -80°C 30 minutes before usage. Slides were blocked for 20 minutes in 20% goat serum (abcam, Cambridge, UK) diluted in PBS-/-. Excess block was tapped off, and slides were incubated with HC IgG or MPO-/PR3-ANCA IgG at 1:20 in PBS-/- for 1-hour at RT. Slides were washed thrice in PBS-/-. Slides were incubated with anti-human IgG FITC (Sigma) conjugation diluted at 1:1000 in PBS-/- for 1 hour in the dark. Slides were washed thrice in PBS-/-. Slides were mounted with Mounting Medium with DAPI – Aqueous Fluoroshield (abcam) and incubated for 30 minutes in the dark prior to imaging. Coverslip was laid on top of slide and imaged using confocal microscopy (Zeiss LSM-780) (**Fig 4**).

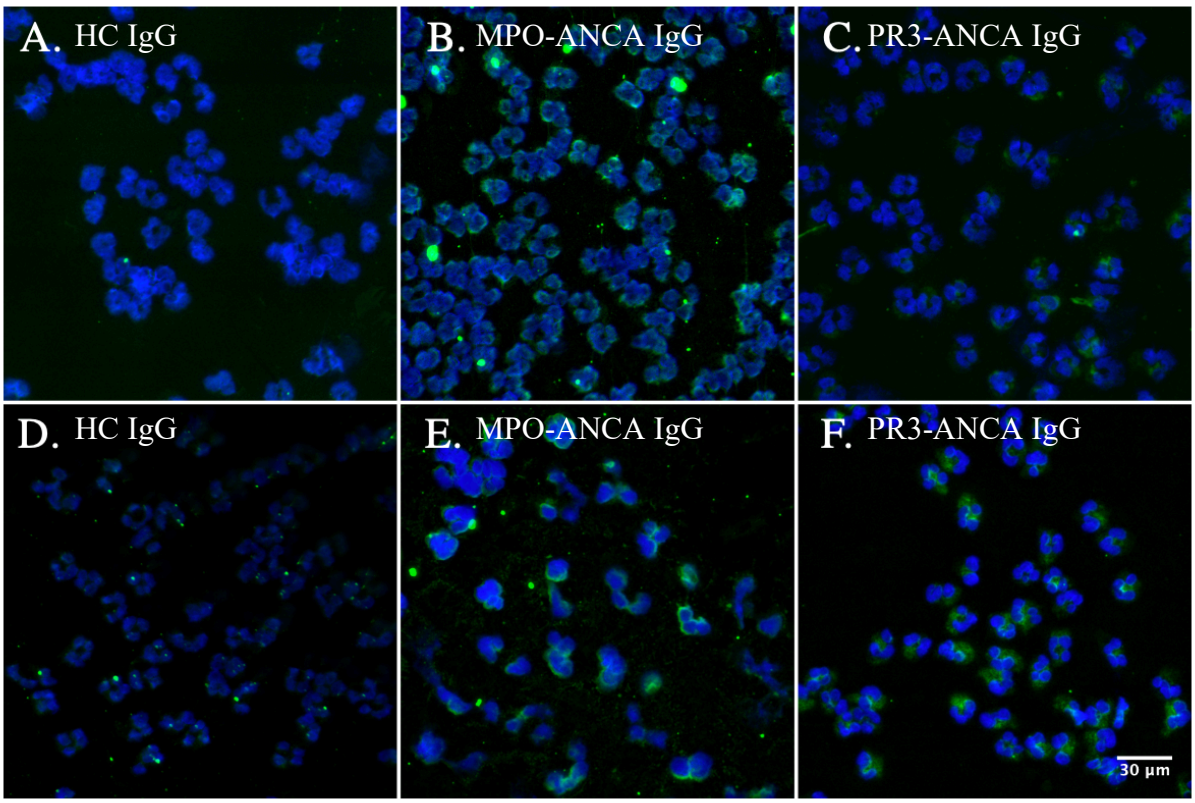


Figure 4. IgG purified from patients with AAV displays typical cANCA and pANCA of binding to ethanol washed neutrophils

Indirect immunofluorescence was performed with anti-MPO-/PR3-ANCA IgG. Isolated neutrophils from AAV patient or HC were applied to microscope slides using cytospin and fixed for 10 minutes with ice cold 100% EtOH onto ThermoFrost slides. Cells were blocked, incubated with MPO-/PR3-ANCA or HC IgG as indicated, followed by anti-human IgG FITC secondary (green) and, and mounted with VectaShield[R] Antifade Mounting Medium with DAPI (blue), and imaged at 40x using an inverted Zeiss LSM-780 (A/D) HC IgG, (B/E) MPO-ANCA IgG, and (C/F) PR3-ANCA IgG (A, B, C) HC neutrophils (D,E, F) AAV neutrophils.

2.2.6. Anti-MPO ELISA

To measure anti-MPO antibody titre from purified IgG preparations, a commercially available human anti-MPO antibody direct ELISA was used (AssayPro, Cambridge, UK). A 96-well polystyrene microplate was pre-coated with myeloperoxidase and the standard curve was prepared with a calibrator of known activity. Patient or control serum was added neat, diluted at 1:5, and 1:50 in MIX diluent (buffered protein base) in duplicates for a 2-hour incubation. Plates were washed five times with a concentrated buffered surfactant and coated with biotinylated anti-human IgG Antibody diluted at 1:50 in MIX Diluent. Plates were sealed at RT for 1 hour, and following incubation, plates were washed. SP conjugate diluted 1:100 in MIX Diluent was added to plates for a 30-minute incubation at RT. Plates were washed, and a stabilised peroxidase chromogen substrate tetramethylbenzidine was added for 12 minutes at RT in the dark. The reaction was stopped with 0.5 N hydrochloric acid solution and read immediately at optical density (OD) 450nm (**Fig 5**).

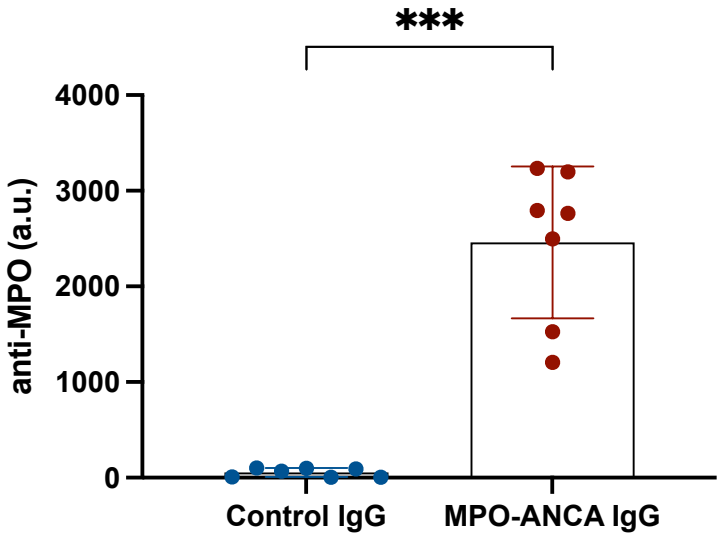


Figure 5. Anti-MPO ELISA
Quantification of IgG purified from plasma exchange fluid from patients with AAV was performed using an anti-MPO ELISA (n=7). HC or MPO-ANCA IgG was serially diluted 1:5 and 1:50 and compared to demonstrate purified IgG preparations contained MPO-ANCA IgG. Data are shown as mean +/- SEM, statistical analysis was performed using Mann-Whitney test. ***p<0.001.

2.2.7. Hypoxic equilibration – Whitley H35 Hypoxystation

The Whitley H35 Hypoxystation (Don Whitley) was used for experimentation analysing the effect of various oxygen tensions on whole blood, neutrophils, and gEC. The front panel of the workstation is transparent, with two sleeves attached to doors with sealed off ports, allowing manual entry into the chamber. External tanks supply nitrogen (N_2), carbon dioxide (CO_2), and compressed air into tubing that feeds into the chamber. Gas levels controlled by an external touch screen electronic panel allows the user to programme the chamber to desired oxygen tensions. The chamber was programmed to adjust N_2 and O_2 levels as required experimentally; CO_2 was kept stable at 5.0%. A thermostat is internally installed allowing incubation conditions to be maintained at temperature 37°C and humidity levels monitored at 70% throughout experimentation to prevent evaporation of media. To prevent oxygen inadvertently entering the main chamber, an enclosed smaller chamber with a sealed opening allows entry from outside of the chamber for the user to add materials; this airlock was flushed with N_2 before entry of materials into the chamber. Before undergoing any experimentation, the chamber needs to equilibrate, along with any materials necessary. To allow for sufficient gas exchange, and pH adjustment, plastics, buffers, and media are placed in the chamber to equilibrate a minimum of 3 hours prior to commencing experiments. To ensure experiments on whole blood were achieving the desired oxygen tension during shorter time points of equilibration, at 15 minutes and 1 hour, blood gas analyses were performed on HC blood. All experiments on whole blood, isolated neutrophils, and gEC were equilibrated first for 15 minutes before starting any time points. All experiments performed under oxygen tensions less than 21% O_2 were conducted in this workstation.

2.2.8. Mechanophenotyping - RT-DC

To perform biomechanical phenotyping of whole blood and isolated neutrophils, the technique of RT-DC was employed. A syringe was filled with sheath fluid, CellCarrierB (Zellmechanik Dresden GmBH) buffer for whole blood, or CellCarrier (Zellmechanik Dresden) buffer for isolated cells. A second syringe contained diluted whole blood 1:20 in CellCarrierB or a cell pellet ($2x10^6$) resuspended in 200 µL of CellCarrier, for the sample syringe. Both were placed onto a syringe pump (neMESYS, Cetoni GmbH) of the AcCellerator (Zellmechanik Dresden), an extension for an inverted microscope (Zeiss). Syringes were connected to polymer PEEK tubing (IDX), attached to the sheath fluid and sample inlet of a Flic20 PDMS microfluidic chip (Zellmechanik Dresden). The chip contains reservoirs connected by a square measurement channel with a 20x20 μm^2 cross-section (**Fig 3**).

RT-DC measurements were collected at a flow rate of 0.12 µL/s (0.03 µL/s of sample flow, and 0.09 µL/s of sheath flow). An inverted microscope (Zeiss) in combination with a high-speed CMOS camera (Mikrotron GmbH) captures images of cells as they reach the end of the constriction channel at a frame rate of 2000 frames/s. For isolated cell populations, an open gating strategy was used. The aspect ratio is set from 1 to 1.2, and the area is set as a gate from 15 μm^2, which is sufficient to in exclude erythrocyte singlets and doublets. Variables measured included cell area, deformability, and elasticity. The Young's modulus, or elasticity coefficient is inversely correlated to the deformability of the cells. For analysis, porosity, or the convex to measured area ratio of the cell, is set to 1.0-1.05 (px: μm^2). ShapeIn is the program used for data collection while running RTDC, and ShapeOut is the analysis software providing kernel graphs, statistical analysis, and recorded visualisation of individual cell populations (**Fig 6**).

Formulas:

deformation = 1 – circularity
= 1 – $(2\sqrt{\pi A})/l$

Young's modulus (E) = stress/strain

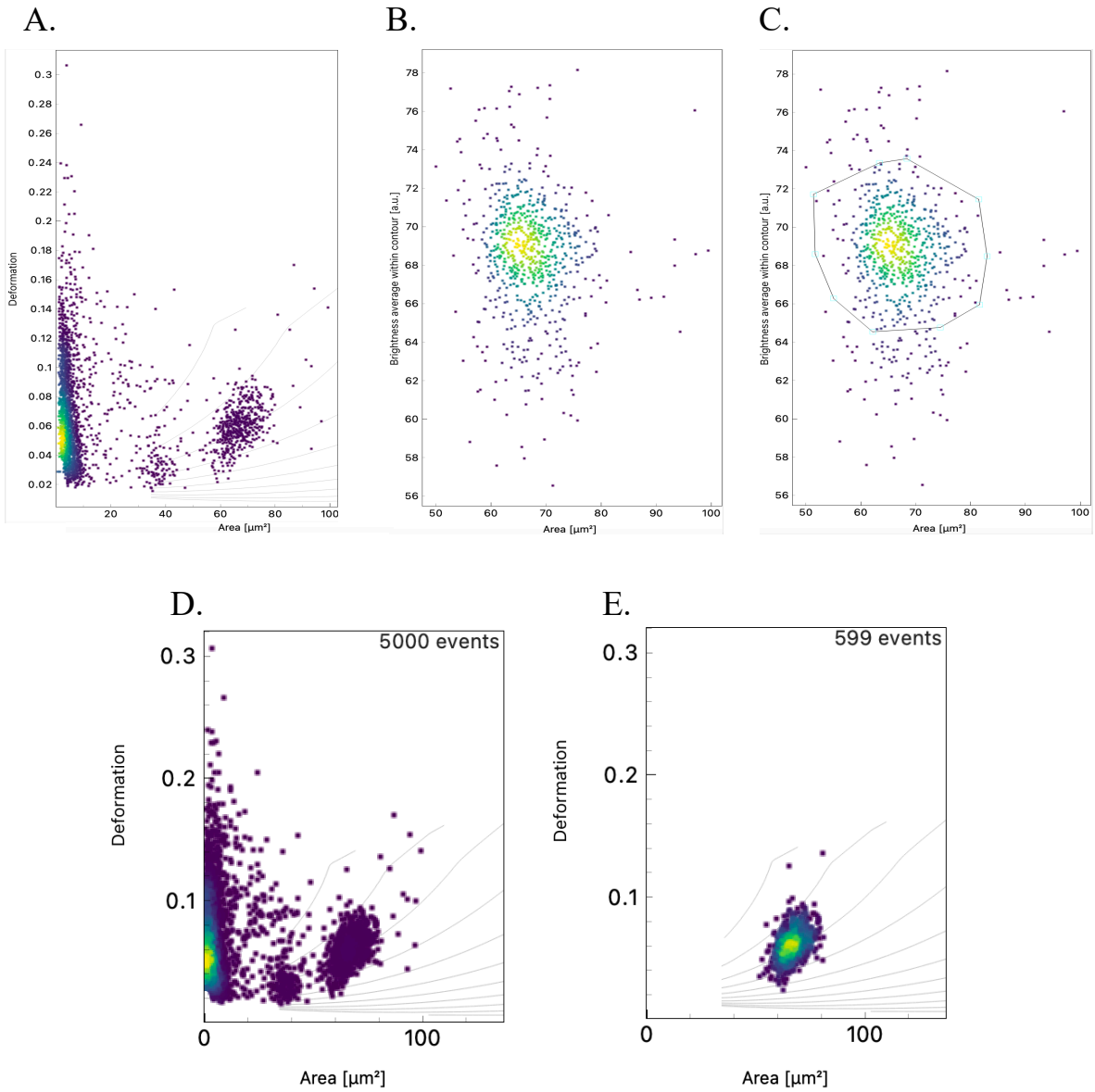


Figure 6. RT-DC gating

Whole blood was subjected to RT-DC. (A) Depicts all recorded cells. The neutrophil gating strategy was then applied, filtering out all other cell types and debris from analysis. (B) Box filters are applied, setting area to neutrophil size, between 50-100µM2, and porosity (convex to measured area ratio) to 1.0-1.05 gating out any cells improperly recorded. (C) Polygon gate is set to include all neutrophils in the density dot plot and exclude monocytes (brighter), eosinophils (darker) or doublets (larger) that may lie within this filtered population by manually assessing cell appearance. (D) Ungated cells after box filters, but polygon gate applied (E) Remaining neutrophils with box filters and polygon gate applied.

2.2.9. Measuring gene expression levels

2.2.9.1. RNA extraction stimulation – neutrophils

To assess a selective myeloid panel of differentially expressed genes, mRNA expression levels were measured by qPCR in neutrophils. Freshly isolated neutrophils were resuspended in neutrophil culture media at $10x10^6$/mL. 1 µL (40 U/µL) of Protector RNase inhibitor (Merck) was added to each sample in 1.5 mL microcentrifuge tubes. Cells were allowed to recover for 15 minutes at 37°C and 5% CO_2. Cells were primed with TNF (2 ng/mL) for 15 minutes and stimulated with control or MPO-ANCA IgG at 100 µg/mL, for 1 hour. Once incubation was completed, cells were centrifuged at 350g for 5 minutes. To lyse neutrophils for RNA extraction, each cell pellet was resuspended in TRIzol (Life Technologies, London, UK) and left to incubate for 10 minutes. To homogenise, cells were resuspended using a 0.30-gauge insulin needle (BD, Wokingham, UK). Cells lysed in TriZol were frozen at -80°C.

2.2.9.2. RNA extraction stimulation – gEC

For isolation of mRNA from gEC, cells were seeded in 12-well plates (as stated in section 2.2.2.6.) in gEC full culture media and incubated at 37°C at 21%, 5%, or 1% O_2 for 24 hours. Once gEC were approximately 80% confluent, gEC full culture media was aspirated, and cells were washed with PBS-/- to remove any remaining serum. Cells were serum starved with gEC media without serum and incubated for 2 hours at 37°C. After 2 hours, gEC media without serum was aspirated, and cells were treated with various conditions including gEC with untreated neutrophil HC SN, HC IgG stimulated neutrophil SN, MPO-ANCA IgG stimulated neutrophil SN, untreated neutrophil rAAV SN, or untreated neutrophil aAAV SN. SN from neutrophils was diluted 1:4 in gEC media with serum before addition to the wells. Cells were treated for 6 hours or 24 hours. After designated time points, reactions were stopped by placing cells on ice for 30 minutes. To lyse gEC for RNA extraction after stimulation, cells were

washed with ice cold Hank's balanced salt solution (HBSS; Sigma) and RLT buffer (Qiagen, Manchester, UK) containing 1:100 dilution of β-mercaptoethanol was added to each well. To harvest, wells were scraped, and aliquoted into 1.5 mL microcentrifuge tubes.

2.2.9.3. RNA extraction

RNA from neutrophils and gEC was extracted on ice using Qiagen mini kit. 70% molecular grade EtOH was added to each sample. After resuspension, each aliquot was transferred to RNeasy tubes for centrifugation at 8000g for 30 seconds at 4°C, discarding flow through. RW1 Buffer was added to each sample and centrifuged at 8000g for 30 seconds at 4°C, discarding flow through. A 1:8 dilution of DNase in RDD buffer was prepared. DNase was aliquoted to the centre of each tube for incubation at RT for 15 minutes. RW1 Buffer was added to each sample and centrifuged at 8000g for 30 seconds at 4°C, discarding flow through. Spin columns were transferred to new collection tubes. RPE Buffer was added to each sample and centrifuged at 8000g for 30 seconds at 4°C, discarding flow through. For a second wash, RPE Buffer was added to each sample and centrifuged at 8000g for 2 minutes at 4°C. Flow through was discarded and samples were centrifuged to dry at 14000g for 1 minute at 4°C. TE buffer (Life technologies) was added to the centre of the column and centrifuged at 14000g for 1 minute at 4°C. Flow through was eluted again, added to the centre of the column, and spun down at 14000g for 1 minute at 4°C. Flow through was transferred to into fresh 1.5 mL microcentrifuge tubes and stored at -80°C prior to analysis. RNA quantity and purity was assessed using A260:A280 ratio and A260:A230 ratio using a Nanodrop 2000c Spectrophotometer (ThermoFisher). gEC samples were stored in -80°C. Neutrophil samples prepared for RNA-seq were stored in -80°C until confirming RNA integrity (RIN) using 4150 TapeStation System (Agilent, Manchester, UK) before sequencing.

2.2.9.4. cDNA synthesis

RNA (250 ng neutrophils and 500 ng for gEC) was diluted in RNase-free H_2O and used for reverse transcription with the MultiScribe Reverse Transcriptase kit (ThermoFisher). Total reaction volume was 20 µL and consisted of 10x RT Buffer, 10x Random Primers, 25x 100 mM dNTP Mix, and 0.2 mL 50U/µL MultiScribe Reverse Transcriptase (ThermoFisher). Reverse transcription was carried out using an Agilent Technologies SureCycler 8800. Primer annealing occurs at 25°C for 10 minutes, RT occurs 37°C for 120 minutes and enzyme inactivation at 85°C for 5 minutes. cDNA was stored at -80°C until usage for validation of differentially expressed targets via RT-qPCR.

2.2.9.5. RT-qPCR

A master mix was prepared containing 5 µL of FastStart SYBR Green Master (Roche, Notttingham, UK), 0.125 µL of forward and reverse primers at 50 mM working concentration, and 2.8 µLof RNase-free H_2O (Qiagen). cDNA was diluted (1:20 in RNase-free H_2O) and 2 µL was added to 8 µL of master mix. Thermal cycling parameters were activation (95°C for 10 minutes), cycles of denaturing (95°C for 10 seconds), annealing (58°C for 45 minutes), cycling [for 39 cycles] (58°C for 10 seconds), and extension (95.0°C for 5 seconds). Real-time qPCR reactions were performed using a QuantStudio 5 thermocycler. Samples were analysed in triplicate and primer pairs are detailed in **Table 3**. All custom primers were synthesised by Sigma-Aldrich and housekeeping primers were synthesised by Qiagen. B2M and 18S expression were used as the housekeeping controls, proven stably expressed across samples, for normalisation of target gene expression of interest. Negative controls were performed using RNase free water or total RNA. Quantification of target gene compared to housekeeping gene was calculated using the comparative Ct method and where appropriate fold change calculated using the 2-ΔΔCT method.

2.2.10. Measuring protein secretion levels in neutrophils and gEC – ELISA

2.2.10.1. Neutrophil and gEC activation analysis

To quantify protein secretion levels, serum, neutrophil, and gEC samples were tested using R&D Human IL-8, VCAM-1, and ICAM-1 DuoSet ELISA kits. Following manufacturer's instructions, 96-well half-well microplates (Greiner Bio-one) were coated with capture antibody diluted in PBS according to manufacturer's instructions and incubated overnight at RT. After coating, plates were washed thrice with washing buffer, blocked with blocking buffer for 1 hour at RT, and washed again. Recombinant protein of interest was serially diluted to create a 7-point standard curve and loaded in duplicates on lanes 1 and 2. Samples were added in duplicate technical replicates to the remainder of the plate. Plates were incubated for 2 hours at RT and then washed. Detection antibody diluted in reagent diluent was added, for a 2-hour incubation at RT, and then washed. Streptavadin horseradish peroxidase (HRP) diluted in reagent diluent was added for 20 minutes at RT in the dark. After washing, 1:1 H_2O_2 and tetramethylbenzidine (substrate solution) was added for maximum 20 minutes at RT in the dark. The reaction was stopped with 2 N H_2SO_4 (stop solution) and read immediately at OD450nm. Background ODs were subtracted from standards and samples and a logarithmic standard curve generated to interpolate sample IL-8, VCAM-1, or ICAM-1 concentration.

2.2.10.2. Co-culture neutrophil SN and gEC treatment conditions

SN from neutrophils stimulated following conditions outlined in 2.2.4.1. were first measured for IL-8, VCAM-1, and ICAM-1 secretion levels before gEC treatment. Harvesting of SN from neutrophil SN treated gEC are outlined in section 2.2.9.3. IL-8, VCAM-1, and ICAM-1 secretion in SN from neutrophil SN treated gEC was quantified by subtracting initial IL-8, VCAM-1 and ICAM-1 secretion levels measured in stimulated neutrophil SN, from the overall IL-8, VCAM-1, or ICAM-1 in SN from neutrophil SN treated gEC (section 2.2.4.1.)

2.2.11. Experiments for neutrophil trans-endothelial migration

2.2.11.1. Neutrophil endothelial trans-well migration assay

To quantify neutrophil trans-migration across endothelial cells, trans-well assays were used. gEC were seeded in 12-well trans-well membrane inserts with 3 μm pores at 5 x 10^5 per well and incubated at 37°C at 21% or 1% O_2 for 48 hours. At 24 hours, 10 ng/mL of TNF was where indicated as a positive control. At 48 hours (24 hours after addition of TNF to selected wells) gEC were treated with neutrophils in conditions outlined in **Table 20**. Neutrophil stimulation conditions were as stated in section 2.2.4.1. Cells were co-cultured for 1.5 hours. SN from the bottom chamber was harvested for counting migrated neutrophils and membrane inserts were fixed for assessing EC monolayer formation and integrity using immunofluorescence.

Oxygen tension	Coculture stimulation conditions					
21% O_2	Neutrophils: Untreated EC: Untreated	Neutrophils: TNF primed EC: Untreated	Neutrophils: Untreated EC: TNF treated	Neutrophils: TNF primed Control IgG stimulated EC: Untreated	Neutrophils: TNF primed MPO-ANCA IgG stimulated EC: Untreated	Neutrophils: TNF primed PR3-ANCA IgG stimulated EC: Untreated
	Neutrophils: Untreated EC: Untreated	Neutrophils: TNF primed EC: Untreated	Neutrophils: Untreated EC: TNF treated	Neutrophils: TNF primed Control IgG stimulated EC: Untreated	Neutrophils: TNF primed MPO-ANCA IgG stimulated EC: Untreated	Neutrophils: TNF primed PR3-ANCA IgG stimulated EC: Untreated
1% O_2	Neutrophils: Untreated EC: Untreated	Neutrophils: TNF primed EC: Untreated	Neutrophils: Untreated EC: TNF treated	Neutrophils: TNF primed Control IgG stimulated EC: Untreated	Neutrophils: TNF primed MPO-ANCA IgG stimulated EC: Untreated	Neutrophils: TNF primed PR3-ANCA IgG stimulated EC: Untreated
	Neutrophils: Untreated EC: Untreated	Neutrophils: TNF primed EC: Untreated	Neutrophils: Untreated EC: TNF treated	Neutrophils: TNF primed Control IgG stimulated EC: Untreated	Neutrophils: TNF primed MPO-ANCA IgG stimulated EC: Untreated	Neutrophils: TNF primed PR3-ANCA IgG stimulated EC: Untreated

Table 20. Stimulation conditions

Optimisation was performed to determine a suitable media cocktail concentration to ensure no activation of either the neutrophils or endothelial cells. A media stock of 1:5 neutrophil culture media in gEC full culture media was made up for further stimulation and incubation from this point of experimentation onward. 30 minutes prior to addition to trans-wells, isolated neutrophils were seeded at 5 million cells per mL into 1.5 mL microcentrifuge tubes and equilibrated at 37°C for 15 minutes. Neutrophils were primed with 2 ng/mL of TNF for 15 minutes. During this neutrophil incubation step, media was aspirated from the top and bottom

chamber of the trans-well membrane insert. 500 µL of media with or without 200 ng/mL of IL-8 was added to bottom chambers. 100 µg/mL of control or ANCA IgG was added to each tube of neutrophils, and directly transferred to the top well insert of each trans-well membrane. Cells were incubated at 37°C and 5% CO_2 for 1.5 hours to allow for trans-endothelial migration to occur. Media from the bottom chamber was carefully removed and pipetted into individual 1.5 mL microcentrifuge tubes. Neutrophils were pelleted at 300g for 5 minutes, resuspended in 100 µL of media, and counted using the haemocytometer.

2.2.12. Immunofluorescence

2.2.12.1. Co-culture trans-well monolayer assessment

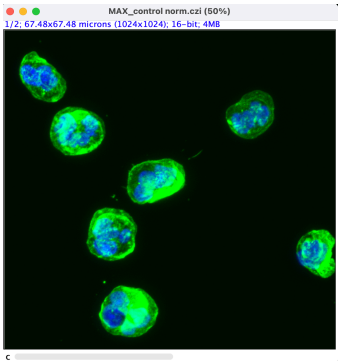
To assess adequate monolayer formation, and integrity of the trans-well membranes, immunofluorescence was performed. Trans-well membrane inserts (from above experiment, section 2.2.11.1.) were removed and transferred to new 12 well plates. Membranes were washed twice in PBS-/-. PBS-/- was aspirated and membranes were fixed in Image-iT Fixative Solution for 15 minutes at RT. PFA was aspirated, and membranes were washed twice in PBS-/-. Membranes were permeabilised with 0.4% Triton X-100 in PBS-/- for 5 minutes. 0.4% Triton X-100 was aspirated, and membranes were washed twice in PBS-/-. Membranes were incubated in blocking buffer for 10 minutes. BSA was aspirated, and membranes were incubated in primary antibodies for VE-Cadherin (R&D) and CD15 (Agilent), diluted in blocking buffer at 4°C overnight. Membranes were washed twice in PBS-/-. PBS-/- was aspirated and membranes were incubated for 1 hour in secondary antibody (donkey anti-goat IgG Alexa555 for VE-Cadherin and donkey anti-mouse IgG Alexa647 for CD15) diluted in blocking buffer at 4°C. Membranes were washed twice in PBS-/-. Using tweezers to hold the chamber, outer edges of the membrane were excised with a scalpel, leaving one point of the membrane attached to the chamber. The chamber was held over a slide, VectaShield DAPI

mount was dropped upon the (still attached) membrane, and the remaining attached portion of membrane was gently removed using tweezers. Coverslip was placed from one corner, carefully avoiding air bubbles to ensure a flat layer sealing of the membrane. Slides were stored at 4°C in the dark until imaging at 20x (Leica Stellaris 8 STED-FALCON).

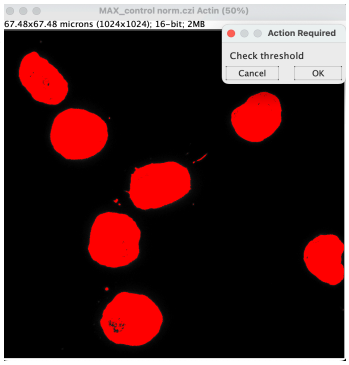
2.2.12.2. Visualisation of actin polymerisation and quantification

Actin polymerisation was quantified by immunofluorescence and confocal microscopy. Freshly isolated neutrophils from healthy control donors were seeded at a density of $2x10^5$ per well into 8 well chamber slides (Ibidi) and allowed to recover for 15 minutes at 37°C. Cells were primed with 2 ng/mL of TNF for 15 minutes then stimulated with 100 µg/mL of HC IgG or MPO-/PR3-ANCA IgG for 1 hour. Following stimulation, SN was aspirated, and wells were washed with PBS-/-. Cells were fixed in Image-iT Fixative Solution (4% PFA; ThermoFisher) for 15 minutes at RT. 4% PFA was aspirated and wells were washed with PBS-/-. Cells were blocked with 1% BSA (Sigma Aldrich) for 1 hour at RT. Serum was aspirated, and Phalloidin (AF488) antibody diluted in PBS-/- was added to each well and left in the dark to incubate overnight at 4°C. Wells were washed with PBS-/-. VectaShield DAPI mount (Vector labs) was added to mount slides. Chamber slides were kept in the dark, at 4°C until imaged using confocal microscopy (Zeiss LSM-780) on 63x immersion oil. Phalloidin staining measures and represents the F-actin signal. A macro developed by Stephen Rothery (Imperial FILM), quantified the area and perimeter of each cell utilising Phalloidin stain, the total cell area staining for Phalloidin was quantified relative to the area of each measured cell, and the total cell perimeter staining for Phalloidin was quantified relative to the perimeter of each measured cell. These variables are individually referred to as area, perimeter, relative area, and relative perimeter. Values generated by the macro were used to quantify protrusions and actin polymerisation (**Fig 7**).

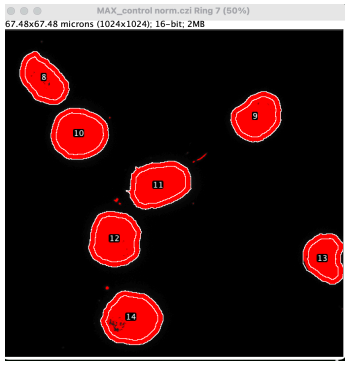
A.



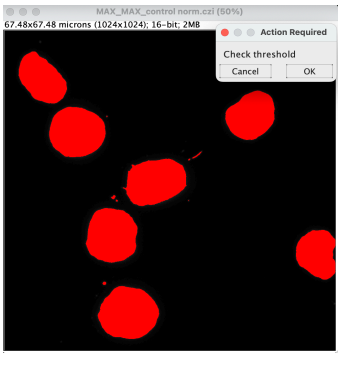
B.



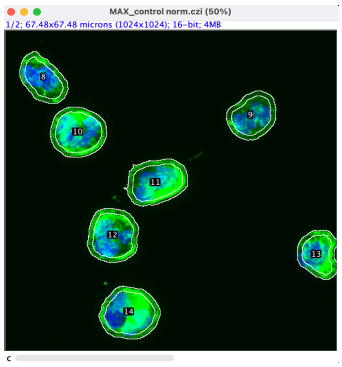
C.



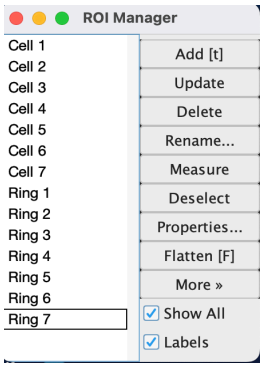
D.



E.



F.



G.

Summary

Slice	Count	Total Area	Average Size	%Area	Mean	Perim.	Circ.	Solidity	Feret	FeretX	FeretY	FeretAngle	MinFeret
MAX_control norm.czi Cell 1	1	69.881	69.881	97.925	31416.156	34.942	0.719	0.960	11.958	67.000	77	121.938	7.451
MAX_control norm.czi Cell 2	1	75.504	75.504	98.399	25775.016	34.667	0.789	0.968	11.016	706.000	329	48.395	8.761
MAX_control norm.czi Cell 3	1	94.726	94.726	98.710	43205.930	39.837	0.750	0.978	11.638	143.000	356	20.898	10.608
MAX_control norm.czi Cell 4	1	93.801	93.801	98.240	42469.613	43.730	0.616	0.948	13.125	368.000	505	15.432	9.302
MAX_control norm.czi Cell 5	1	94.891	94.891	98.530	37555.215	40.082	0.742	0.973	11.796	287.000	576	118.713	10.196
MAX_control norm.czi Cell 6	1	63.984	63.984	97.267	43190.098	32.912	0.742	0.958	10.762	954.000	639	105.994	8.039
MAX_control norm.czi Cell 7	7	101.543	14.506	96.533	18017.756	6.069	0.885	0.898	1.902	336.143	928	92.436	1.622
MAX_control norm.czi Ring 1	1	27.724	27.724	96.145	33452.367	34.942	0.285	0.381	11.958	67.000	77	121.938	7.451
MAX_control norm.czi Ring 2	1	27.672	27.672	95.993	23319.252	34.667	0.289	0.355	11.016	706.000	329	48.395	8.761
MAX_control norm.czi Ring 3	1	30.785	30.785	96.149	36009.406	39.837	0.244	0.318	11.638	143.000	356	20.898	10.608
MAX_control norm.czi Ring 4	1	31.792	31.792	95.054	37285.789	43.730	0.209	0.321	13.125	368.000	505	15.432	9.302
MAX_control norm.czi Ring 5	1	31.263	31.263	95.910	35764.441	40.082	0.245	0.321	11.796	287.000	576	118.713	10.196
MAX_control norm.czi Ring 6	1	25.670	25.670	93.456	37807.289	32.912	0.298	0.384	10.762	954.000	639	105.994	8.039
MAX_control norm.czi Ring 7	1	32.409	32.409	95.607	36013.680	40.862	0.244	0.305	12.517	289.000	912	5.741	10.877

Figure 7. Actin polymerisation quantification macro steps

(A) Z-stacks were projected to maximum intensity images. (B) Auto threshold was set to Huang dark and a mask was created, filling any holes. (C) Area and perimeter were measured within a 1 µm sized ring around each individual cell. (D) Auto threshold was set to Otsu dark. (E) Relative area and relative perimeter were measured within a 1 µm sized ring around each individual cell. (F) Individual cells were divided by cell and ring; cell denoting area and perimeter measurement, and ring denoting relative area and relative perimeter measurement. (G) A quantified labelled list of variables is generated.

2.2.12.3. Visualisation of NET formation

To quantify NET formation, immunofluorescence and confocal microscopy was performed. Freshly isolated neutrophils from healthy control donors were seeded at a density of $2x10^5$ per well into an 8 well chamber slide (Ibidi) and allowed to recover for 15 minutes at 37°C. Cells were primed with 2 ng/mL of TNF for 15 minutes and stimulated with 100 µg/mL of HC IgG or MPO-/PR3-ANCA IgG for 4 hours. PMA at 60 ng/mL was used as a positive control. Following stimulation, SN was aspirated, and wells were washed twice with PBS-/-. Cells were fixed in Image-iT Fixative Solution for 15 minutes at RT. PFA was aspirated, and wells were washed twice with PBS-/-. Cells were blocked with 2.5% horse serum (Vector labs) for 10 minutes at RT. Serum was aspirated, and anti-Citrullinated histone H3 (H3Cit; abcam) antibody diluted in PBS-/- was added to each well and left in the dark to incubate overnight at 4°C. Wells were washed with PBS-/- twice. Secondary antibody (horse anti-rabbit IgG DyLight 594) in PBS-/- was added to each well for 1 hour. Wells were washed with PBS-/- twice. Slides were mounted with VectaShield DAPI mount. Chamber slides were kept in the dark at 4°C until imaged using confocal microscopy (Zeiss LSM-780) at 40x immersion oil.

2.2.13. Statistical analysis

Values for statistical analysis were generated using Excel (Microsoft). Graphs and statistical analysis were carried out in ShapeOut2 (Zellmechanik Dresden) or Prism Software Version 10 (Graphpad). Where statistical tests are used, this is detailed in the text or figure legend. For non-parametric data or datasets with a small number of replicates, non-parametric tests were used included a Mann-Whitney test to compare two conditions, Kruskal-Wallis test, with Dunn's post-hoc test to compare multiple conditions. For normally distributed data t test for two variables or one way analysis of variance (ANOVA) for multiple variables with Dunnett's post-hoc correction to compare groups to a control group or Bonferroni post-hoc correction for

multiple comparisons. To compare multiple groups across different conditions, two-way ANOVA with Geisser-Greenhouse correction, with Tukey's multiple comparisons post-hoc test was used. For liner correlation Pearson correlation coefficient was used.

RNA-seq analysis was performed by GeneWiz. Sequence reads were trimmed using Trimmomatic v.0.36 mapped to Homo sapiens GRCh38.p14 reference genome on EMSEBL using STAR aligner v.2.5.2b. Hit counts for genes were calculated using featureCounts from the Subread package v.1.5.2. Downstream differential expression analysis using DESeq2 was performed; p-values and log2 fold changes were generated using the Wald test. Presentation of results were displayed using EnhancedVolcano (505,506) package in R for volcano plots and WebGestalt (507–510) for gene ontology analysis.

3. Chapter 3 – Characterising the biomechanical phenotype of neutrophils following stimulation with ANCA IgG

3.1. Introduction

Neutrophils are key to the pathogenesis of AAV as ANCA activated neutrophils are direct mediators of vascular and tissue injury. A chemoattractant, such as IL-8, signals neutrophil recruitment to sites of vascular damage due to inflammation, localising neutrophils activated by ANCA to the endothelium and increasing the inflammatory response. As a result of activation by ANCA, stimulation of neutrophil pathogen killing mechanisms occurs, mediating tissue injury through ROS generation, degranulation, and NET formation. There is sufficient evidence for ANCA IgG activation of neutrophils leading to pathogenic responses from several *in vitro* studies (289,327,511,512).

Neutrophil priming by inflammatory mediators has been shown to result in a biophysical phenotypic change whereby neutrophils become smaller and stiffer. Once neutrophils shrink following priming, they then undergo a second phase of morphological change of enlargement and softening, displaying yet another example of neutrophil plasticity (41). Activation of neutrophils has, in other studies, been described to induce both stiffening and softening of cells (41,513). As such biomechanical changes are likely to depend on the timing, the exact stimulus used and potentially whether whole blood or isolated neutrophils are used.

RT-DC, a method used for high-throughput characterisation of single cell mechanics, can detect biomechanical changes in primed and activated cells using a range of conventional stimuli such as PAF, FMLP, or LPS. Although ANCA IgG is known to induce a range of pathogenic neutrophil responses, there is only one study of biomechanics, which used single cell micropipette aspiration to identify that neutrophils may become stiffer following ANCA IgG stimulation (342). Therefore, it is unknown what the impact of ANCA stimulation is on cell biophysical phenotype using a high throughput technique capable of fully phenotyping

morphorheological properties. Increased neutrophil stiffness in AAV would be consistent with its specificity for small blood vessels as stiffer neutrophils are more likely to become trapped in the microvasculature (514). Previous studies, in other settings than AAV, have identified that mechanical changes such as stiffening are associated with a stiffer actin cortex (216); this is also a typical cytoskeletal feature of neutrophil priming (40). Actin cytoskeletal changes are also of key importance for neutrophil functions, such as NETosis, as detailed previously in section 1.3.2.

Determining whether changes in the cytoskeleton and neutrophil biophysical phenotype occur following ANCA stimulation may lead to identification of novel ways of targeting pathogenic ANCA responses, such as preventing increased neutrophil stiffness by targeting the regulation of actin polymerisation.

Hypothesis of this chapter

Stimulation of neutrophils with ANCA IgG induces morphorheological changes due to changes in the actin cytoskeleton.

Aims

1 To optimise experimental conditions for use of RT-DC

2 Investigate the effect of ANCA IgG stimulation on neutrophil mechanophenotype

3 Investigate the link between neutrophil mechanophenotype and actin cytoskeletal changes

4 To measure if ANCA IgG induced changes in neutrophils are transcriptionally regulated

3.2. Optimisation of RT-DC

As RT-DC is a novel technique, an important part of my project was optimising conditions for experimental work. The effect of several experimental parameters on neutrophil biomechanical phenotype were measured including anticoagulant, cell culture media, processing time, and cell isolation method. I also explored the effects of different priming agents over a time course, in addition to initial optimisation of basic conditions.

3.2.1. Whole blood neutrophils in sodium citrate have lower deformability than EDTA

Previous studies showed platelets collected in heparin and EDTA exhibited the lowest deformability whereas those collected into sodium citrate had the highest deformability (515). As such, I investigated the effects of different anticoagulants on neutrophil deformability. To determine if anticoagulants influence deformability of neutrophils in whole blood, RT-DC was used to analyse this population. Intra-donor and inter-donor effects of anticoagulants (sodium citrate or EDTA) were compared.

No significant difference in neutrophil size, deformability, or elastic modulus was seen between different anticoagulants compared in a single donor (**Fig 8A, C, and E**; ns). Additionally, the single donor results validated the reproducibility of RT-DC measurement. Neutrophils in citrate from multiple donors showed no change in size (**Fig 8B**), significantly lower deformation (**Fig 8D**; p=0.0295), and a trend towards having higher elastic modulus (**Fig 8F**; p=0.0531) in comparison to cells in EDTA. EDTA is commonly available for the collection of samples in the clinical setting (516) and is required for usage in for EasySep Direct Human Neutrophil Isolation Kit. From this, EDTA was the selected anticoagulant of choice for blood donation from healthy donors and patients.

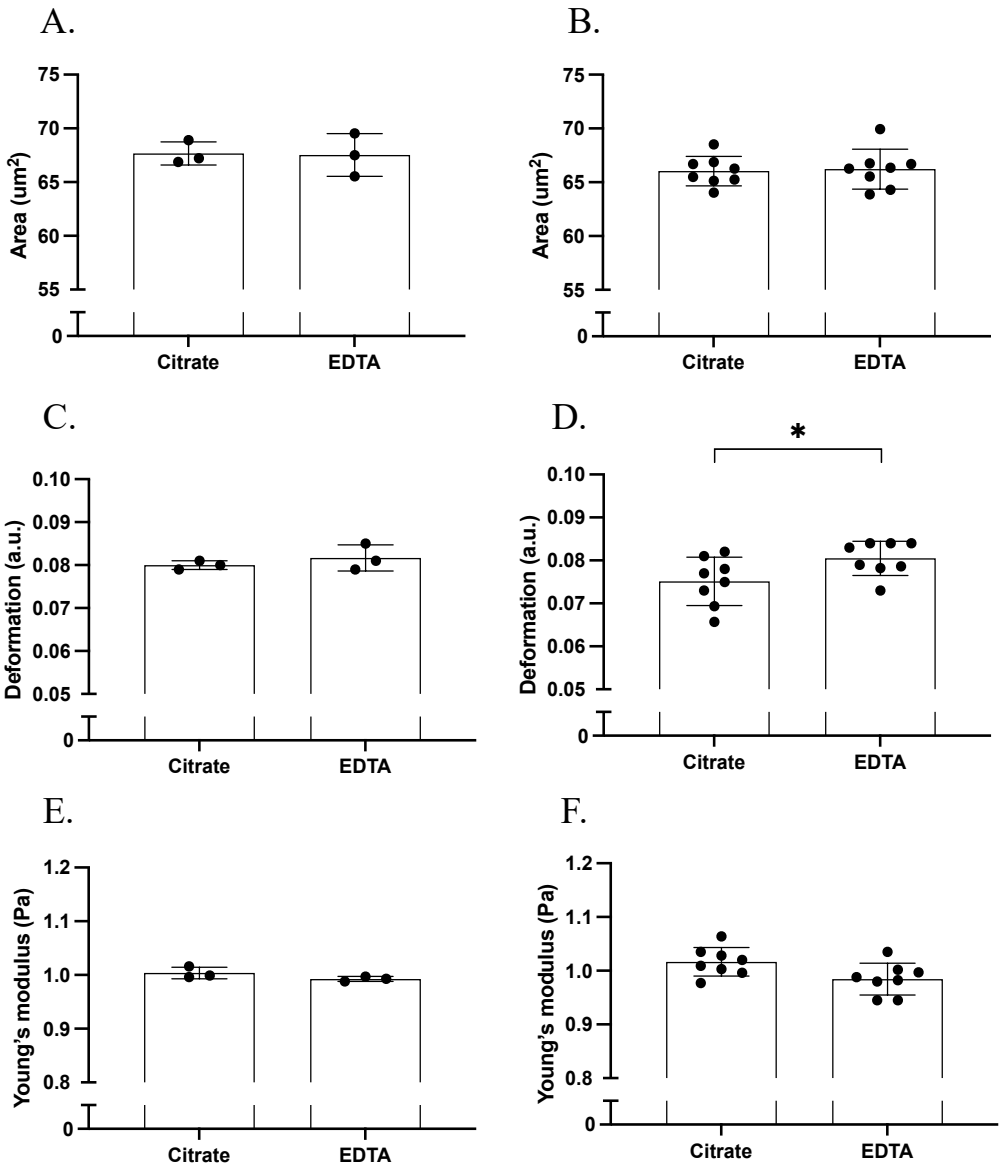


Figure 8. Whole blood neutrophils in sodium citrate have lowest deformability
(A/C/E) Neutrophils in whole blood from the same HC donor on different days. (n=3 separate collection days) collected in sodium citrate or EDTA were analysed using RT-DC. Neutrophil populations were gated and analysed for (A) Cell size, (B) Cell deformability, and (C) Elasticity. (B/D/F) Neutrophils in whole blood from HC (n=8 volunteers) collected in sodium citrate or EDTA were analysed using RT-DC. Neutrophil populations were gated and analysed for (B) Cell size, (D) Cell deformability, and (F) Elasticity. More than 1000 events were recorded for each sample and results were visualised and analysed in ShapeOut2 software. Data are shown as mean +/- SEM, statistical analysis was performed using Mann-Whitney test; *$p<0.05$.

3.2.2. Isolation methods do not alter neutrophil mechanophenotype

Previous work has shown that different methods of neutrophil isolation do not activate neutrophils but may result in different functional responses (67). I compared if methods of neutrophil isolation impact morphorheological characteristics of neutrophils using two different methods of cell isolation: dextran sedimentation/Percoll gradient *versus* immunomagnetic negative selection beads (EasySep) (517,518). Neutrophils were isolated using both methods in parallel and analysed using RT-DC.

No significant differences were observed between isolation methods when examining biomechanical profile of isolated neutrophils (**Fig 9A-C**; ns). For most experiments, Percoll gradient isolation method was the isolation method of choice. For RNA-Sequencing experiments neutrophils were isolated using immunomagnetic negative selection beads to ensure pure cell populations without contaminating eosinophils (or other rare granulocytes). Each experiment was performed using a consistent isolation method as there is a trend to increased deformability in the cells isolated using immunomagnetic negative selection.

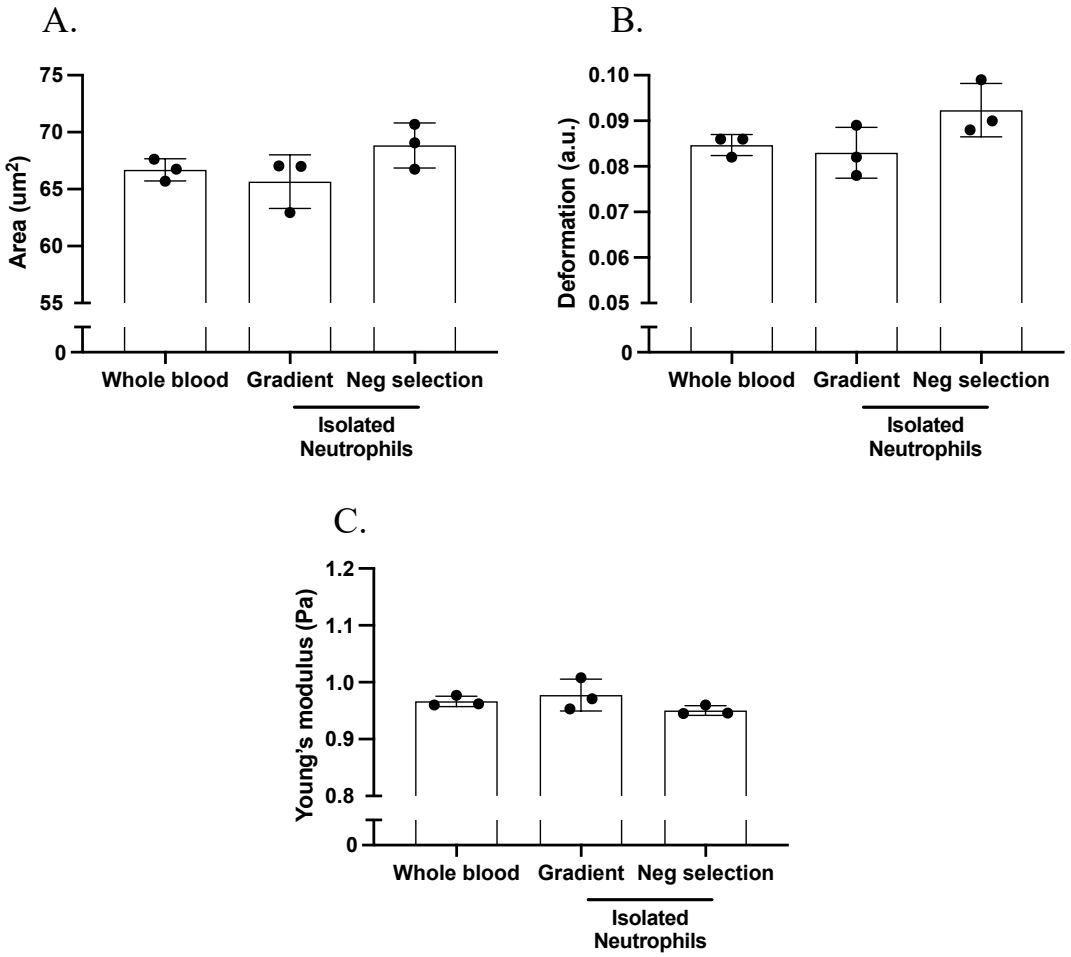


Figure 9. Isolation methods do not alter neutrophil mechanophenotype
(A-C) Neutrophils from HC (n=3) were examined in whole blood, or isolated using Percoll density gradient or EasySep Direct Neutrophil Isolation and analysed using RT-DC. Neutrophil populations were gated and analysed for (A) Cell size, (B) Cell deformability, and (C) Elasticity. More than 1000 events were recorded for each sample and results were visualised and analysed in ShapeOut2 software. Data are shown as mean +/- SEM, statistical analysis was performed using Kruskal-Wallis test, with Dunn's multiple comparisons test.

3.2.3. Time post-venepuncture does not alter neutrophil mechanophenotype

As this project involves analysis of patient samples, there was the potential for unavoidable time interval between venesection in the hospital clinic/ward setting and processing of samples. As such, I investigated the effect of delayed processing on morphorheological characteristics of neutrophils in whole blood and isolated cells using RT-DC. Whole blood and isolated neutrophils were measured at time of venepuncture in comparison to blood incubated at room temperature in collection tubes for 30 minutes post-venepuncture.

All parameter readouts are of similar magnitude when comparing isolated neutrophils versus whole blood neutrophils (**Fig 10A-C**). Importantly, there was no difference between immediate processing and 30 minutes delay. Up to 30 minutes time from venesection to sample retrieval for analysis was therefore eliminated as a variable which might contribute to changes in size, deformability, and elasticity.

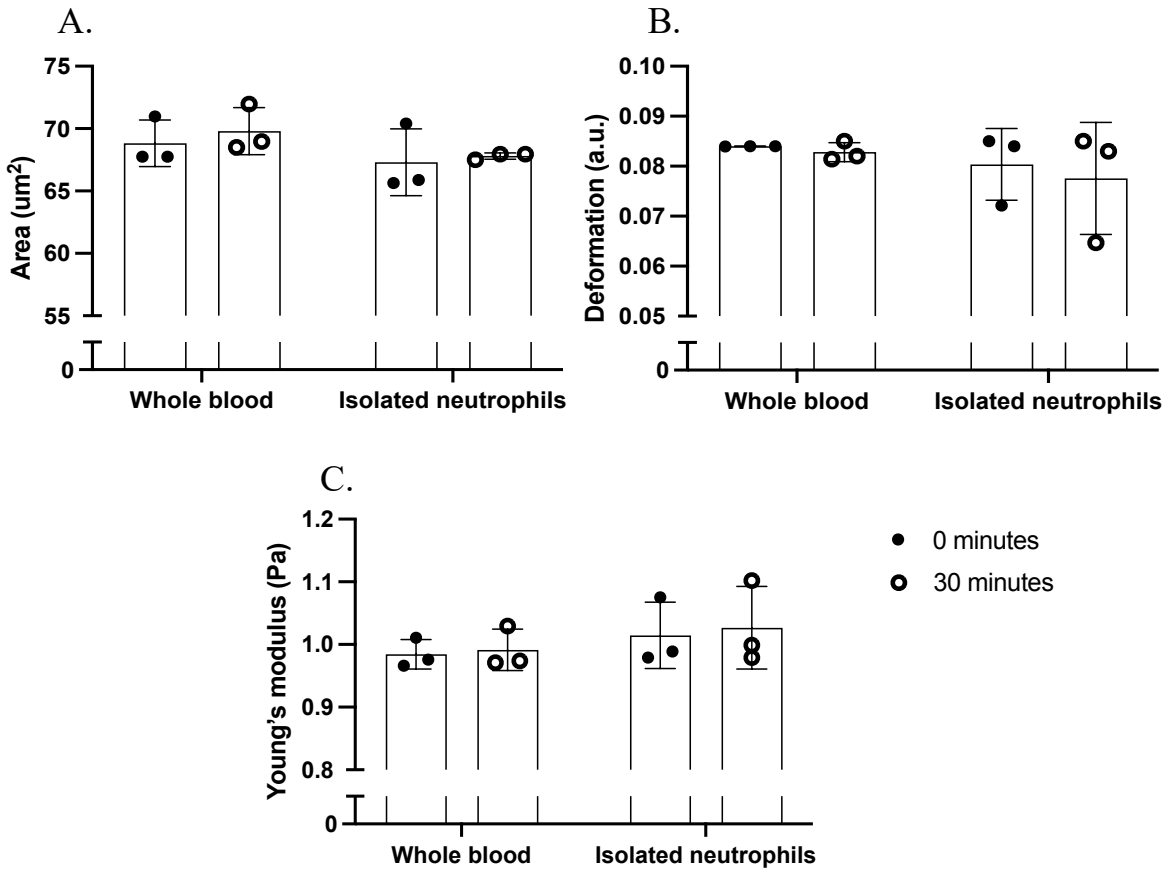


Figure 10. Time post-venepuncture does not alter neutrophil mechanophenotype
(A-C) Neutrophils in whole blood from HC (n=3) were analysed using RT-DC at time of venepuncture and 30 minutes post venepuncture. Neutrophils were isolated either at time of venepuncture of after 30 minutes delay followed by immediate and analysis using RT-DC. Neutrophil populations were gated and analysed for (A) Cell size, (B) Cell deformability, and (C) Elasticity. More than 1000 events were recorded for each sample and results were visualised and analysed in ShapeOut2 software. Data are shown as mean +/- SEM, statistical analysis was performed using Mann-Whitney test.

3.2.4. Neutrophil deformability is not altered by cell culture media calcium concentration

Previous studies have shown the influence of calcium regulation and signalling on neutrophil cytoskeletal rearrangement (239). I assessed if calcium concentration influenced neutrophil deformability at baseline by comparing media with different calcium concentrations: IMDM (1.49 mM) and RPMI (0.42 mM). Untreated isolated neutrophils resuspended in serum free IMDM or RPMI were analysed using RT-DC at 15 minutes or 60 minutes after isolation.

No significant changes in RT-DC parameters of untreated neutrophils were seen between different media suspensions at either time point (**Fig 11A-C**; ns). This data indicates that increased media calcium content does not alter untreated neutrophil mechanophenotype. As media calcium content did not alter neutrophil mechanophenotype and majority of experiments would be performed in suspension culture, future experiments were carried out utilising RPMI.

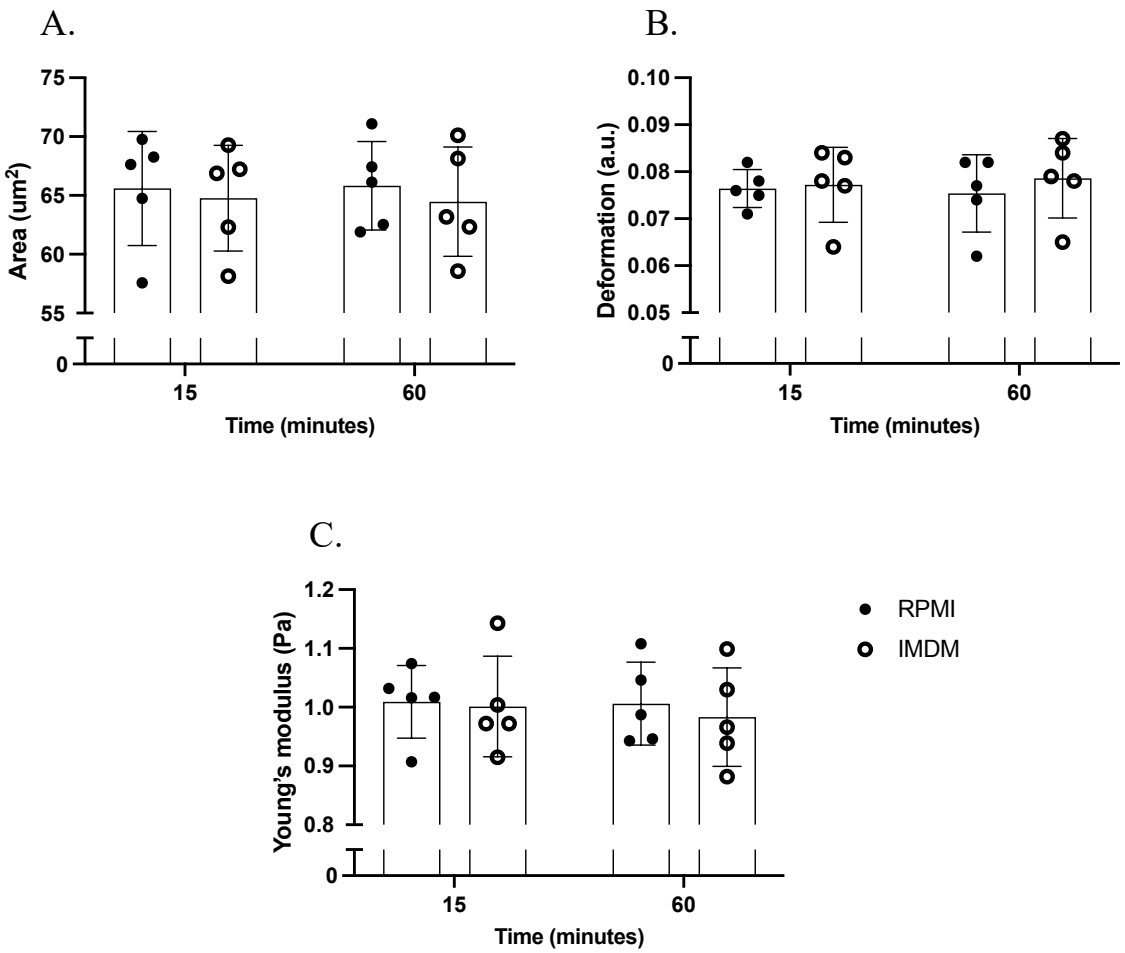


Figure 11. Neutrophil deformability is not altered by media calcium concentration
(A-C) Neutrophils from HC (n=5) were isolated, incubated in RPMI or IMDM for 15 minutes or 60 minutes, and analysed using RT-DC. Neutrophil populations were gated and analysed for (A) Cell size, (B) Cell deformability, and (C) Elasticity. More than 1000 events were recorded for each sample and results were visualised and analysed in ShapeOut2 software. Data are shown as mean +/- SEM, statistical analysis was performed using Mann-Whitney test..

3.2.5. Low dose TNF priming does not alter neutrophil deformability

Stimulation with TNF has been reported to impact neutrophil function, with increasing doses of TNF stimulation resulting in generation of ROS (Wright et al., 2010). Priming of neutrophils is required prior to stimulation with ANCA IgG to elicit a robust stimulation response, and low-dose TNF (2ng/mL) is commonly used in many published studies as a priming agent that is relevant to AAV (519–521). Previous work has shown some priming agents LPS and PAF can alter RT-DC parameters, although TNF was not studied (41). It was important to understand if TNF priming influenced mechanophenotype so the effect of ANCA could be examined. I therefore compared the effect of two concentrations of TNF: 2 ng/mL, which I planned to use in ANCA IgG stimulation experiments, and 20 ng/mL, to examine the effect on morphorheological characteristics using RT-DC.

Neither TNF concentration had a significant effect on neutrophil size, deformability, or elasticity (**Fig 12**). As the sole purpose of TNF in this set of experiments is to prime neutrophils, which is known to be achieved using low dose TNF (2 ng/mL), this concentration was used in the remainder of experiments.

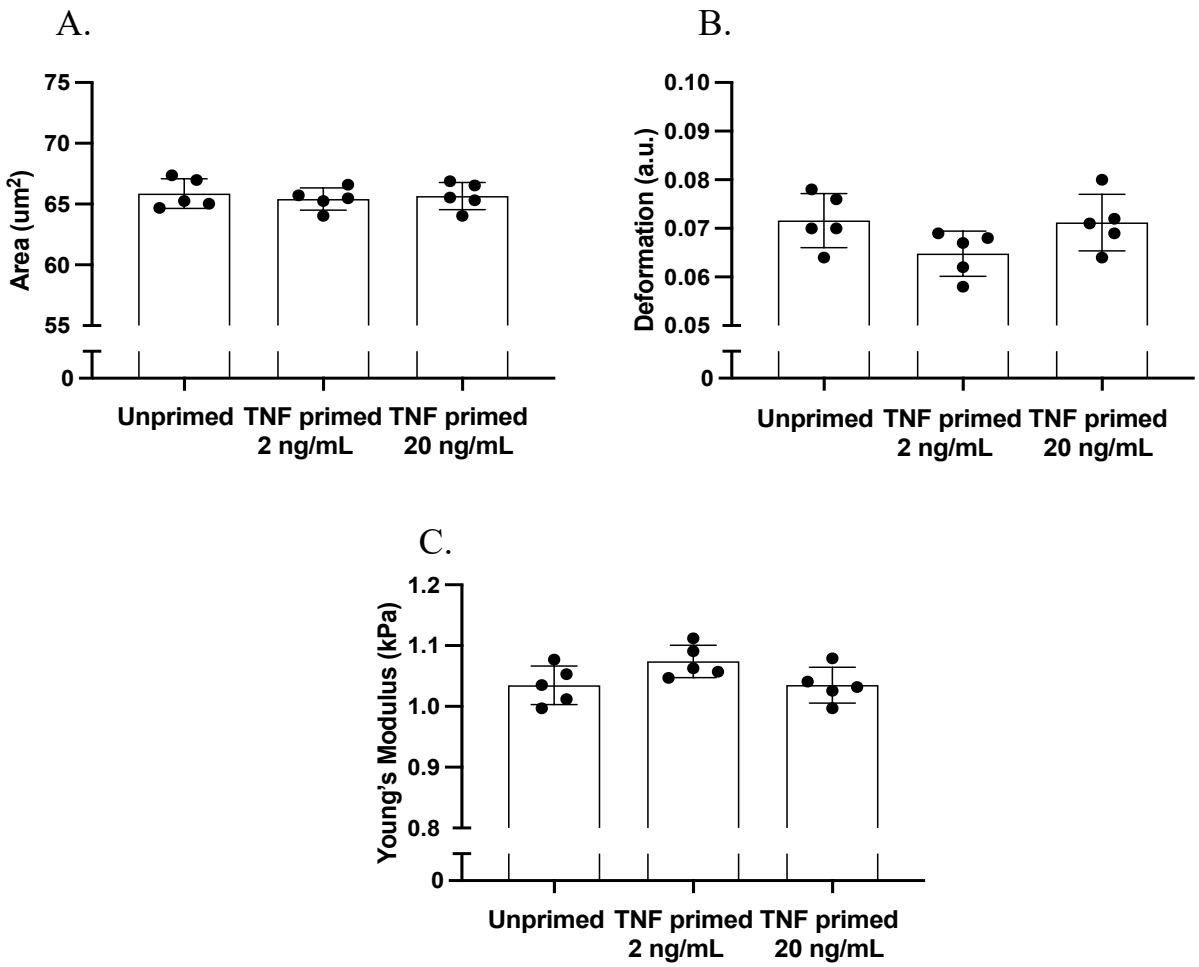


Figure 12. Low-dose TNF priming does not alter neutrophil deformability
(A-C) Neutrophils from HC (n=5) were isolated, primed with 2 ng/mL or 20 ng/mL TNF for 15 minutes, and analysed using RT-DC. Neutrophil populations were gated and analysed for (A) Cell size, (B) Cell deformability, and (C) Elasticity. More than 1000 events were recorded for each sample and results were visualised and analysed in ShapeOut2 software. Data are shown as mean +/- SEM, statistical analysis was performed using Kruskal-Wallis test, with Dunn's multiple comparisons test.

3.3. Neutrophil pathogenic responses following stimulation with ANCA

ANCA IgG stimulation of neutrophils has been described to induce cytokine release, ROS production, and NETosis (289,393). To ensure the ANCA I isolated were pathogenic, two of these responses were investigated; IL-8 production and NETosis.

3.3.1. MPO- and PR3-ANCA increases neutrophil IL-8 secretion

IL-8 is a key chemoattractant of neutrophils, shown to be upregulated in serum from patients with aAAV and present in kidney tissue of patients with AAV associated GN (327). To confirm the ANCA IgG I isolated were pathogenic, IL-8 secretion from neutrophils was measured over a time-course of ANCA stimulation using ELISA. Neutrophils were primed with 2 ng/mL TNF (15 minutes) and stimulated with HC or MPO- or PR3- ANCA IgG for 15 minutes, 1h, 2h, 3h, or 4h.

IL-8 production peaked at 4h stimulation (**Fig 13A**; ns) and was higher in MPO-/PR3-ANCA IgG stimulated cells compared to untreated at all timepoints. As for many of my experimental protocols, I planned to use 1h stimulation time course. I thereafter measured in a shorter time course of 15 minutes and 1h stimulation identifying significant IL-8 secretion in MPO-ANCA or PR3-ANCA stimulated cells in comparison to untreated at 1h (**Fig 13B**; MPO: $p=0.0012$, PR3: $p=0.0150$). These results confirmed that for techniques where a shorter time course is optimal for technical reasons, 1h of MPO- or PR3-ANCA IgG stimulation is sufficient to induce significant neutrophil activation.

Although IL-8 secretion from cells stimulated with PR3-ANCA for 1h was not significantly different to MPO-ANCA, the magnitude of change compared to untreated cells was lower for

PR3-ANCA (**Fig 13B)**. Thus, comparing ANCA subtypes, MPO-ANCA significantly induces greater IL-8 secretion from neutrophils at 15 minutes and 1h (**Fig 13B**; 15 minutes: p=0.0149, 1h: p=0.0012).

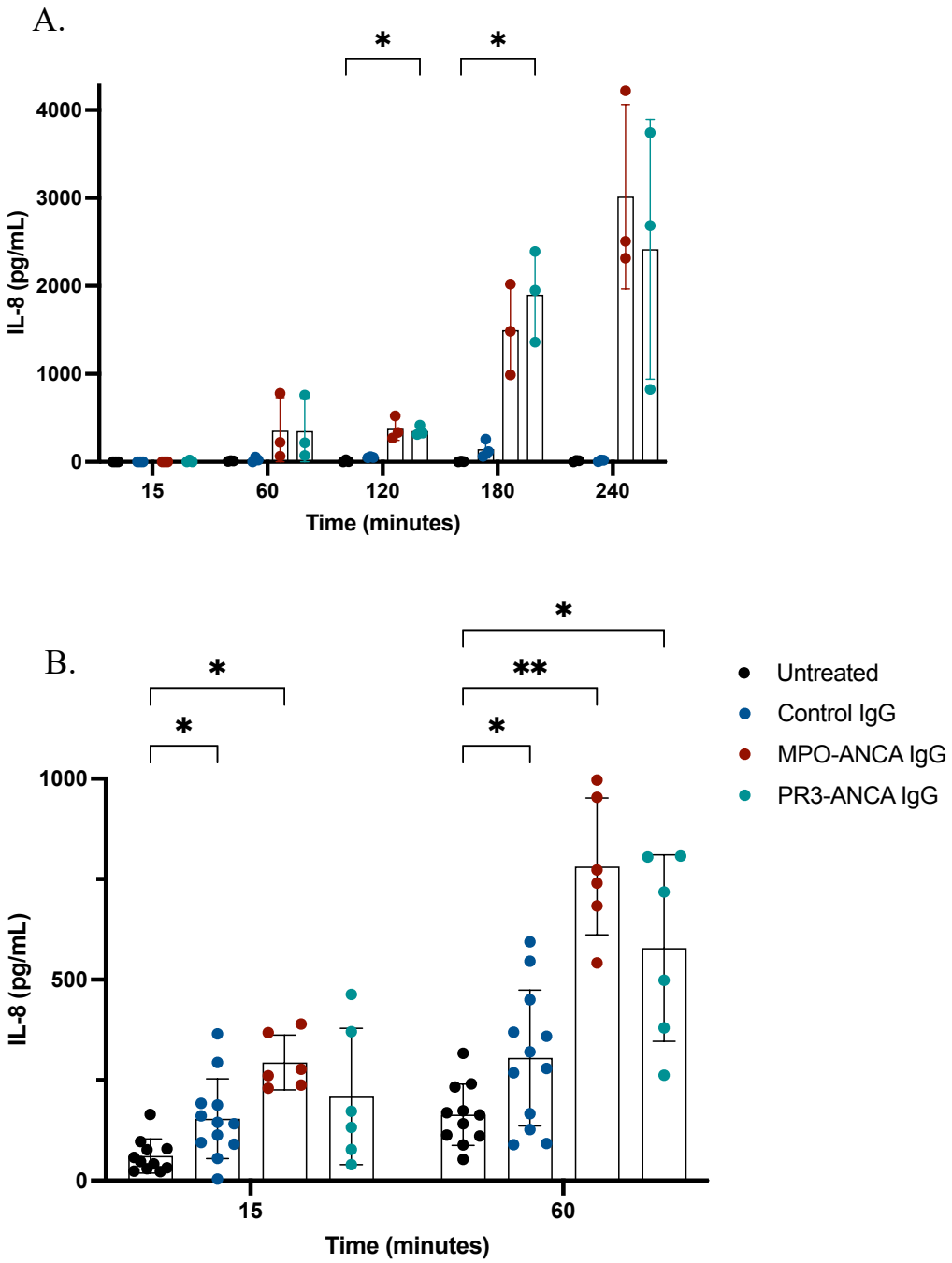


Figure 13. ANCA induced IL-8 secretion

(A) Isolated neutrophils from HC (n=3) were untreated with media only (neutrophil culture media, 'untreated') or primed with 2 ng/mL TNF (15 minutes) and stimulated with 100 µg/mL HC IgG, MPO-ANCA IgG for 1h or 4h. (B.) Isolated neutrophils from HC were untreated with media only (neutrophil culture media, 'untreated') (n=12) or primed with 2 ng/mL TNF (15 minutes) and stimulated with 100 µg/mL HC IgG (n=12), MPO-/PR3-ANCA IgG (n=6) for 15 minutes, or 1h. Untreated and HC IgG data points were pooled from MPO- and PR3-ANCA experiments. SN IL-8 content was measured by ELISA. Data are shown as mean +/- SEM, statistical analysis was performed using Kruskal-Wallis test, with Dunn's multiple comparisons test; *p<0.05 **p<0.01 ***p<0.001 ****p<0.0001.

3.3.2. Increased NET production in ANCA stimulated neutrophils

Increased NET formation occurs when neutrophils are exposed to pathogenic ANCA IgG, and measurement of NET formation can be used to determine pathogenicity of purified IgG (317). To visualise NET formation, neutrophils were primed with 2 ng/mL TNF (15 minutes) and stimulated with HC or MPO- or PR3- ANCA IgG for 4h and stained for H3Cit, a marker of NET formation, using immunofluorescence (522).

Minimal NET formation was shown in untreated neutrophils (representative images shown in **Fig 14A**). Upon visual inspection, there was a substantial increase in NET production in both MPO- and PR3-ANCA IgG stimulated neutrophils, in comparison to untreated neutrophils, and to HC IgG stimulated neutrophils (**Fig 14A-D**). While some NETs were present in HC IgG stimulated neutrophils, this was to a much lesser degree than seen following ANCA stimulation, which displayed noticeably thicker and more confluent NETs (**Fig 14C and D**). Previous work has shown serum can inhibit NET formation in response to other stimuli such as LPS or calcium ionophores, but not in response to PMA. In my experiments using ANCA, the addition of healthy serum to culture media when using 10% RPMI with Human AB serum, serum did not inhibit NET formation (523). Consideration of how NETosis may contribute to other experimental findings is discussed in future sections.

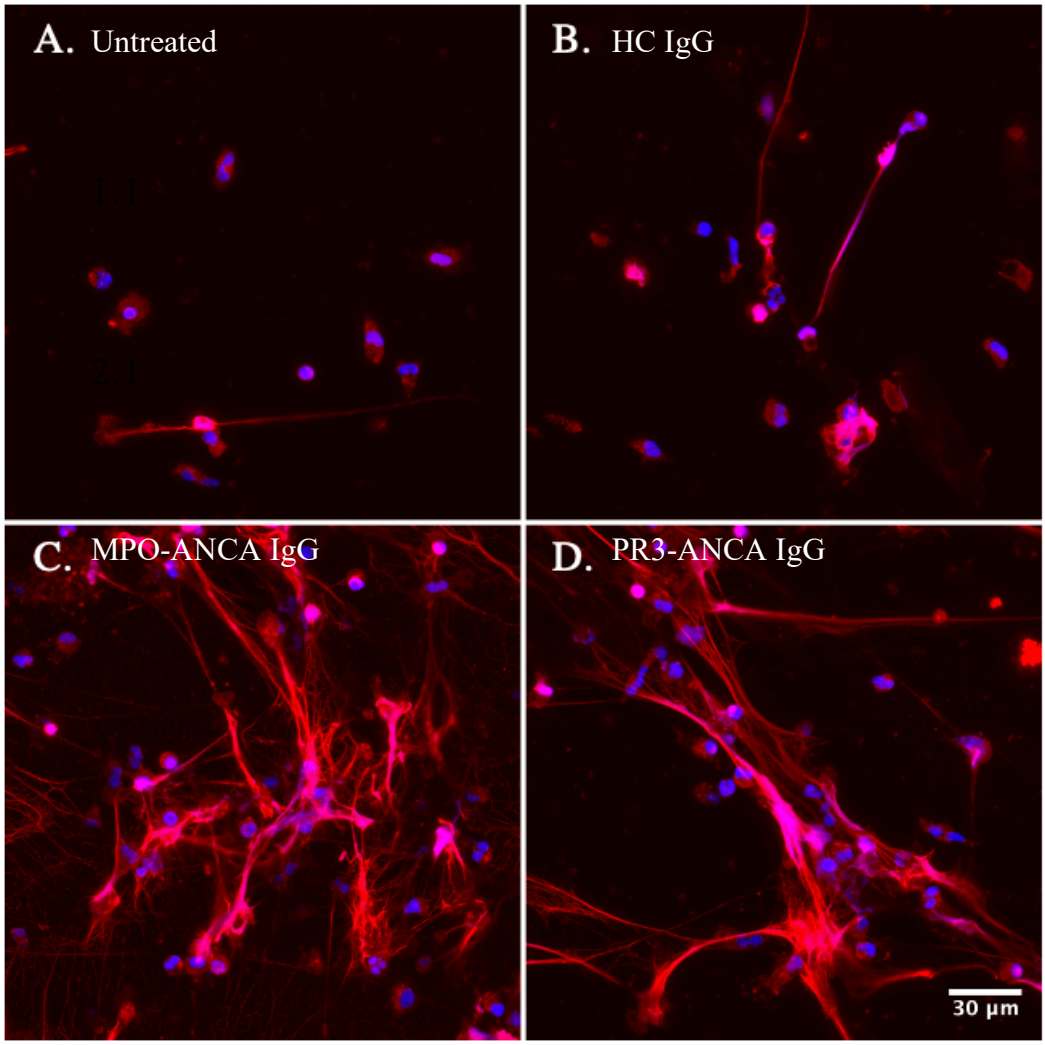


Figure 14. Increased NET production in ANCA simulated neutrophils
Isolated neutrophils from HC were untreated with media only (neutrophil culture media, 'untreated') or primed with 2 ng/mL TNF for 15 minutes and stimulated with 100 µg/mL HC IgG, MPO- or PR3-ANCA IgG for 4h (A) Untreated, (B) HC IgG, (C) MPO-ANCA IgG, and (D) PR3-ANCA IgG. Neutrophils were fixed, stained for H3Cit (red) (AF647), mounted with VectaShield[R] Antifade Mounting Medium with DAPI (blue), and imaged at 20x using an inverted Zeiss LSM-780. Representative images from n=10 experiments are shown.

3.4. Effect of ANCA on neutrophil mechanophenotype

Once the pathogenic effect of purified ANCA upon neutrophils was established, I investigated the effect of ANCA stimulation on neutrophil mechanophenotype using RT-DC.

3.4.1. Neutrophil deformability decreases over time

To assess ANCA stimulation on neutrophil mechanophenotype over time using RT-DC, a 4h time course experiment was performed. Neutrophils were primed with 2 ng/mL TNF (15 minutes) and stimulated with HC or MPO-ANCA-IgG for 15 minutes, 1h, 2h, 3h, or 4h.

There was sequential decrease in cell size and deformability from 1h onwards under all conditions suggesting this was a non-specific effect of prolonged neutrophil culture (**Fig 15**). The differences between stimulation conditions were not significant although changes in deformability were most marked in MPO-ANCA IgG stimulated cells (change of 0.006 and 0.011 a.u. from baseline in untreated and MPO-ANCA IgG stimulated neutrophils respectively) with a significant decrease in deformability from 15 minutes to 4h of stimulation (**Fig 15B**; p=0.0290). Following prolonged stimulation at 3h and 4h time points, ANCA stimulated neutrophils were more challenging to measure using RT-DC. Strands of material, which were thought to potentially be NETs, would block single cells flowing through the microfluidic channel. This is in keeping with the known effect of ANCA stimulation in inducing NETosis which I described in section 3.3.2. To prevent further interference from this variable, and to maintain technical feasibility, a 1h stimulation was used for further studies investigating the effect of ANCA IgG stimulation.

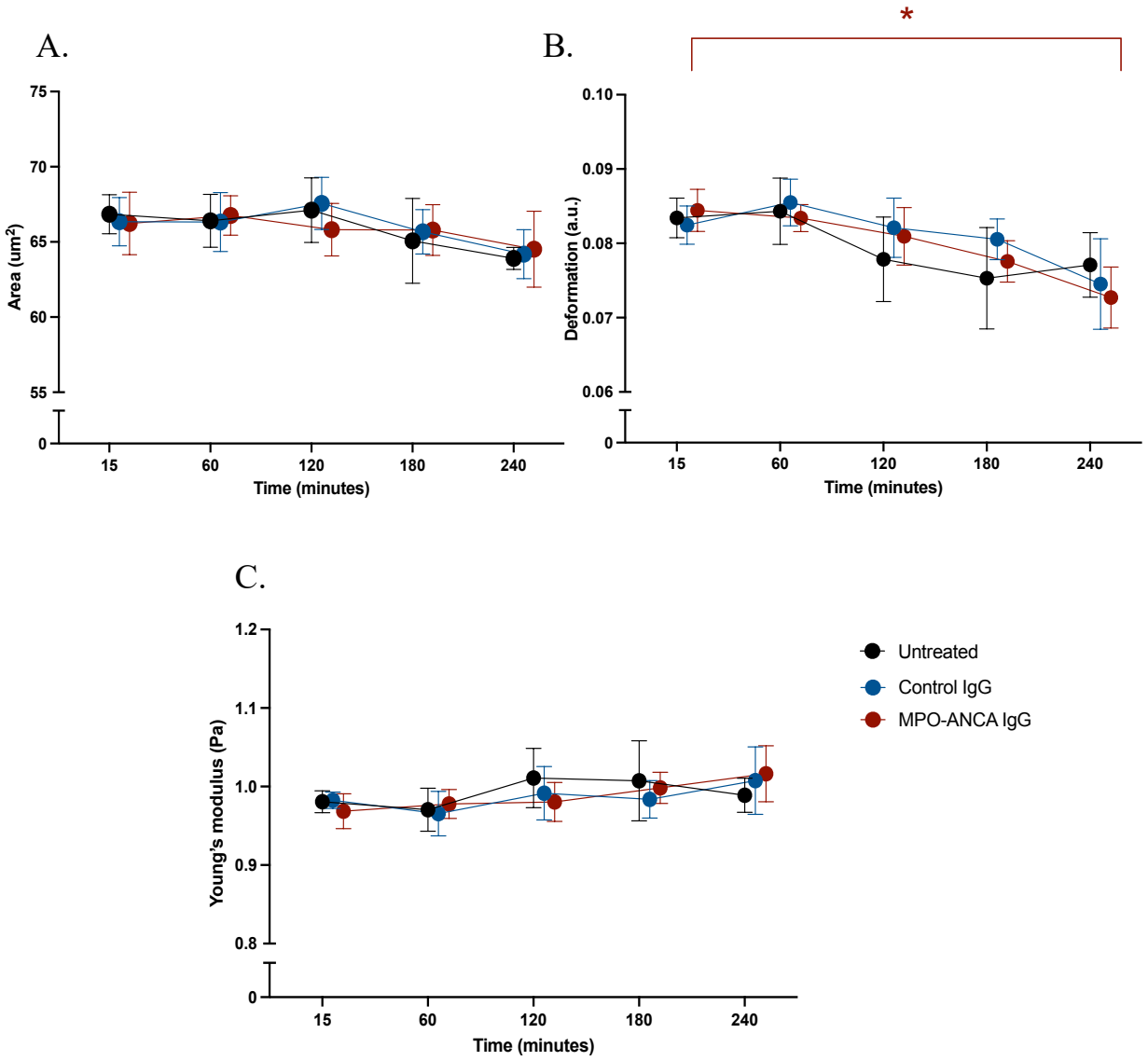


Figure 15. Neutrophil deformability decreases over time

(A-C) Neutrophils from HC (n=5) were untreated with media only (neutrophil culture media, 'untreated') or primed with 2 ng/mL TNF for 15 minutes and stimulated with 100 µg/mL HC IgG, MPO-ANCA IgG for 15 minutes, 1h, 2h, 3h, or 4h. Neutrophil populations were gated and analysed by RT-DC for (A) Cell size, (B) Cell deformability, and (C) Elasticity. More than 1000 events were recorded for each sample and results were visualised and analysed in ShapeOut2 software. Data are shown as mean +/- SEM, statistical analysis was performed using two-way ANOVA mixed effects model with Geisser-Greenhouse correction, with Tukey's multiple comparisons test; *$p<0.05$.

3.4.2. No difference between MPO- or PR3-ANCA stimulation on isolated neutrophil deformability

Clinical studies highlight the difference between ANCA serotype in disease pathogenesis (524). I measured whether there was a difference between pathogenic ANCA subtypes on neutrophil deformability by comparing MPO-ANCA and PR3-ANCA IgG stimulated neutrophils using RT-DC. Neutrophils were primed with 2 ng/mL TNF (15 minutes) and stimulated with HC IgG or MPO-/PR3-ANCA-IgG for 15 minutes or 1h.

The results suggest stimulation with MPO- or PR3-ANCA do not induce a decrease in neutrophil deformability compared to untreated neutrophils at 15 minutes and 1 hour. The data did not achieve significance and similar results were also seen with HC IgG by 1h (**Fig 16**). While MPO- and PR3-ANCA may have different effects on other processes in AAV disease pathogenesis, ANCA subtypes do not differ in their effects on isolated neutrophil biomechanics.

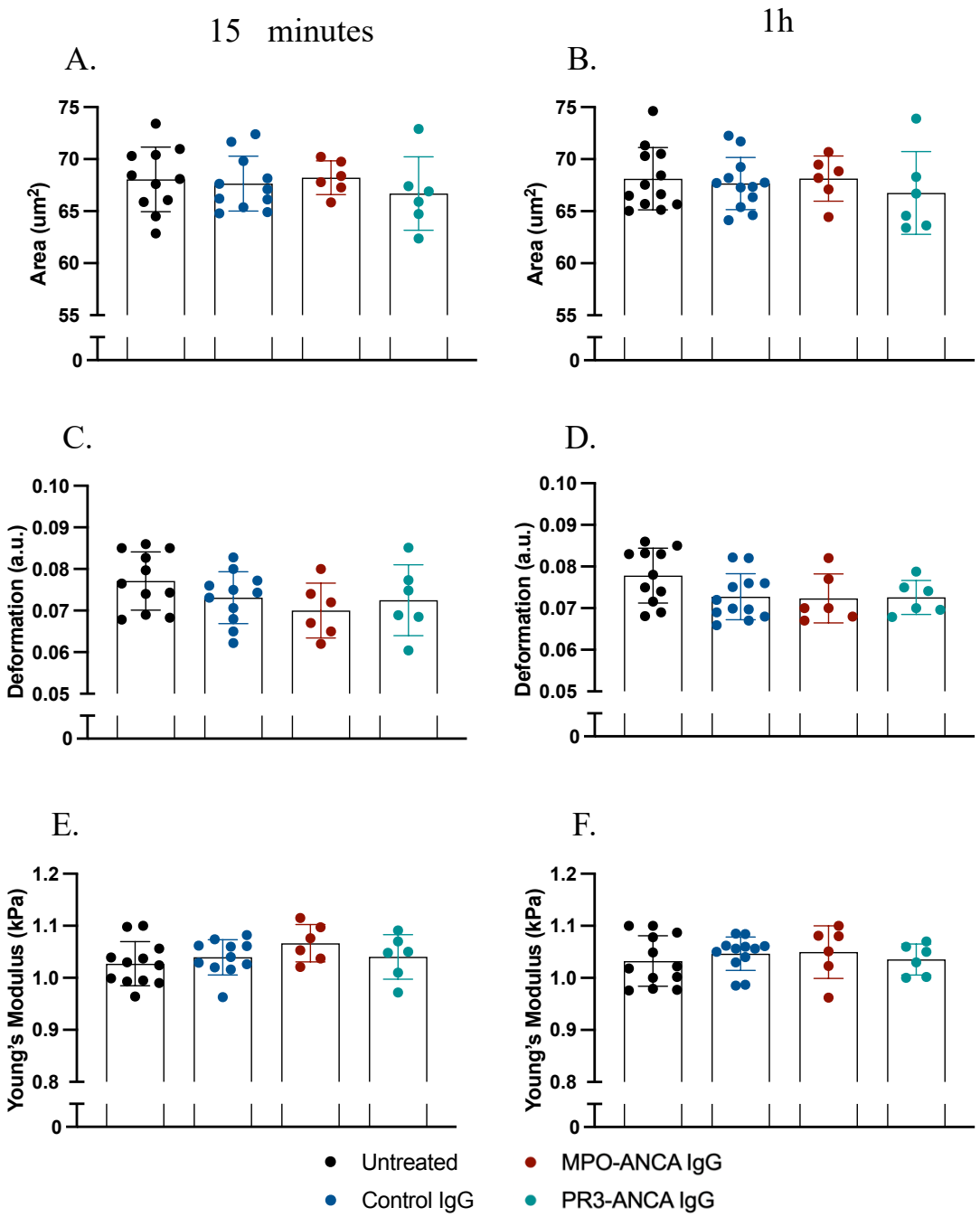


Figure 16. No difference between MPO- or PR3-ANCA stimulation on isolated neutrophil deformability

(A-F) Isolated neutrophils from HC (n=6) were untreated with media only (neutrophil culture media, 'untreated') or primed with 2 ng/mL TNF for 15 minutes and stimulated with 100 ug/mL HC IgG, MPO-/PR3-ANCA IgG for 15 minutes (A/C/E) or 1h (B/D/F) and analysed using RT-DC. Untreated and HC IgG data points were pooled from MPO- and PR3-ANCA experiments. Neutrophil populations were gated and analysed for (A/B) Cell size, (C/D) Cell deformability, and (E/F) Elasticity. More than 1000 events were recorded for each sample and results were visualised and analysed in ShapeOut2 software. Data are shown as mean +/- SEM, statistical analysis was performed using two-way ANOVA mixed effects model with Geisser-Greenhouse correction, with Tukey's multiple comparisons test.

3.5. Whole blood treatment with ANCA

3.5.1. Increased IL-8 secretion in whole blood treated with MPO-ANCA

It is possible that neutrophil isolation was a confounding factor in my results investigating the biomechanical phenotype of neutrophils following ANCA stimulation (section 3.4.2.). As such, I next investigated if neutrophils in whole blood exhibited changes in deformability when treated with ANCA as this may be more physiologically relevant. To ensure ANCA stimulation remained pathogenic in this experimental protocol, IL-8 release was investigated as this is well characterised in isolated cells. Whole blood was treated with 2 ng/mL TNF (15 minutes) and then with HC IgG or MPO-ANCA-IgG for 1h. IL-8 secretion in serum from whole blood stimulation was measured using ELISA.

There was little to no IL-8 secretion in untreated or HC IgG treated whole blood. HC IgG treated whole blood exhibited minimal IL-8 secretion. MPO-ANCA IgG treated whole blood displayed a significant increase in IL-8 secretion in comparison to untreated whole blood (**Fig 17;** $p=0.0001$). Overall, these results indicate that ANCA can exert a similar pathogenic effect in this whole blood experimental protocol as compared to isolated cells.

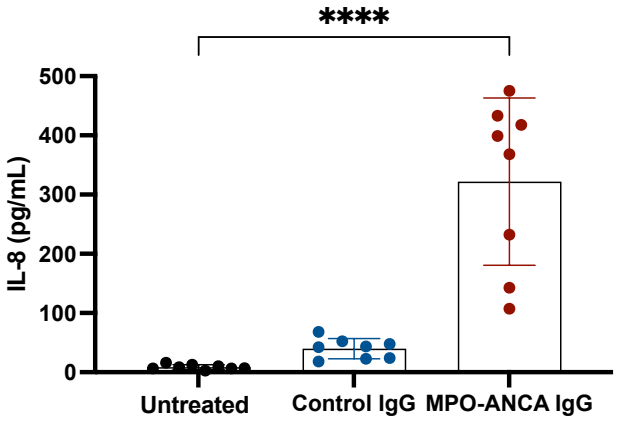


Figure 17. MPO-ANCA promotes IL-8 secretion in serum following whole blood stimulation

Whole blood from HC (n=8) was untreated or treated with 2 ng/mL TNF (15 minutes) and treated with 100 µg/mL HC IgG, MPO-ANCA IgG, or untreated for 1h. Serum IL-8 content was measured by ELISA. Data are shown as mean +/- SEM, statistical analysis was performed using Kruskal-Wallis test, with Dunn's multiple comparisons test; ****$p<0.0001$.

3.5.2. Neutrophil deformability decreases in whole blood stimulated with MPO-ANCA

To eliminate the effect of cell preparation on ANCA induced responses, whole blood treated with HC IgG or MPO-ANCA IgG was analysed using RT-DC. Whole blood was primed with 2 ng/mL TNF (15 minutes) and treated with HC or MPO-ANCA IgG for 1h.

There was a significant decrease in neutrophil deformability in whole blood treated with ANCA IgG in comparison to untreated (**Fig 18**; p=0.0365) and a significant increase in elastic modulus (**Fig 18**; p=0.0291). The change in deformability in whole blood neutrophils between conditions was greater than that seen in isolated neutrophils. This suggests that either isolation method may be impacting cell deformability, or that a more representative physiological environment *ex vivo* results in a greater neutrophil response (**Fig 18**).

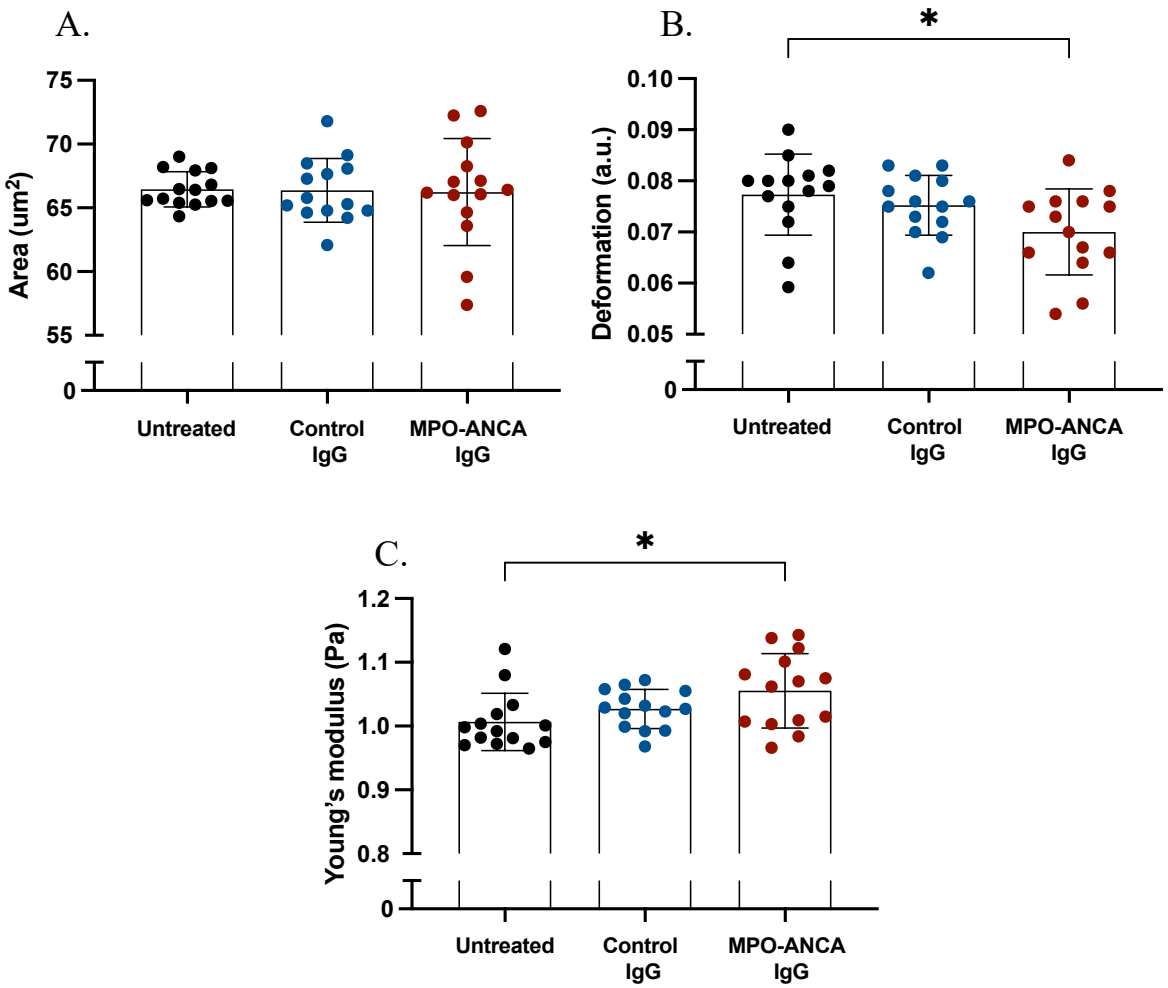


Figure 18. Neutrophil deformability decreases in whole blood stimulated with MPO-ANCA (A-C) Whole blood from HC (n=14) was primed with 2 ng/mL TNF for 15 minutes, treated with 100 µg/mL HC IgG or MPO-ANCA IgG for 1h, and analysed using RT-DC. Neutrophil populations were gated and analysed for (A) Cell size, (B) Cell deformability, and (C) Elasticity. More than 1000 events were recorded for each sample and results were visualised and analysed in ShapeOut2 software. Data are shown as mean +/- SEM, statistical analysis was performed using one-way ANOVA Kruskal-Wallis test, with Dunn's multiple comparisons test; *$p<0.05$.

3.6. Increase in actin polymerisation in MPO/PR3-ANCA stimulated neutrophils

3.6.1. MPO/PR3-ANCA promotes actin polymerisation in HC stimulated neutrophils

My previous results have established that pathogenic ANCA stimulation alters neutrophil deformability in whole blood (section 3.5.2.). To determine if ANCA induced cytoskeletal changes could explain decreased cell deformability, isolated HC neutrophils were stimulated with ANCA followed by measurement of actin polymerisation using Phalloidin immunofluorescence staining for F-actin. Neutrophils were primed with 2 ng/mL TNF (15 minutes), stimulated with HC or MPO-/PR3-ANCA IgG for 1h, fixed, and stained for F actin using phalloidin immunofluorescence.

Representative images shown in **Figure 19** display a visually brighter stain, extended protrusion formation, and distorted cell shape in MPO-/PR3-ANCA stimulated neutrophils in comparison to untreated and HC IgG. Untreated and HC IgG stimulated neutrophils exhibit minimal Phalloidin staining. Actin "caps" (focal areas of polymerised actin) are present in ANCA and HC IgG stimulated neutrophils but not in untreated cells. Other variables and cytoskeletal protrusions were quantified using a macro. Phalloidin staining measures and represents the F-actin signal. The area and perimeter of each cell were quantified utilising Phalloidin stain. The total cell area staining for Phalloidin was quantified relative to the area of each measured cell, and the total cell perimeter staining for Phalloidin was quantified relative to the perimeter of each measured cell. These variables are individually referred to as area, perimeter, relative area, and relative perimeter.

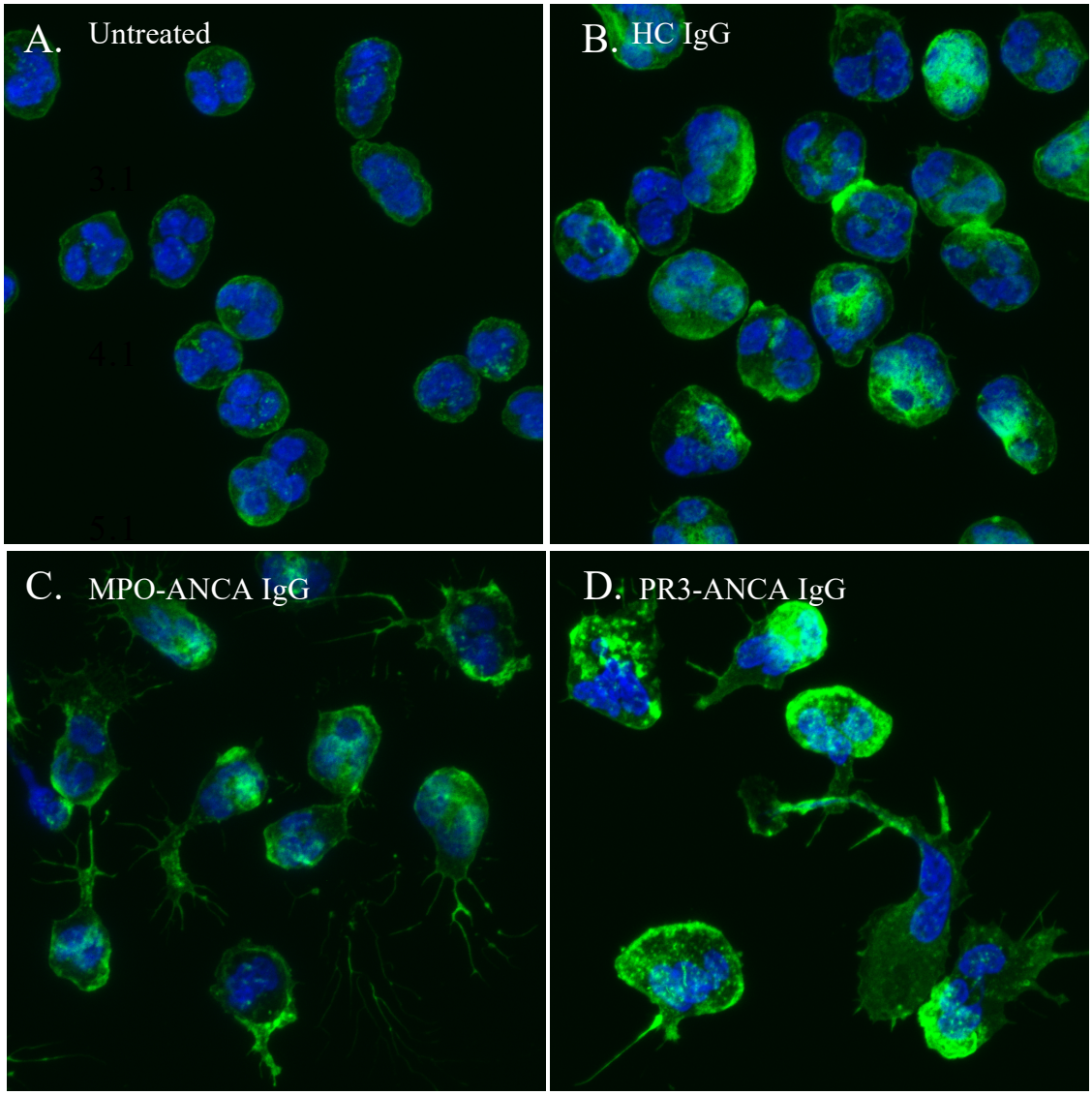


Figure 19. MPO/PR3-ANCA stimulation promotes actin polymerisation in HC neutrophils (A-D) Neutrophils from HC were isolated, untreated with media only (neutrophil culture media, 'untreated') or primed with 2 ng/mL TNF (15 minutes) and stimulated with 100 µg/mL HC IgG, MPO-ANCA IgG (n=30), PR3-ANCA IgG (n=16) for 1h. Neutrophils were fixed, stained with Phalloidin (F actin, AF488, green), and mounted with VectaShield[R] Antifade Mounting Medium with DAPI (nucleus, blue), and imaged at 63x using an inverted Zeiss LSM-780 (A) Untreated, (B) HC IgG, (C) MPO-ANCA IgG, and (D) PR3-ANCA IgG. Representative images from n=30 (MPO-ANCA IgG) or n=16 (PR3-ANCA IgG) experiments are shown.

An increase in area was seen in HC neutrophils when stimulated with MPO-ANCA or PR3-ANCA in comparison to untreated neutrophils (**Fig 20A**; MPO p=0.0002, PR3 p=0.0001). Similar results were seen for perimeter (**Fig 20B**; MPO p=0.0001, PR3 p=0.0001). However, the relative area and relative perimeter were only significantly increased in PR3-ANCA stimulated cells compared with untreated cells (**Fig 20C and D**; relative area p=0.0006, relative perimeter p=0.0006). On visual inspection, the changes of greater magnitude following PR3-ANCA stimulation compared to MPO-ANCA are likely due to larger cell protrusions and distortion of cell shape (representative images shown in **Fig 20**). All cells stained positively for F-actin as expected, but untreated and HC IgG stimulated neutrophils exhibited low intensity F-actin fluorescence, which was localised to the cell itself with no protrusions, in contrast to ANCA stimulated neutrophils. Increased F-actin, and cytoskeletal protrusions could result in not only a deformed cytoskeleton, but increased stiffness of the cell as well.

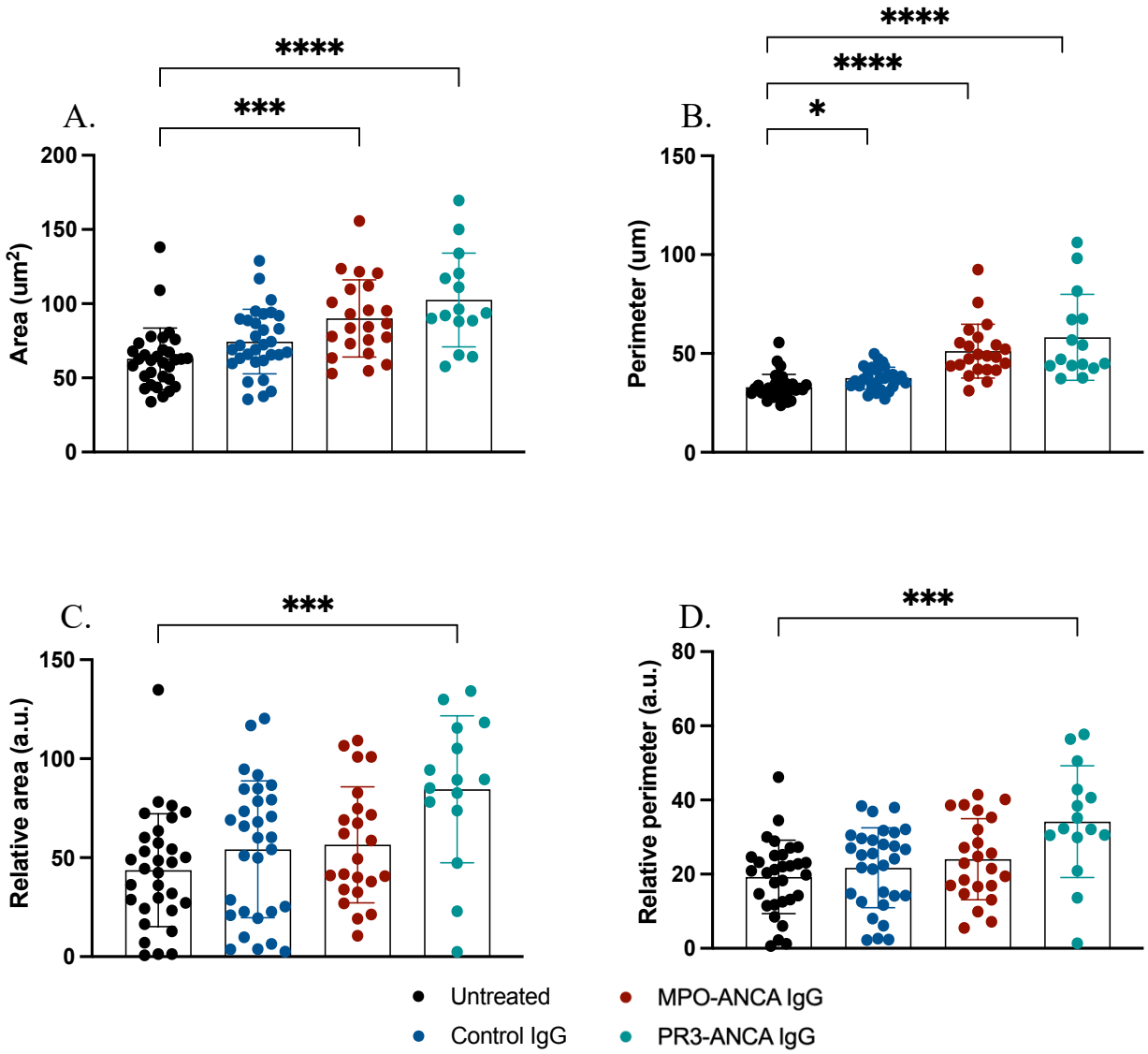


Figure 20. MPO/PR3-ANCA promotes actin polymerisation in HC stimulated neutrophils (A-D) Neutrophils in whole blood from HC were isolated, untreated with media only (neutrophil culture media, 'untreated') or primed with 2 ng/mL TNF (15 minutes) and stimulated with 100 µg/mL HC IgG, MPO-ANCA IgG (n=30), PR3-ANCA IgG (n=16) for 1h. Neutrophils were fixed, stained with Phalloidin (F actin, AF488, green), and mounted with VectaShield[R] Antifade Mounting Medium with DAPI (nucleus, blue), and imaged at 63x using an inverted Zeiss LSM-780 (A) Area, (B) Perimeter, (C) Relative area, and (D) Relative perimeter. Data was analysed using a macro developed for use with ImageJ to measure area, perimeter, relative area, and relative perimeter. Data are shown as mean +/- SEM, statistical analysis was performed using Kruskal-Wallis test, with Dunn's multiple comparisons test; *p<0.05 **p<0.01 ***p<0.001. ****p<0.00001.

3.7. Effect of inhibitors of cytoskeletal remodelling on ANCA mediated neutrophil actin polymerisation

3.7.1. Cytochalasin D best inhibits ANCA induced actin polymerisation

Having shown ANCA IgG stimulation resulted in increased actin polymerisation and filopodia formation, I investigated whether this could be inhibited using a range of cytoskeletal inhibitors. Para-aminoblebbistatin, blebbistatin, cytochalasin B and D were chosen for treatment. Inhibitors were diluted in neutrophil media and incubated with cells for 10 minutes after priming and prior to the addition of IgG. Inhibitor mechanisms and concentrations used are detailed in **Table 21**. Stimulated neutrophils were treated with actin filament formation or myosin-ii inhibitors to determine if inhibition of either cytoskeletal element could affect ANCA-induced actin polymerisation. Neutrophils were primed with 2 ng/mL TNF (15 minutes), treated with one of the selected inhibitors (10 minutes), stimulated with HC or MPO-ANCA-IgG for 1h, fixed, and stained for Phalloidin using immunofluorescence.

None of the inhibitors used exerted any influence on the actin cytoskeleton in untreated cells; there was no significant change in any of the parameters measured (**Fig 21**, **Table 21**).

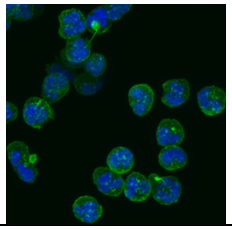
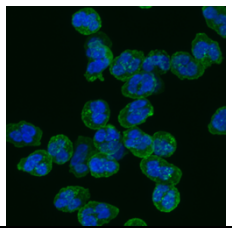
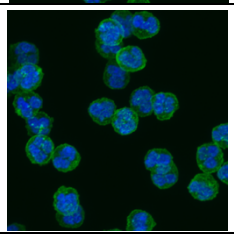
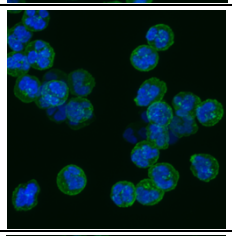
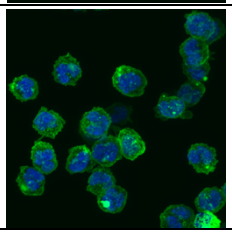
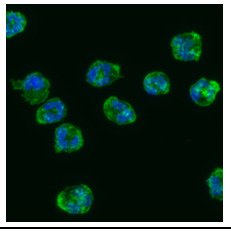
Inhibitor	Site of action	Concentration	Representative confocal image
Para-aminoblebbistatin	Inhibits myosin II A/B/C motor domains	50 μM	
Blebbistatin	Inhibits myosin II and myosin ATPase activity	100 μM	
Cytochalasin B	Binds to barbed end of F-actin filaments and inhibits building of filament network	10 μM	
Cytochalasin D	Binds to F-actin polymer and prevents actin monomer polymerisation	2 μM	
Cytochalasin D	Binds to F-actin polymer and prevents actin monomer polymerisation	20 μM	
DMSO	Vehicle		

Table 21. Cytoskeletal inhibitors
Neutrophils in whole blood from HC were isolated, untreated with media only (neutrophil culture media, 'untreated') or primed with 2 ng/mL TNF (15 minutes), treated with actin polymerisation inhibitors for 10 minutes at concentrations stated above, and incubated in media (neutrophil culture media) for 1h. Neutrophils were fixed, stained with Phalloidin (F actin, AF488, green), and mounted with VectaShield[R] Antifade Mounting Medium with DAPI (nucleus, blue), and imaged at 63x using an inverted Zeiss LSM-780. Representative images from n=6 experiments are shown.

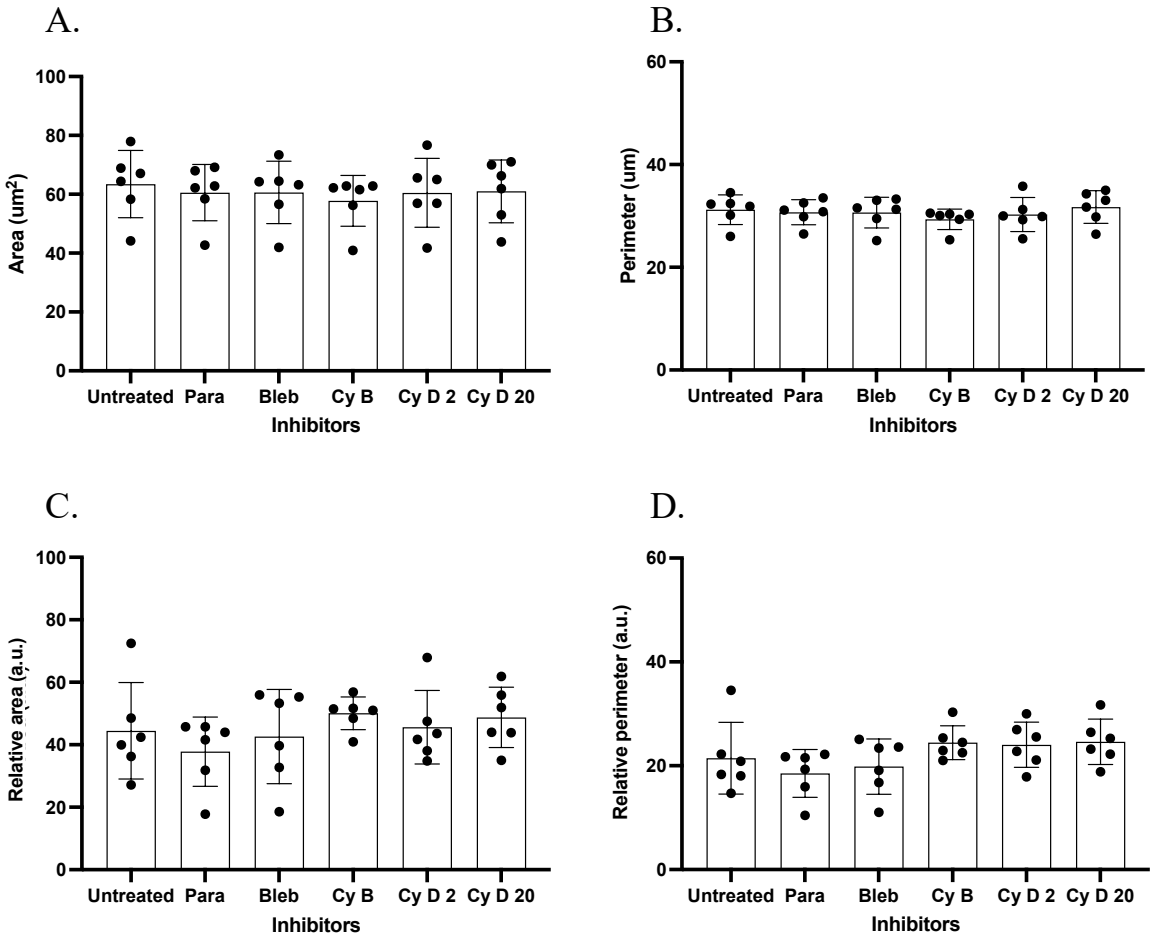


Figure 21. No change in parameters of untreated neutrophils with cytoskeletal inhibitors
Neutrophils in whole blood from HC (n=6) were isolated, untreated with media only (neutrophil culture media, 'untreated') or primed with 2 ng/mL TNF (15 minutes), treated with cytochalasin B 10µm, cytochalasin D 2µm, paraminoblebbistatin 50 µm, or blebbistatin 100µm, and incubated with media (neutrophil culture media) for 1h. Neutrophils were fixed, stained with Phalloidin (F actin, AF488, green), and mounted with VectaShield[R] Antifade Mounting Medium with DAPI (nucleus, blue), and imaged at 63x using an inverted Zeiss LSM-780 (A) Area, (B) Perimeter, (C) Relative area, and (D) Relative perimeter. Data was analysed using a macro developed for use with ImageJ to measure area, perimeter, relative area, and relative perimeter. Data are shown as mean +/- SEM, statistical analysis was performed using Kruskal-Wallis test, with Dunn's multiple comparisons test.

Inhibitors resulted in decreased MPO-ANCA induced cytoskeletal changes as measured by for area and perimeter, with the greatest magnitude of reduction in perimeter seen with cytochalasin D at 2 μM (representative images shown in **Fig 22**, **Fig 23**; p=0.0244) and the smallest effect on morphology seen with blebbistatin, where protrusions were still formed in ANCA stimulated neutrophils. Comparing the blebbistatins by visual inspection, para-aminoblebbistatin was more effective than blebbistatin with some protrusion formation seen in para-aminoblebbistatin treated ANCA neutrophils, but not as many as seen in blebbistatin treated ANCA neutrophils. On an observational level, cytochalasin B resulted in visually more rounded, circular cells. Cytochalasin D at 20 μM resulted in bleb-like formation around the cell in ANCA stimulated neutrophils, which has been reported to occur in untreated neutrophils as well (525), and therefore is unlikely to be related to ANCA stimulation. In comparison to the other inhibitors used, cytochalasin D at 2 μM had the greatest inhibitory effect. This suggests MPO-ANCA promotion of actin polymerisation may be inhibited through the elongation step of actin polymerisation.

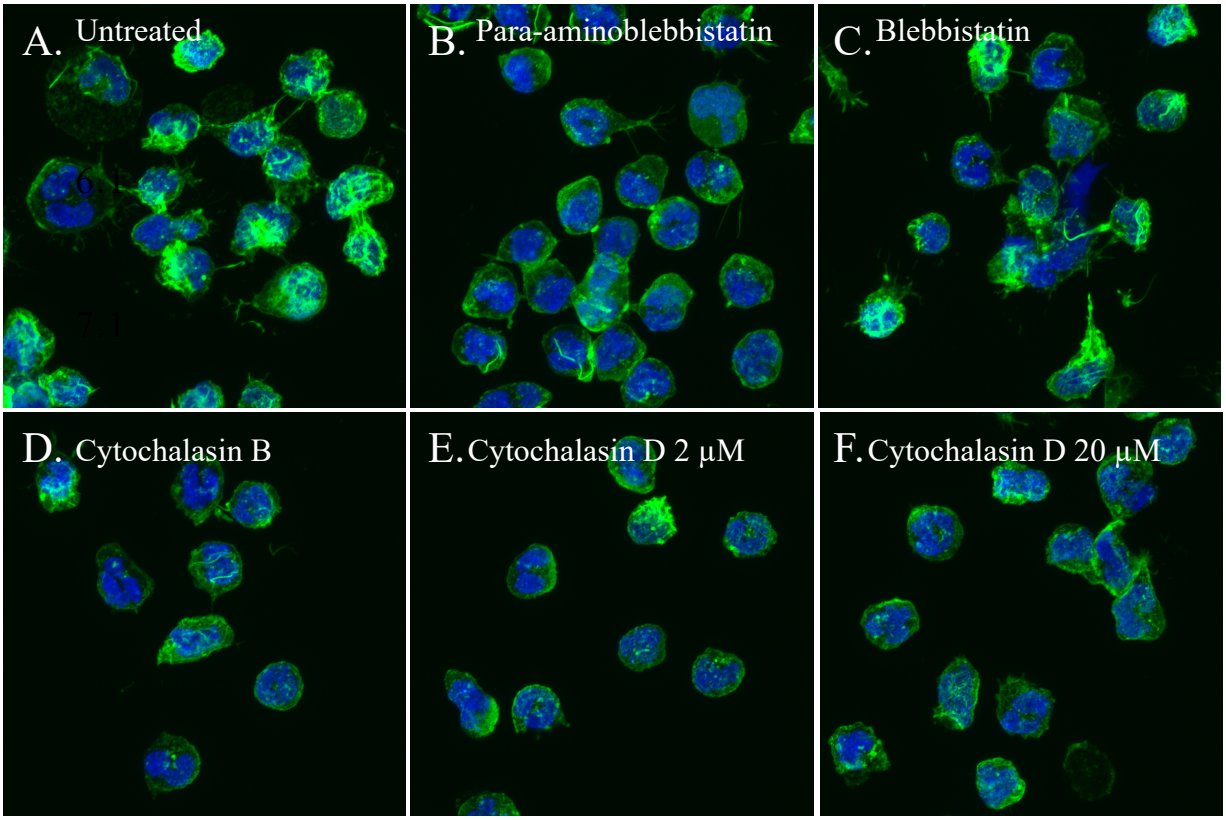


Figure 22. Inhibitors of cytoskeletal remodelling inhibit MPO-ANCA promotion of actin polymerisation in HC stimulated neutrophils

(A-D) Neutrophils in whole blood from HC (n=6) were isolated, untreated with media only (neutrophil culture media, 'untreated') or primed with 2 ng/mL TNF (15 minutes), treated with cytochalasin B 10µm, cytochalasin D 2µm, paraminoblebbistatin 50 µm, or blebbistatin 100µm for 10 minutes, and stimulated with 100 µg/mL HC IgG, or MPO-ANCA IgG for 1h. Neutrophils were fixed, stained with Phalloidin (F actin, AF488, green), and mounted with VectaShield[R] Antifade Mounting Medium with DAPI (nucleus, blue), and imaged at 63x using an inverted Zeiss LSM-780 (A) Untreated, (B) para-aminoblebbistatin, (C) blebbistatin, (D) cytochalasin B, (E) cytochalasin D 2 µM, and (F) cytochalasin D 20 µM. Images presented are MPO-ANCA stimulated conditions. Representative images from n=6 experiments are shown.

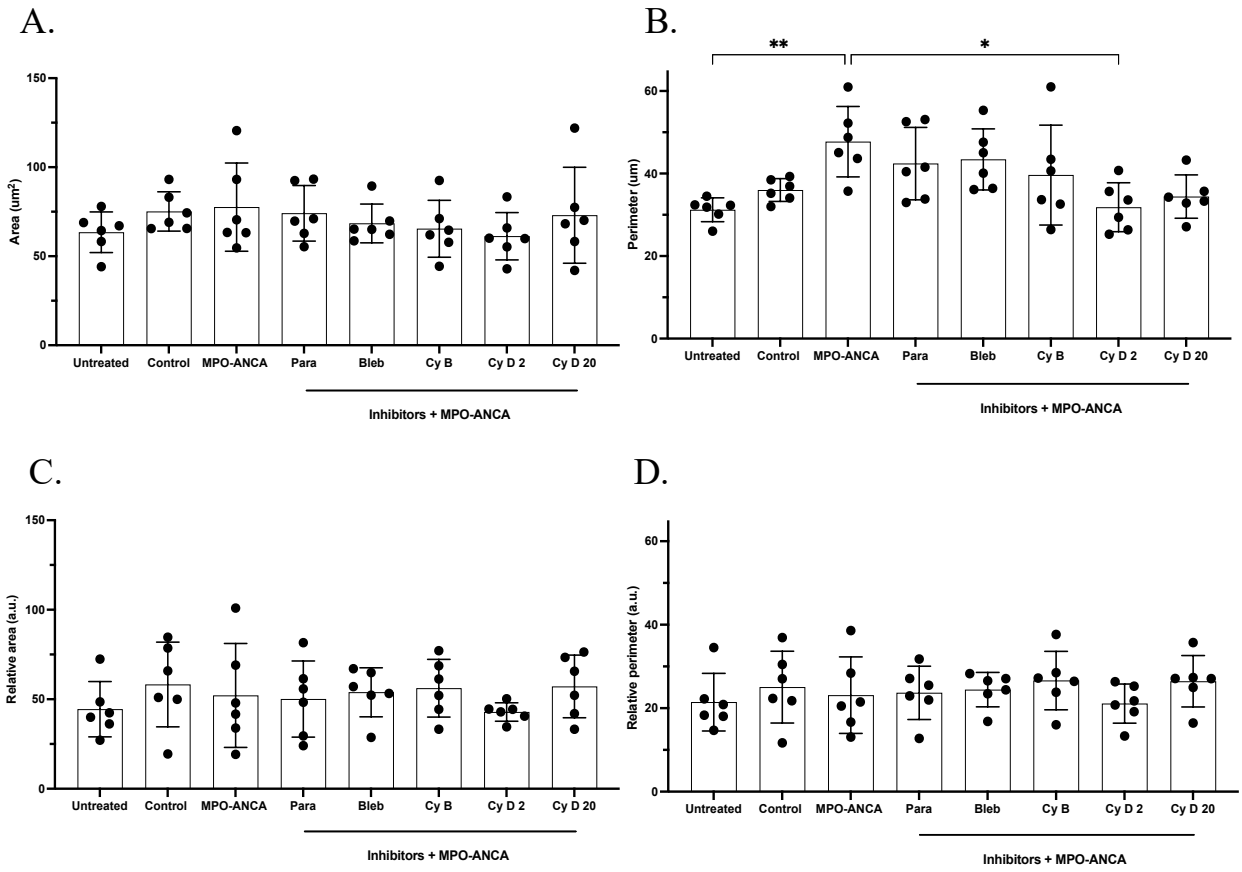


Figure 23. Cytochalasin D best inhibits ANCA promotion of actin polymerisation
Neutrophils in whole blood from HC (n=6) were isolated, untreated with media only (neutrophil culture media, 'untreated') or primed with 2 ng/mL TNF (15 minutes), treated with cytochalasin B 10µm, cytochalasin D 2µm, paraminoblebbistatin 50 µm, or blebbistatin 100µm for 10 minutes, and stimulated with 100 µg/mL HC IgG, or MPO-ANCA IgG for 1h. Neutrophils were fixed, stained with Phalloidin (F actin, AF488, green), and mounted with VectaShield[R] Antifade Mounting Medium with DAPI (nucleus, blue), and imaged at 63x using an inverted Zeiss LSM-780 (A) Area, (B) Perimeter, (C) Relative area, and (D) Relative perimeter. Data was analysed using a macro developed for use with ImageJ to measure area, perimeter, relative area, and relative perimeter. Data are shown as mean +/- SEM, statistical analysis was performed using Kruskal-Wallis test, with Dunn's multiple comparisons test; *p<0.05. **p<0.01.

3.7.2. No change in deformability in ANCA stimulated neutrophils treated with Cytochalasin B or D

Cytochalasin B and D were the inhibitors that had the greatest effect on actin polymerisation in ANCA stimulated neutrophils (section 3.7.1.). As such I selected these inhibitors for use in further experiments to investigate cell deformability using RT-DC. Isolated neutrophils were primed with 2 ng/mL TNF (15 minutes), treated with one of the selected inhibitors (10 minutes), and stimulated with HC or MPO-ANCA-IgG for 1h.

Examining neutrophils at baseline without exposure to ANCA IgG in comparison to untreated neutrophils, neither cytochalasin B nor cytochalasin D significantly altered neutrophil size, deformability, or elasticity (**Fig 24A-C**; ns).

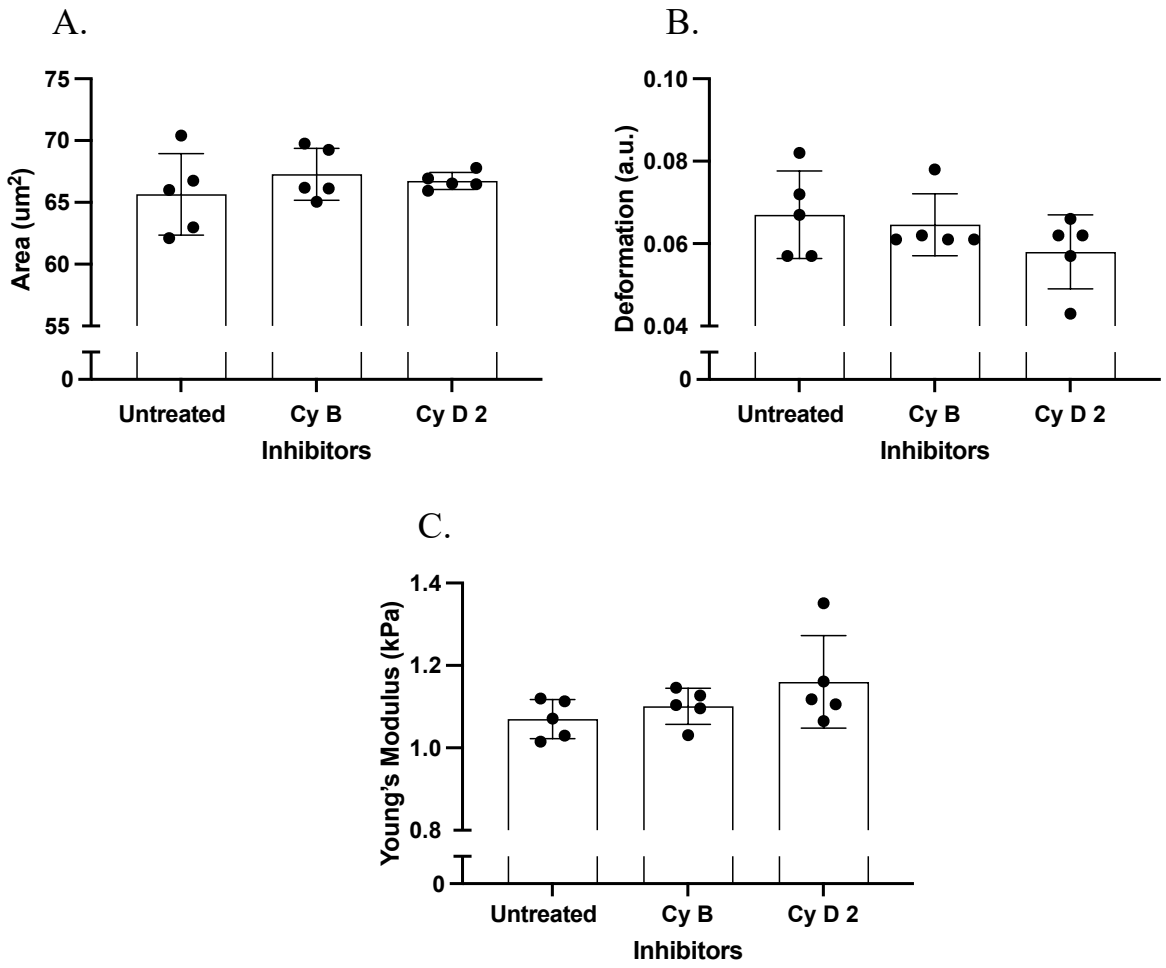


Figure 24. No change in deformability in untreated neutrophils treated with Cytochalasin B/D

(A-C) Neutrophils in whole blood from HC (n=5) were incubated for 15 minutes, untreated with media only (neutrophil culture media, 'untreated') or primed with 2 ng/mL TNF (15 minutes), treated with cytochalasin B 10µm or cytochalasin D 2µm, and incubated in media (neutrophil culture media) for 1h. Neutrophil populations were gated and analysed for (A) Cell size, (B) Cell deformability, and (C) Elasticity. More than 1000 events were recorded for each sample and results were visualised and analysed in ShapeOut2 software. Data are shown as mean +/- SEM, statistical analysis was performed using Kruskal-Wallis test, with Dunn's multiple comparisons test.

No significant changes in size or elasticity were observed when utilising either actin polymerisation inhibitor on neutrophils stimulated with ANCA (**Fig 25**; ns). There is a potential trend towards decreased deformability with inhibitors (**Fig 25**; ns) and will be further discussed in section 3.9. This indicates that under these experimental conditions, neither cytochalasin B nor D alter ANCA-induced decreased deformability.

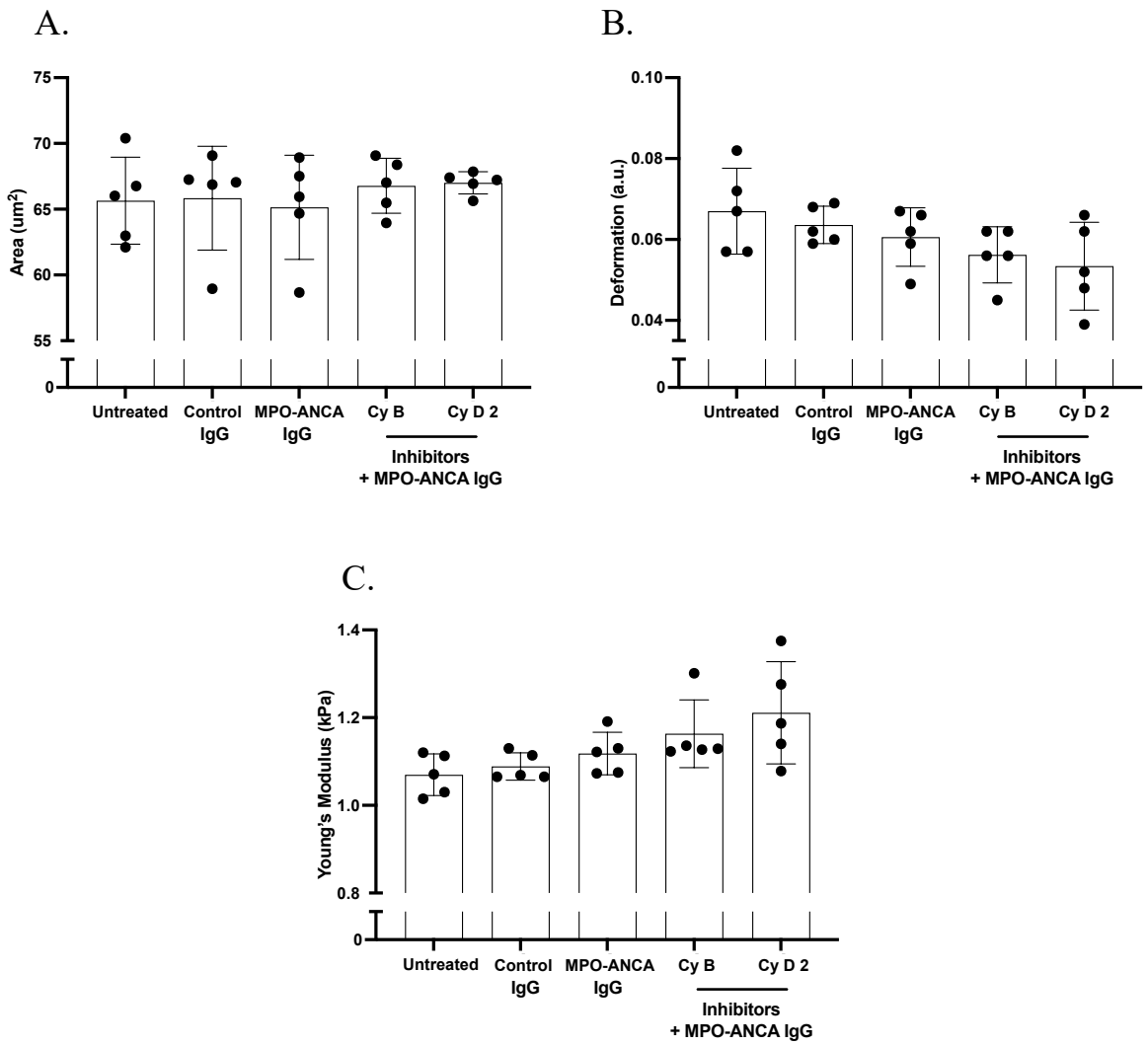


Figure 25. No change in deformability in ANCA stimulated neutrophils treated with Cytochalasin B or D

(A-C) Neutrophils isolated from whole blood from HC (n=5) were incubated for 15 minutes, untreated with media only (neutrophil culture media, 'untreated') or primed with 2 ng/mL TNF (15 minutes), treated with cytochalasin B 10µm or cytochalasin D 2µm (10 minutes), then stimulated with 100 µg/mL of HC or MPO-ANCA IgG for 1h. Neutrophil populations were gated and analysed for (A) Cell size, (B) Cell deformability, and (C) Elasticity. More than 1000 events were recorded for each sample and results were visualised and analysed in ShapeOut2 software. Data are shown as mean +/- SEM, statistical analysis was performed using Kruskal-Wallis test, with Dunn's multiple comparisons test

3.7.3. Inhibitors of actin polymerisation do not influence ANCA stimulated neutrophil protein secretion levels

Previous studies have shown that exocytosis, or degranulation in neutrophils, is regulated by actin (55). I next investigated whether actin polymerisation inhibitors can alter ANCA induced cytokine secretion in addition to their effects on the actin cytoskeleton. I selected cytochalasins as these inhibitors had the greatest effect on ANCA induced actin polymerisation in isolated cells. To assess the influence on protein secretion levels, stimulated neutrophils in culture were treated with inhibitors and SN levels of IL-8, VCAM-1, and ICAM-1 were measured using ELISA.

As before, IL-8 secretion levels were significantly increased following ANCA stimulation in comparison to untreated cells (**Fig 26A**). The addition of cytochalasin B or D had no significant effect on ANCA induced IL-8 secretion. Although ANCA stimulation had no significant effect on neutrophil VCAM-1 secretion, in untreated neutrophils there was a decrease in VCAM-1 secretion in with cytochalasin D in comparison to untreated neutrophils without inhibitors but no effect of cytochalasin D on VCAM-1 secretion from HC IgG or ANCA stimulated cells (**Fig 26B**; ns). A similar effect was seen with cytochalasin B, although this was of less magnitude than seen with cytochalasin D and results were not statistically significant.

An increase in ICAM-1 secretion was seen in ANCA stimulated neutrophils compared to untreated or HC IgG stimulated cells (without either inhibitor), but data was not significant (**Fig 26**; ns). Like VCAM-1, there was a decrease in ICAM-1 secretion in untreated neutrophils with cytochalasin D in comparison to untreated neutrophils without inhibitors (**Fig 26**; ns). When comparing ANCA stimulated neutrophils treated with cytochalasin B or D to untreated neutrophil conditions, an increase in ICAM-1 secretion levels was seen (**Fig 26C**; ns).

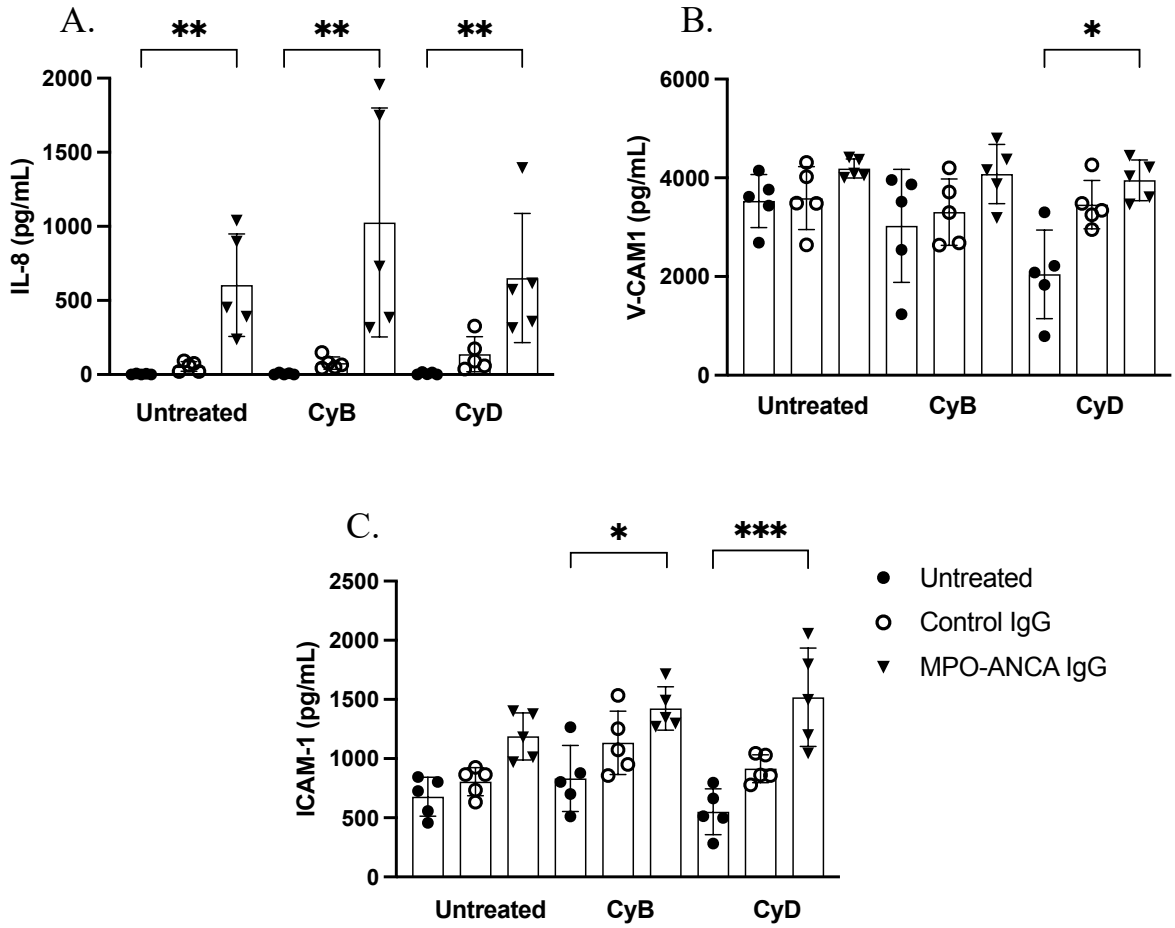


Figure 26. Inhibitors do not influence ANCA stimulated neutrophil protein secretion levels
Neutrophils in whole blood from HC (n=5) were incubated for 15 minutes, untreated with media only (neutrophil culture media, 'untreated') or primed with 2 ng/mL TNF (15 minutes), treated with cytochalasin B 10µm or cytochalasin D 2µm, and stimulated with 100 µg/mL of HC or MPO-ANCA IgG for 1h. SN IL-8 content was measured by ELISA (A) IL-8, (B) VCAM-1, and (C) ICAM-1. Data are shown as mean +/- SEM, statistical analysis was performed using two-way ANOVA with Geisser-Greenhouse correction, with Tukey's multiple comparisons test; *p<0.05.

3.8. RNA-Sequencing of untreated v MPO-ANCA v PR3-ANCA stimulated HC neutrophils

Neutrophils isolated from age match healthy controls were compared to TNF primed (15 minutes) and MPO-ANCA (100 ug/mL) or PR3-ANCA (100 ug/mL) IgG 1h stimulated cells using poly(A) RNA-seq. LDGs were separated from this population for future work. There are several published studies of transcriptional phenotype of leucocytes from patients with active AAV, identifying up-regulation of genes involved in neutrophil degranulation, activation, NET formation, and inflammatory pathways. Whether a similar phenotype is seen following ANCA stimulation of neutrophils, is unknown. I expected to correlate results of other findings from previous sections, including mechanophenotyping, actin polymerisation, and protein secretion levels, with gene expression.

3.8.1. Identification of a gene signature comparing 21% untreated neutrophils to 21% MPO-ANCA or PR3-ANCA stimulated neutrophils

I have shown that ANCA stimulation, modulates the neutrophil cytoskeleton and induces pathogenic neutrophil responses such as cytokine production and NETosis. I next investigated whether transcriptional changes may underpin these processes. Untreated HC isolated neutrophils were equilibrated (15 minutes), TNF primed (15 minutes) and stimulated with MPO- or PR3-ANCA IgG (100 µg/mL) for 1h. Untreated samples were incubated in culture media for an equivalent time period. Samples were prepared following method outlined in 2.2.9.1 and 2.2.9.3. in preparation for RNA-seq.

Figure 27 display top DE genes in MPO-ANCA stimulated neutrophils and **Figure 28** display top differentially expressed (DE) genes in PR3-ANCA stimulated neutrophils in comparison to untreated cells. In MPO-ANCA, there were 14,374 DE genes overall, and of those, 1,933

were significant (**Fig 27**; adjusted p value cut off=0.05). In PR3-ANCA, there were 13,798 DE genes overall, and of those, 1,797 were significant (**Fig 28**; adjusted p value cut off=0.05 adjusted p value cut off=0.05). The top 20 upregulated and top 10 downregulated significant DE genes are presented in **Table 22** (untreated v MPO-ANCA IgG) and **Table 23** (untreated PR3-ANCA IgG). Potential genes of interest that were upregulated following both MPO- and PR3-ANCA stimulation included *ICAM-1*, *TAGAP*, *TRAF1*, *CD83*, *NLRP3*, *IL1-B*, *CCL20*, *CXCL8*, *TNF*, *VEGFA*, *IL-6*, *NFKB1*, *C3*, *CD48*, *RAB21*, *SRC*, and *TNFRSF12A*. These genes are involved in processes such as inflammation, chemotaxis, immune response, and PI3K/AKT signalling. Gene ontology analysis displayed enrichment for several pathways in both MPO-ANCA stimulated neutrophils (**Fig 27**) and PR3-ANCA stimulated neutrophils (**Fig 28**). Of the dysregulated biological processes, inflammatory response, response to bacterium, and response to external stimulus were pathways of interest due to the alteration of neutrophil pathogen killing mechanisms in AAV. As for cellular components, pathways involved in the cell surface and whole membrane were dysregulated, which potentially may link with the effect found of ANCA stimulated neutrophil mechanophenotype. No significant DE were found when comparing MPO-ANCA stimulated neutrophils to PR3-ANCA stimulated neutrophils either.

Gene name	P value	FDR	Log_2FC
Upregulated			
F3	1.35E-72	1.94E-68	6.70979363
ICAM1	1.09E-51	5.23E-48	3.91251196
SLC35B2	6.35E-47	1.82E-43	4.06351762
MIR3945	2.26E-45	5.40E-42	4.25624469
ETS2	1.60E-44	2.86E-41	3.29961192
TAGAP	3.41E-43	5.43E-40	3.25254019
AC079753.1	2.48E-42	3.56E-39	6.6129507
AP003086.1	7.33E-40	9.56E-37	3.89649174
TRAF1	4.87E-38	5.37E-35	5.8130019
PDYN-AS1	4.53E-38	5.37E-35	5.25134472
XBP1	2.01E-36	2.06E-33	4.80994934
CD83	8.87E-34	8.49E-31	5.2910612
OLR1	4.76E-33	4.26E-30	5.47025307
AC020907.4	2.76E-32	2.33E-29	3.51851425
AC010980.1	3.90E-32	3.11E-29	7.40184026
C1orf61	5.08E-32	3.84E-29	5.79125926
GCH1	1.12E-31	8.00E-29	4.14758737
SFR1	1.76E-31	1.20E-28	3.83350988
PTX3	4.11E-31	2.68E-28	3.13419511
PPP1R15A	7.66E-31	4.78E-28	4.32530085
Downregulated			
PELO	1.36E-69	9.75E-66	-4.8310703
AC010542.5	1.19E-48	4.27E-45	-4.8297583
TNFRSF12A	9.07E-45	1.86E-41	-4.571081
AL662844.3	3.58E-30	2.05E-27	-3.7830795
CMTM1	1.22E-28	5.30E-26	-3.4585086
AL513327.1	1.49E-26	4.96E-24	-2.5465909
PPP1R3D	2.07E-26	6.59E-24	-3.1430274
LINC00324	9.68E-23	2.07E-20	-2.0021266
PEAK3	1.41E-21	2.69E-19	-2.4336105
THBD	4.35E-21	7.67E-19	-3.2945092

Table 22. Top upregulated and downregulated genes in MPO-ANCA treated neutrophils in comparison to untreated neutrophils

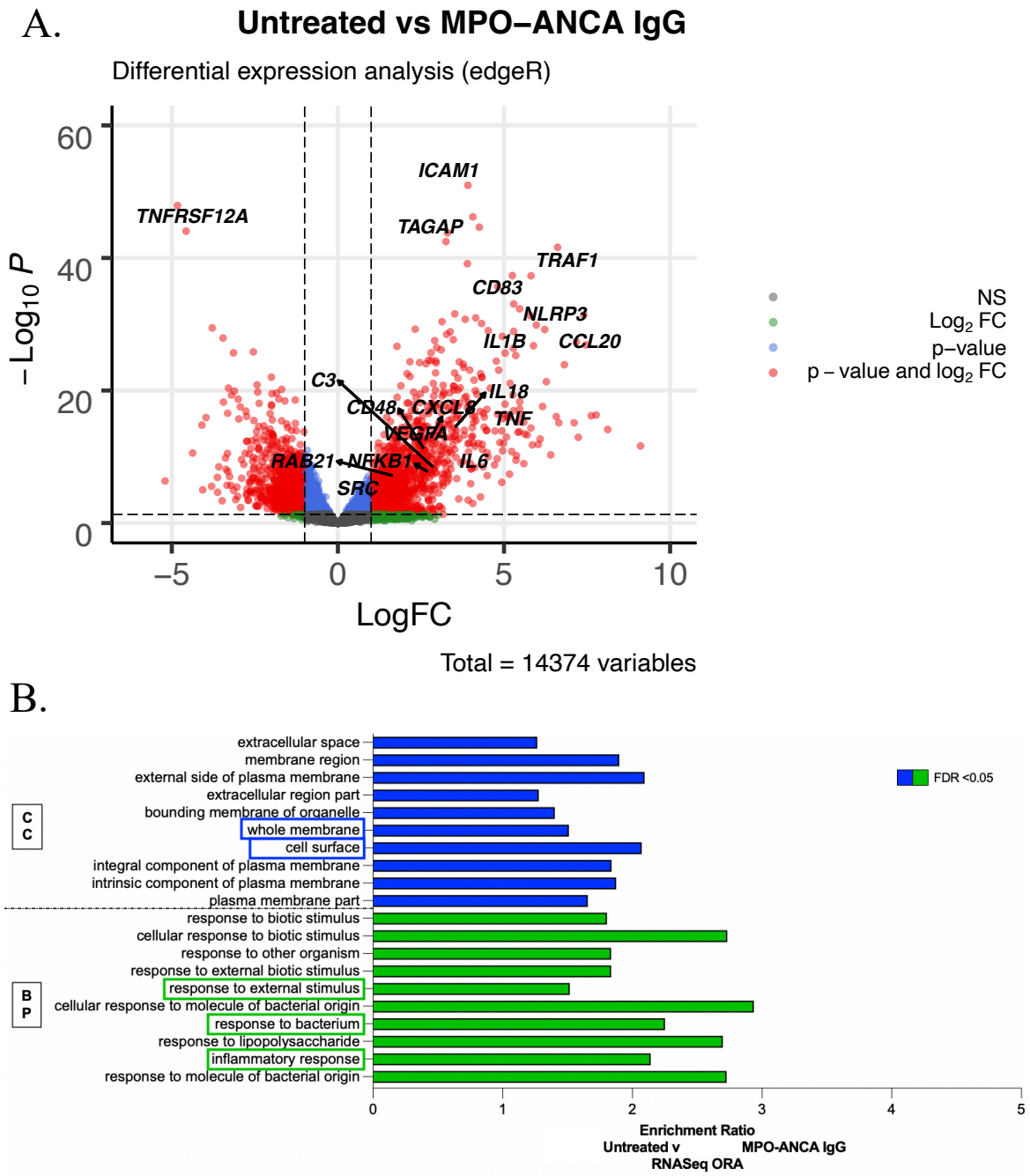


Figure 27. Transcriptomic analysis of untreated versus MPO-ANCA stimulated neutrophils (A) Volcano plot of untreated versus MPO-ANCA treated. One dot signifies each gene. Red dots represent genes meeting p-value (<0.05) and Log_2FC (<0.05), blue data points represent genes meeting p-value alone, green data points represent genes meeting Log_2 FC alone, and grey data points represent nonsignificant genes. In MPO-ANCA in comparison to untreated, downregulated genes are presented on the left panel from -5 to 0, and in MPO-ANCA in comparison to untreated, upregulated genes are presented on the right panel from 0-10. ns=nonsignificant, p<0.05; Log_2 FC signifies mean gene expression level of individual genes. (B) Gene ontology classification of untreated v MPO-ANCA DEGs (Log_2FC <0.05, p<0.05). Over-representation analysis (ORA) was performed on enrichment of cellular component and molecular function pathway dysregulation.

Gene name	P value	FDR	Log_2FC
Upregulated			
ICAM1	1.09E-51	5.23E-48	3.91251196
SLC35B2	6.35E-47	1.82E-43	4.06351762
MIR3945	2.26E-45	5.40E-42	4.25624469
ETS2	1.60E-44	2.86E-41	3.29961192
TAGAP	3.41E-43	5.43E-40	3.25254019
AC079753.1	2.48E-42	3.56E-39	6.6129507
AP003086.1	7.33E-40	9.56E-37	3.89649174
TRAF1	4.87E-38	5.37E-35	5.8130019
PDYN-AS1	4.53E-38	5.37E-35	5.25134472
XBP1	2.01E-36	2.06E-33	4.80994934
CD83	8.87E-34	8.49E-31	5.2910612
OLR1	4.76E-33	4.26E-30	5.47025307
AC020907.4	2.76E-32	2.33E-29	3.51851425
AC010980.1	3.90E-32	3.11E-29	7.40184026
C1orf61	5.08E-32	3.84E-29	5.79125926
GCH1	1.12E-31	8.00E-29	4.14758737
SFR1	1.76E-31	1.20E-28	3.83350988
PTX3	4.11E-31	2.68E-28	3.13419511
PPP1R15A	7.66E-31	4.78E-28	4.32530085
AC112198.2	1.34E-30	7.99E-28	5.97127306
Downregulated			
PELO	1.36E-69	9.75E-66	-4.8310703
AC010542.5	1.19E-48	4.27E-45	-4.8297583
TNFRSF12A	9.07E-45	1.86E-41	-4.571081
AL662844.3	3.58E-30	2.05E-27	-3.7830795
CMTM1	1.22E-28	5.30E-26	-3.4585086
AL513327.1	1.49E-26	4.96E-24	-2.5465909
PPP1R3D	2.07E-26	6.59E-24	-3.1430274
LINC00324	9.68E-23	2.07E-20	-2.0021266
PEAK3	1.41E-21	2.69E-19	-2.4336105
THBD	4.35E-21	7.67E-19	-3.2945092

Table 23. Top upregulated and downregulated genes in PR3-ANCA treated neutrophils in comparison to untreated neutrophils

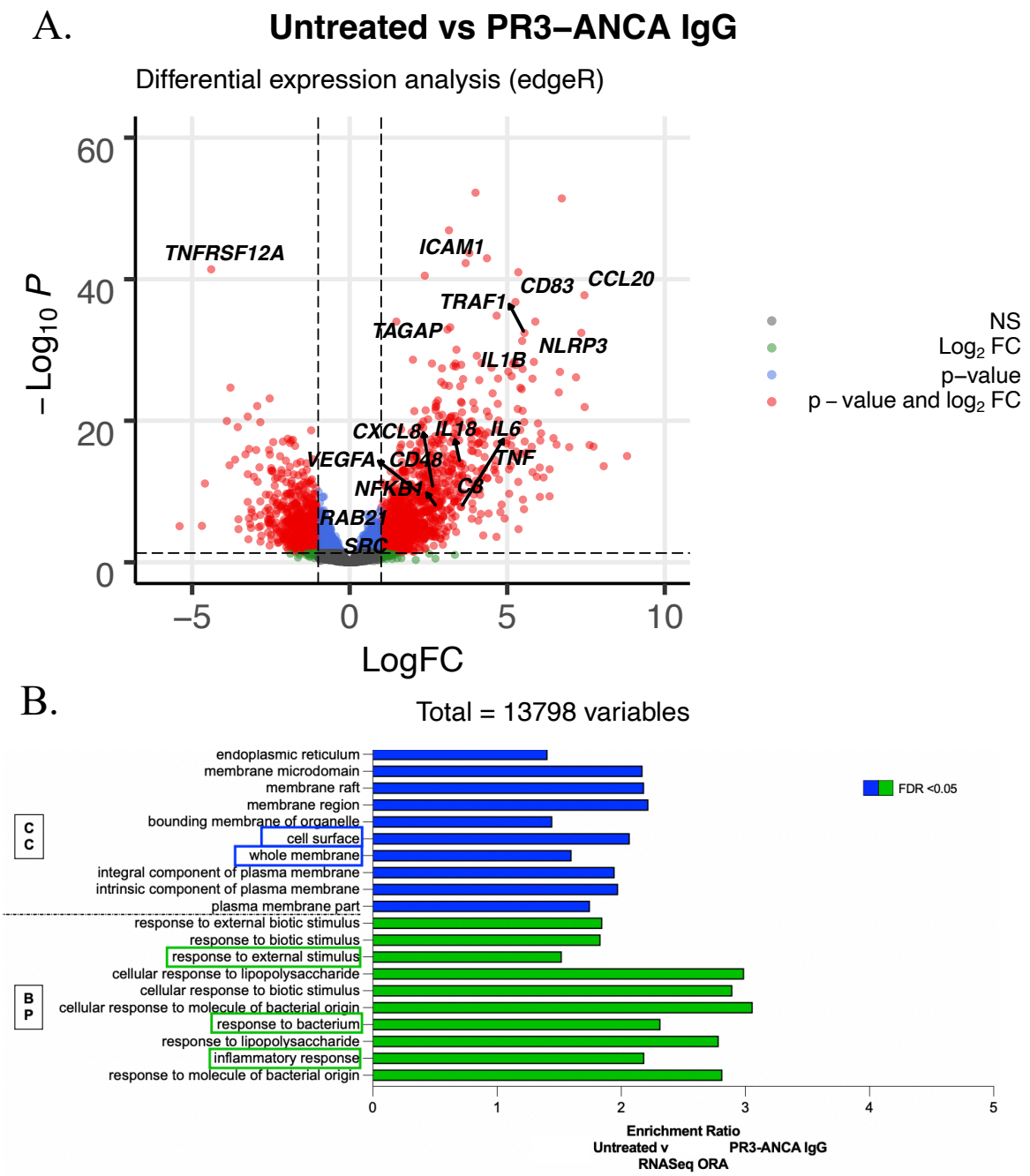


Figure 28. Transcriptomic analysis of untreated versus PR3-ANCA stimulated neutrophils (A) Volcano plot of untreated versus PR3-ANCA. One dot signifies each gene. Red dots represent genes meeting p-value (<0.05) and Log_2FC (<0.05), blue data points represent genes meeting p-value alone, green data points represent genes meeting Log_2 FC alone, and grey data points represent nonsignificant genes. In PR3-ANCA in comparison to untreated, downregulated genes are presented on the left panel from -5 to 0, and in PR3-ANCA in comparison to untreated, upregulated genes are presented on the right panel from 0-10. ns=nonsignificant, p<0.05; Log_2 FC signifies mean gene expression level of individual genes. (B) Gene ontology classification of untreated v PR3-ANCA DEGs (Log_2FC <0.05, p<0.05). ORA was performed on enrichment of cellular component and molecular function pathway dysregulation.

3.9. Discussion

The main objectives of this chapter were to optimise the use of RT-DC and phenotype the effect of pathogenic ANCA IgG on HC neutrophil biomechanics and actin polymerisation. I compared untreated HC neutrophil responses to stimulation with HC IgG, MPO-ANCA and PR3-ANCA IgG. My key findings were that ANCA IgG stimulation promoted a small increase in cell stiffness in neutrophils in whole blood, and that ANCA induced an increase actin polymerisation with filopodia formation and deformation of the cell membrane.

Several technical aspects were optimised to ensure my experiments were robust and to ensure I was seeing an effect of ANCA, not another variable. Importantly, in whole blood and HC/untreated cells isolated using the same conditions, RT-DC was reproducible with minimal inter-donor and intra-donor variability across multiple assays. The only variable shown to significantly alter neutrophil biomechanics during optimisation was that of whole blood anticoagulant. Previous studies showed heparin and EDTA decrease deformability of platelets, whereas sodium citrate increases deformability (523). Interestingly, the opposite result was found in neutrophils, where sodium citrate decreased deformability (section 3.2.1.). EDTA can optimally preserve blood cells, potentially explaining more deformable cells in comparison to citrate (516).

EDTA is a calcium chelating agent: blood anticoagulated using EDTA is therefore exposed to decreased Ca (++) ion. While exposure of whole blood to EDTA still allows ANCA-induced pathogenic responses that require calcium signalling to occur, the availability of exogenous calcium may contribute to neutrophil biomechanics and was therefore investigated by resuspending isolated cells in media with different calcium concentrations. Extracellular calcium has shown to influence stiffness of other cell types (526). While media calcium

concentration is lower in comparison to serum (2.1-2.6 mmol/L) (527), IMDM has three times the amount of calcium concentration than RPMI, yet no significant difference in size, deformability, and elasticity was found in untreated neutrophils. Potentially recalcification of isolated neutrophils in greater concentrations may influence these parameters (459) so, following optimisation, further experiments were kept consistent using RPMI.

Prior to investigating the effect of ANCA stimulation on neutrophil biomechanics, I confirmed the ANCA I had isolated were pathogenic, measuring the well characterised responses of IL-8 production and NETosis. Not all ANCA are pathogenic (528), but the ANCA I selected were pathogenic in terms of cytokine release and NETosis. Additionally, I identified the MPO-ANCA I isolated induced greater IL-8 secretion in neutrophils than PR3-ANCA, aligning with previous work showing MPO-ANCA stimulates primed neutrophils greater than PR3-ANCA (529). I then tested my hypothesis that ANCA IgG can alter neutrophil biomechanics. My results using RT-DC identified that once neutrophils are primed with TNF, subsequent MPO- or PR3-ANCA IgG stimulation both induce a small decrease in deformability in whole blood neutrophils from healthy volunteers. MPO- and PR3-ANCA IgG did not show a difference in the magnitude of decreased deformability. These results are perhaps surprising because ANCA serotypes have a different effect *in vivo* and may differ in their role in disease pathogenesis; *in vitro* data also has shown different activation and responses between MPO- and PR3-ANCA (529,530). Additionally, healthy donors may respond differently due to variability in PR3 cell surface expression. My results suggest that MPO- and PR3-ANCA behave similarly in biomechanics but possible reasons for not detecting a difference could be due to the variability in TNF responders and PR3 expressors (287) between healthy donors recruited. There may also be variability in the pathogenicity of isolated ANCA IgG (512).

For most of my experiments using MPO-ANCA (any experimental technique with more than an n=5), more than one MPO-ANCA was used; I had access to multiple patients' plasma exchange with MPO-ANCA positivity, but only one PR3-ANCA positive patient at the time of batch purification. The focus of my project was initially investigating MPO-ANCA's pathogenic effect, but developed into involving PR3-ANCA as I began recruiting more patients with PR3 positivity. As such, for PR3-ANCA, I have used one patient's purified IgG for all experiments and have fewer replicates as a result. It may be that expanding the pool of PR3 ANCA IgG used identifies some IgG preparations which have a greater effect on neutrophils. Therefore, this is a limitation in terms of definitively determining a difference between MPO- and PR3-ANCA stimulation *in vitro*.

In whole blood, MPO-ANCA IgG induced a greater effect of decreased deformability than seen in isolated neutrophils. Stimulation of isolated neutrophils resulted in smaller changes in biomechanics suggesting cells may be less susceptible to ANCA stimulation, perhaps due to being 'pre-primed' during the isolation process. Particularly as the HC IgG had a small impact on deformability too, perhaps due to cells being partially primed. However, isolated neutrophils did not have significantly different deformability at baseline compared to whole blood. Not only do these results suggest RT-DC may phenotype biomechanics of cells in whole blood more adequately than in isolated cells, but this experiment is a more accurate representation of ANCA exposure *ex vivo*. In circulation and in resident tissue, neutrophils are continually exposed to other cell types, therefore whole blood experiments more representative of crosstalk which may occur *in vivo*. Whole blood neutrophils are also subject to less *in vitro* manipulation than isolated neutrophils, resulting in less chance for inadvertent activation of cells. Overall, whole blood is more physiological including cell-cell crosstalk, physiological environment

rather than artificial buffers or cell culture media. These variables may explain the increased variability seen between donors for isolated neutrophils in comparison to whole blood.

RT-DC is a highly sensitive, high-throughput technique, capable of detecting small changes in biomechanical phenotype in cell populations. As previously discussed, following ANCA stimulation of isolated cells, the changes detected by RT-DC are small, and less significant than results seen in whole blood. This could be due to RT-DC's sensitivity, limiting changes detected in isolated cells, whole blood being of more physiological relevance, or it could also be argued this set of stimulation experiments does not alter parameters of neutrophils biomechanically. Moreover, due to the length per run in RT-DC setup, a maximum of 4 conditions can be measured per time point, therefore requiring separate experiments to measure several variables. In turn, this limits the number of comparisons that can be performed within an experiment. Overall, from my results, it likely that the difference in ANCA-induced deformability between whole blood and isolated cells was due to neutrophil isolation. Although there is unavoidable variability between healthy control donors, this was more apparent in isolated cell runs compared to the more consistent whole blood runs. Technical aspects of analysing activated, NETosing cells may also have an impact on results. Additionally, cells may be lost due to the number of cells acquired within the gate set varying between runs dependent upon donors, and therefore, the time taken to acquire a set number of cells varies. These cells acquired may be gated out once the porosity gate (<1.05) is set, therefore decreasing the number of events analysed in comparison to the number of cells measured in other time points, and stimulation conditions.

My results showing MPO- and PR3-ANCA promote a decrease in neutrophil deformability necessitated further investigation on what contributes to this. Various parameters can influence

cell deformability including nuclear morphology, cell osmolality (41), actin cytoskeleton, and other cytoskeletal components. I initially chose to study the actin cytoskeleton based on RT-DC findings of increased stiffness of neutrophils when stimulated with ANCA. One previous study using electron microscopy has investigated neutrophil actin polymerisation in the context of ANCA stimulation, comparing FMLP, as a positive control, to up to 20 minutes of PR3-ANCA stimulation (342). In keeping with my findings, this study also identified significant F-actin polymerisation following ANCA stimulation. Increased F-actin polymerisation could explain why neutrophils stimulated with ANCA are stiffer. Stiffer cells, potentially due to an increase in F-actin, may lead to increased migration of neutrophils through the vasculature and transmigration through the vessel wall. This hypothesis of increased migration is further investigated in Chapter 4.

As I identified ANCA IgG promotes neutrophil actin polymerisation and that this likely contributes to biomechanical RTDC phenotype, I questioned whether this effect could be inhibited and if this would impact on ANCA induced decreases in neutrophil deformability. Multiple actin polymerisation inhibitors, targeting different stages of actin polymerisation, have proven efficacy *in vitro* in other cell types. It is unknown which stage of actin polymerisation ANCA IgG stimulation promotes, therefore I tested several inhibitors with different mechanisms of action. Actin filament formation inhibitors, cytochalasin B and D were more effective than myosin-ii inhibitors, para-aminoblebbistatin and blebbistatin in inhibiting ANCA induced changes in the actin cytoskeleton. Previous studies have shown cytochalasin D increases cell deformability, although this has not been studied extensively (Elson 1984). Surprisingly, my results using RT-DC indicated a trend towards decreased neutrophil deformability in the presence of cytochalasin B or D. Incubation with cytochalasins resulted in visually rounder cells, which has been shown to be a phenotype for stiffer neutrophils, as

previously shown in primed neutrophils (234,531,532). Cells which are rounder at baseline are less likely to be deformed by mechanical force, which may explain why there was a trend towards increased stiffness in ANCA stimulated neutrophils treated with cytochalasins in comparison to ANCA stimulated neutrophils without an inhibitor treatment.

Cytochalasin D best inhibited ANCA promotion of actin polymerisation both using quantitative analysis and upon visual inspection of protrusion formation. However, when neutrophil biomechanics were measured using RT-DC no significant change in size, deformability, or elasticity was shown between ANCA stimulated neutrophils with or without inhibitor treatment. In isolated cells, the inhibitors used prevented additional actin polymerisation promoted by ANCA simulation. This suggests that in the context of ANCA stimulation there are factors other than actin cytoskeletal changes which underlie the decrease in neutrophil deformability. One hypothesis is that the inhibitory effect may only be effective in a static setting with no additional forces applied *in vitro*. Another hypothesis is that the inhibitor may need to be added before the TNF priming. There was also minimal effect of cytoskeletal inhibitors on ANCA-induced cytokine secretion. Cytochalasin B and D did not alter MPO-ANCA IgG induced IL-8 and ICAM-1 protein secretion levels, suggesting actin filament formation inhibition does not impact neutrophil secretory capabilities in the presence of ANCA. However, untreated neutrophil protein secretion was reduced. It is possible that cytochalasins decrease baseline neutrophil protein secretion, but this effect can be over-ridden by an additional stimulus such as ANCA. These results require further investigation to interpret why inhibiting actin polymerisation in the presence of ANCA stimulation has no effect on cell deformability under flow conditions.

Key findings:

1. Healthy neutrophil deformability significantly decreases following stimulation with MPO-ANCA IgG in whole blood
2. ANCA stimulation induces neutrophil actin polymerisation
3. Cytochalasin D inhibits ANCA stimulation induced neutrophil actin polymerisation but does not change neutrophil deformability in isolated neutrophils

4. Chapter 4 – The effect of hypoxia on neutrophil biomechanics following stimulation with ANCA IgG

4.1. Introduction

Organs such as the kidney and the lung exist in what is conventionally perceived as a low oxygen level, (533), however, due to physiological adaptations, the oxygen delivered is adequate for requirements. As such, this is better described not as hypoxia but rather physiological normoxia. During inflammation, however, tissues and blood vessels can become characteristically hypoxic with an insufficient supply of oxygen to meet demands. Neutrophils are adapted to not only survive under hypoxic conditions, but to function effectively while carrying out their programmed capabilities. However, these processes can be impacted by the availability of oxygen or pathological hypoxia, as described in section 1.10. The effect of changing oxygen tensions on neutrophil mechanical properties is unknown.

Most laboratory research is carried out at atmospheric oxygen levels which are not usually experienced by cells *in vivo*. Measuring neutrophil responses under more physiologically relevant oxygen tensions may allow for more representative *ex vivo* modelling when studying neutrophils in the vasculature. Under usual physiological conditions, 10-12% O_2 is the highest oxygen tension cells are exposed to as they circulate *in vivo.* In this set of experiments, I therefore use 10% as an *in vitro* representation of the oxygen tension experienced by circulating cells in arterial blood, 5% O_2 represents the O_2 level that cells experience in venous blood, and 1% O_2 replicates pathological hypoxia of vessel inflammation (534). As AAV is a disease of the small vessels, experiments were mostly carried out at 1% and 5% O_2 compared to 21% O_2. In pathological conditions, pathological hypoxia (1% O_2 or less) has been shown to influence neutrophil responses to a multitude of stimuli, including fMLP, GM-CSF, and TNF, thereby impacting on processes such as apoptosis, NET formation, and migration (430,535). Therefore, performing experimental setups under physiological normoxia and hypoxia *in vitro* allows for a more representative model of what occurs *in vivo*, particularly in AAV.

In Chapter 3, I identified ANCA stimulation induced neutrophil biomechanical changes at 21% O_2 and was associated with increased actin polymerisation. Therefore, in this chapter, I use RT-DC to determine if there is an effect of hypoxia on untreated neutrophils and what the subsequent effect of ANCA stimulation is on neutrophil mechanical properties. Actin polymerisation can also be promoted in neutrophils in response to other stimuli including chemoattractants (234). Studies have shown hypoxia changes neutrophil actin polymerisation in response to stimulus such as fMLP (459). This raises the question of whether hypoxia alone may act as an inducer of actin polymerisation in neutrophils, and whether an enhanced effect is seen once cells are stimulated with ANCA. By correlating biophysical phenotype of ANCA stimulated neutrophils using RT-DC with actin cytoskeletal changes, I may identify a neutrophil signature associated with aAAV in the context of pathological hypoxia.

Hypothesis of current chapter

Hypoxia exacerbates the effect of ANCA on neutrophil biomechanics.

Aims

1 Evaluate effect of hypoxia on neutrophil mechanophenotype

2 Determine the effect of hypoxia on neutrophil biomechanics following ANCA stimulation

3 Measure the effect of hypoxia on neutrophil actin cytoskeletal changes in untreated cells and following ANCA stimulation

4.2. Oxygen tensions

4.2.1. Oxygen tension alters whole blood neutrophil mechanophenotype at 5% O_2

I performed blood gas analysis on whole blood in microcentrifuge tubes after 15 minutes and 1h incubation at 5% O_2. Measured oxygen tensions reflected the setting of the hypoxic workstation. This included showing ample blood gas equilibration and the blood maintained physiological pH, between 7.35 to 7.45 (536). Once I confirmed blood equilibrated to the oxygen level set for the workstation by 15 minutes, this was chosen as the initial experimental timepoint. I then used RT-DC to measure the impact oxygen tension has on neutrophil biomechanical profiles. To select oxygen tensions for future experiments, I carried out a series of measurements investigating a titration from 1%-21% O_2 using whole blood equilibrated for 15 or 60 minutes followed by measurement of biophysical properties of cells using RT-DC.

Oxygen tension exhibited no change on whole blood neutrophil deformability following 15 minutes or 1h exposure to the indicated oxygen tension, except for 5% O_2. Compared to 21% O_2, neutrophil deformability remained unchanged at 10% O_2, 7% O_2, 3% O_2, and 1% O_2 (**Fig 29B; ns**). Although, 5% O_2 displayed a trending increase in deformability. There were no significant differences though in neutrophil size, deformation, or elasticity in any of the oxygen tensions studied. These findings suggest oxygen tension can influence neutrophil mechanophenotype in the absence of stimulation and is dependent upon the degree of oxygen tension. For future experiments, 1%, 5%, and 10% O_2 tensions were selected as the most physiologically relevant. 10% O_2 is representative of arterial blood *in vitro*, 5% O_2 is representative of venous blood *in vitro*, and 1% O_2 is representative of pathological hypoxia. Standard culture conditions of 21% O_2, is non-physiological but was used as baseline comparison as most neutrophil phenotyping experiments in the literature have been performed in atmospheric oxygen.

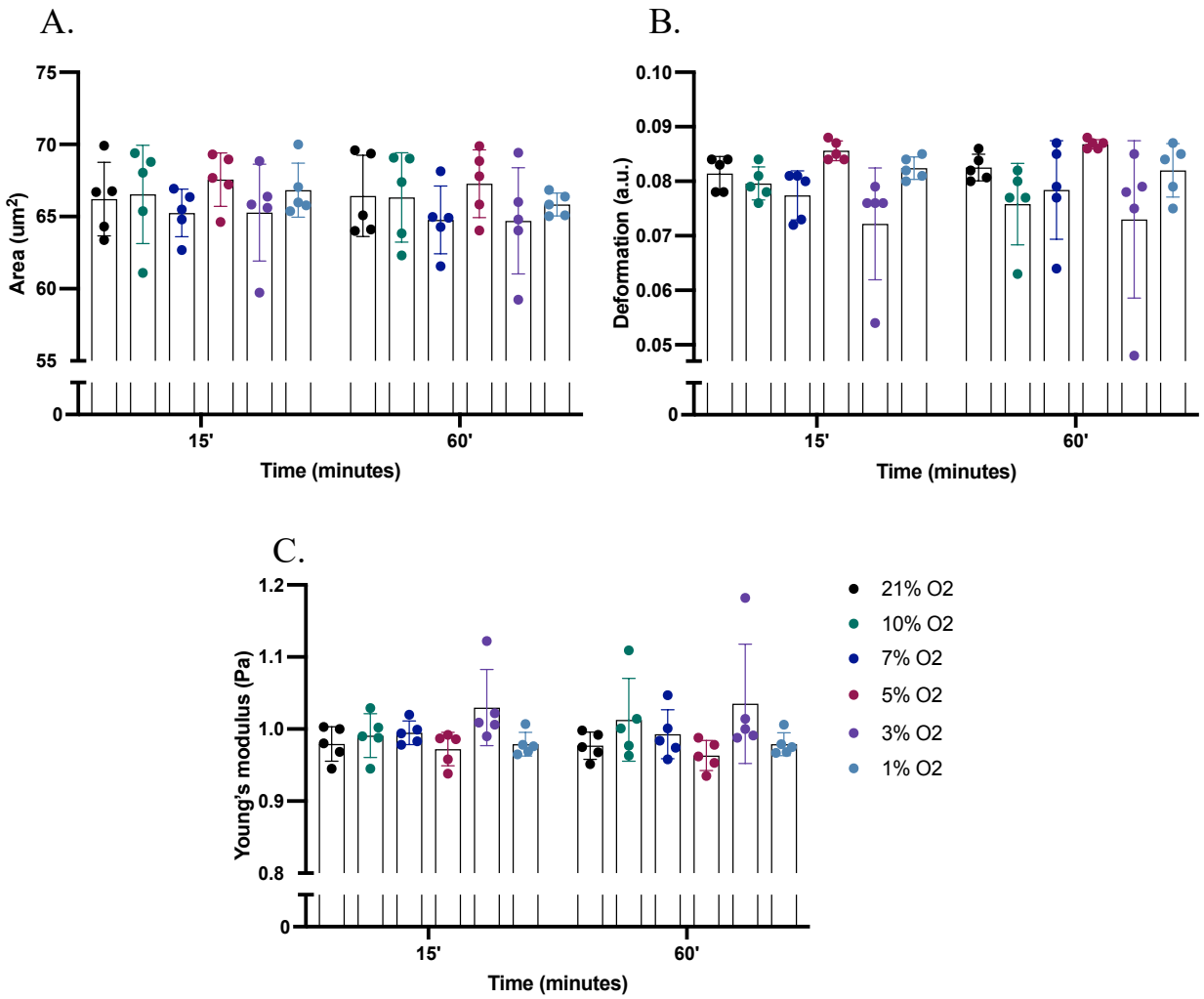


Figure 29. Oxygen tension alters whole blood neutrophil mechanophenotype at 5% O_2
(A-C) Whole blood from HC (n=5) was aliquoted, incubated for 15 minutes and 1h at 1%, 3%, 5%, 7%, 10%, or 21% O_2, and analysed using RT-DC. Data are not matched as it was not possible to assess this many oxygen tensions simultaneously. Neutrophil populations were gated and analysed for (A) Cell size, (B) Cell deformability, and (C) Elasticity. More than 1000 events were recorded for each sample and results were visualised and analysed in ShapeOut2 software. Data are shown as mean +/- SEM, statistical analysis was performed using Kruskal-Wallis test, with Dunn's multiple comparisons test.

4.3. Oxygen tension alters isolated neutrophil deformability

Having demonstrated that oxygen tension likely alters whole blood neutrophil mechanophenotype, I next investigated whether different oxygen tensions would similarly alter the phenotype of isolated neutrophils. Neutrophils were isolated at 21% O_2, equilibrated for 15 or 60 minutes at desired oxygen concentrations, and measured using RT-DC.

There were no significant differences in neutrophil size or elasticity between any oxygen tensions studied, following either 15- or 60-minutes incubation (**Fig 30A-C**). In comparison to 21% O_2, no change in deformability was seen at 1% O_2, but a significant decrease was seen at 5% O_2 (**Fig 30B**; p=0.0207). Interestingly, this is in direct contrast to experiments carried out under the same oxygen tension using whole blood, where an increase in neutrophil deformability was seen. These findings suggest oxygen tension influences neutrophil mechanophenotype dependent upon the oxygen concentration cells are exposed to but that the cell isolation procedure also has an impact, particularly as the cell isolation process was performed under 21% O_2.

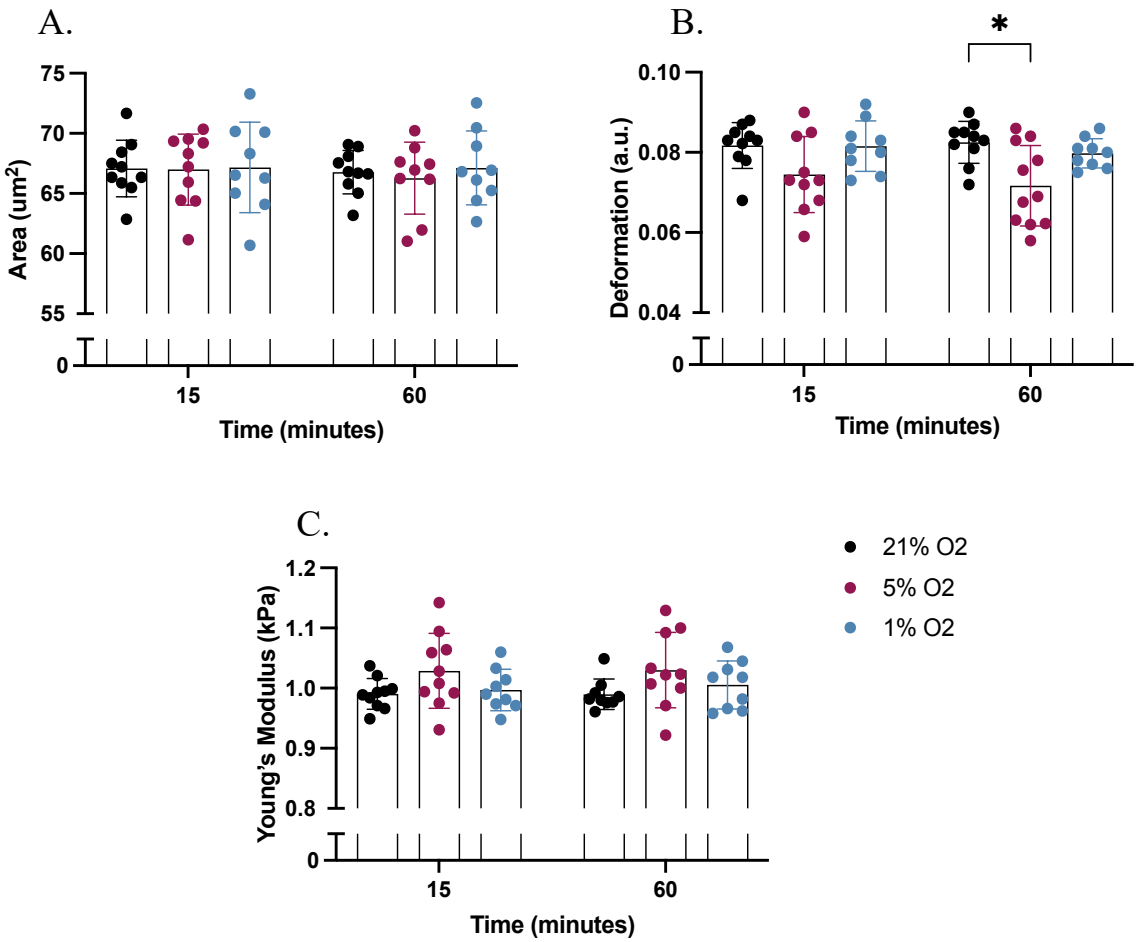


Figure 30. Oxygen tension alters isolated neutrophil deformability

(A-C) Neutrophils from HC (n=10) were isolated at 21% O_2, incubated in neutrophil culture media for 15 minutes or 1h at 1%, 5%, or 21% O_2 from different donors recruited on different days and analysed using RT-DC. Neutrophil populations were gated and analysed for (A) Cell size, (B) Cell deformability, and (C) Elasticity. More than 1000 events were recorded for each sample and results were visualised and analysed in ShapeOut2 software. Data are shown as mean +/- SEM, statistical analysis was performed using Kruskal-Wallis test, with Dunn's multiple comparisons test; *$p<0.05$.

4.4. The effect of oxygen tension on ANCA stimulated neutrophil deformability

Hypoxia has previously been shown to augment some neutrophil functional responses but is dependent upon the stimulus used. For example, GM-CSF promotes neutrophil degranulation under hypoxia, but this effect is not seen with TNF (459). In this section, I will investigate this by measuring the biomechanics of ANCA stimulated neutrophils under hypoxia.

4.4.1. Oxygen tension alters neutrophil deformability in whole blood stimulated with ANCA IgG

To assess the impact of differing oxygen tensions on role of ANCA-IgG stimulation induced changes in neutrophil deformability in whole blood, I compared the effect of MPO-ANCA IgG stimulation at 1% O_2, 5% O_2, 10% O_2 and 21% O_2 using RT-DC. Whole blood was equilibrated for 15 minutes at indicated oxygen tensions, primed with 2 ng/mL TNF (15 minutes), and stimulated with HC or MPO- IgG for 1h.

As shown previously, there was no difference in untreated neutrophil size or deformability comparing 21% and 10% O_2 (**Fig 31A**). The reproducible effect of a decrease in neutrophil deformability in ANCA stimulated whole blood was again shown in comparison to untreated whole blood neutrophil deformability under 21% O_2 (**Fig 31B**; p=0.0566). The effect of ANCA on deformation was slightly more pronounced under 10% but was not significantly different between the two oxygen tensions (**Fig 31B**; ns).

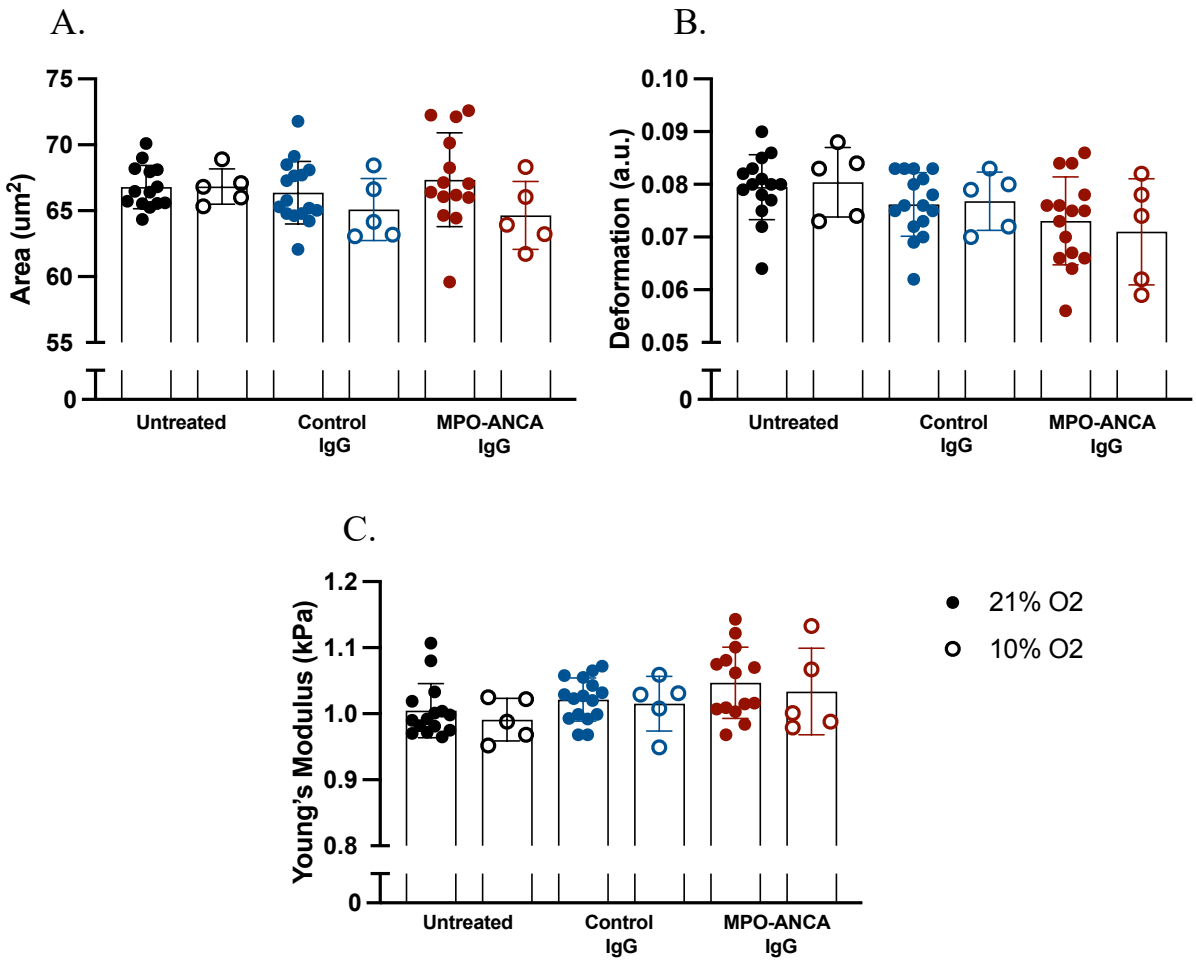


Figure 31. Oxygen tension alters neutrophil deformability in whole blood stimulated with ANCA

(A-C) Whole blood from HC (n=10 (21% O_2), n=5 (10% O_2)) was incubated for 15 minutes at 10%, or 21% O_2, primed with 2 ng/mL TNF for 15 minutes, stimulated with 100 ug/mL HC IgG or MPO-ANCA IgG for 1h, and analysed using RT-DC. Neutrophil populations were gated and analysed for (A) Cell size, (B) Cell deformability, and (C) Elasticity. More than 1000 events were recorded for each sample and results were visualised and analysed in ShapeOut2 software. Data are shown as mean +/- SEM, statistical analysis was performed using two-way ANOVA mixed effects model with Geisser-Greenhouse correction, with Tukey's multiple comparisons test.

No difference in size was shown at 5% O_2 in either HC or MPO-ANCA stimulated whole blood either in comparison to 21% O_2 or between stimulation conditions (**Fig 32A**). As previously shown in section 4.2., there is increased neutrophil deformability in untreated whole blood at 5% O_2 in comparison to 21% O_2 (**Fig 32B**). At 5% O_2, neutrophils remain more deformable despite MPO-ANCA IgG stimulation in contrast to 21% O_2 (**Fig 32B-C**; ns).

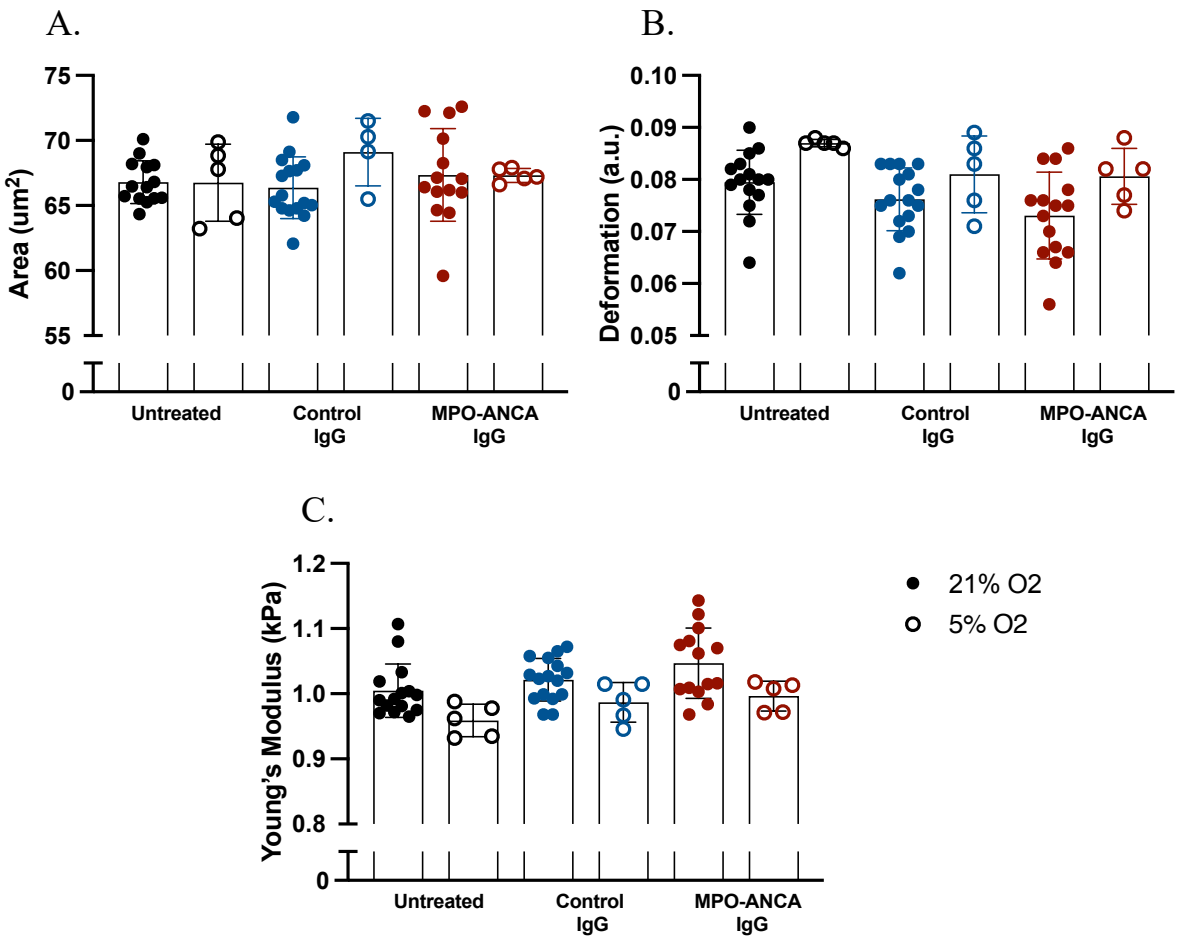


Figure 32. 5% O_2 alters neutrophil deformability in whole blood stimulated with ANCA
A-C) Whole blood from HC (n=10 (21% O_2), n=5 (10% O_2)) was incubated for 15 minutes at 5% or 21% O_2, untreated, or primed with 2 ng/mL TNF for 15 minutes, stimulated with 100 ug/mL HC IgG or MPO-ANCA IgG for 1h, and analysed using RT-DC. Neutrophil populations were gated and analysed for (A) Cell size, (B) Cell deformability, and (C) Elasticity. More than 1000 events were recorded for each sample and results were visualised and analysed in ShapeOut2 software. Data are shown as mean +/- SEM, statistical analysis was performed using two-way ANOVA mixed effects model with Geisser-Greenhouse correction, with Tukey's multiple comparisons test.

There is no change in size between any stimulation condition or oxygen tension comparing neutrophils in WB under 1% O_2 with 21% O_2 (**Fig 33A**). However, at 1% O_2, decreased deformability was seen with HC IgG, to a greater extent than seen in 21% O_2. This effect was also seen, although to a lesser degree, in untreated cells, suggesting that decreases in deformability at 1% O_2 may not ANCA specific and may be related to the effect of hypoxia in addition to TNF priming (**Fig 33B-C**; ns).

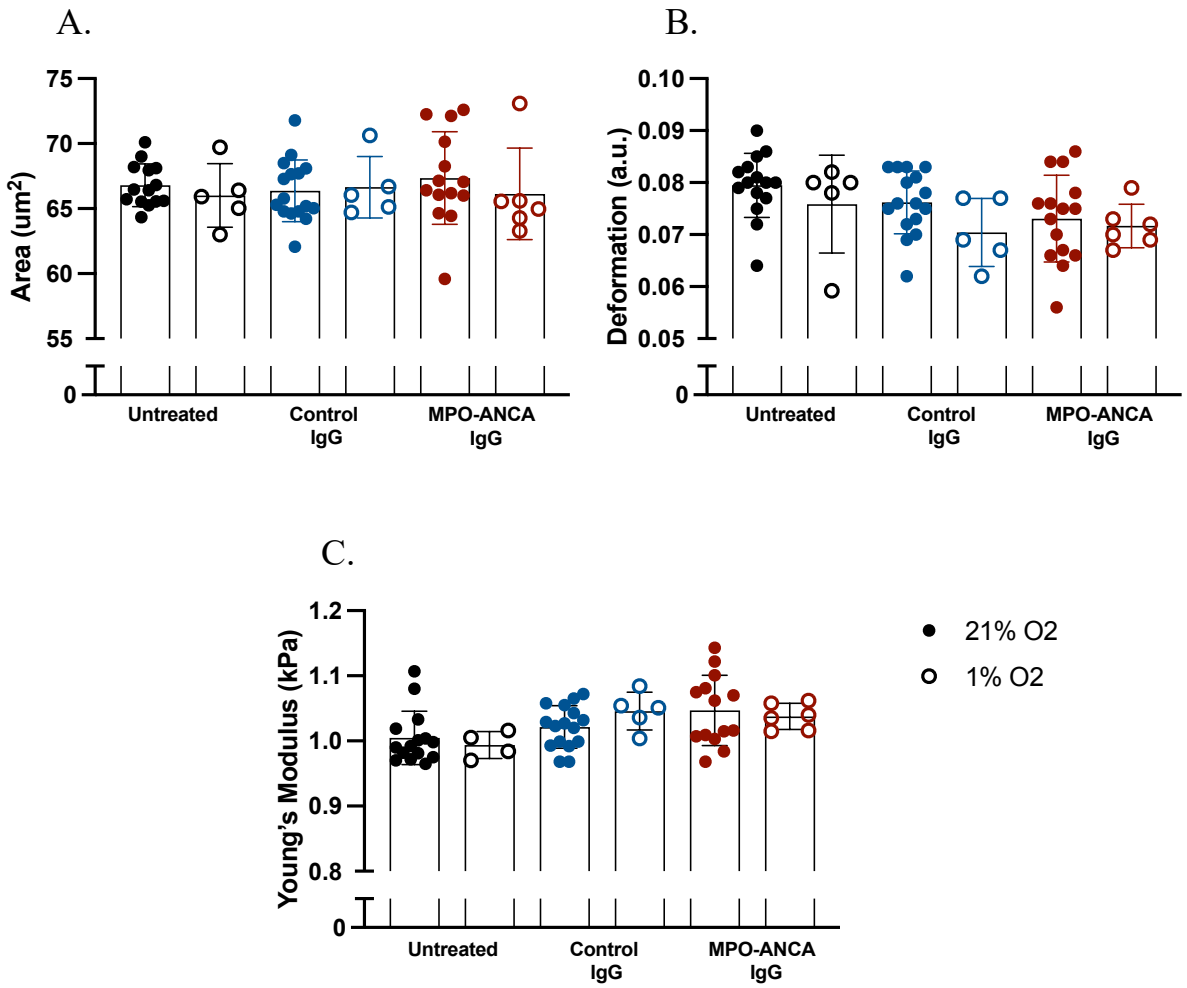


Figure 33. Hypoxia alters neutrophil deformability in whole blood stimulated with ANCA (A-C) Whole blood from HC (n=10 (21% O_2), n=5 (10% O_2)) was incubated for 15 minutes at 1% or 21% O_2, untreated, or primed with 2 ng/mL TNF for 15 minutes, stimulated with 100 ug/mL HC IgG or MPO-ANCA IgG for 1h, and analysed using RT-DC. Neutrophil populations were gated and analysed for (A) Cell size, (B) Cell deformability, and (C) Elasticity. More than 1000 events were recorded for each sample and results were visualised and analysed in ShapeOut2 software. Data are shown as mean +/- SEM, statistical analysis was performed using two-way ANOVA mixed effects model with Geisser-Greenhouse correction, with Tukey's multiple comparisons test.

4.4.2. Hypoxia decreases the effect of ANCA on isolated neutrophil deformability

As I had previously identified differences in the effect of hypoxia on neutrophil deformability between whole blood and isolated neutrophils, I next assessed the impact of differing oxygen tensions on ANCA IgG induced changes in neutrophil deformability using isolated cells. I compared MPO-ANCA and PR3-ANCA IgG stimulated neutrophils at 1% O_2, 5% O_2, or 21% O_2 using RT-DC. Neutrophils were incubated at the indicated oxygen tension for 15 minutes, primed with 2 ng/mL of TNF (15 minutes) and stimulated with 100 µg/mL MPO-/PR3-ANCA IgG for 15-minutes and 1h, followed by measurement using RT-DC.

No additional effect of ANCA IgG on size beyond that seen with 5% O_2 alone was small (**Fig 34A-B**). In untreated cells, lower neutrophil deformability was seen at 5% O_2 compared to 21% O_2 following 15 minutes or 1h incubation (**Fig 34C-D**; median deformability at 15 min: 0.072 a.u., 1h: 0.077 a.u. in 5% O_2 and 15 min: 0.077 a.u. and 1h: 0.078 a.u. in 21% O_2, ns). The small decrease in deformability seen following MPO-ANCA IgG stimulation at 21% O_2 is inhibited by 5% O_2 (**Fig 34D**; median deformability at 15 min: 0.074 a.u. and 1h: 0.076 a.u. in 5% O_2, median deformability at 15 min: 0.070 a.u. and 1h: 0.072 a.u. in 21% O_2, ns). Stimulation with PR3-ANCA induces a decrease in deformability following 15 minutes and 1h stimulation at 21% O_2 (**Fig 34C and D**; median deformability at 15 min: 0.072 a.u., 1h: 0.067 a.u.). Unexpectedly, in contrast to MPO-ANCA IgG stimulation, this effect is preserved when experiments were carried out at 5% O_2 with median deformability of 0.067 a.u. at 15 minutes and 0.064 a.u. at 1h (**Fig 34C and D;** ns). Interestingly, at both time points HC IgG stimulated neutrophils at 5% O_2 were less deformable than MPO-ANCA stimulated neutrophils, but more deformable than PR3-ANCA stimulated neutrophils.

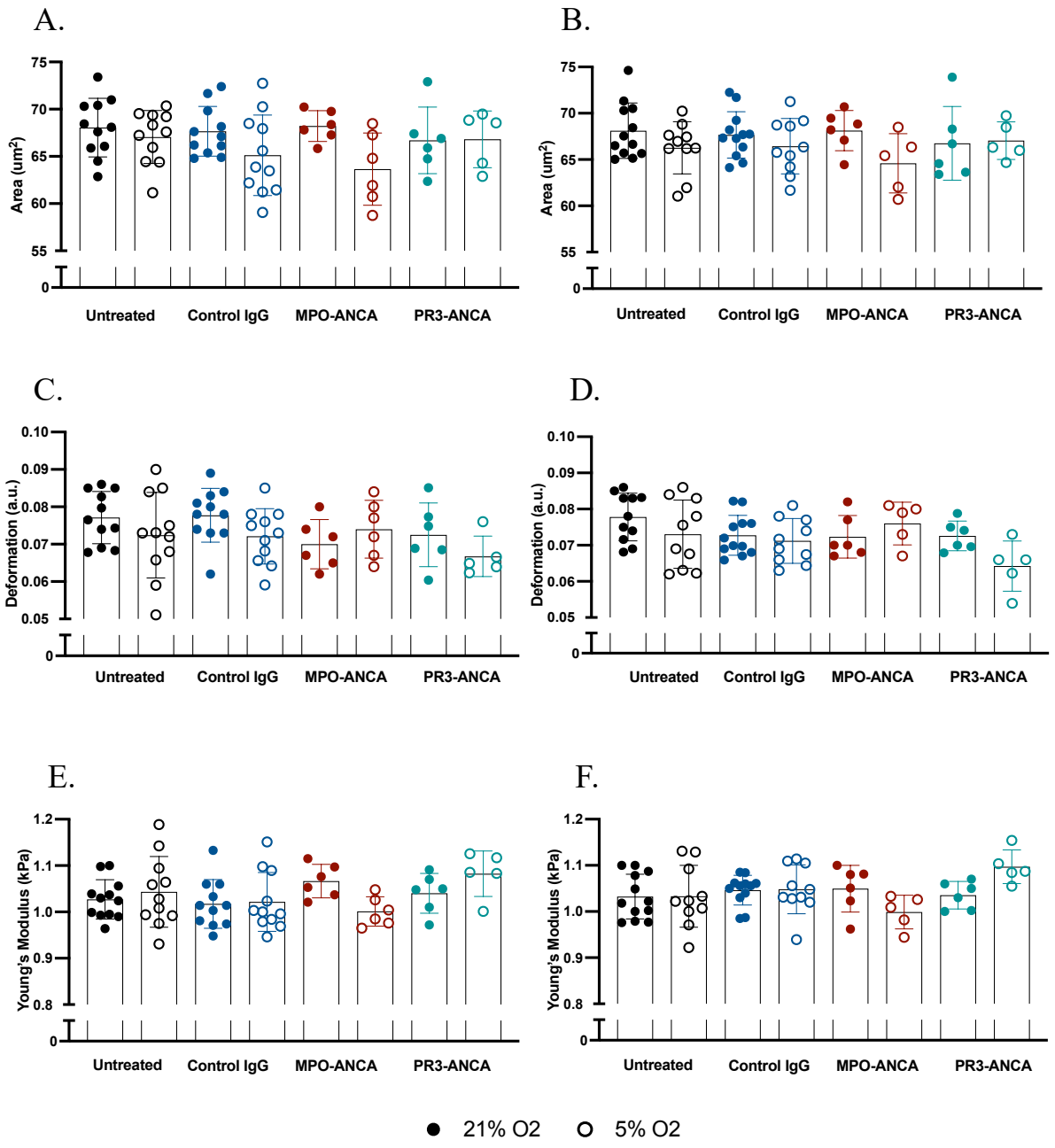


Figure 34. 5% O_2 decreases the effect of ANCA on isolated neutrophil deformability
(A-C) Neutrophils from HC (n=5) were isolated at 21% O_2, incubated for 15 minutes at 5% O_2, untreated with media only (neutrophil culture media, 'untreated') or primed with 2 ng/mL TNF for 15 minutes and stimulated with 100 ug/mL HC IgG, MPO-/PR3-ANCA IgG for 15 minutes or 1h, and were analysed using RT-DC. Neutrophil populations were gated and analysed for (A/B) Cell size, (C/D) Cell deformability, and (E/F) Elasticity, (A, C, E) 15 minutes, (B, D, F) 1h. More than 1000 events were recorded for each sample and results were visualised and analysed in ShapeOut2 software. Data are shown as mean +/- SEM, statistical analysis was performed using two-way ANOVA mixed effects model with Geisser-Greenhouse correction, with Tukey's multiple comparisons test; *p<0.05.

Following incubation at 1% O_2 for 15 minutes or 1h, untreated cells are the same size as they are in 21% O_2 (**Fig 35A-B**). Yet, both HC IgG and MPO-ANCA stimulation decreases the size of cells at 1% O_2 but not at 21% O_2; PR3-ANCA stimulation did not influence cell size (**Fig 35A and B**). There is no difference in deformability of untreated cells between neutrophils incubated at 1% O_2 at either time point (15 min: 0.077 a.u., 1h: 0.078 a.u.) or 21% O_2 (15 min: 0.077 a.u., 1h: 0.078 a.u.) (**Fig 35C and D**; ns). MPO ANCA IgG induced a small decrease in deformability at 21% O_2 in comparison to untreated cells (15 min: 0.070 a.u., 1h: 0.0723 a.u.), and this was inhibited at 1% O_2 (15 min: 0.080 a.u., 1h: 0.076 a.u.) (**Fig 35C and D**; ns). Interestingly, at both time points HC IgG stimulated neutrophils at 1% O_2 (15 min: 0.079 a.u., 1h: 0.077 a.u.) were more deformable than HC IgG stimulated neutrophils at 21% O_2 (15 min: 0.073 a.u., 1h: 0.073 a.u.). At 1% O_2, PR3-ANCA stimulated neutrophils were stiffer than MPO-ANCA IgG stimulated neutrophils at both time points (**Fig 35C and D**; 15 min: 0.075 a.u., 1h: 0.078 a.u., ns). For all IgG stimulations, incubation at 1% O_2 inhibited the decrease in deformability seen at 21% O_2, with the most striking results seen with MPO-ANCA IgG stimulation.

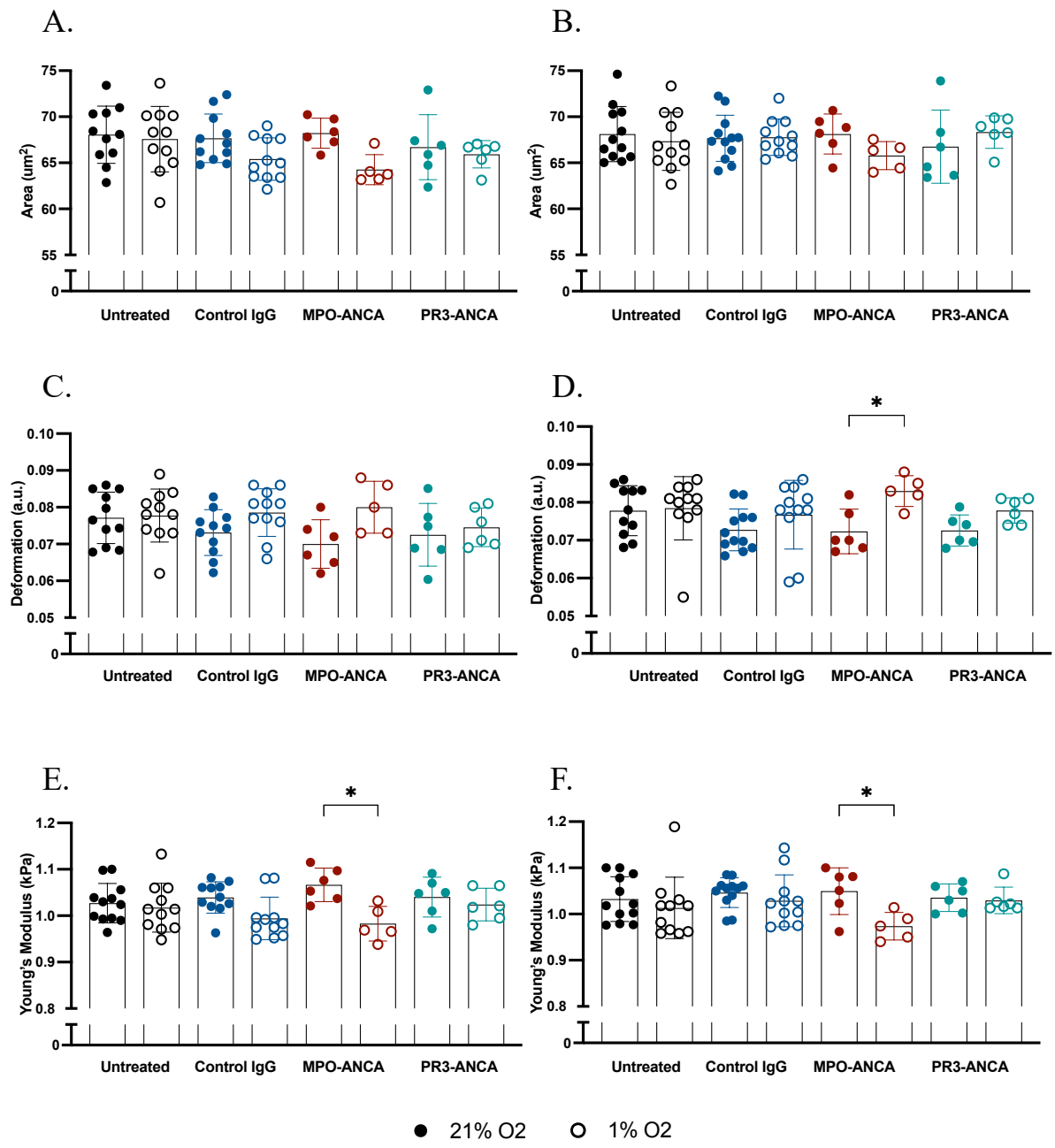


Figure 35. 1% O_2 decreases the effect of ANCA on isolated neutrophil deformability
(A-C) Neutrophils from HC (n=5) were isolated at 21% O_2, incubated for 15 minutes at 1% O_2, untreated with media only (neutrophil culture media, 'untreated') or primed with 2 ng/mL TNF for 15 minutes and stimulated with 100 ug/mL HC IgG, MPO-/PR3-ANCA IgG for 15 minutes or 1h, and were analysed using RT-DC. Neutrophil populations were gated and analysed for (A/B) Cell size, (C/D) Cell deformability, and (E/F) Elasticity, (A, C, E) 15 minutes, (B, D, F) 1h. More than 1000 events were recorded for each sample and results were visualised and analysed in ShapeOut2 software. Data are shown as mean +/- SEM, statistical analysis was performed using two-way ANOVA mixed effects model with Geisser-Greenhouse correction, with Tukey's multiple comparisons test; *p<0.05.

I have identified that in whole blood 5% O_2 inhibits ANCA induced changes in deformability whereas 1% O_2 promotes these changes (**Table 24**). In contrast, in experiments using isolated neutrophils, both 1%, and to a lesser degree, 5% O_2 diminish the MPO-ANCA IgG induced decrease in deformability seen at 1h in 21% O_2. These results suggest oxygen tension coupled with ANCA stimulation impacts biophysical properties of neutrophils in comparison to 21% O_2. As displayed, the relationship is complex and cell isolation method has a significant impact on results. It is likely that results are also stimulation, timing, and degree of oxygen tension dependent as outlined in **Table 24**.

	Oxygen Tension (O_2)	HC IgG	MPO-ANCA IgG	PR3-ANCA IgG
Whole blood	21%	↓	↓	
	5%	↑	↑	
	1%	↓	↓	
Isolated neutrophils	21%	↓	↓	↓
	5%	No change	↑	↓
	1%	No change	↑	↑

Table 24. Summary of stimulation conditions in comparison to untreated neutrophil deformability
'↓' denotes a decrease in deformability in comparison to untreated and '↑' denotes an increase in deformability in comparison to untreated.

4.5. Effect of hypoxia and ANCA on actin cytoskeleton

At 21% O_2, ANCA stimulation resulted in significant promotion of actin polymerisation in neutrophils (section 3.6). Having demonstrated that oxygen tension can have additional effects on biomechanical profiles, I next investigated whether this effect of ANCA-promoted actin polymerisation was changed under venous physiological normoxia or pathological hypoxia.

4.5.1. Oxygen tension influences neutrophil actin polymerisation

The increased F-actin polymerisation I have identified in neutrophils treated with ANCA IgG may contribute to their phenotype of increased cell stiffness. As I have also seen biomechanical changes in neutrophils in response to changing oxygen tensions, I wished to assess the cytoskeletal response of untreated neutrophils to hypoxia. HC isolated neutrophils were cultured at 21%, 5%, or 1% O_2 for 1h, fixed and stained for Phalloidin to visualise actin polymerisation. Experiments were performed simultaneously comparing 21% v 5% O_2, or 21% v 1% O_2. Variables and cytoskeletal protrusions were quantified using a macro. Phalloidin staining measures and represents the F-actin signal. The area and perimeter of each cell were quantified utilising Phalloidin stain, the total cell area staining for Phalloidin was quantified relative to the area of each measured cell, and the total cell perimeter staining for Phalloidin was quantified relative to the perimeter of each measured cell. These variables are individually referred to as area, perimeter, relative area, and relative perimeter.

Representative images shown in **Figure 36** display a visually brighter stain, blebbing at the cell perimeter and increased actin cap formation at 5% and 1% O_2 in untreated neutrophils in comparison to 21% O_2.

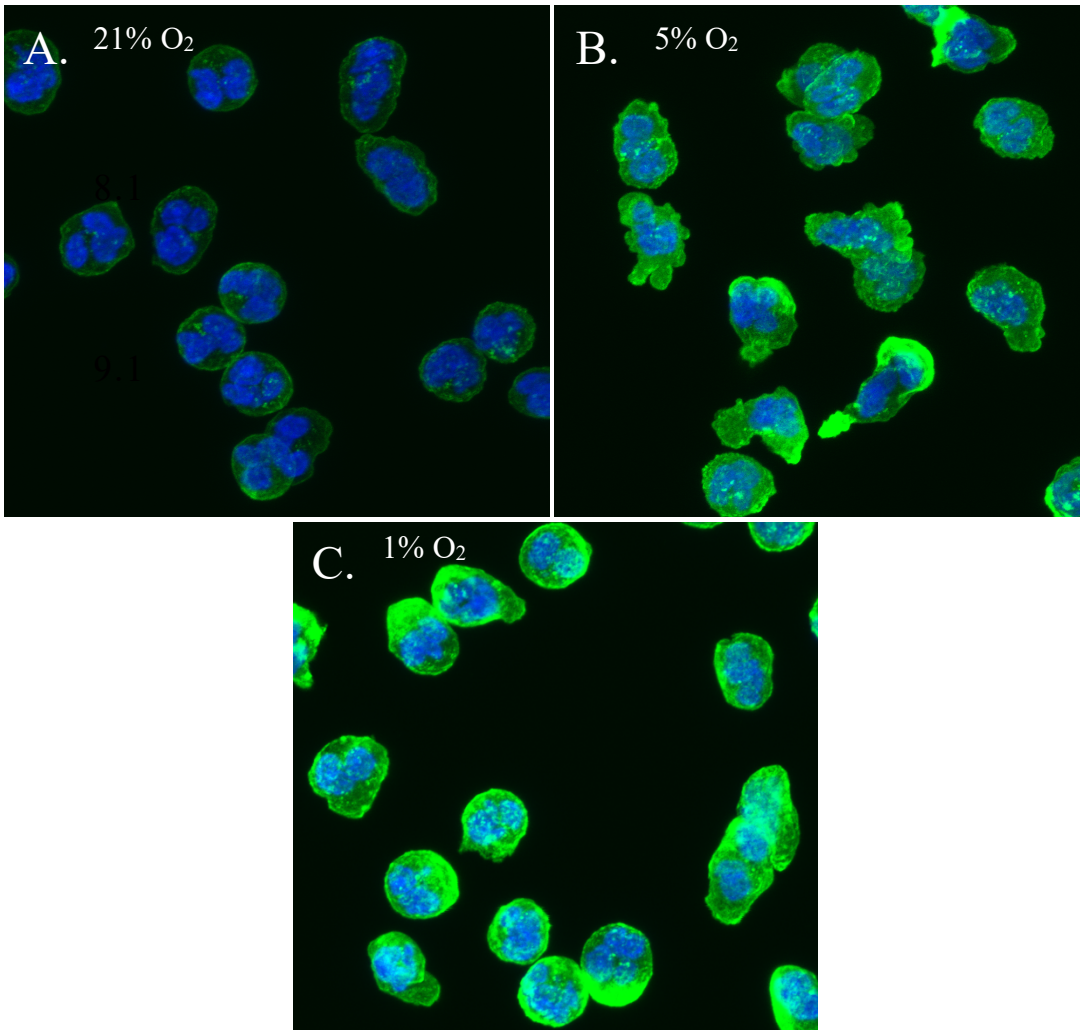


Figure 36. Oxygen tension influences actin polymerisation in neutrophils
Neutrophils from HC were isolated, cultured at 21%, 5%, or 1% O_2 (15 minutes), and incubated in media only (neutrophil culture media, 'untreated') for 1h. Neutrophils were fixed, stained for Phalloidin (green) (AF488), and mounted with VectaShield[R] Antifade Mounting Medium with DAPI (blue), and imaged at 63x using confocal microscopy (A) 21% O_2, (B) 5% O_2, (C) 1% O_2. Representative images from 21% O_2 n=31, 5% O_2 n=18, 1% O_2 n=12 experiments are shown.

There was no significant difference in area, perimeter, relative area, and relative perimeter at 5% O_2 in comparison to 21% O_2 (**Fig 36**; ns). However, at 1% O_2, there was a significant increase in area and perimeter (**Fig 36A and B**; p=0.0002, p=0.0005), and relative area and perimeter in comparison to 21% O_2 (**Fig 36C and D**; p=0.0001, p=0.0002).

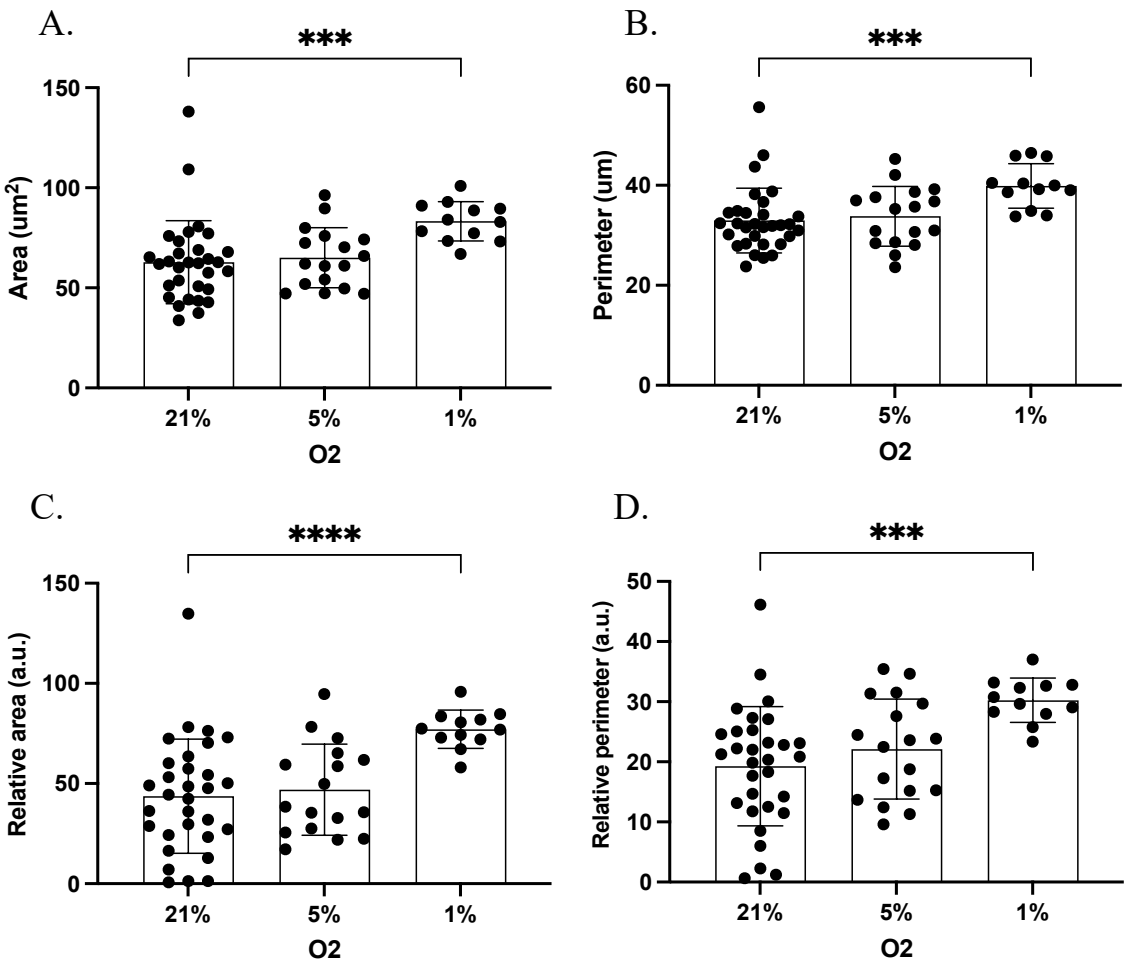


Figure 37. Oxygen tension influences neutrophil actin polymerisation
(A-D) Neutrophils from HC were isolated and incubated with media only (neutrophil culture media, 'untreated') for 1h (21% O_2 n=31, 5% O_2 n=18, 1% O_2 n=12). Neutrophils were fixed, stained for Phalloidin (AF488), and mounted with VectaShield[R] Antifade Mounting Medium with DAPI, and imaged at 63x using an inverted Zeiss LSM-780 (A) Area, (B) Perimeter, (C) Relative area, and (D) Relative perimeter. Data was analysed using a macro developed for use with ImageJ to measure area, perimeter, relative area, and relative perimeter. Data are shown as mean +/- SEM, statistical analysis was performed using two-way ANOVA mixed effects model with Geisser-Greenhouse correction, with Tukey's multiple comparisons test; ***p<0.001. ****p<0.00001.

4.6. Oxygen tension influences actin polymerisation in neutrophils stimulated with ANCA

Next, to determine if alterations in oxygen tension modulate the effect of ANCA on actin polymerisation, I cultured isolated neutrophils at 21%, 5%, or 1% O_2 (15 min), primed them with 2 ng/mL TNF (15 minutes) and stimulated with HC or MPO-/PR3-ANCA IgG for 1h. Cells were fixed, stained for Phalloidin, and assessed as above.

Neutrophils in all stimulation conditions displayed brighter phalloidin staining at 5% O_2 (Representative images shown in **Figure 38**) than 21% O_2 (Representative images shown in **Figure 38A-D**). Untreated and HC IgG stimulated neutrophils at 5% exhibit a visually brighter stain and blebbing at the cell perimeter in comparison to untreated or HC IgG treated neutrophils at 21% O_2. Some actin caps were present at 21% O_2 following stimulation of neutrophils with HC IgG, but this was present to a greater extent seen at 5% O_2. Following MPO-/PR3-ANCA stimulation at 5% O_2 there was a further visual increase in intensity of staining and increased actin cap formation in comparison to untreated and HC IgG treated cells. Incubation at 5% O_2 resulted in some decrease in ANCA induced protrusions. Visually, protrusions could still be identified, but they were not as frequent as those seen in ANCA stimulated neutrophils at 21% O_2. It could also be seen that more actin was retained at the cell periphery compared to 21% O_2.

Quantification of phalloidin staining identified that incubation at 5% O_2 prevented the MPO-ANCA induced increase in area (**Fig 38A**) and perimeter (**Fig 38B**) that were seen at 21% O_2. There was no significant change in relative area at either 21% or 5% O_2 (**Fig 38C**), however the MPO-ANCA induced increase in relative perimeter found at 21% O_2 was also inhibited at 5% O_2 (**Fig 38D**). In contrast to these results seen with MPO-ANCA, my results suggest the

actin polymerisation effect in PR3-ANCA stimulated neutrophils seen at 21% is preserved at 5% O_2 (**Fig 38A-D**). This may be as the magnitude of effect seen following PR3-ANCA stimulation is greater than seen with MPO-ANCA.

Similar to at 5% O_2, neutrophils in all conditions displayed visually brighter phalloidin staining at 1% O_2 compared to 21 % O_2 (**Fig 40I-L**). Untreated and HC IgG stimulated neutrophils at 1% O_2 exhibit a visually brighter stain and blebbing at the cell perimeter in comparison to 21% O_2 untreated or HC IgG (**Fig 39A-B**). Again, following MPO-/PR3-ANCA stimulation, there was an increase in the brightness of phalloidin staining and cell protrusions were formed (**Fig 39C and D**).

Quantification of area, relative area, and relative perimeter were all significantly increased in untreated neutrophils at 1% O_2 in comparison to 21% O_2, (**Fig 39A, C, and D**; area p= 0.0350, relative area p= 0.0258, relative perimeter p=0.0212). In contrast to cells at 5% O_2, when cells were incubated at 1% O_2 an increase in area and perimeter in response to MPO-ANCA stimulation was still seen (**Fig 39A and B**; ns). Incubation at 1% O_2 significantly enhanced increased relative area and relative perimeter in MPO-ANCA stimulated neutrophils to a greater degree than was seen at 21% O_2 (**Fig 39C and D**; relative area MPO p=0.0033, relative perimeter MPO p=0.0034). Results for PR3-ANCA exhibited a similar pattern of results, displaying an increase in all measurements following stimulation in 1% O_2 in comparison to 21% O_2, but data did not achieve significance for any of the variables measured. However, the magnitude of the increase in actin parameters was similar to that seen at 21% O_2, suggesting the greater area/perimeter staining seen at 1% O_2 is based upon the initial hypoxic uplift seen at baseline.

Collectively, 1% O_2 enhances actin polymerisation overall, in comparison to 5% and 21% O_2, at baseline in untreated cells and synergising with MPO-/PR3-ANCA to further promote actin polymerisation in stimulated neutrophils. Conversely, the actin polymerisation effect of MPO-ANCA stimulation at 21% O_2 was completely lost at 5% O_2. In contrast to MPO ANCA responses, the polymerisation effect of PR3-ANCA stimulation was maintained at 5% O_2 and only slightly increased at 1% O_2 (representative images shown in **Fig 38**). Thus, not only does oxygen tension alone have a significant effect on actin polymerisation in untreated neutrophils, but it can impact ANCA-induced responses in both directions dependent upon the degree of hypoxia and the specificity of ANCA. These experiments indicate pathological hypoxia promotes neutrophil actin polymerisation to a similar extent as previously seen with ANCA stimulation (section 3.6.1).

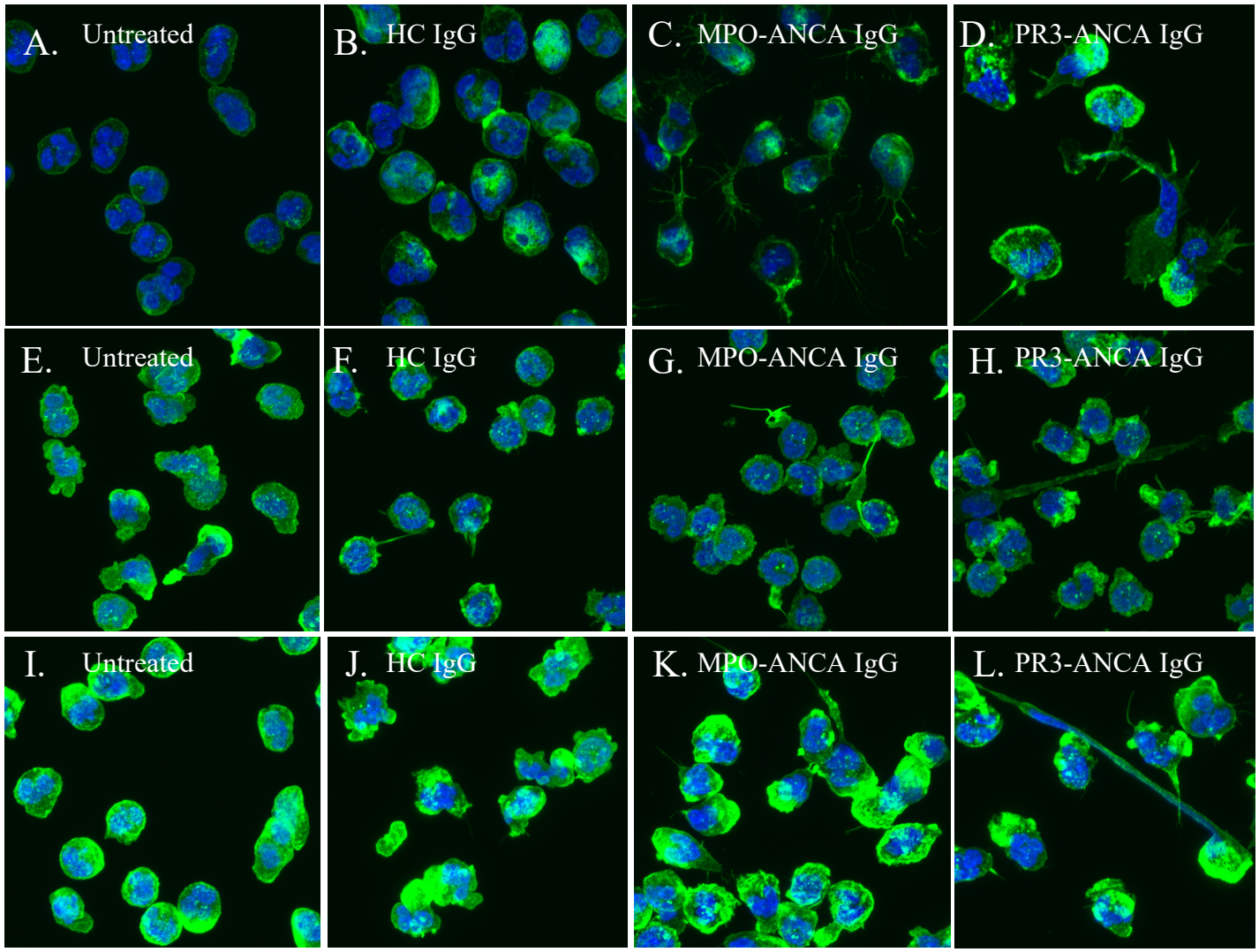


Figure 38. Oxygen tension alters ANCA induced actin polymerisation in HC stimulated neutrophils

(A-L) Neutrophils from HC were isolated, untreated with media only (neutrophil culture media, 'untreated') or primed with 2 ng/mL TNF (15 minutes) and stimulated with 100 ug/mL HC IgG, MPO-ANCA IgG, PR3-ANCA IgG for 1h at 21%, 5% or 1% O_2. Neutrophils were fixed, stained with Phalloidin (F actin, AF488, green), and mounted with VectaShield[R] Antifade Mounting Medium with DAPI (nucleus, blue), and imaged at 63x using an inverted Zeiss LSM-780 (A-D) 21% O_2, (E-H) 5% O_2, (I-L) 1% O_2, (A/E/I) Untreated, (B/F/J) HC IgG, (C/G/K) MPO-ANCA IgG, and (D/H/L) PR3-ANCA. Representative images from 21% O_2 n=31, 5% O_2 n=18, 1% O_2 n=12 experiments are shown.

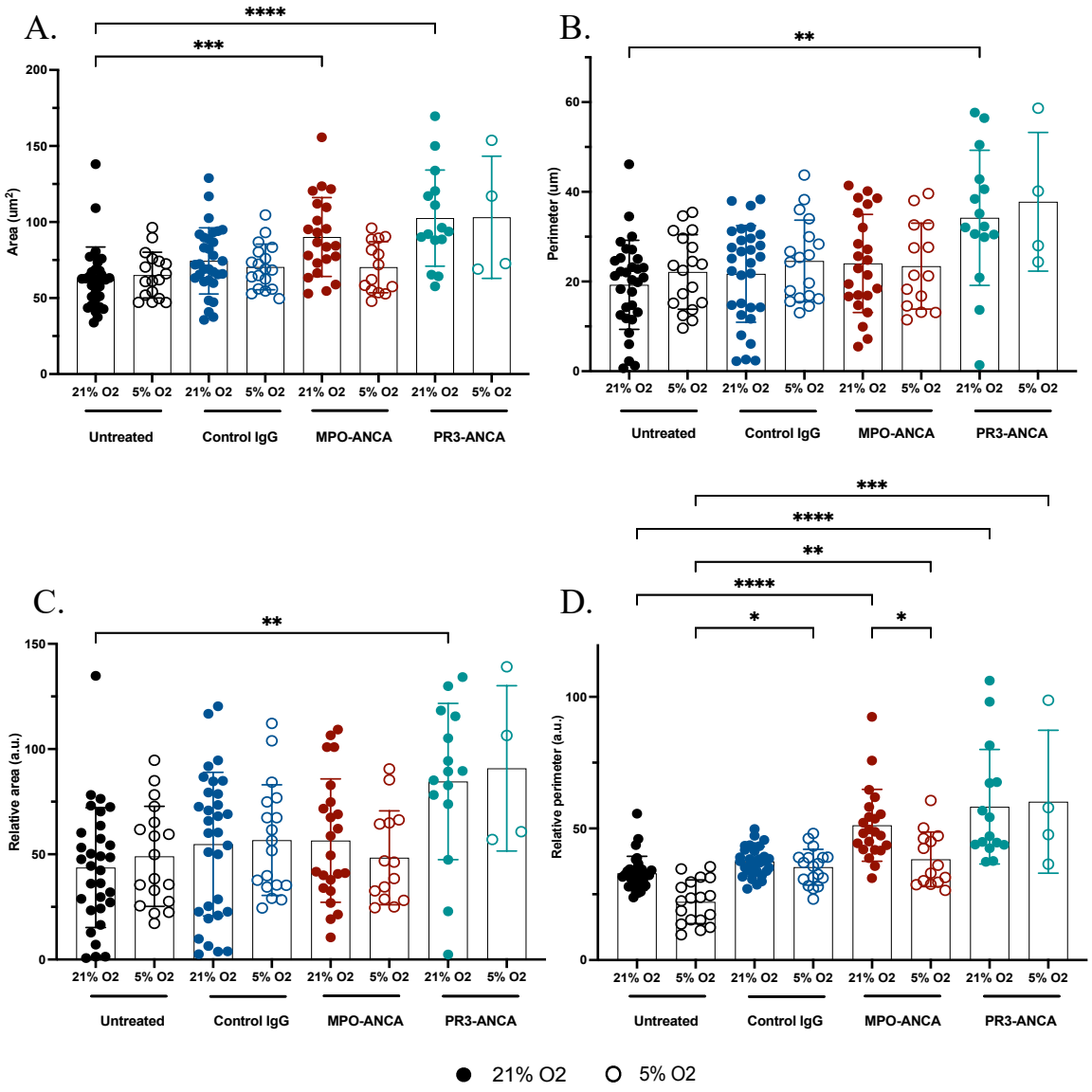


Figure 39. 5% O_2 influences actin polymerisation in MPO-ANCA stimulated neutrophils
(A-D) Neutrophils from HC were isolated, cultured at 21% or 5% O_2 (15 minutes), untreated with media only (neutrophil culture media, 'untreated') or primed with 2 ng/mL TNF (15 minutes) and stimulated with 100 ug/mL HC IgG, MPO-ANCA IgG (n=14), PR3-ANCA IgG (n=4) for 1h. Neutrophils were fixed, stained for Phalloidin (AF488), and mounted with VectaShield[R] Antifade Mounting Medium with DAPI, and imaged at 63x using an inverted Zeiss LSM-780 (A) Area, (B) Perimeter, (C) Relative area, and (D) Relative perimeter. Data were analysed using a macro developed for use with ImageJ to measure area, perimeter, relative area, and relative perimeter. Data are shown as mean +/- SEM, statistical analysis was performed using two-way ANOVA mixed effects model with Geisser-Greenhouse correction, with Tukey's multiple comparisons test; *p<0.05. **p<0.01 ***p<0.001. ****p<00001.

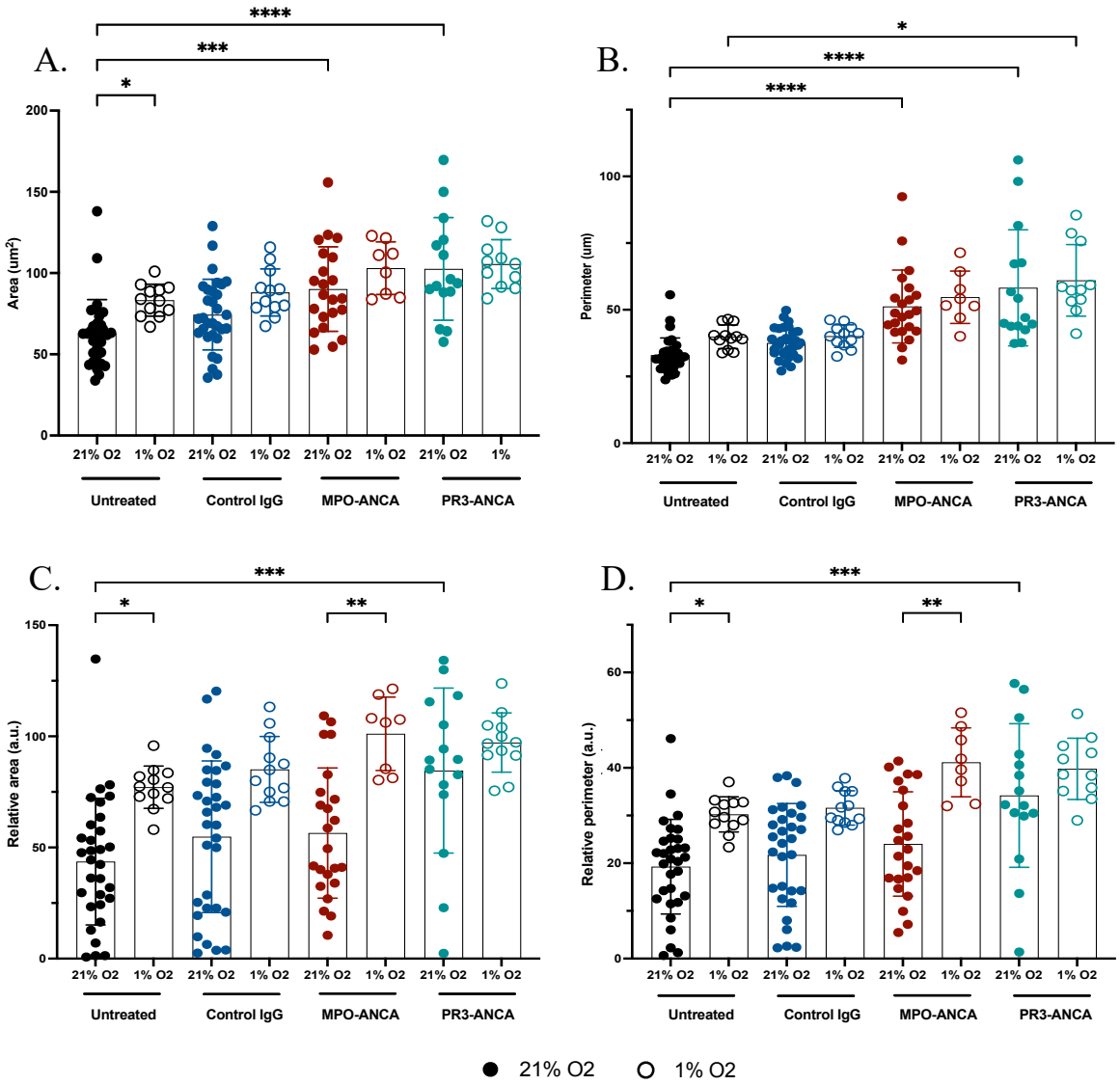


Figure 40. <u>1% O_2 influences actin polymerisation in ANCA stimulated neutrophils</u>
(A-D) Neutrophils in whole blood from HC were isolated, cultured at 21% or 5% O_2 (15 minutes), untreated with media only (neutrophil culture media, 'untreated') or primed with 2 ng/mL TNF (15 minutes) and stimulated with 100 ug/mL HC IgG, MPO-ANCA IgG (n=8), PR3-ANCA IgG (n=12) for 1h. Neutrophils were fixed, stained for Phalloidin (AF488), and mounted with VectaShield[R] Antifade Mounting Medium with DAPI, and imaged at 63x using an inverted Zeiss LSM-780 (A) Area, (B) Perimeter, (C) Relative area, and (D) Relative perimeter. Data were analysed using a macro developed for use with ImageJ to measure area, perimeter, relative area, and relative perimeter. Data are shown as mean +/- SEM, statistical analysis was performed using two-way ANOVA mixed effects model with Geisser-Greenhouse correction, with Tukey's multiple comparisons test; *p<0.05. **p<0.01 ***p<0.001. ****p<0.00001.

4.7. Effect of inhibitors on ANCA mediated neutrophil response

4.7.1. Cytochalasin B best inhibits ANCA induced actin polymerisation under hypoxia

At 21% O_2, MPO-ANCA induced promotion of actin polymerisation was inhibited by Cytochalasin D. However, as shown in previous sections, results may differ under different oxygen tensions. Therefore, I tested the same set of inhibitors I used previously in section 3.7.1., but under different oxygen tensions of 1% or 5% O_2 to determine whether the effect of ANCA on neutrophil actin polymerisation under hypoxia could be inhibited using inhibitors of actin filament formation or myosin-ii. Neutrophils were cultured for 15 minutes at 21%, 5%, or 1% O_2, primed with 2 ng/mL TNF (15 minutes), treated with one of the selected inhibitors (10 minutes), stimulated with HC or MPO-ANCA IgG for 1h, fixed, and stained for Phalloidin using immunofluorescence.

No inhibitor influenced the actin cytoskeleton at 5% O_2 for any stimulation condition (**Fig 41**). This was not surprising as data from section 4.6 suggests that incubation under 5% O_2 alone (without any additional inhibitors) prevented ANCA induced actin polymerisation and therefore there was no ANCA stimulation effect to inhibit.

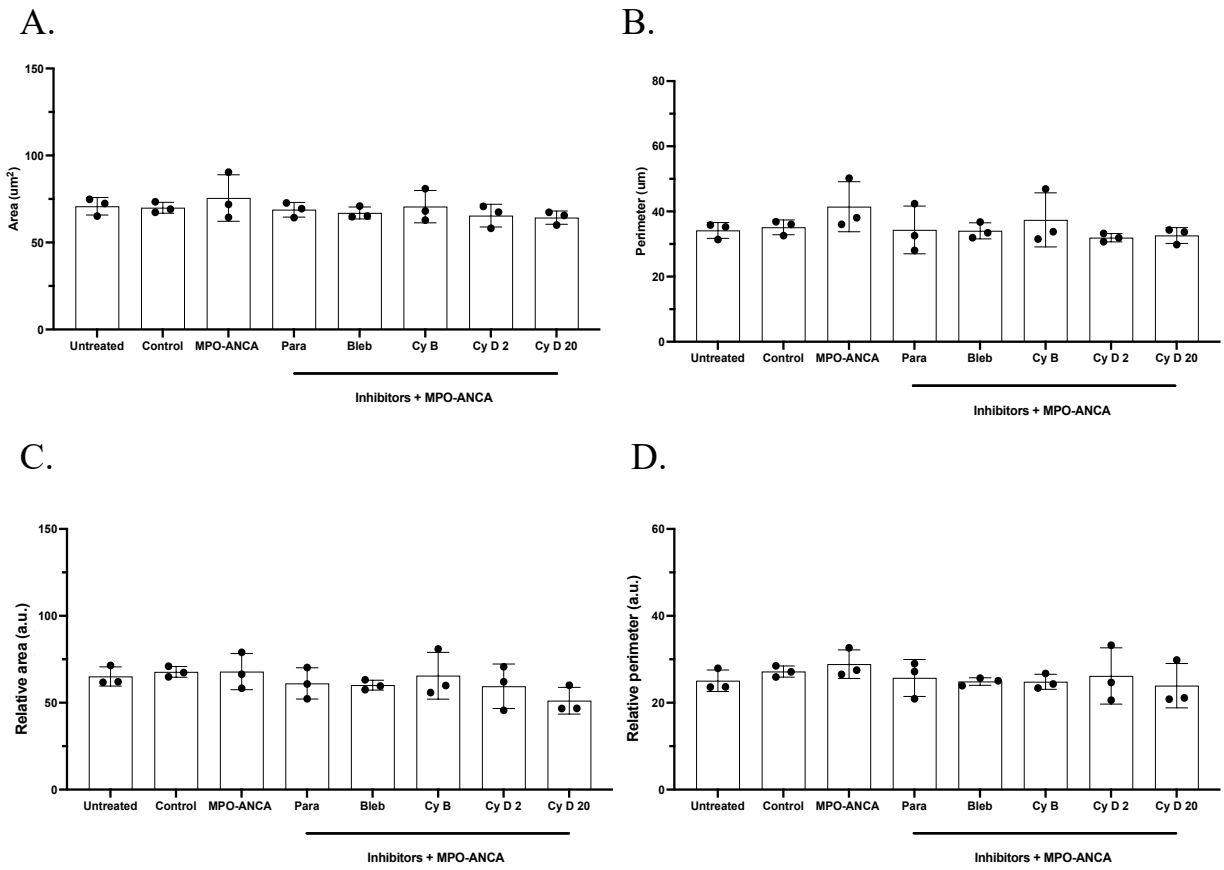


Figure 41. <u>No change in parameters at 5% O_2 with actin polymerisation inhibitors</u>
(A-D) Neutrophils in whole blood from HC (n=3) were isolated, cultured at 5% O_2 (15 minutes), untreated with media only (neutrophil culture media, 'untreated') or primed with 2 ng/mL TNF (15 minutes), treated with cytochalasin B 10µm, cytochalasin D 2µm, paraminoblebbistatin 50 µm, or blebbistatin 100µm, and stimulated with 100 µg/mL HC IgG, MPO-ANCA IgG for 1h. Neutrophils were fixed, stained for Phalloidin (AF488), and mounted with VectaShield[R] Antifade Mounting Medium with DAPI, and imaged at 63x using confocal microscopy (A) Area, (B) Perimeter, (C) Relative area, and (D) Relative perimeter. Data was analysed using a macro developed for use with ImageJ to measure area, perimeter, relative area, and relative perimeter. Data are shown as mean +/- SEM, statistical analysis was performed using one-way ANOVA Kruskal-Wallis test, with Dunn's multiple comparisons test.

At 1% O_2 upon visual inspection, blebbistatin resulted in the smallest morphology effect, and significant protrusions were still formed in ANCA stimulated neutrophils (representative images shown in **Fig 42**). Similar results were seen with para-aminoblebbistatin which again showed significant ANCA induced neutrophil protrusion, although not as many as seen in blebbistatin treated, ANCA stimulated neutrophils. By visual inspection, cytochalasin B resulted in more rounded, circular cells. As I also identified at 21% O_2, cytochalasin D at 20 μm resulted in bleb-like formation around the cell membrane in ANCA stimulated neutrophils, which was identified in untreated neutrophils as well, it seems this is unlikely to be a result of ANCA stimulation (537,538). In comparison to all the other inhibitors used, cytochalasin B had the greatest inhibitory effect, particularly upon visual inspection. All inhibitors resulted in a decrease in MPO-ANCA induced cytoskeletal changes for all variables at 1% O_2 (**Fig 43**). The smallest effect was seen with the blebbistatins. The greatest magnitude of inhibition on perimeter was seen with cytochalasin B, which suppressed actin polymerisation to that seen in untreated cells (**Fig 43**; ns). This suggests MPO-ANCA promotion of actin polymerisation under hypoxia may be inhibited through the annealing step of actin polymerisation. Once again, neutrophil phenotype is altered under hypoxia and in the context of ANCA stimulation.

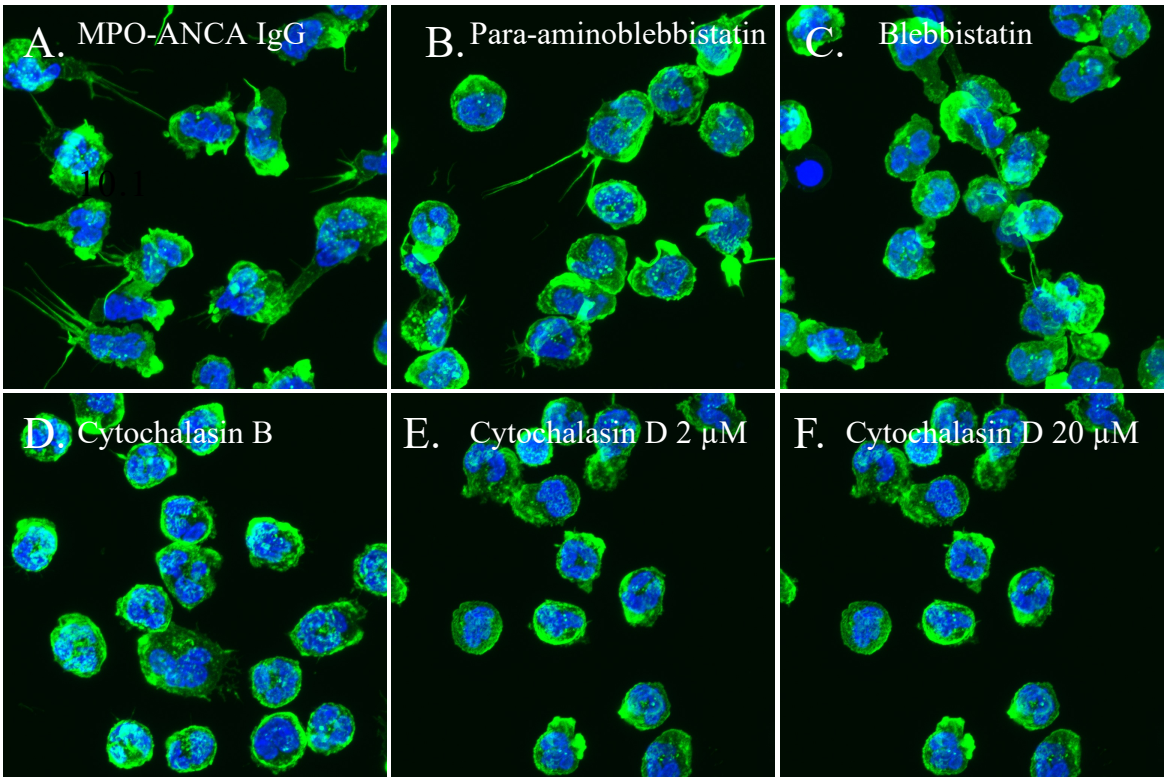


Figure 42. ANCA promotion of actin polymerisation in HC is inhibited by Cytochalasin B at 1% O_2

(A-D) Neutrophils in whole blood from HC (n=3) were isolated, untreated with media only (neutrophil culture media, 'untreated') or primed with 2 ng/mL TNF (15 minutes), treated with cytochalasin B 10µm, cytochalasin D 2µm, paraminoblebbistatin 50 µm, or blebbistatin 100µm, and incubated for 1h at 1% O_2. Neutrophils were fixed, stained with Phalloidin (F actin, AF488, green), and mounted with VectaShield[R] Antifade Mounting Medium with DAPI (nucleus, blue), and imaged at 63x using an inverted Zeiss LSM-780 (A) Untreated, (B) para-aminoblebbistatin, (C) blebbistatin, (D) cytochalasin B, (E) cytochalasin D 2mM, and (F) cytochalasin D 20mM.

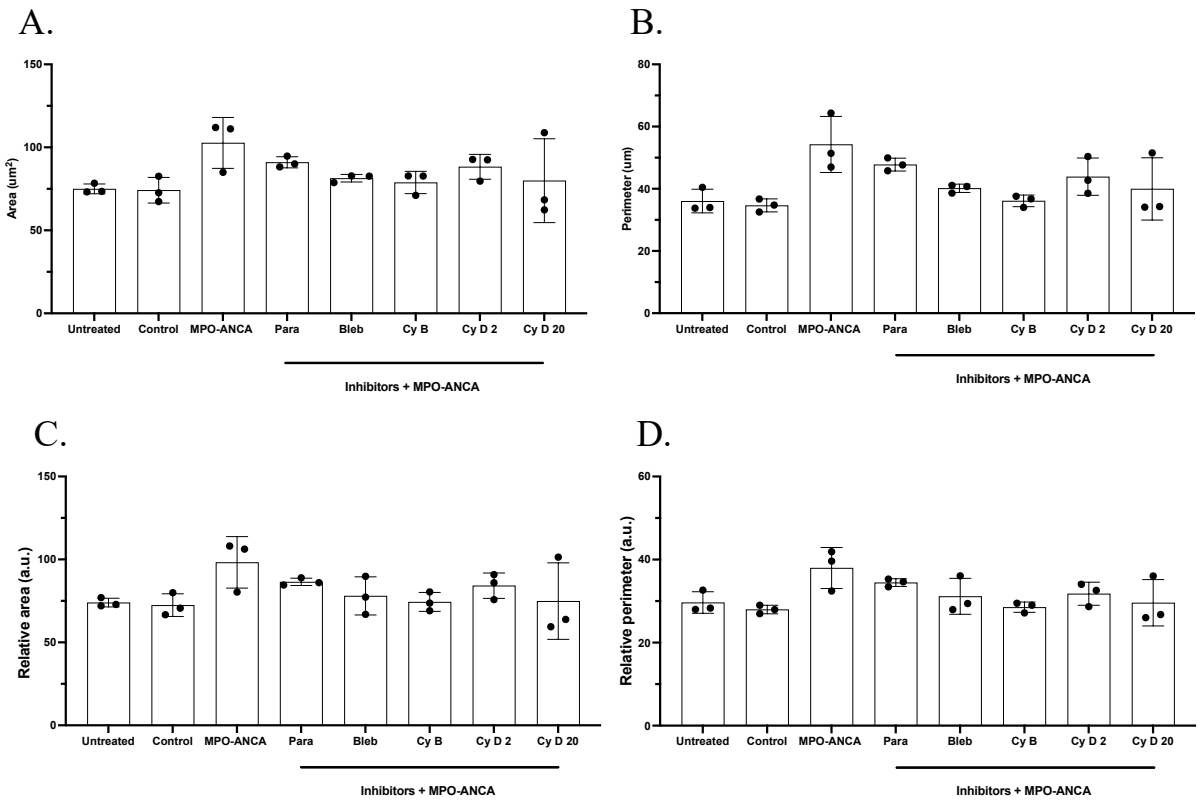


Figure 43. Cytochalasin B best inhibits ANCA promotion of actin polymerisation under hypoxia

(A-D) Neutrophils in whole blood from HC (n=3) were isolated, cultured at 1% O_2 (15 minutes), untreated with media only (neutrophil culture media, 'untreated') or primed with 2 ng/mL TNF (15 minutes), treated with cytochalasin B 10µm, cytochalasin D 2µm, paraminoblebbistatin 50 µm, or blebbistatin 100µm, and stimulated with 100 µg/mL HC IgG, MPO-ANCA IgG for 1h. Neutrophils were fixed, stained for Phalloidin (AF488), and mounted with VectaShield[R] Antifade Mounting Medium with DAPI, and imaged at 63x using confocal microscopy (A) Area, (B) Perimeter, (C) Relative area, and (D) Relative perimeter. Data was analysed using a macro developed for use with ImageJ to measure area, perimeter, relative area, and relative perimeter. Data are shown as mean +/- SEM, statistical analysis was performed using one-way ANOVA Kruskal-Wallis test, with Dunn's multiple comparisons test.

4.8. Discussion

The hypothesis for this chapter was based on the theory that neutrophils trapped in the inflamed microvasculature, as found in AAV, will be exposed to a characteristically hypoxic environment. Therefore, in effort to model *ex vivo* the most representative physiological/pathological conditions of what occurs *in vivo*, I used different oxygen tensions with the intention of more accurately measuring neutrophil function in AAV. The main objective was to determine the effect of hypoxia alone, and then the combined effect of hypoxia and ANCA on neutrophil mechanics and actin polymerisation. In Chapter 3, I established the capability of RT-DC to identify the biomechanical phenotype of neutrophils under various conditions at 21% O_2. I identified an ANCA induced decrease in cell deformability and promotion of actin polymerisation. In this chapter I explored whether this mechanism in neutrophils was influenced or replicated under more physiological oxygen tensions in comparison to pathological hypoxia. ANCA promotion of actin polymerisation was inhibited at 21% O_2 using Cytochalasin D. Therefore, I questioned whether inhibition of ANCA promoted actin polymerisation was similar under physiological or pathological oxygen tensions, or whether hypoxia acted as an independent stimulus.

Untreated neutrophil responses at 21% O_2 differed from untreated neutrophil responses at various oxygen tensions, and 5% (venous) O_2 or 1% (hypoxia) O_2 also impacted neutrophil responses to control and ANCA IgG. The changes in neutrophil biomechanics and cytoskeletal changes such as actin polymerisation, were dependent upon the oxygen tension measured, and often occurred in synergy with ANCA IgG stimulation.

In this chapter, I initially identified how different oxygen tensions influence the biomechanical properties of untreated neutrophils. Unexpectedly, incubation of whole blood at 5% O_2 resulted

in an increase in neutrophil deformability, which was a reproducible and consistent effect throughout my experiments. In Chapter 3, my experiments performed under 21% O_2 indicated variability in isolated cell runs, but more consistent effects were displayed in whole blood. As for experiments under decreased oxygen tensions in Chapter 4, this same relationship held true, specifically at 5% O_2. Thus, in contrast, a significant decrease in deformability at 5% O_2 in untreated isolated neutrophils was shown in comparison to 21% O_2. Minimal change was shown in whole blood or in isolated untreated neutrophils at 1% O_2 in comparison to 21% O_2. Therefore, this opposite effect shown between whole blood and isolated neutrophil mechanophenotype may not be an effect of oxygen tension but instead may be related to the impact of cell isolation on RT-DC measurements of neutrophil biomechanics, as it is also shown in Chapter 3 at 21% O_2.

While there is a different baseline for each oxygen tension, my results suggest that when whole blood ANCA IgG stimulation is performed, 5% O_2 inhibits the ANCA IgG induced decrease in neutrophil deformation that was seen at 21% O_2. However, at 1% O_2, following whole blood stimulation with ANCA IgG, the effect of decreased neutrophil deformability persists, but is also seen following HC IgG stimulation suggesting cells may be primed or pre-activated by pathological hypoxia. This effect in HC IgG was equivalent to the effect of decreased deformability seen in ANCA stimulated whole blood at 1% O_2. Due to the differences in isolated cells, it is difficult to interpret the data. This may be due to performing neutrophil isolation under 21% O_2 to then a new challenge of 1 or 5% O_2, whereas blood is kept in its physiological environment in the EDTA vacutainer up until any treatment. At 5% O_2, cells are somehow more quiescent in their physiological O_2. This result has not been examined before and has important implications for laboratory neutrophil functional work. Hypoxia enhancing

this result aligns with hypoxia further promoting other function responses in combination with other stimuli such as degranulation (456).

In Chapter 3, once isolated neutrophils were stimulated with ANCA at 21% O_2, there was a small decrease in neutrophil deformability following stimulation with both MPO- and PR3-ANCA. At 5% O_2, this effect was diminished in MPO-ANCA stimulated neutrophils, consistent with my results using whole blood. Surprisingly, in contrast, in PR3-ANCA stimulated neutrophils, at 5% O_2 the effect of decreased deformability persisted. At 1% O_2, a similar effect was seen with inhibition of MPO-ANCA induced decreases in deformability in comparison to 21% O_2 conditions. Unexpectedly, PR3-ANCA stimulated neutrophils exhibited a different effect at 1% and 5% O_2. At 5% O_2, a PR3-ANCA induced decrease in neutrophil deformability was still seen, but this was inhibited at 1% O_2.

Following identification of the impact of hypoxia on neutrophil mechanophenotype and the effect on ANCA induced changes in deformability this prompted further investigation to determine if hypoxia also altered neutrophil cytoskeleton in conjunction with ANCA stimulation. Hypoxia has been shown to induce and modulate actin cytoskeletal rearrangement in multiple cell types (539). Studies of the effects of hypoxia on neutrophil actin cytoskeleton are limited but hypoxia has been identified to promote actin cap formation in neutrophils (459). At baseline, untreated neutrophil cytoskeleton was visually altered at 1% and 5% O_2, with increased actin polymerisation and cap formation, but in quantified data, a significant increase was only shown at 1% O_2 in comparison to 21% O_2.

My results assessing the actin cytoskeleton following ANCA stimulation were broadly in keeping with measurements of cell deformability in isolated neutrophils. Incubation at 5% O_2

inhibited MPO- but not PR3- ANCA induced changes in area and perimeter whereas incubation at 1% O_2 increased the magnitude of these changes. At 1% O_2, the proportional increase in area/perimeter following MPO-ANCA stimulation was greater than that seen at 21% O_2, whereas following PR3-ANCA stimulation, the proportional increase in actin area/perimeter was similar between 21% and 1% O_2 after the initial shift upwards in untreated cells at 1% O_2. At 21% O_2, PR3-ANCA induced a greater effect in area/perimeter than MPO-ANCA, therefore there was not as great of a difference between 21% O_2 PR3-ANCA and 1% O_2 PR3-ANCA conditions. Yet, at 21% O_2, MPO-ANCA induced less of an effect on area/perimeter than PR3-ANCA, and therefore, hypoxia enhanced this effect more so in comparison to 21% O_2, than shown with PR3-ANCA. This was an interesting result as some studies have shown MPO-ANCA to have a greater effect on neutrophil programmed mechanisms than PR3-ANCA such as ROS production and degranulation (529). In my previous results, confirming the pathogenicity of the IgG preparations I had isolated, PR3-ANCA induced similar levels of cytokine production and NETosis. In general, my results were more variable using PR3-ANCA than MPO-ANCA. This could potentially be explained due to differences in cell surface PR3 expression between donors (287).

In Chapter 3, I showed that cytochalasin D inhibited actin polymerisation promoted by MPO-ANCA IgG. However, given neutrophil responses at baseline, in addition to when stimulated with ANCA IgG, are different at 21% O_2 than other decreased oxygen tensions it was unknown whether cytochalasin D would inhibit ANCA promoted actin polymerisation under hypoxia (540). At 1% O_2, cytochalasin B best inhibited ANCA promotion of actin polymerisation. While cytochalasin D was most effective at 21% O_2 and cytochalasin B under hypoxia, this identified the potential step of actin polymerisation involved in ANCA induced cytoskeletal changes, as the cytochalasins have similar mechanisms of action by binding to F-actin directly.

The blebbistatins were less effective, both at 21% O_2 or under hypoxia. The consistency of cytochalasins being the most effective inhibitor across oxygen tensions suggests that the mechanism of ANCA induced promotion of actin polymerisation is consistent. Possibly, although modulated by hypoxia, the pathways involved may not change, or the cytochalasins may act on a final common pathway in inhibiting cytoskeletal changes.

In conclusion, my results have identified that hypoxia modulates neutrophil deformability and actin polymerisation both in untreated cells and following ANCA stimulation. A key finding is that pathological hypoxia (1% O_2) enhances actin polymerisation in response to ANCA stimulation. It may be that this enhancement is also seen *in vivo* at sites of tissue injury. Whether this response of increased actin polymerisation has a protective effect, promotes cell interaction, locomotion, and communication, or leads to enhanced pathological responses warrants further investigation. As a result, in the next chapter I investigated functional neutrophil responses such as TEM, NETosis and cytokine responses (234).

Key findings:

1. Untreated whole blood neutrophil deformability is increased at 5% O_2
2. 5% O_2 prevents ANCA stimulated whole blood neutrophil deformability and actin polymerisation whereas 1% O_2 further enhances these effects
3. MPO- and PR3-ANCA promoted neutrophil actin polymerisation response differs under decreased oxygen tension
4. Cytochalasins best inhibit MPO-ANCA IgG promoted actin polymerisation in neutrophils

5. Chapter 5 – The effect of hypoxia on ANCA induced functional responses

5.1. Introduction

Having identified an ANCA-induced neutrophil mechanophenotype that is influenced by oxygen tension, I next performed neutrophil functional analysis and examine functional responses and neutrophil-endothelial interaction in physiological normoxia and pathological hypoxia environments. In chapter 4, I identified that decreased oxygen tension modulates neutrophil deformability, both at baseline and following stimulation with ANCA. This was associated with changes in actin polymerisation. As previously discussed, remodelling of the actin cytoskeleton is a key process in several neutrophil functions such as exocytosis, degranulation, and NETosis (55,541,542). In this chapter, I therefore investigated the impact of physiological and pathological oxygen tensions on functional neutrophil responses in the context of ANCA stimulation.

In Chapter 3, at 21% O_2, an increase in NET production was shown in neutrophils stimulated with MPO- or PR3-ANCA IgG. Considering pathological hypoxia enhances the effect of ANCA stimulated neutrophil actin polymerisation as shown in Chapter 4, it was important to determine whether hypoxia also synergises with the effect of ANCA shown at 21% O_2 to promote NET formation. Yet, ANCA stimulated neutrophils at physiological normoxia displayed an unexpected phenotype, therefore I wanted to determine whether 5% O_2 can inhibit a pathogenic programmed mechanism, such as NETs.

I also employed a co-culture system with glomerular endothelial cells (gEC) as a more representative model *ex vivo* of what interactions, communication, and signalling may occur *in vivo* with neutrophils and their surrounding environment. The kidney is a main site of organ involvement in AAV, therefore gEC were chosen for this model. Whether the relationship I

identified in Chapter 4 between hypoxia and neutrophil mechanophenotype could impact neutrophil-endothelial interactions and injury is currently unknown.

Hypothesis of current chapter

Hypoxia exacerbates the effect of ANCA on neutrophil mediated responses and contributes to endothelial injury.

Aims

1 Determine the impact of hypoxia on ANCA induced functional neutrophil responses

2 Investigate the effect of hypoxia on ANCA mediated responses in a neutrophil-endothelial cell co-culture setting

3 Identify if transcriptional changes contributed to any differences in neutrophil phenotype following ANCA stimulation in hypoxic conditions

5.2. Impact of hypoxia on ANCA induced pathogenic neutrophil responses

My previous results have identified that oxygen tension can modulate ANCA IgG induced changes in neutrophil biomechanics. In this chapter I aimed to identify if oxygen tension can also influence key pathogenic effects of ANCA I identified in earlier sections, by assessing IL-8 secretion and NET release.

5.2.1. Hypoxia alters MPO-ANCA induced neutrophil IL-8 secretion

The induction of IL-8 secretion following ANCA stimulation of neutrophils is well established (327) and was replicated at 21% O_2 in my experimental work in section 3.3.1. Hypoxic neutrophils have displayed a 'hyper-secretory' phenotype, promoting secretion of several histotoxic granule proteins. However, there is also evidence that decreased oxygen tension may decrease IL-8 production in PMN, although results varied depending on stimuli used (543). The impact of hypoxia on IL-8 responses induced by ANCA is not known. I therefore investigated if oxygen tension modulates IL-8 secretion following ANCA stimulation. Isolated neutrophils were primed with 2 ng/mL TNF (15 minutes) and stimulated with MPO-ANCA for 1h and 4h at 1%, 5% or 10% O_2 in comparison to 21% O_2. SNs were collected and IL-8 was measured using ELISA at 1%, 5%, or 10% O_2 in comparison to 21% O_2.

At 21% O_2, as previously described, an increase in IL-8 secretion was seen in MPO-ANCA stimulated neutrophils in comparison to HC IgG stimulated or untreated neutrophils with increased cytokine release at 1h (**Fig 44A**; ns) and at 4h (**Fig 44B**; ns). At 1% O_2, this level of oxygen tension led to decreased MPO-ANCA stimulated neutrophil IL-8 secretion in comparison to 21% O_2 at 1h and 4h (**Fig 44A**; 1h: ns, **Fig 44B**; 4h: 0.0359). A decrease in PR3-ANCA IL-8 secretion was shown at 1% O_2 in comparison to 21% O_2 at 1h and 4h, but neither

achieved significance (**Fig 44A**; 1h: ns, **Fig 44B**; 4h: ns). At 5% O_2, there was a decrease in both ANCA stimulated neutrophil IL-8 secretion at 1h, but this effect was not significant, nor was there a change IL-8 secretion at 4h (**Fig 44A**; ns, **Fig 44B**; ns). At 10% O_2, this level of oxygen tension displayed a slight decrease in MPO-ANCA IL-8 secretion at 4h in comparison to 21% O_2 but did not achieve significance at either 1h or 4h (**Fig 44A**; ns, **Fig 44B**; ns). Minimal difference in IL-8 secretion was shown when comparing MPO- or PR3-ANCA stimulation under all oxygen tensions and at both time points (**Fig 44A and B**).

Overall, at 5% and 10% O_2, cytokine release did not significantly differ from 21% O_2, suggesting ANCA promoted neutrophil IL-8 secretion is maintained under physiological oxygen tensions. However, 1% O_2 promotes a slight decrease in IL-8 secretion in in ANCA stimulated neutrophils in comparison to 21% O_2 at 4h, but more replicates are necessary before confirming this effect.

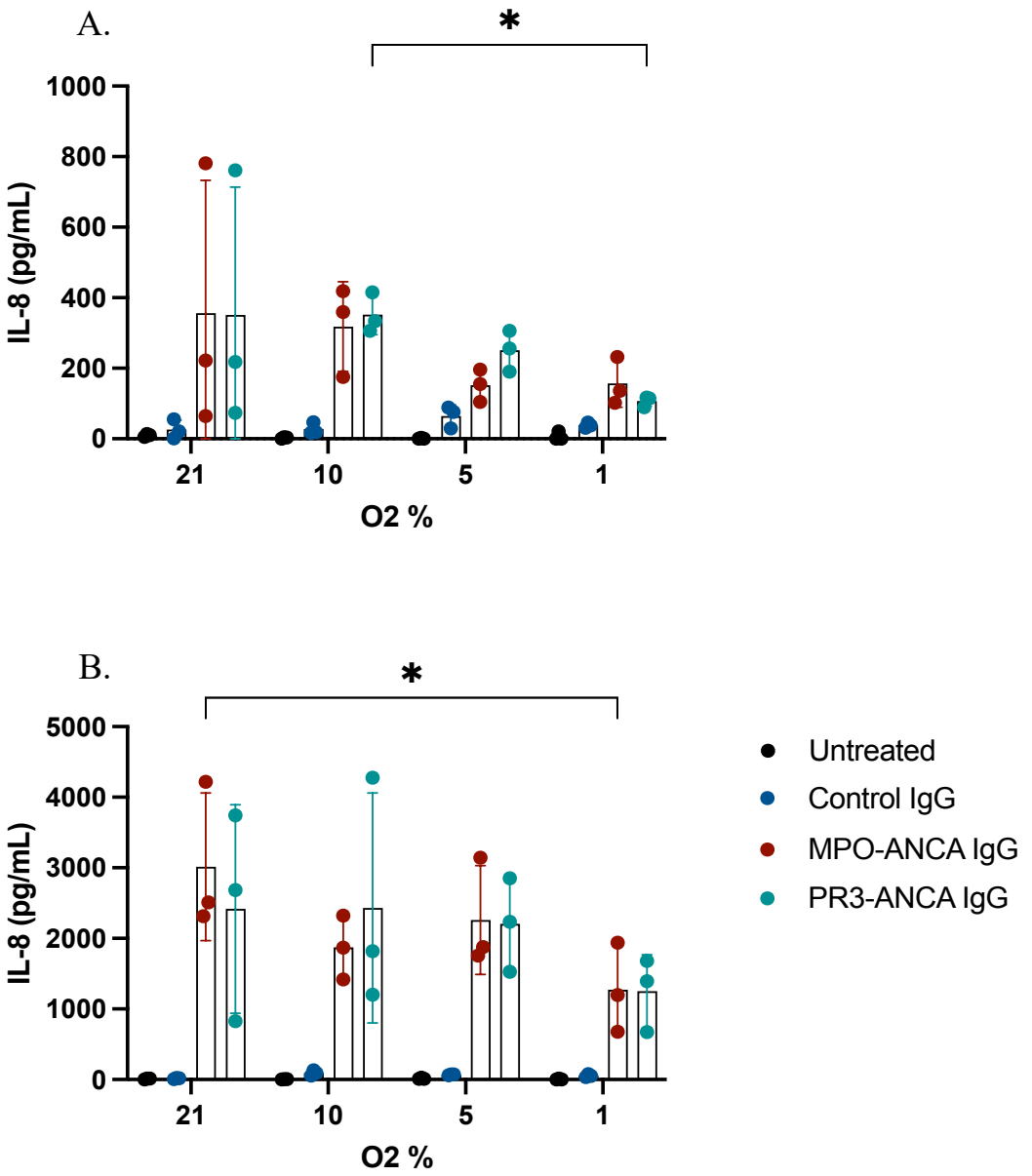


Figure 44. Hypoxia alters MPO-ANCA stimulated neutrophil IL-8 secretion
Isolated neutrophils from HC (n=3) were incubated for 15 minutes at 1%, 5%, 10%, or 21% O_2, untreated with media only (neutrophil culture media, 'untreated') or primed with 2 ng/mL TNF (15 minutes) and stimulated with 100 µg/mL HC or MPO-/PR3-ANCA IgG for 1h (A) and 4h (B). SN IL-8 content was measured by ELISA. Data are shown as mean +/- SEM, statistical analysis was performed using two-way ANOVA mixed effects model with Geisser-Greenhouse correction, with Tukey's multiple comparisons test; *$p<0.05$.

5.2.2. Whole blood ANCA stimulation IL-8 production

In Chapter 3, a greater effect of MPO-ANCA stimulation on neutrophil deformability was seen in whole blood at 21% O_2 than in experiments where isolated cells were used. Additionally, in comparison to isolated cells there was less IL-8 secretion in whole blood, but presumably neutrophil count was comparable in whole blood compared to stimulation of isolated cells. As I saw differing results in terms of deformability between whole blood and isolated cells, I also looked at IL-8 release in both whole blood and isolated cells.

To assess the impact of differing oxygen tensions on the role of ANCA-IgG stimulation induced changes in neutrophil IL-8 secretion in whole blood, I compared the effect of MPO-ANCA IgG stimulation at 1% O_2, 5% O_2, 10% O_2 and 21% O_2 using ELISA. Whole blood (1 mL) was equilibrated for 15 minutes at indicated oxygen tensions, primed with 2 ng/mL TNF (15 minutes), and stimulated with HC or MPO- IgG for 1h. Serum was used for measurement of IL-8 secretion levels.

ANCA induced a significant increase in IL-8 release compared to untreated at 21%O_2 (**Fig 45;** p=0.0003). While there was peak IL-8 release in response to MPO-ANCA at 21% O_2, there was a significant decrease in IL-8 in 5% O_2 (**Fig 45**; p=0.0015) and 1% O_2 (**Fig 45**; p=0.0010) and a trend towards decreased IL-8 in 10% O_2 (**Fig 45**; p=0.0656). A significant decrease in IL-8 secretion in MPO-ANCA stimulated neutrophils was displayed at 10%, 5% and 1% O_2 in comparison to 21% O_2 (**Fig 45**; 10%: p=0.0001, 5%: p= 0.0023, 1%: p=<0.0001). There was no effect of oxygen tension on IL-8 release from untreated or HC IgG treated WB. These results display how changing oxygen tension alters the pathogenic effect of MPO-ANCA on neutrophil IL-8 release.

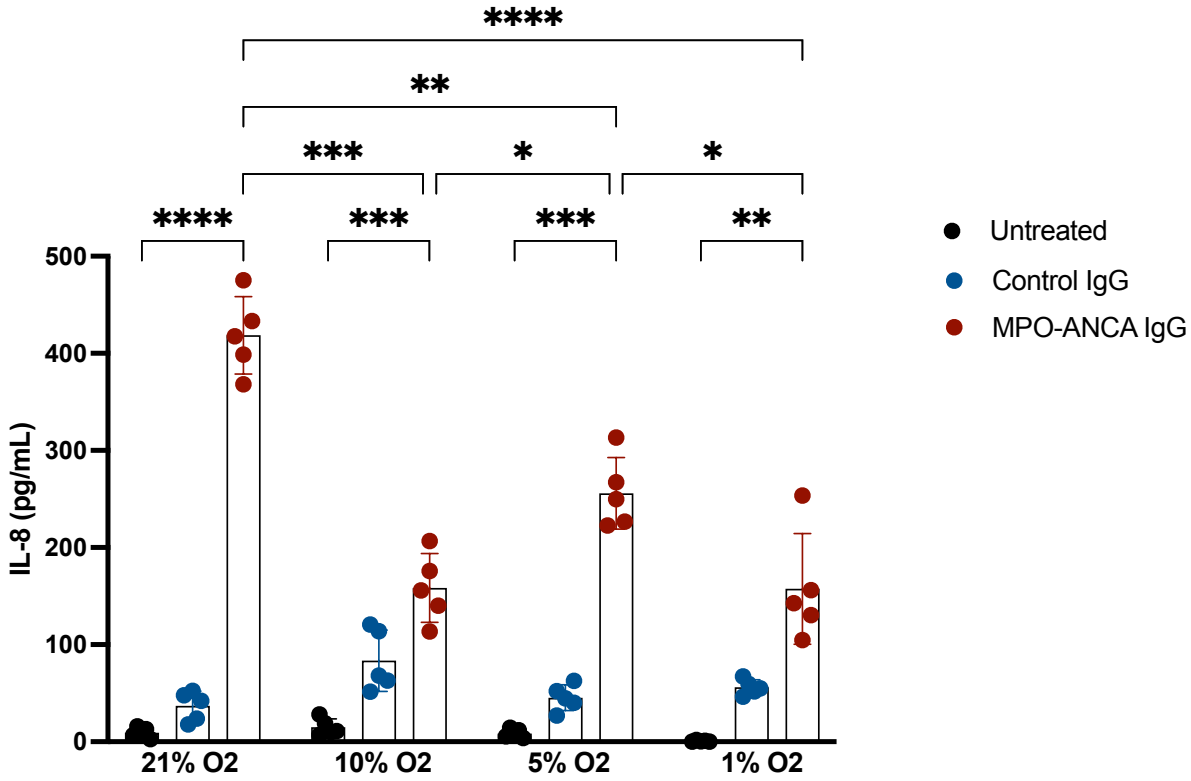


Figure 45. Oxygen tension alters MPO-ANCA stimulated whole blood neutrophil IL-8 secretion

Whole blood from HC (n=5) was incubated for 15 minutes at 1%, 5%, 10%, or 21% O_2, untreated or primed with 2 ng/mL TNF for 15 minutes, stimulated with 100 ug/mL HC IgG or MPO-ANCA IgG for 1h, and centrifuged to generate serum. IL-8 levels in serum were analysed using ELISA. Data are shown as mean +/- SEM, statistical analysis was performed using two-way ANOVA mixed effects model with Geisser-Greenhouse correction, with Tukey's multiple comparisons test; *$p<0.05$.

5.3. Effect of oxygen tension on ANCA induced NETosis

I identified the pathogenic effect of ANCA stimulation in promoting NET formation at 21% O_2 in section 3.3.2. (**Fig 46**). Pathological hypoxia at 1% O_2 has been shown to enhance NET formation in untreated neutrophils (544). Other studies, however, have identified either reduction in, or similar levels of NETosis in hypoxia (535,545). Therefore, studies are conflicting and the effect of ANCA on NETs in hypoxia is unknown.

5.3.1. NET production in ANCA stimulated neutrophils is enhanced at 1% O_2 and diminished at 5% O_2

To assess if hypoxia impacts NET formation in neutrophils stimulated with ANCA, I identified NETosis using immunofluorescence in neutrophils incubated at 1% and 5% O_2. Neutrophils were primed with 2 ng/mL TNF (15 minutes), stimulated with HC or MPO-ANCA-IgG for 4h, fixed, and stained for H3Cit.

Interestingly, at 5% O_2, no NET formation was seen, either in untreated or in MPO- or PR3-ANCA stimulated cells (representative images shown in **Fig 46**). Untreated and HC IgG stimulated neutrophils at 1% O_2 exhibit a visually brighter stain (representative images shown in **Fig 46**) and potentially more NET formation in comparison to the same stimulation conditions at 21% O_2 (representative images shown in **Fig 46**). Ultimately, this data shows hypoxia has the potential to regulate the pathogenic effect of ANCA stimulation with marked differences depending on degree of oxygen tension.

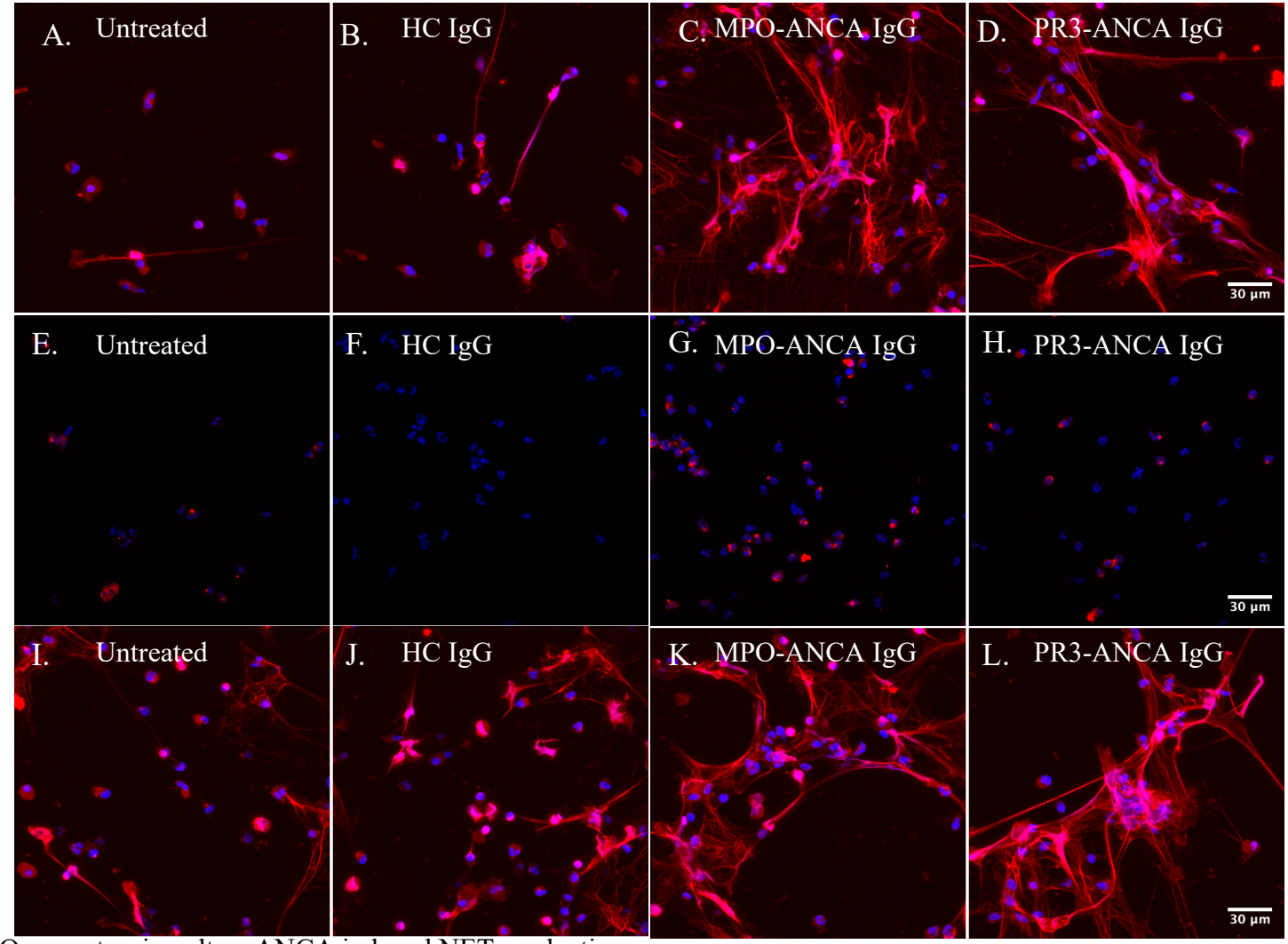


Figure 46. Oxygen tension alters ANCA induced NET production

(A-L) Isolated neutrophils from HC were incubated for 15 minutes at 21% O_2, untreated with media only (neutrophil culture media, 'untreated') or primed with 2 ng/mL TNF for 15 minutes, and stimulated with 100 µg/mL HC IgG, MPO-/PR3-ANCA IgG for 4h at 21%, 5% or 1% O_2. Neutrophils were fixed, stained for H3Cit (red) (AF647), mounted with VectaShield[R] Antifade Mounting Medium with DAPI (blue), and imaged at 40x using an inverted Zeiss LSM-780 (A-D) 21% O_2, (E-H) 5% O_2, (I-L) 1% O_2, (A) Untreated, (B) HC IgG, (C) MPO-ANCA IgG, (D) PR3-ANCA IgG. Representative images from 21% O_2 (n=10), 5% O_2 (n=5), and 1% O_2 (n=5) experiments are shown.

5.4. Effect of ANCA and hypoxia on protein secretion levels from neutrophil and gEC

In AAV, increased secretion and expression of cell adhesion and inflammatory molecules has been shown in neutrophils in addition to increased neutrophil induced endothelial activation (339). Hypoxia has also shown to alter EC secretion profile by promoting increase in IL-6 and VEGF secretion once EC are cultured in hypoxia (546,547). I next investigated whether this response is modulated in hypoxic conditions with gEC co-cultured with ANCA stimulated supernatant.

5.4.1. Oxygen tension influences gEC protein secretion levels following treatment with neutrophil-conditioned SNs

In the presence of ANCA, interaction of activated neutrophils with the endothelium results in inflammatory cytokine release from neutrophils which leads to endothelial injury (339). To determine whether secretions from neutrophils induce a difference in endothelial cell release of cytokines (IL-8), or adhesion molecules (ICAM-1 and VCAM-1) under different oxygen tensions, at 21%, 5%, or 1% O_2, I treated gEC with previously harvested ANCA stimulated neutrophil SN. Experimental set-up included initial incubation of gEC for 24h at 1%, 5%, or 21% O_2 followed by serum starvation for 2 hours. I then used SN harvested from untreated neutrophils, or neutrophils primed with 2 ng/mL TNF (15 minutes) and stimulated with 100 µg/mL HC or MPO-ANCA-IgG, and added the SN to gEC under 21%, 5%, or 1% O_2. Degree of oxygen tension was matched between cell types e.g., neutrophil SN collected from neutrophils incubated at 1% O_2 was used to stimulate gEC at 1% O_2. Protein secretion levels at 1%, 5%, or 21% O_2 following 6h and 24h incubation with neutrophil SN were measured using ELISA. Of note, different donor stimulated SN was used for each biological replicate (n=3), potentially influencing the variability in 21% O_2 results between experiments. While IL-

8, VCAM-1, and ICAM-1 levels were initially quantified in SN used before treatment, other inflammatory cytokines and levels of such cytokines could be present in the SN, also influencing endothelial activation.

Minimal IL-8 secretion was seen from gEC following 6h stimulation with neutrophil SNs, at both 21% and 5% O_2. At 24h, there was increased IL-8 secretion from gEC following incubation with SN from ANCA stimulated neutrophils compared to incubation with SN from untreated or HC IgG stimulated neutrophils. There was no difference between 21% and 5% O_2 (**Fig 47A**). Similarly, there was low levels of VCAM-1 secretion at 6h. There was a small increase in VCAM-1 secretion from neutrophils incubated with SN from ANCA stimulated neutrophils, although this was not statistically significant, and there was no difference between 21% and 5% O_2. By 24h there was a significant increase in VCAM-1 secretion following incubation of gEC with SN from ANCA stimulated neutrophils (**Fig 47B**; p=0.0269). This effect was of greater magnitude at 21% O_2 compared to 5% O_2, as VCAM-1 levels at 21% O_2 (3467.83 pg/mL) were nearly doubled in comparison to VCAM-1 levels at 5% O_2 (1932.63 pg/mL) (**Fig 47B**; ns). While there was a small increase in ICAM-1 secretion from gEC following incubation with SNs from ANCA stimulated neutrophils, these results were not significant and there was no difference in ICAM-1 secretion between either oxygen tension or time point (**Fig 47C**).

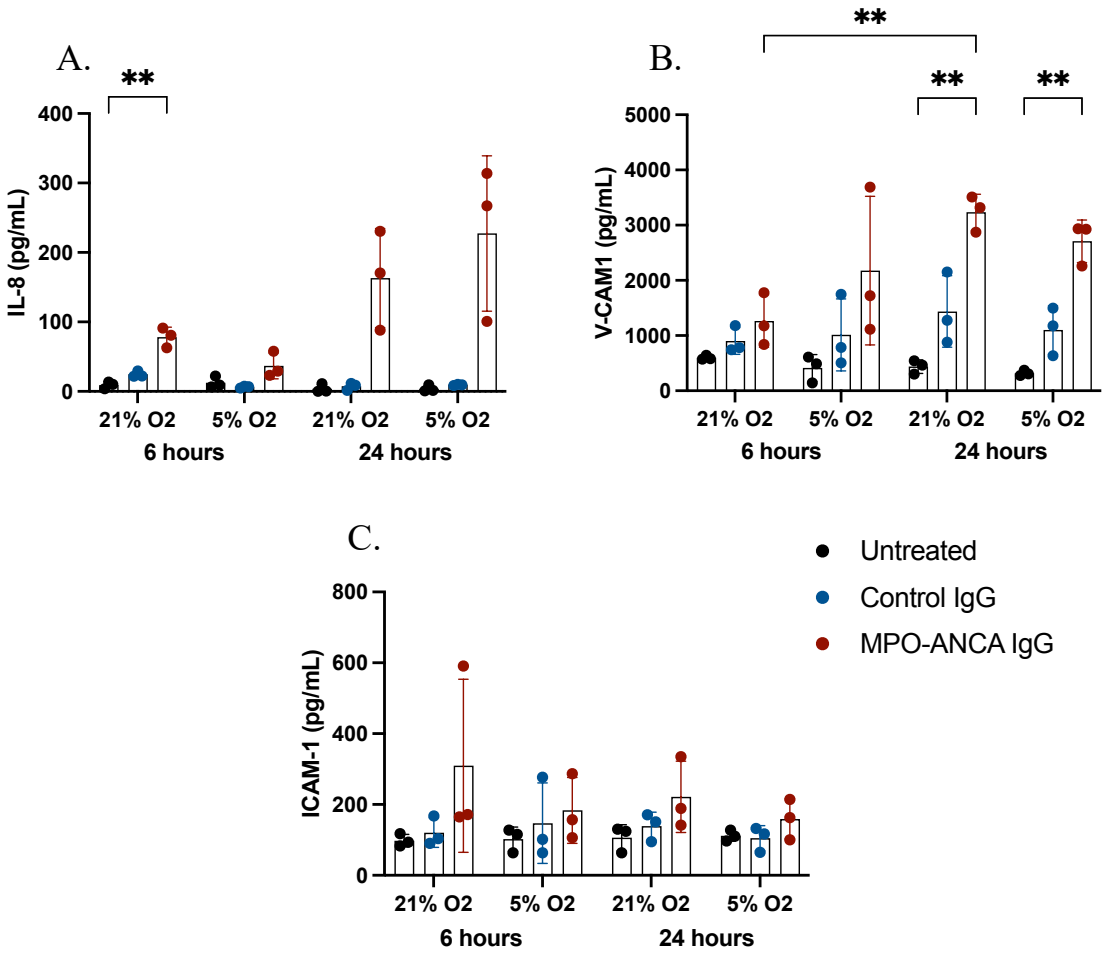


Figure 47. 5% O_2 influences gEC protein secretion levels when treated with ANCA SN
Neutrophils ($2x10^5$) were incubated for 15 minutes, untreated with media only (neutrophil culture media, 'untreated') or primed with 2 ng/mL TNF (15 minutes), stimulated with 100 µg/mL of HC or MPO-ANCA IgG, and SN added directly to the gEC wells for 6h or 24h incubation (n=3). SN IL-8, VCAM-1, and ICAM-1 content was measured by ELISA. The amount of cytokine/CAM in the added neutrophil SN was subtracted from the total value and results presented are EC secretion levels only. (A) IL-8, (B) VCAM-1 (C) ICAM-1. Data are shown as mean +/- SEM, statistical analysis was performed using two-way ANOVA with Geisser-Greenhouse correction, with Dunnett's multiple comparisons test. ns, non-significant. *p<0.05. **p<0.01.

The H35 can be set to 1 oxygen tension at a time; therefore, I compared 21% O_2 and 1% O_2 in a different set of experiments than 21% O_2 and 5% O_2. There is a significant increase in IL-8 secretion from gEC following incubation with SNs from MPO-ANCA treated neutrophils compared to SNs from untreated at 6h (**Fig 48A**; p=0.0190) or untreated neutrophils at 24h (**Fig 48A**; p=0.0218) in 21% O_2. At 1% O_2, there was a trend exhibiting increased IL-8 at 6h (**Fig 48A**; p=0.0550) and 24h (**Fig 48A**; p=0.0051) in the presence of ANCA in comparison to untreated. Yet, there were no significant differences in IL-8 when comparing 21% versus 1% O_2 stimulations. The increase in VCAM-1 secretion from gEC following treatment with SN from MPO-ANCA stimulated neutrophils was more variable. At 24h in 1% O_2, there is a decrease in VCAM-1 secretion gEC following treatment with SN from MPO-ANCA stimulated neutrophils in comparison to 21% O_2 (**Fig 48B**, ns). Following 6h stimulation, there is an increase in ICAM-1 release from gEC incubated with SN from MPO-ANCA stimulated neutrophils. Following 6h stimulation there was a small, non-significant increase in 1% O_2 compared to 21% O_2. In contrast, following 24h there was less ICAM-1 release at 1% O_2 (**Fig 48C**; p=0.0884).

In conclusion, when gEC are exposed to SN from ANCA stimulated neutrophils, this leads to release of IL-8, VCAM-1, and ICAM-1 from gEC. Hypoxia may modulate this although a consistent pattern of results was not seen and there was considerable inter-donor variability. IL-8 secretion was not significantly altered by oxygen tension at either time point, VCAM-1 release was reduced at 24h by both 5% and 1% O_2, and ICAM-1 release was augmented at 6h and reduced at 24h by 1% O_2; 5% O_2 had no effect.

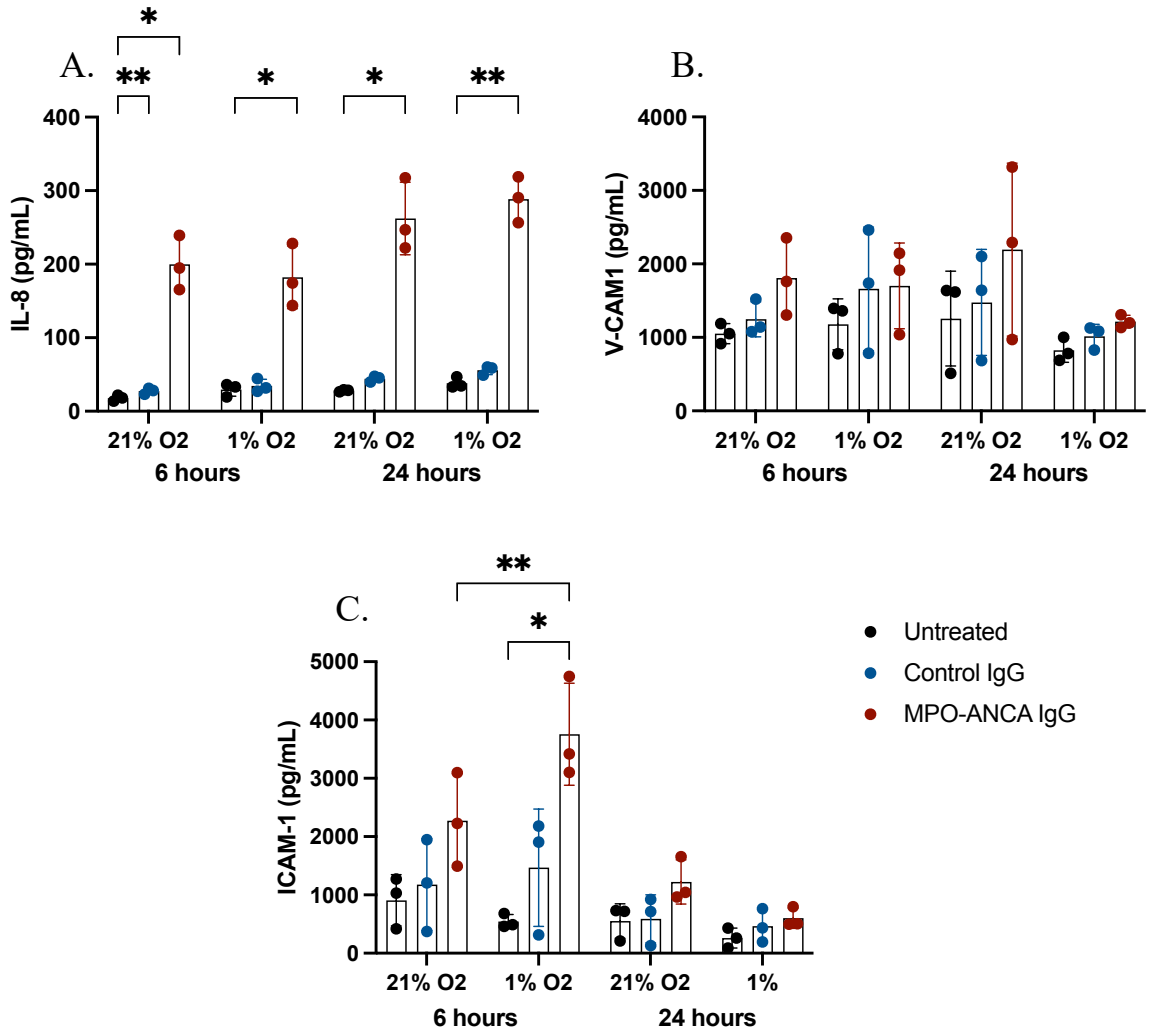


Figure 48. 1% O_2 influences gEC protein secretion levels when treated with ANCA SN
Neutrophils ($2x10^5$) were incubated for 15 minutes, untreated with media only (neutrophil culture media, 'untreated') or primed with 2 ng/mL TNF (15 minutes), stimulated with 100 ug/mL of HC or MPO-ANCA IgG, and added directly to the gEC wells for 6h or 24h incubation (n=3). SN IL-8, VCAM-1, and ICAM-1 content was measured by ELISA. The amount of cytokine/CAM in the added neutrophil SN was subtracted from the total value and results presented are EC secretion levels only. (A) IL-8, (B) VCAM-1, (C) ICAM-1. Data are shown as mean +/- SEM, statistical analysis was performed using two-way ANOVA with Geisser-Greenhouse correction, with Dunnett's multiple comparisons test. ns, non-significant. *p<0.05. **p<0.01.

5.4.2. Increased IL-8, ICAM-1, and VCAM-1 secretion following co-culture of gEC and ANCA stimulated neutrophils

Having identified an effect of conditioned SN, I next investigated the direct effect of neutrophils on gEC using co-culture. These experiments had to be conducted at a shorter timepoint due to the limited survival of isolated neutrophils *ex vivo*. As I had seen the greatest impact on gEC secretion at 1% O_2 in my previous set of experiments, and this represents pathological hypoxia, this was the oxygen tension I used in this set of experiments. As a positive control, 10 ng/mL of TNF was added directly to gEC for 24h. All wells included gEC and neutrophils with stimulation conditions outlined in **Table 20** in section 2.2.11.1.

At 21% O_2 co-culture of gEC and neutrophils in the presence of ANCA IgG resulted in a small increase in IL-8, VCAM-1, and ICAM-1 production compared to wells of untreated cells (neutrophils and gEC). At 1% O_2, there was an overall increase in IL-8 release compared to 21% O_2, with significant increases shown between untreated and MPO-ANCA (**Fig 49A**; 21% O_2: p=0.0004, 1% O_2: p=0.0001) and untreated and PR3-ANCA (**Fig 49A**; 21% O_2: p=0.0003, 1% O_2: p=0.0001). This effect of hypoxia-potentiated IL-8 release in the presence of ANCA may be dependent on neutrophils rather than gEC. No effect on IL-8 was seen when gEC alone were treated with TNF, but the role of ANCA on gEC alone remains elusive. It may also be dependent on neutrophil-TNF interactions, rather than ANCA stimulation as augmentation was seen in all conditions where the neutrophils had been primed directly for 15 minutes with TNF irrespective of the addition of IgG, rather than 24h gEC treatment with TNF. This therefore compared the difference between the effect of an activated endothelium with unprimed neutrophils, to resting endothelium with primed neutrophils.

At 1% O_2, there was also augmentation of VCAM-1 release, although this was of smaller magnitude than the difference in IL-8 secretion. There was an increase in VCAM-1 secretion from gEC cultured with TNF in the absence of neutrophils, suggesting increases in VCAM-1 production may be gEC dependent to a greater degree than IL-8 (**Fig 49B**). It also seemed to be more specific to the effect of ANCA stimulation; there was no change in VCAM-1 secretion in TNF primed co-culture wells, untreated wells, or HC IgG stimulated wells. An increase was seen in MPO-/PR3-ANCA treated wells at both 21% and 1% O_2 in comparison to untreated (**Fig 49B**; 21% O_2: MPO: p=0.0034, PR3: p=0.0007, 1% O_2: MPO: p=0.0001, PR3: p=0.0001).

At baseline at 21% O_2, ICAM-1 secretion levels were already elevated in untreated co-culture wells, with a small increase seen in the presence of ANCA stimulation (**Fig 49C;** MPO: p=0.0166 and PR3: p=0.0083 comparing untreated wells to MPO- and PR3- ANCA stimulation respectively). 1% O_2 had a small effect on enhancing ICAM-1 release in all conditions but the effect size was similar between all conditions; a small, but significant additional effect of ANCA stimulation was shown (**Fig 49;** MPO: p=0.0120 and PR3: p=0.0006 comparing untreated wells to MPO- and PR3- ANCA stimulation respectively). From this, hypoxia increases baseline secretion from neutrophils (IL-8, VCAM-1, and ICAM-1) and gEC (VCAM-1 and ICAM-1) and synergises with ANCA to further increase secretion in comparison to 21% O_2.

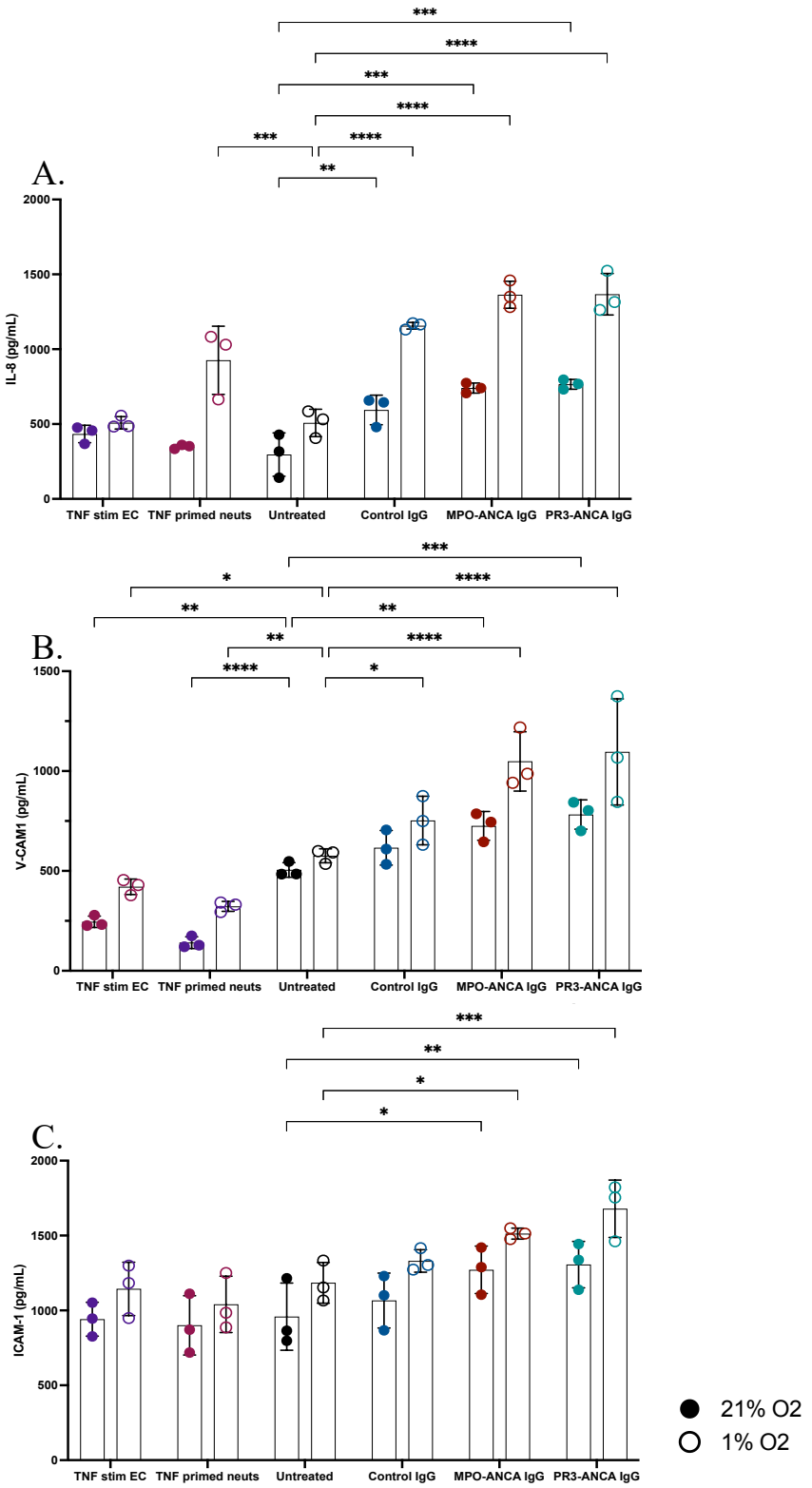


Figure 49. Increased IL-8, ICAM-1, and VCAM-1 levels in ANCA stimulated co-culture
Neutrophils ($2x10^5$) were incubated for 15 minutes, untreated with media only (neutrophil culture media, 'untreated') or primed with 2 ng/mL TNF (15 minutes), stimulated with 100 ug/mL of HC or MPO-/PR3-ANCA IgG, and added directly to the gEC wells for 1.5 h incubation (n=3). SN IL-8, ICAM-1, and VCAM-1 content was measured by ELISA. Data are shown as mean +/- SEM, statistical analysis was performed using two-way ANOVA with Geisser-Greenhouse correction, with Dunnett's multiple comparisons test. *p<0.05. **p<0.01. ***p<0.001. ****p<0.0001

5.5. ANCA IgG and hypoxia promote neutrophil trans-endothelial migration through gEC

Having established that both ANCA and hypoxia can increase neutrophil/endothelial secretion of adhesion molecules, I next performed trans-well migration experiments to assess if ANCA and hypoxia promote neutrophil endothelial transmigration at the glomerular endothelium, I performed trans-well migration experiments. I selected IL-8 as the chemoattractant used, to mimic the disease state in AAV *in vivo* since IL-8 has been identified at the site of inflammatory damage in AAV microvasculature (327). I used untreated EC co-cultured with neutrophils as a negative control and for baseline comparison as previous sections have shown hypoxia alone can have an effect on gEC. I used gEC treated with 10 ng/mL TNF for 24 hours prior to the addition of untreated neutrophils as a positive control. Experimental conditions included neutrophils in microcentrifuge tubes primed with 2 ng/mL TNF (15 minutes), stimulated with 100 µg/mL HC or MPO-ANCA-IgG, and added immediately to respective wells. Neutrophils were then added to respective EC wells, incubated with EC for 90 minutes, and migrated cells were quantified.

In the absence of chemoattractant, minimal neutrophil migration was seen at 21% O_2 with minimal effect of ANCA stimulation in comparison to untreated (**Fig 50A**; ns). At 1% O_2, without chemoattractant, untreated neutrophil migration increased in comparison to untreated neutrophils at 21% O_2 (**Fig 50A**; ns). Neutrophils migrating at 1% O_2 without IL-8 displayed a significant increase in migration in MPO- and PR3-ANCA treated wells (**Fig 50A**; MPO: p=0.0037, PR3: p=0.0069).

Once the chemoattractant was added there was an increase in neutrophil migration seen at both oxygen tensions. At 21% O_2 when comparing untreated to MPO-ANCA IgG treated wells,

there was a significant increase in migration (**Fig 50A**; p=0.0188 compared to untreated neutrophils). More of an effect was present at 21% O_2 once IL-8 was added, and the percentage of migration increased in the presence of ANCA (**Fig 50B**; MPO: p=0.0017, PR3: p=0.0021). This effect is further increased at 1% O_2 in MPO- and PR3-ANCA treated wells (**Fig 50B**; MPO: p=0.0099, PR3: p=0.0066). Therefore, hypoxia potentiates the effect of both ANCA and itself, and in ANCA combination with IL-8. However, at 1% O_2 in the presence of IL-8 there was significant migration of even untreated neutrophils meaning the magnitude of the effect of additional ANCA stimulation was less than was seen at 21% O_2 with hypoxia. In summary, in the absence of chemoattractant, little TEM is seen at 21% O_2 even in the presence of ANCA stimulation. Both hypoxia, and the addition of chemoattractant permit neutrophil TEM and the greatest neutrophil migration is seen when they are present in combination. There was the greatest differential effect of ANCA at 21% O_2 in the presence of IL-8.

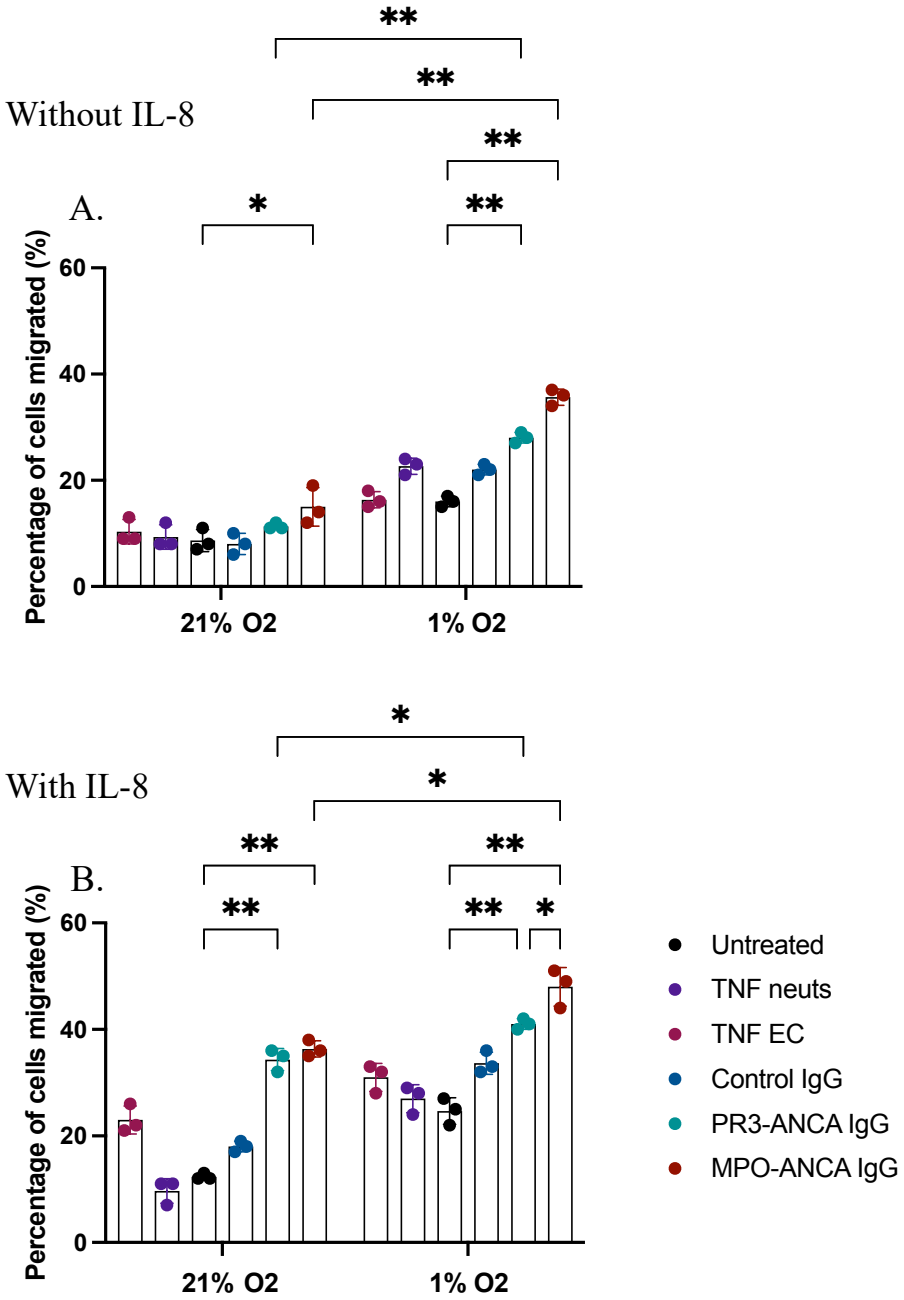


Figure 50. Increased migration in neutrophils stimulated with ANCA IgG at 1% O_2
Neutrophils ($2x10^5$) were incubated for 15 minutes, untreated with media only (neutrophil culture media, 'untreated') or primed with 2 ng/mL TNF (15 minutes), stimulated with 100 µg/mL of HC or MPO-/PR3-ANCA IgG, and added directly to the gEC wells treated with (B) IL-8 (200 pg/mL) or (A) untreated (media) with recombinant for 90-minute incubation (n=3). Neutrophil migration was measured by counting migrated cells from bottom chamber using haemocytometer and brightfield microscopy. (A) Untreated, without IL-8, (B) Treated, with 200 pg/mL IL-8. Data are shown as mean +/- SEM, statistical analysis was performed using two-way ANOVA with Geisser-Greenhouse correction, with Dunnett's multiple comparisons test. ns, non-significant. *p<0.05. **p<0.01.

5.5.1. gEC form confluent monolayers under pathological hypoxia

gEC were cultured as stated above in section 5.4.2., therefore in total gEC were exposed to 1% O_2 for approximately 48 hr. I imaged the trans-well membranes to confirm a confluent monolayer formed and that cell viability was not impacted when EC were cultured at 1% O_2 during this longer time course. gEC were stained for VE-Cadherin (magenta) and neutrophils were stained for CD15 (yellow) with nuclear staining using DAPI (cyan). Representative images display wells from 1% O_2 with MPO-ANCA IgG stimulation in **Figure 51A-F**. These images identify a confluent gEC monolayer with no morphological differences compared to 21% O_2 (**Fig 51B**). In addition, these images displayed neutrophils migrating through the membrane, towards chemoattractant, IL-8 (**Fig 51E**).

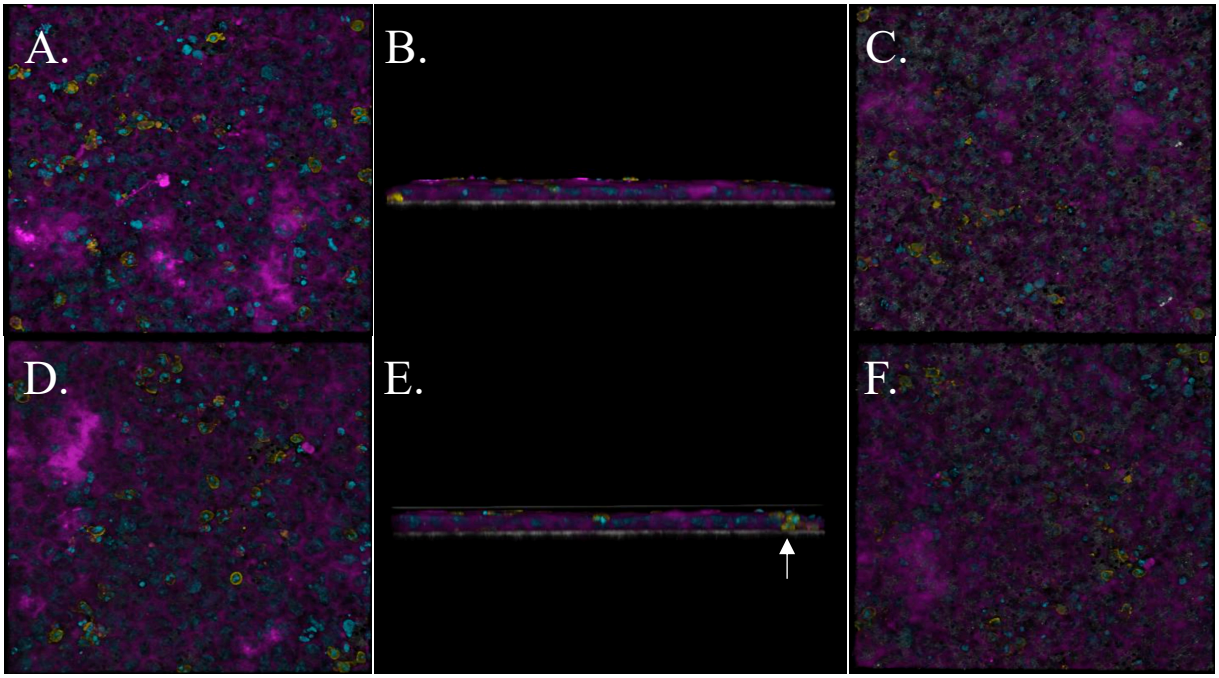


Figure 51. ANCA IgG promotes neutrophil migration through gEC, and hypoxia enhances this effect

Neutrophils ($2x10^5$) were incubated for 15 minutes, untreated with media only (neutrophil culture media, 'untreated') or primed with 2 ng/mL TNF (15 minutes), stimulated with 100 µg/mL of HC or MPO-/PR3-ANCA IgG, and added directly to the gEC wells for 1.5 h incubation (n=3). Transwell membranes were fixed, stained for VE-Cadherin (magenta) (AF555) and CD15 (yellow) (AF647), and mounted onto coverslips with VectaShield[R] Antifade Mounting Medium with DAPI (cyan), and imaged at 20x using a Leica-Stellaris 9 STED-Falcon. (A/B/C) MPO ANCA IgG neutrophil/gEC well at 21% O_2, (D/E/F) MPO ANCA IgG neutrophil/gEC well at 1% O_2. (A/D) Top of membrane (B/E) Cross section (C/F) Bottom of membrane.

5.6. RNA-Sequencing of neutrophils in 1% O_2; untreated v MPO-ANCA v PR3-ANCA stimulation

I next investigated whether hypoxia had any effect on gene profile of untreated neutrophils or on the ANCA induced transcriptional changes identified in Chapter 3.

5.6.1. Identification of a gene signature comparing 21% O_2 untreated neutrophils to 1% O_2 untreated neutrophils

Untreated neutrophils in previous sections displayed different responses dependent upon the oxygen tension neutrophils were exposed to. Although, I expected a longer period of hypoxia would be needed to induce transcriptional changes in untreated cells, I initially determined if 1% O_2 had an impact (548). Isolated neutrophils were cultured at 21% or 1% O_2 (1h). Samples were prepared following the method outlined in 2.2.9.1. in preparation for RNA-seq.

There were no significant DE genes when comparing untreated neutrophils at 21% O_2 to untreated neutrophils at 1% O_2. This suggests that any significant differences identified in previous experiments in hypoxia were not due to transcriptional changes at this short time point.

5.6.2. Identification of a gene signature comparing 1% untreated neutrophils to 1% MPO- or PR3-ANCA stimulated neutrophils

In previous sections, neutrophils stimulated with MPO- or PR3-ANCA displayed different responses dependent upon the oxygen tension stimulated neutrophils were exposed to. Untreated HC isolated neutrophils were equilibrated (15 minutes) and cultured at 1% O_2 (1h) or TNF primed (15 minutes) and stimulated with MPO- or PR3-ANCA IgG (100 µg/mL) for

1h at 1% O_2. Samples were prepared following method outlined in 2.2.9.1. in preparation for RNA-seq.

Results displayed in **Figure 52** display top DE genes for MPO-ANCA or PR3-ANCA stimulation compared to untreated cells at 1% O_2. Following MPO-ANCA stimulation there were 14,007 amount of DE genes overall, and of those, 1,816 were significant in MPO-ANCA stimulations (**Fig 52A**). Following PR3-ANCA stimulations, there were 13,658 of DE genes overall, and of those, 1,806 were significant (**Fig 52B**). The top 20 upregulated and top 10 downregulated significant DE genes are presented in Table 25 (1% O_2 untreated v MPO-ANCA IgG) and Table 26 (1% O_2 untreated v PR3-ANCA IgG). Targets up-regulated were similar to those seen at 21% O_2 and potential genes of interest included *F3*, *IL1-B*, *CD83*, *NLRP3*, *TRAF1*, *CCL4*, *CCL20*, *TNF*, *TAGAP*, *IL-18*, *CXCL8*, *ICAM-1*, *NFKB1*, *CD48*, *C3, VEGFA*, *RAB21*, *IL-6*, *SRC*, *TLR6*, *TLR1,* and *TNFRSF12A*. These genes are involved in processes such as bacteria response, complement, inflammation, recruitment, and coagulation. Gene ontology analysis was used to identify enrichment for genes involved in top dysregulated processes of MPO- or PR3-ANCA stimulated neutrophils exposed to hypoxia (**Fig 53**). Of the dysregulated biological processes, cell-cell signalling, inflammatory response, response to bacteria, response to external stimulus, and cytokine-mediated signalling pathway were pathways of interest – particularly cell adhesion, due to findings of increased cell adhesion molecule protein secretion presented in section 5.4. As for cellular components, pathways involved in the cell surface, whole membrane, cytoskeleton, and cell projection were dysregulated, which may link with hypoxia exacerbating ANCA stimulated neutrophil actin polymerisation (section 4.7).

These dysregulated pathways at 1% O_2 are similar to results found at 21% O_2 (section 3.8.1.). Differentially regulated genes at 21% O_2 comparing untreated and MPO-ANCA, or untreated and PR3-ANCA stimulated neutrophils are similar in comparison to hypoxia. Interestingly, despite 1% O_2 exacerbating some neutrophil functional responses to ANCA stimulation, there were no significant DEG between MPO- or PR3-ANCA stimulations at 21% O_2 versus MPO- or PR3-ANCA stimulations at 1% O_2 suggesting this is not due to transcriptional regulation.

Gene name	P value	FDR	Log_2FC
Upregulated			
AD000864.1	6.73E-52	9.07E-48	2.32824839
ZFP36	4.91E-36	2.20E-32	2.86750502
F3	7.19E-36	2.42E-32	6.29796458
AC020907.3	2.12E-35	5.71E-32	4.66271479
AC023813.1	1.90E-33	4.27E-30	5.51003228
AP003086.1	3.36E-33	6.47E-30	3.9165307
IL23A	9.51E-33	1.60E-29	5.92620214
AC079753.1	1.78E-32	2.66E-29	6.36147944
XBP1	1.42E-30	1.74E-27	4.87238836
CCL3	4.21E-30	4.72E-27	6.47143242
REPIN1	5.29E-30	5.49E-27	4.87212533
GCH1	6.48E-30	6.24E-27	4.17938989
CD83	1.14E-29	1.03E-26	5.43956285
ATP2B1-AS1	1.49E-29	1.26E-26	2.21618342
PPP1R15A	3.72E-29	2.95E-26	4.3819196
NFKBID	2.24E-28	1.68E-25	3.21818674
AL391832.3	3.30E-28	2.34E-25	2.59736348
BTN2A2	1.23E-27	8.27E-25	3.75033065
FFAR2	2.21E-27	1.42E-24	2.70784765
RHOH	3.03E-27	1.85E-24	3.7372393
Downregulated			
PELO	8.81E-39	5.93E-35	-4.7064261
TNFRSF12A	6.94E-31	9.35E-28	-4.6847834
CARD8-AS1	6.16E-26	2.77E-23	-2.4008292
TBCC	3.40E-23	1.02E-20	-2.8823938
AC010542.5	1.92E-22	5.24E-20	-4.6898722
TMEM92-AS1	1.28E-20	2.70E-18	-2.9056381
LINC00324	1.09E-19	1.81E-17	-1.785722
CLP1	1.45E-19	2.35E-17	-1.9022647
FADD	2.64E-18	3.52E-16	-3.4753977
AL662844.3	8.81E-17	9.65E-15	-3.4529004

Table 25. Top upregulated and downregulated genes in 1% O_2 MPO-ANCA treated neutrophils in comparison to untreated neutrophils

Gene name	P value	FDR	Log_2FC
Upregulated			
AC020907.3	2.23E-59	3.04E-55	5.11733101
AC079753.1	3.89E-44	1.77E-40	6.57621517
F3	1.91E-40	6.49E-37	6.53310808
LDLR	1.63E-36	3.70E-33	3.52793394
CCL3	4.60E-35	8.96E-32	6.9526774
PPP1R15A	1.12E-34	1.90E-31	4.48124018
C1orf61	3.59E-33	5.44E-30	5.66362089
GPR4	8.34E-33	1.14E-29	3.72691024
AC023813.1	1.03E-32	1.28E-29	5.80736011
SFR1	5.14E-31	5.84E-28	4.09390623
CD83	5.87E-31	6.16E-28	5.44596312
AD000864.1	6.61E-31	6.43E-28	2.41255527
IL23A	7.28E-31	6.62E-28	5.77704611
IL1B	2.17E-30	1.74E-27	5.91321745
CCL3L1	8.51E-30	6.45E-27	5.74839785
FDPSP3	1.27E-29	9.08E-27	4.28919992
TRAF1	1.93E-29	1.32E-26	5.54763434
IL1RN	4.33E-29	2.81E-26	5.57395596
XBP1	1.03E-28	6.40E-26	4.81050169
NFKBID	1.18E-28	6.98E-26	3.23027872
Downregulated			
PELO	1.96E-58	1.33E-54	-4.7710965
TBCC	2.60E-38	7.09E-35	-3.213148
TNFRSF12A	1.40E-30	1.20E-27	-4.4829675
AC010542.5	7.45E-27	3.50E-24	-4.0885581
AL662844.3	1.82E-26	8.01E-24	-4.0350465
CARD8-AS1	5.10E-25	1.88E-22	-2.7126422
PEAK3	2.86E-24	9.29E-22	-2.6773814
CLP1	3.80E-24	1.18E-21	-2.0654583
FADD	4.61E-24	1.40E-21	-3.9437396
AL513327.1	2.38E-21	5.22E-19	-2.431101

Table 26. Top upregulated and downregulated genes in 1% O_2 PR3-ANCA treated neutrophils in comparison to untreated neutrophils

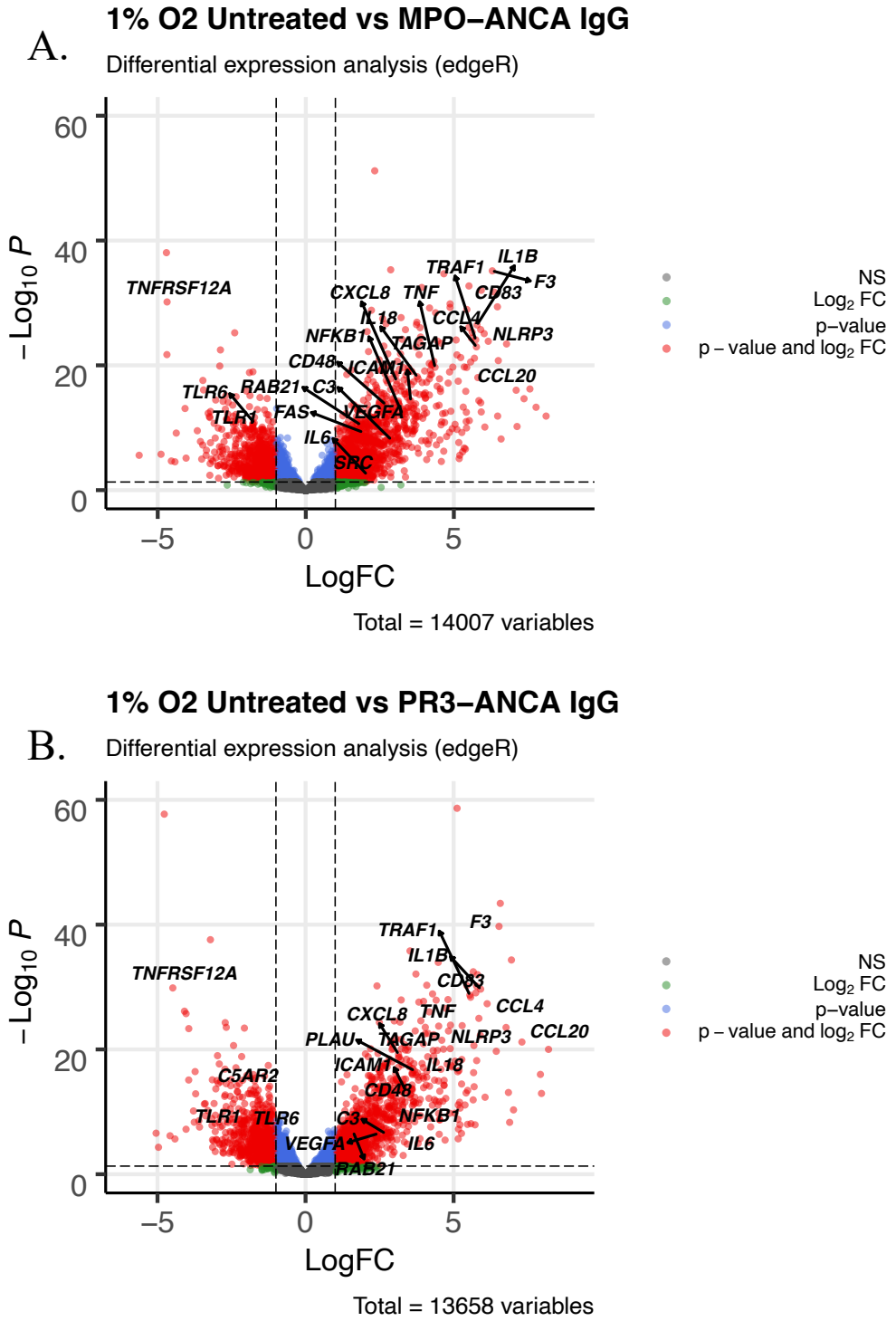


Figure 52. Differential expression analysis of 1% O_2 untreated v MPO-ANCA v PR3-ANCA

(A) Volcano plot of 1% O_2 untreated versus MPO-ANCA. (B) Volcano plot of 1% O_2 untreated versus PR3-ANCA. One dot signifies each gene. Red data points represent genes meeting p-value (<0.05) and Log_2FC (<0.05), blue data points represent genes meeting p-value alone, green data points represent genes meeting Log_2FC alone, and grey data points represent nonsignificant genes. In MPO- or PR3-ANCA in comparison to untreated, downregulated genes are presented on the left panel from -5 to 0, and in MPO- or PR3-ANCA in comparison to untreated upregulated genes are presented on the right panel from 0-10. ns=nonsignificant, p<0.05; Log_2 FC signifies mean gene expression level of individual genes.

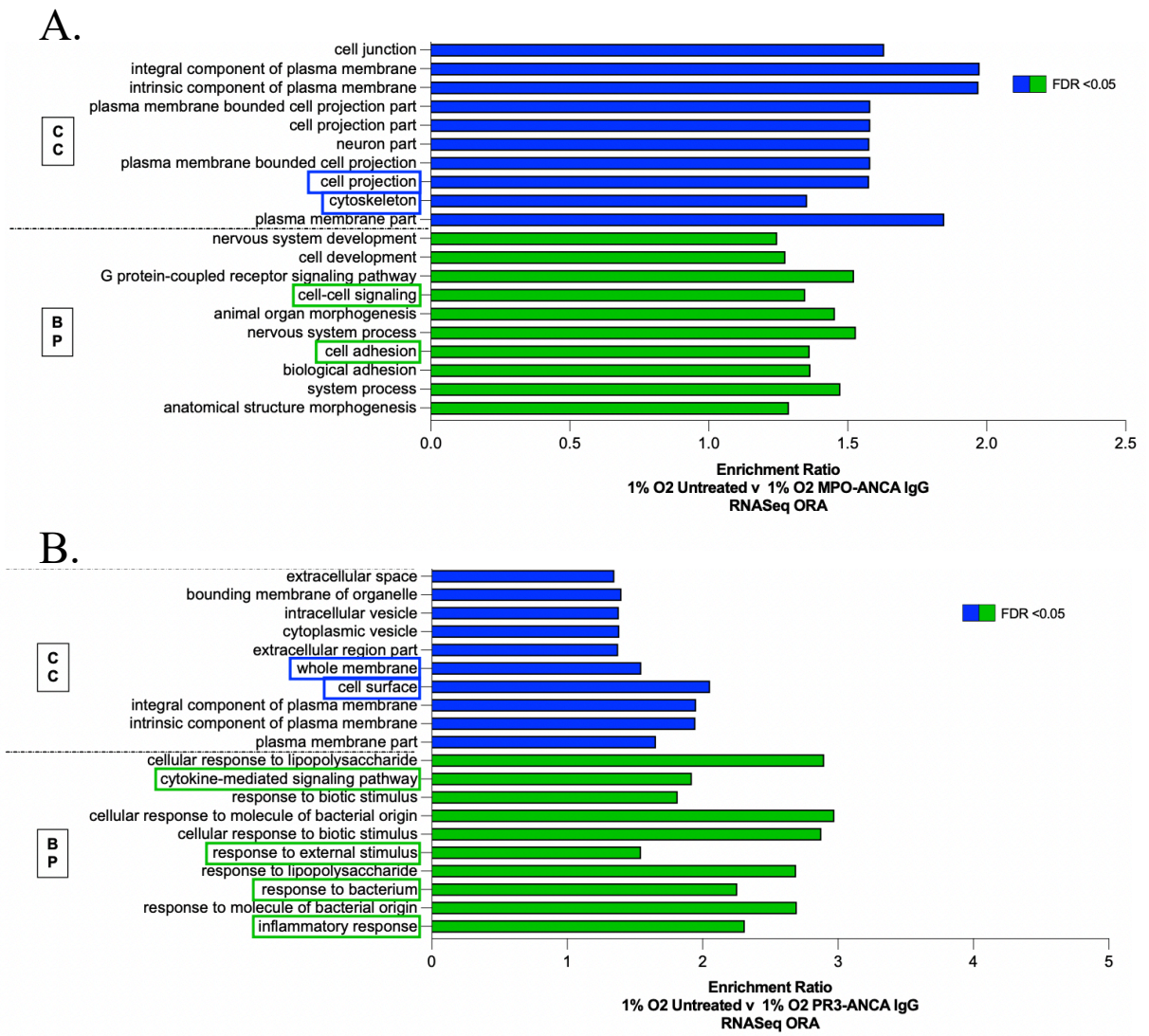


Figure 53. Enrichment ratio of 1% O_2 untreated v MPO-ANCA v PR3-ANCA
(A) Gene ontology classification of 1% O_2 untreated v MPO-ANCA DEGs (Log_2FC <0.05, p<0.05). (B) Gene ontology classification of 1% O_2 untreated v PR3-ANCA DEGs (Log_2FC <0.05, p<0.05). ORA was performed on enrichment of cellular component and molecular function pathway dysregulation.

5.7. Discussion

The main objectives of this chapter were to determine the effect of hypoxia and pathogenic ANCA IgG on HC neutrophil mediated responses in neutrophils alone and in co-culture setting with gEC. I compared untreated HC neutrophil responses to different secondary stimuli, HC IgG and ANCA IgG, under 1% and 5% O_2. Decreased oxygen tension coupled with ANCA IgG stimulation resulted in alteration of protein (IL-8) secretion levels, NET formation, trans-endothelial migration, and endothelial injury/activation (ICAM-1 and VCAM-1).

Firstly, having shown different effects of 5% and 1% O_2 on neutrophil biomechanics suggested that 5% O_2 reduced and 1% O_2 promoted ANCA induced cytoskeletal responses, I investigated whether there were effects on functional responses by examining pathogenic effects of IL-8 secretion and NETs. Although stimulation of isolated neutrophils with ANCA resulted in increased IL-8 secretion at 21% O_2, no additional effect on cytokine release was shown at 5% or 10% O_2, and at 1% O_2, an unexpected decrease in IL-8 secretion occurred. Increased IL-8 in serum has been found in multiple disease types, including AAV (327,550). As shown in Chapter 3, ANCA stimulated whole blood led to increased IL-8 secretion in serum in comparison to untreated and HC IgG stimulation, which presumably neutrophils as the predominant source of this cytokine release. Yet, once whole blood was incubated at decreased oxygen tensions (1%, 5% or 10% O_2) a decrease in IL-8 secretion in serum in MPO-ANCA IgG stimulated whole blood was seen in comparison to 21% O_2 MPO-ANCA IgG stimulated whole blood. More IL-8 secretion was displayed in MPO-ANCA stimulated neutrophils at 5% O_2 in comparison to 1% or 10% O_2, which were comparable in secretion amount of IL-8. This effect of IL-8 secretion in serum is modulated by MPO-ANCA IgG stimulation but is therefore also coupled with the effect of oxygen tension. Although the effect in size was small, in both whole blood and isolated cells, decreasing oxygen tension seemed to lead to the same or lower

levels of IL-8 secretion. Previous work has shown ~3% O_2 does not increase IL-8 release in fMLP or TNF stimulated neutrophils at 2h and 4h (439), but this result additionally displays the stimulation effect of ANCA does not surpass the effect decreased oxygen tension has on neutrophil TNF stimulated IL-8 secretion. While in T cells, cytokine exocytosis has shown to be dependent upon cytoskeletal remodelling through Rho-GTPase Cdc42, this effect has not been shown in neutrophils (549).

Increased NETs have been described in AAV at areas of microvascular inflammation (320). Sites of vascular inflammation are also known to be a hypoxic environment (551,552). I then hypothesised that hypoxia would impact on the pathogenic effect of ANCA IgG induced NET formation. My results identified that when neutrophils primed with TNF and stimulated with ANCA IgG are incubated at the physiological oxygen tension of 5% O_2, NET formation is profoundly diminished in comparison to both 21% and 1% O_2. Although physiological normoxia displayed no effect on isolated neutrophil cytokine release, the main finding under this oxygen tension was the complete absence of NETosis, even in the presence of ANCA IgG. This finding again displayed 5% O_2 may therefore be more physiological, resulting in neutrophils being more quiescent under this oxygen tension. This therefore suggests neutrophils at 1% and 21% O_2 may be equally stressed. Whereas neutrophils primed with TNF and stimulated with ANCA IgG, incubated under 1% O_2, NET formation was equivalent or more pronounced in comparison to 21% O_2. It is likely therefore, that modulation of NETosis by hypoxia is both dependent on stimulus and degree of oxygen tension used, and whether this effect is due to pharmacological manipulation or HIF, rather than hypoxia. While pathological hypoxia displayed decreased IL-8 production from ANCA stimulated neutrophils, the pathogenic effect of NETosis was increased at 1% O_2.

In the context of the increased actin polymerisation I identified in 1% O_2, my results investigating neutrophil functional responses suggest cytoskeletal changes are more relevant to NET formation rather than cytokine release. In keeping with this, it has been identified in other studies that cytoskeletal rearrangements are an essential step neutrophils must undergo to release NETs (108,553). This finding *in vitro* may also provide insight regarding what occurs *in vivo* with NET production correlating with vascular leakage in the microvasculature in AAV (350). While active NET release can be beneficial in trapping bacteria, in disease context, NETosis may also initiate or perpetuate the autoimmune response in AAV in addition to promoting endothelial damage. This suggests a two-hit hypothesis is necessary, so that ANCA alone in normal venous blood does not mean neutrophils will produce NETs, but ANCA and hypoxia does so if there is already inflammation present. This would be an interesting future hypothesis to investigate in co-culture settings.

Having examined the impact of oxygen on neutrophil pathogenic responses to ANCA and identified the potential for enhanced neutrophil-mediated endothelial damage under hypoxia, I next examined the effect of hypoxia on neutrophil-endothelial interactions. Due to the limitation of short neutrophil life span *ex vivo*, the longest time point of IL-8 secretion measured in neutrophils alone was 4h. For gEC, a longer time course was performed, using neutrophil SN from 1h stimulations, as peak cell adhesion molecule secretion from gEC was expected to occur later (6h or 24h) than the shorter time points measured for neutrophils. At 6h, there was minimal release of IL-8 secretion in ANCA condition wells at all oxygen tensions, and a small increase was shown at 24h in all oxygen tensions in ANCA condition wells in comparison to untreated and HC IgG conditions. However, the CAM secretion profiles are altered by oxygen tension. At 24h in 21% O_2 there was a reproducible effect of an increase in VCAM-1 secretion in ANCA conditioned wells in comparison to untreated and HC IgG, but

incubation at both 1% and 5% O_2 resulted in a reduction of this effect. ANCA condition wells promoted ICAM-1 secretion at 1% O_2 at 6h, but in comparison to 5% and 21% O_2, there was no increase in ICAM-1 secretion at 6h. Considering the diminishment of effects previously seen at 5% O_2, no difference in secretion levels found at 5% O_2 was unsurprising. While 1% O_2 results in different cytokine profiles, these results show 5% O_2 may not alter only neutrophil responses, but endothelial responses as well. Neutrophil endothelial interaction has shown to be altered under hypoxic conditions including EC ROS generation (554), recruitment (555), NE release and adherence (456). Endothelial activation is also well established in AAV and is shown to occur after multiple steps in ANCA activation through other cell types such as monocytes and neutrophils (556). The increased gEC secretion of adhesion molecules shown in this experiment could be due to activation from cytokine release from previous stimulation before gEC treatment, which is already present in the cultured SN such as IL-17 (393), BAFF (381), or IL1-β (557). Although, this effect could potentially be due to the presence of ANCA alone. Previous work suggests ANCA may activate the endothelium directly, but this has not been thoroughly investigated in the field (558). Further experimentation is necessary with ANCA alone to measure its direct effect on the endothelium and eliminate the potential of ANCA directly activating the endothelium.

Based on the protein secretion levels measured, I hypothesised that hypoxia would alter neutrophil-endothelial interactions. As I have shown that 1% O_2 increases ICAM-1 secretion, I expected hypoxia may promote neutrophil migration under these conditions. Although utilisation of neutrophil SN was necessary to examine longer time points, it is hard to visualise a situation *in vivo* where EC would be in contact with neutrophil secretion products, but not neutrophils themselves. I therefore extended these experiments to a co-culture setting where I demonstrated a significant increase in IL-8, VCAM-1, and ICAM-1 release was found in MPO-

and PR3-ANCA stimulated conditions in comparison to untreated, and all other conditions. In comparison to the positive control of TNF activated gEC, the stark increase in ANCA stimulated conditions, displays how the pathogenic effect of activating neutrophils with ANCA promotes increased proinflammatory cytokine release and EC activation. At 1% O_2 in comparison to 21% O_2, hypoxia further increased secretion levels of IL-8, VCAM-1, and ICAM-1 in all conditions, acting synergistically with ANCA stimulation. In contrast to isolated neutrophils alone and neutrophil SN-treated gEC, there was increased IL-8 in co-culture SNs, suggesting that neutrophils are the source but only secrete it once in contact with the endothelium. Additionally, increased CAM present in co-culture, suggests that hypoxia may promote neutrophil adherence or recruitment to the endothelium in the context of ANCA. These findings led me to further investigate neutrophil interaction with the endothelium to measure TEM under the same conditions later in this chapter.

As findings from section 5.4.3. confirmed increased co-culture IL-8 secretion in MPO- and PR3-ANCA also correlate with increased adhesion molecule secretion, this suggests this combination with increased TEM may perpetuate endothelial damage. Having confirmed an intact endothelial monolayer, hypoxia alone, even without the usage of a chemoattractant, promoted neutrophil endothelial migration in all stimulation conditions in comparison to 21% O_2, but the greatest increase was shown with MPO- and PR3-ANCA stimulation. Once the chemoattractant was added, an increase in migration was shown in both ANCA conditions at 21% O_2, yet these levels of migration were comparable to what was found at 1% O_2 without any chemoattractant, and a further increase was seen in hypoxia, again in synergy with ANCA stimulation. This result displays how significant the effect hypoxia is on neutrophil TEM. Although secretion of IL-8 is down-regulated in neutrophils alone in 1% O_2, neutrophils clearly display enhanced capacity to injure and transmigrate across endothelium in hypoxia,

potentially due to increase in ICAM-1. Hypoxia has been previously shown to increased neutrophil TEM in the context of increased EC CD108 expression, which promotes integrin binding (559). Monocyte TEM has also been shown to be increased at 3% O_2 (560). My results show that this is also the case for neutrophil TEM across gEC, in the context of ANCA stimulation. Therefore, it may be that a hypoxia micro-environment promotes neutrophil TEM, which increases the capacity for resultant tissue damage as shown *in vivo* in AAV.

To investigate whether increased neutrophil transmigration under hypoxia was due tohypoxia leading to damage of the endothelial cell monolayer, I examined gEC monolayer formation by imaging transwells using confocal microscopy. Not only did gEC achieve a confluent monolayer formation under hypoxia alone, but this was also maintained in the presence of ANCA, with and without the chemoattractant. I also identified neutrophils which did not completed migration prior to fixation, migrating through the endothelium as well at time of fixation. Neutrophil migration through endothelium to resident tissue in AAV causes extensive tissue damage, inflammation to the area, and prolonged exposure of activated neutrophils as they are not properly cleared once leaving the circulation. These results require further investigation regarding how ANCA may activate and damage the endothelium directly. Additionally, indirect endothelial activation and damage may occur as neutrophil and endothelial functions were proven altered under different oxygen tensions and in the presence of ANCA in this chapter. Future work would require quantified measurement of permeability to assess further vascular damage mimicked *in vitro*.

Lastly, although 1% O_2 altered certain neutrophil responses, there was no transcriptional changes between 21% and 1% O_2 in either presence or absence of ANCA stimulation. HIF dependent neutrophil responses under hypoxia may therefore require a longer time point than

1h to transcriptionally regulate neutrophils under the conditions (407). Although, hypoxia has shown to be capable of regulating neutrophil responses at a short time point; neutrophils have displayed retained oxidative potential upon exposure to hypoxia for 2h and once reoxygenated for 4h (430). Otherwise, 1% O_2 enhanced neutrophil responses and in the context of ANCA. Whereas in 5% O_2 pathogenic neutrophil responses were diminished, which is in line with evidence displaying 5% O_2 may be more physiological for neutrophils (561). To measure the granulocytic output of cell production, prolonged maintenance of human cord blood and bone marrow mononuclear cells has been shown at 5% O_2 (561). Human neutrophil precursors, peripheral blood CD34+ cells, cultured at 5% O_2 over the course of 13 days of culture showed 5% O_2 enhanced granulocytic differentiation in comparison to 20% O_2 culture; therefore, *ex vivo*, 5% O_2 may be a more suitable culture condition for neutrophils (561). Additionally, some of the responses found in these results may have been altered by exposing neutrophils to 21% O_2 initially during the isolation process and thereafter subjecting the neutrophils to different oxygen tensions. Isolating neutrophils under 5% O_2 then carrying out experiments directly at physiological normoxia may result in different readouts. Therefore, it is of interest to conduct future experiments following these conditions.

Overall, incubation at 5% or 1% O_2 alters ANCA stimulated HC neutrophil responses differently, displaying a reduction or enhancement of ANCA's pathogenic effect, respectively. More responses were reduced under 5% O_2 and promoted by 1% O_2 in general, supporting that 1% O_2 promotes a neutrophil phenotype with increased capacity for EC and tissue damage. Thereafter determining mechanisms by which the pathogenic effect of ANCA promotes endothelial damage is influenced by oxygen tension in HC neutrophils, the pathogenic effect of ANCA on aAAV neutrophils under 1% and 5% O_2 were investigated in the next chapter.

Additionally, multiple experiments performed using HC neutrophils were then replicated using rAAV and aAAV neutrophils.

Key findings:

1. Oxygen tension alters ANCA's pathogenic effect on neutrophils, with decreased NET production at 5% O_2, increased NET production at 1% O_2
2. Oxygen tension alters protein secretion levels of gEC stimulated with ANCA SN
3. Co-culture with MPO- and PR3-ANCA results in greater protein secretion levels, and this effect increases under hypoxia
4. Co-culture with MPO- and PR3-ANCA results in increased TEM, and this effect increases under hypoxia
5. Hypoxia does not transcriptionally regulate the effects seen in neutrophils stimulated with ANCA for 1h at 1% O_2

6. Chapter 6 – AAV

6.1. Introduction

Previous work using RT-DC has shown its capability in defining myeloid cell changes in whole-blood in disease states, including SLE and COVID-19. There have been no studies to date using this technique to identify a morpho-rheological phenotype of neutrophils in AAV, or the biomechanical effect of hypoxia and/or ANCA stimulation on neutrophils *in vitro*. Changes in neutrophil deformability can impact their ability to traffic through the microvasculature, with stiffer cells becoming trapped. I hypothesise that distinct biophysical properties of neutrophils in patients with active AAV (aAAV) contributes to endothelial injury, thereby driving disease pathogenesis. Since morphorheological parameters are recorded using a small volume (50 μL) of whole blood, RT-DC may be a useful technique in the clinical setting to aid identification of disease activity in aAAV and to guide treatment.

My results from Chapters 4 and 5 identified ANCA induced altered actin polymerisation in HC neutrophils, that was further enhanced by pathological hypoxia (1% O_2). As aAAV neutrophils may exhibit a different phenotype to those from healthy volunteers (369,562,563), I hypothesise that neutrophils from patients with aAAV exhibit enhanced responses to ANCA IgG stimulation and there will be differences in ANCA induced actin polymerisation to that seen in HC neutrophils. It is possible that clinical parameters in patients with aAAV such as MPO/PR3 positivity, treatment, lung/kidney involvement, and disease activity, may influence neutrophil phenotype and responsiveness to ANCA *in vitro*.

Hypothesis of current chapter

Neutrophils from patients with active AAV have a distinct morpho-rheological phenotype and show exaggerated responses to ANCA stimulation *in vitro*.

Aims

1 Identify the biomechanical phenotype of neutrophils in patients with active AAV

2 Measure the effect of ANCA on actin polymerisation in neutrophils from patients with aAAV

3 Investigate the effect of ANCA and hypoxia in co-culture setting with aAAV SN

6.2. AAV

Healthy controls included in this study were age and sex matched to patients with active and remission AAV. Under the terms of my ethical approvals, information available for healthy volunteers is limited to age and sex. Clinical and demographic characteristics of patients and volunteers is shown in **Table 27**.

		Active	**Remission**	**Healthy control**
Characteristic		n=46 (%)	n=33 (%)	n=27 (%)
Age	Years (IQR)	60 (40-76.2)	67 (39-78)	42 (34-63.6)
Sex	Male	23 (50)	12 (36.4)	14 (51.8)
Comorbidities	T2DM Cancer Asthma/COPD CVD HTN	6 (13.0) 1 (2.0) 8 (17.3) 0 13 (28.2)	8 (24.2) 5 (15.2) 11 (33.3) 2 (6.1) 17(51.5)	
ANCA specificity	MPO PR3 Negative	22 (37.5) 24 (62.5) 0	9 (27.3) 18 (54.5) 6 (18.2)	
Immunotherapy-induction	Prednisolone/ Methylprednisolone	28 (60.8)	19 (57.6)	
Immunotherapy-maintenance	Prednisolone <5mg Azathioprine Rituximab MMF MTX Nil		18 (54.5) 8 (24.2) 17 (51.5) 2 (6.0) 2 (6.0) 1 (3.1)	
Presentation	First presentation Relapse	38 (82.6) 8 (17.4)		
Haematology/ Biochemistry	CRP (mg/dL) (IQR) Creatinine (μmol/L) (IQR) BVAS (IQR) WCC ($x10^9$) (IQR) Neutrophil count ($x10^9$) (IQR)	30 (3.45-164.8) 175 (65.5-558) 15 (8-21) 11 (4.5-13.8) 9 (6.65-17.6)	2.5 (0.5-27.5) 84 (59-239) N/A 8 (3.4-22.3) 5.2 (2.5-13.6)	
Organ involvement	Renal ENT Lung Eye Skin Cardiac	37 (80.4) 17 (40.0) 21 (46.0) 6 (13.0) 2 (4.3) 1 (2.0)	5 (15.2) 10 (30.3) 2 (6.1) 0 2 (6.1) 2 (6.1)	

Table 27. Characteristics of patients included in study
Data are median with IQR. MPO-myeloperoxidase, PR3- Proteinase-3, T2DM- Type 2 diabetes mellitus, CVD- cardiovascular disease, HTN- hypertension, MMF- mycophenolate mofetil, MTX- methotrexate, CRP- C reactive protein, BVAS- Birmingham vasculitis activity score, WCC- white cell count, ENT- ear, nose, and throat.

6.2.1. Biomechanical phenotype of neutrophils in whole blood is altered in AAV

Having shown ANCA can affect mechanical properties of healthy neutrophils *in vitro*, I investigated whether neutrophils from patients with AAV exhibited a similar phenotype *ex vivo*, potentially reflecting their exposure to ANCA *in vivo*. To establish if there is a mechanophenotype of neutrophils in whole blood from patients with aAAV, cells were phenotyped using RT-DC.

Whole blood neutrophil biomechanical properties from age matched HC, rAAV, aAAV were compared. Neutrophils from aAAV samples exhibited no change in size (**Fig 54A**), but a significant decrease in deformability (**Fig 54B**; rAAV: p=0.0001, HC: p=0.0175) and a significant increase in elasticity (**Fig 54C**; rAAV: p=0.0001, HC: ns) in comparison to rAAV and age matched HC. Interestingly, neutrophils from rAAV samples were the most deformable and displayed a small increase in deformability and decrease in elasticity in comparison to HC (ns) as well as aAAV ($p<0.0001$). This may suggest that treatments used for remission maintenance may have an additional impact on cell biomechanics, rather than just returning circulating neutrophils to a baseline state. A larger sample set of the different maintenance treatments is required to potentially determine a correlation between therapies and deformability.

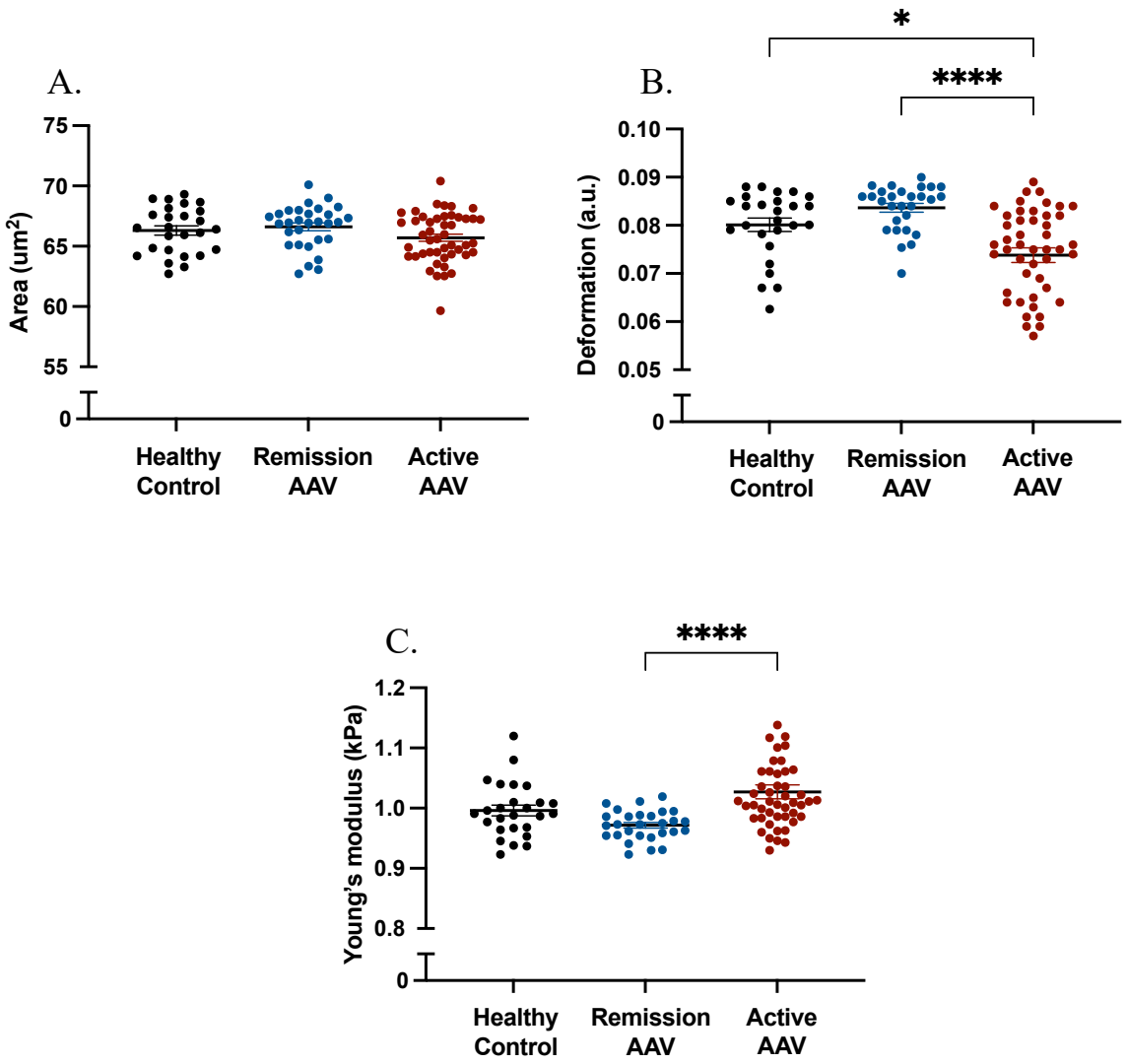


Figure 54. Biomechanical phenotype of neutrophils is altered in AAV
(A-C) Neutrophils in whole blood from patients with aAAV (n=39), rAAV (n=33) and HC (n=27) were analysed using RT-DC. Neutrophil populations were gated and analysed for (A) Cell size, (B) Cell deformability, and (C) Elasticity. More than 1000 events were recorded for each sample and results were visualised and analysed in ShapeOut2 software. Data are shown as median with IQR, statistical analysis was performed using one-way ANOVA Kruskal-Wallis test, with Dunn's multiple comparisons test; *p<0.05. ****p<0.0001.

6.2.2. Disease correlations

6.2.2.1. Disease severity (BVAS) correlates with neutrophil deformability

To determine whether this phenotype correlated with disease-specific clinical manifestations from patients in this study, I compared BVAS score to neutrophil deformability. A significant inverse correlation between BVAS disease activity score and neutrophil deformability was found (**Fig 55B**; r=-0.4039, p=0.0002). In keeping with an association between neutrophil deformability and disease activity, there was also weak inverse correlation between deformability and CRP, although this was not statistically significant (**Fig 55A**; ns).

6.2.2.2. ANCA specificity does not influence neutrophil deformability

MPO-ANCA IgG and PR3-ANCA IgG do not result in different mechanophenotypic changes in stimulated HC neutrophils, and no difference is seen between neutrophils from patients with MPO-AAV versus those with PR3-AAV (**Fig 56A**; ns). Additionally, there is no correlation between ANCA titre and neutrophil deformability in presented heat map. This suggests that factors other than, or in addition to, a direct effect of ANCA on cells may underlie the decreased deformability seen in neutrophils from patients with aAAV.

6.2.2.3. Steroids do not alter neutrophil deformability

Previous work using a microfluidic veins model has shown glucocorticoids (equivalent to 75 mg of prednisolone) induce a cell softening phenotype in leucocytes *in vitro* , and similar results were seen *in vivo* in response to a single dose administered to healthy volunteers (43). My results show that neutrophils from aAAV patients treated acutely with steroids prior to blood sampling exhibited no change in deformability in comparison to patients not receiving treatment (**Fig 56B**; ns). A larger cohort is required to compare the effect of prednisolone *versus* methylprednisolone, as majority of patients on steroid treatment were prescribed

prednisolone. No correlation was found when comparing the total amount of steroid and deformability either, with the maximum dose of prednisolone that patients were prescribed in this study being 60 mg, and most were prescribed 30 mg. Therefore, while previous data suggested steroids can affect leukocyte biomechanics, in this cohort deformation did not correlate with steroid treatment. This result may be due to patients in my experiments having received a lower dosage of steroids.

6.2.2.4. Association between clinical phenotype and neutrophil deformability

There was a trend towards patients with kidney involvement as part of their AAV having decreased deformability, although the number of patients included without kidney disease was small (n=8) (**Fig 56C**; p=0.0710). In keeping with this, there was no correlation between neutrophil deformability and serum creatinine (**Fig 55A**). There was a significant decrease in deformability in patients with lung involvement compared to no lung involvement (**Fig 56D**; p=0.0227).This may be due to neutrophils acquiring a phenotype of decreased deformability after transiting inflamed lung microvasculature, or that neutrophils with decreased deformability are more likely to lodge in the extensive capillary filtering network of the lung and lead to microvascular injury. A larger cohort is required to determine if these findings are specific to disease manifestations or a reflection of greater disease activity in those with pulmonary disease.

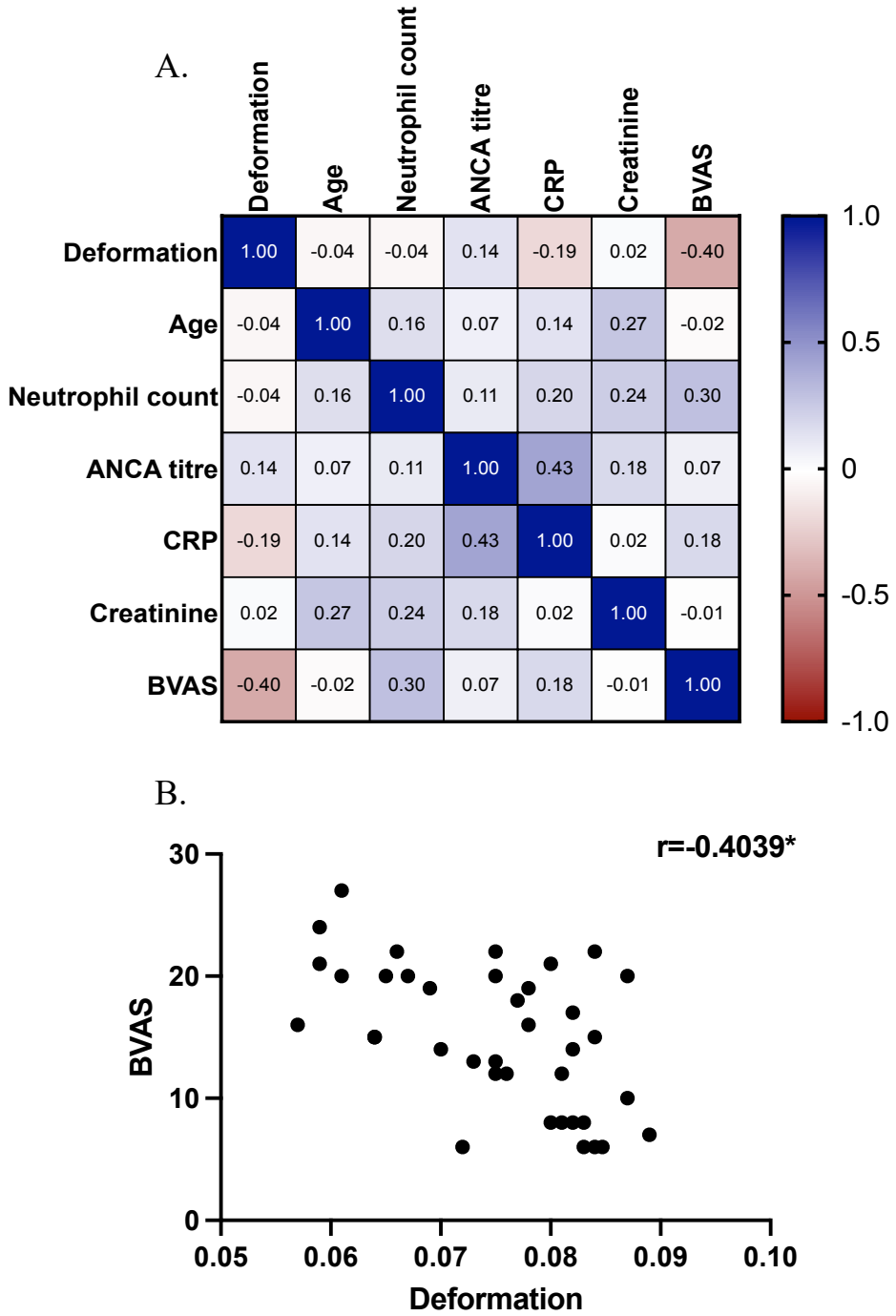


Figure 55. Decreased neutrophil deformability significantly correlates with BVAS
(A) Clinical data from patients with aAAV (n=39) are shown as continuous variables (age, neutrophil count, ANCA titre, CRP, creatinine) in a correlation matrix associated with neutrophil deformability measured in a gated whole blood population, using RT-DC as before. (B) BVAS score correlation with neutrophil deformability. Data are shown as continuous variables, statistical analysis was performed computing Pearson correlation coefficients, two-tailed summary, with 95% confidence interval; *=$p<0.05$.

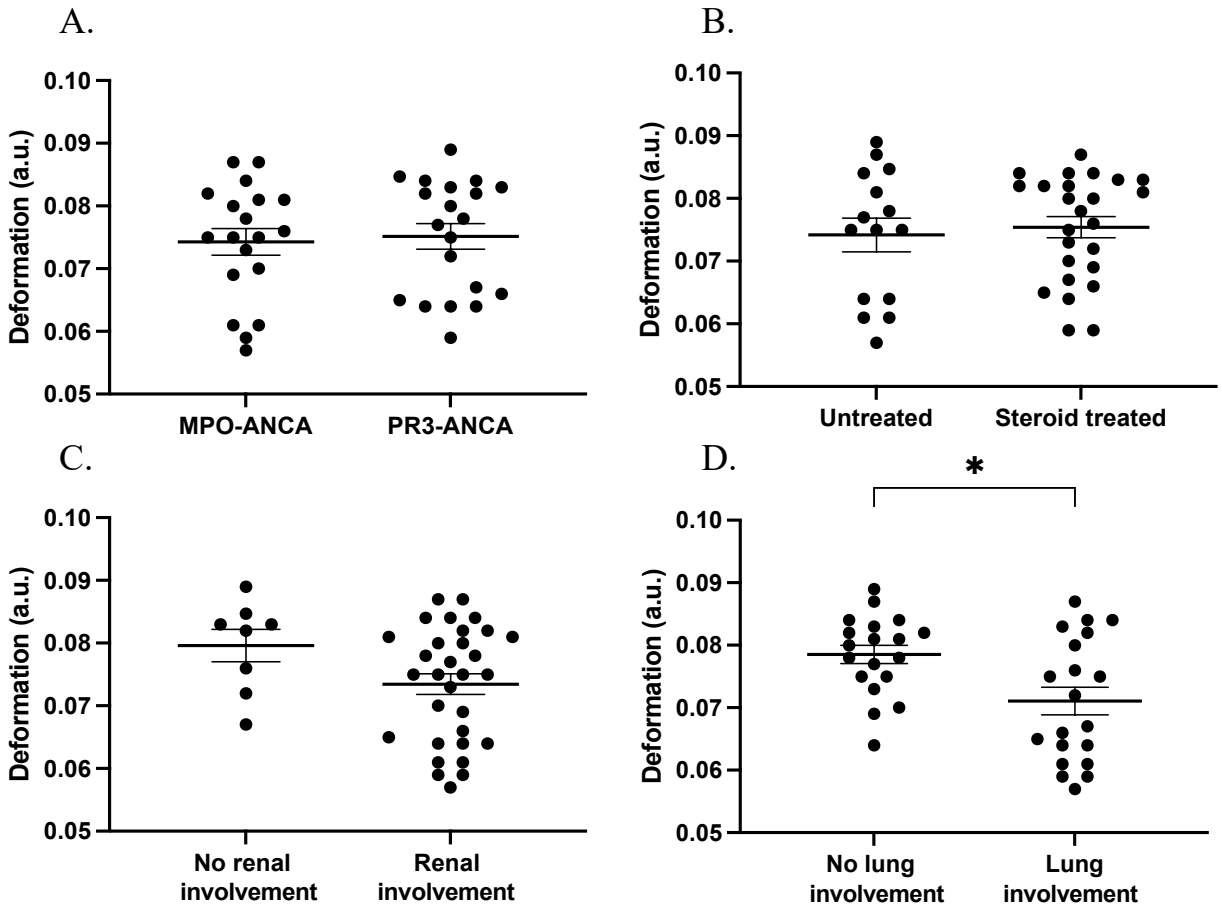


Figure 56. Decreased neutrophil deformability in patients with renal and lung disease
(A-D) Neutrophils in whole blood from patients with aAAV (n=39) were analysed using RT-DC. Neutrophil populations were gated and analysed for (A) MPO v PR3, (B) Steroid treatment, (C) Renal involvement, (D) Lung involvement. More than 1000 events were recorded for each sample and results were visualised and analysed in ShapeOut2 software. Data are shown as median with IQR, statistical analysis was performed using Mann-Whitney test; *=$p<0.05$.

6.3. Increased elasticity in AAV is a myeloid phenotype

When comparing HC, rAAV, and aAAV, monocytes from whole blood exhibited no significant change in size (**Fig 57A**). There is a trend towards decreased deformability and a significant increase in elasticity in aAAV in comparison to HC (**Fig 57B and C**; p=0.0816, p=0.0146). Due to the limitation of sample recordings having small event counts, runs with events recorded in the monocyte population below 100 events were excluded, therefore explaining the reduced number of samples compared to neutrophils. Further limitations regarding monocyte phenotyping are reviewed in section 6.8. Data suggests the robust phenotype of decreased deformability is specific to neutrophils in AAV, but more replicates are necessary to determine if there is a significant myeloid phenotype of decreased deformability in AAV.

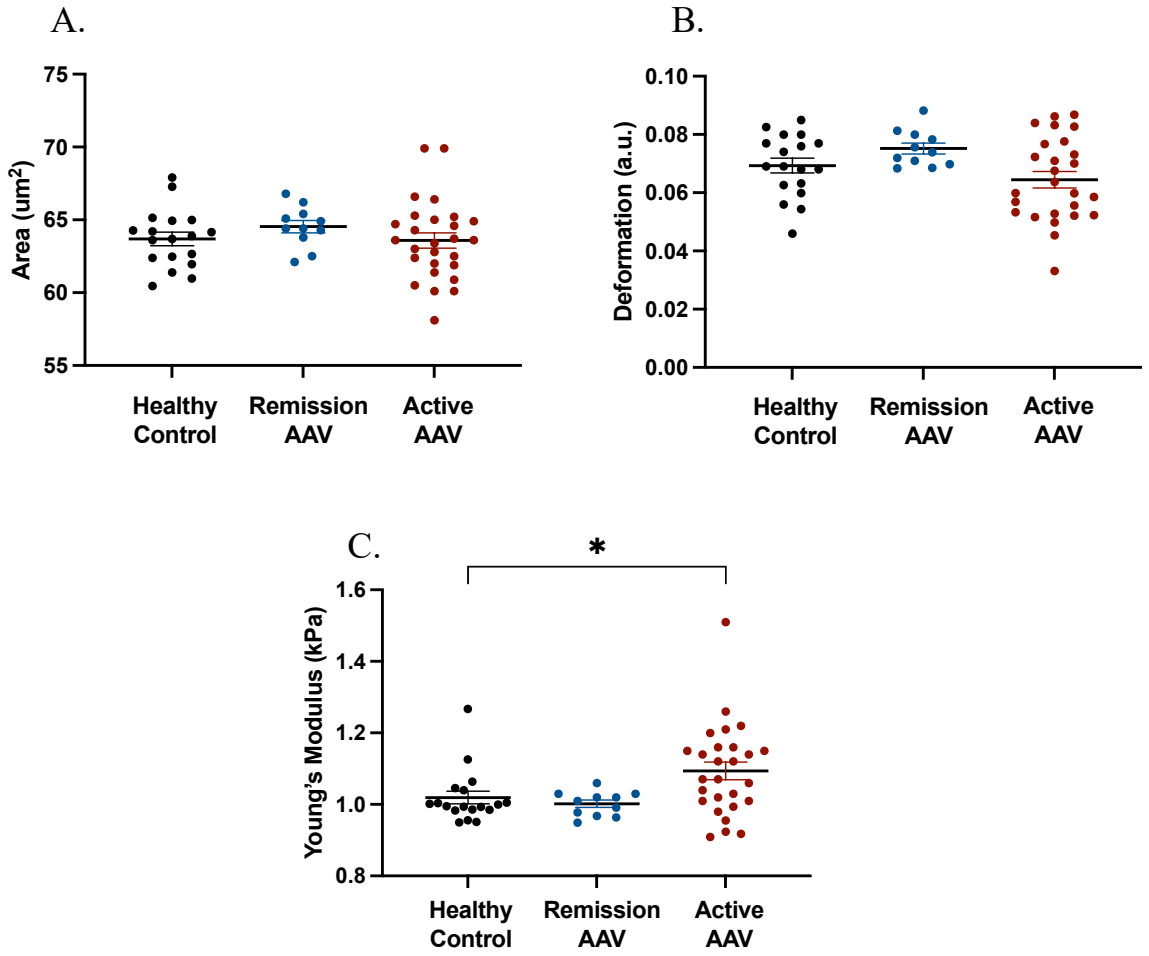


Figure 57. Decreased deformability in AAV is a myeloid phenotype
(A-C) Monocytes in whole blood from patients with aAAV (n=27), rAAV (n=11) and HC (n=18) were analysed using RT-DC. Monocyte populations were gated and analysed for (A) Cell size, (B) Cell deformability, and (C) Elasticity. More than 1000 events were recorded for each sample and results were visualised and analysed in ShapeOut2 software. Data are shown as median with IQR, statistical analysis was performed using one-way ANOVA Kruskal-Wallis test, with Dunn's multiple comparisons test; *p<0.05.

6.4. Actin polymerisation is altered in neutrophils from patients with AAV

HC neutrophils stimulated with ANCA exhibit decreased deformability (section 3.4.) and increased actin polymerisation (section 3.6.1.). As I also identified that neutrophils from patients with aAAV exhibit a stiffer phenotype than HC at baseline, I next investigated actin polymerisation in neutrophils from patients with AAV.

6.4.1. Untreated HC v Untreated AAV

HC or aAAV isolated neutrophils were cultured at 21% O_2 for 1h, fixed and stained for Phalloidin to visualise actin polymerisation. As previously determined, the area and perimeter of each cell were quantified utilising Phalloidin stain, the total cell area staining for Phalloidin was quantified relative to the area of each measured cell, and the total cell perimeter staining for Phalloidin was quantified relative to the perimeter of each measured cell. These variables are individually referred to as area, perimeter, relative area, and relative perimeter.

Representative images shown in **Figure 58** display a visually brighter stain and increased actin cap formation in untreated aAAV neutrophils in comparison to untreated HC neutrophils at 21% O_2. Quantification of actin parameters did not identify any significant differences in untreated HC or aAAV neutrophils under 21% O_2 (**Fig 59**; ns). Therefore, I next investigated the effect of ANCA stimulation of neutrophils from patients with AAV in comparison to HC.

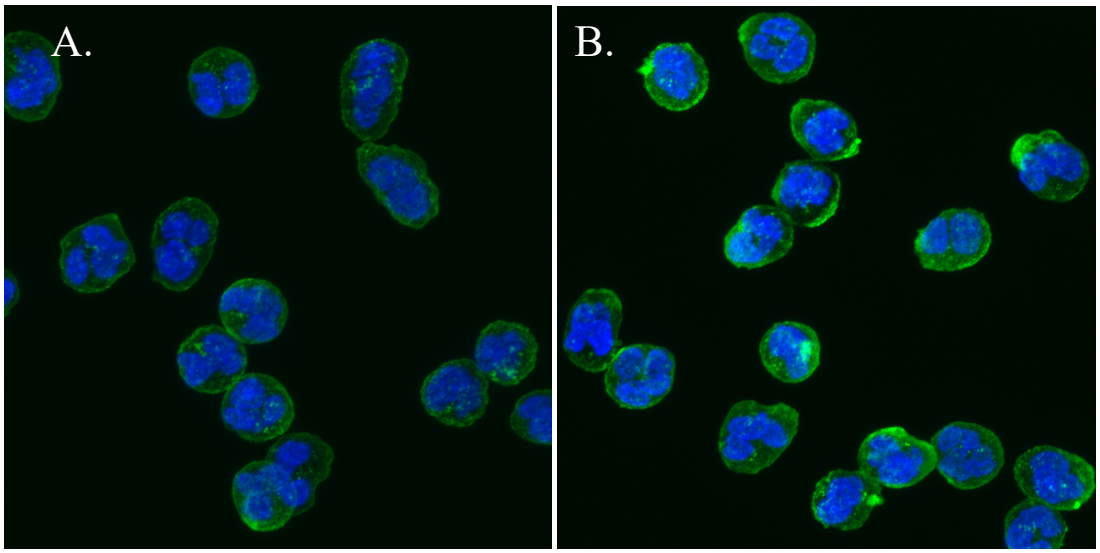


Figure 58. Increased actin capping in AAV neutrophils at baseline
Neutrophils from HC (A) or aAAV (B) were isolated, cultured at 21% O_2 (15 minutes), and incubated in media only (neutrophil culture media, 'untreated') for 1h. Neutrophils were fixed, stained for Phalloidin (green) (AF488), and mounted with VectaShield[R] Antifade Mounting Medium with DAPI (blue), and imaged at 63x using confocal microscopy. Representative images from HC (n=31) and AAV (n=22) experiments are shown.

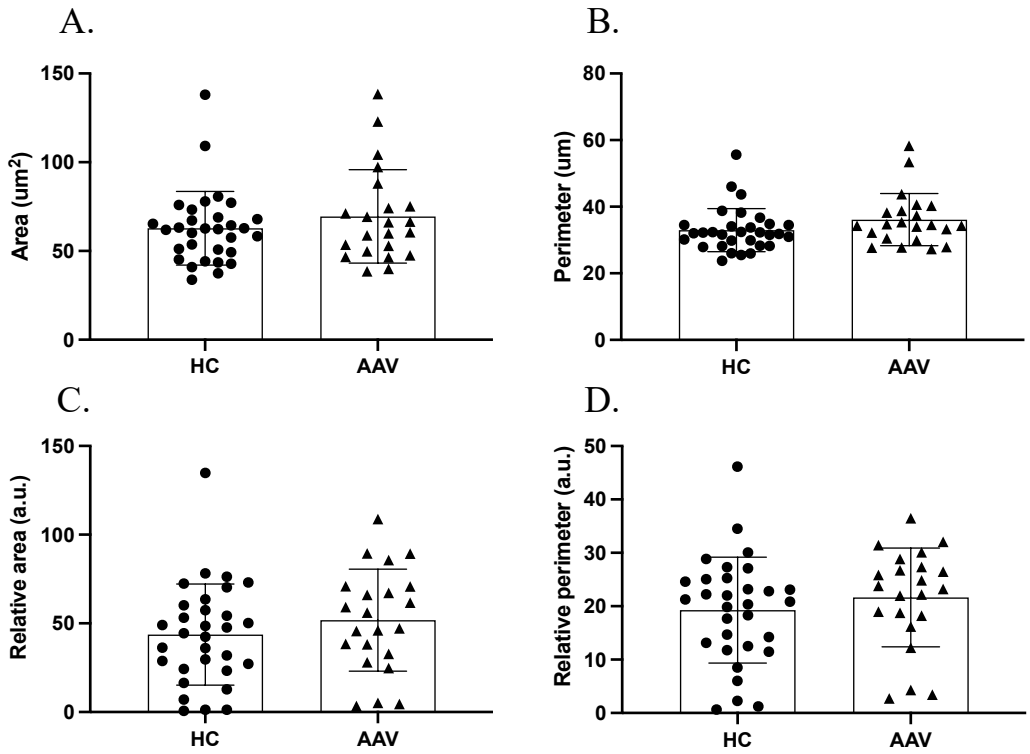


Figure 59. Baseline actin polymerisation is increased in aAAV
(A-D) Neutrophils from HC or AAV were isolated and incubated with media only (neutrophil culture media, 'untreated') for 1h at 21% O_2 (HC n=31, aAAV n=22). Neutrophils were fixed, stained for Phalloidin (AF488), and mounted with VectaShield[R] Antifade Mounting Medium with DAPI, and imaged at 63x using an inverted Zeiss LSM-780 (A) Area, (B) Perimeter, (C) Relative area, and (D) Relative perimeter. Data was analysed using a macro developed for use with ImageJ to measure area, perimeter, relative area, and relative perimeter. Data are shown as mean +/- SEM, statistical analysis was performed using Mann-Whitney test.

6.4.2. Increase in actin polymerisation in MPO/PR3-ANCA stimulated AAV neutrophils at 21% O_2

To determine if ANCA promotes increased cytoskeletal changes in AAV, I stimulated AAV neutrophils with ANCA to measure actin polymerisation using immunofluorescence. Neutrophils were primed with 2 ng/mL TNF (15 minutes), stimulated with HC or MPO-/PR3-ANCA IgG for 1h, fixed, and stained for Phalloidin.

As described previously, when HC neutrophils are stimulated with MPO-/PR3-ANCA, (representative images shown in **Fig 61A/C/E/G**), this results in a visually brighter stain, extended protrusion formation, and distorted cell shape in MPO-/PR3-ANCA stimulated neutrophils in comparison to untreated and HC IgG. Untreated and HC IgG stimulated neutrophils exhibit less actin staining, with actin caps present in HC IgG stimulated neutrophils. I then compared aAAV to HC neutrophils, and the visual features described were all heightened in aAAV in all stimulation conditions (representative images shown in **Fig 61B/D/F/H**). Images were quantified using the same macro from section 6.4.1. to measure actin area, perimeter, relative area, and relative perimeter.

Although non-significant, untreated aAAV neutrophils in 21% O_2, exhibit a small increase across all parameters in comparison to untreated HC neutrophils. A greater magnitude of change is then displayed in aAAV neutrophils once stimulated with ANCA in comparison to HC neutrophils responses. Although, this increase in area, perimeter, relative area, and relative perimeter seen in ANCA stimulated aAAV neutrophils in comparison to ANCA stimulated HC did not achieve significance for any parameter (**Fig 60ABCD**; ns). The most striking difference was that aAAV neutrophils were more responsive to stimulation with HC IgG, compared to HC neutrophils which exhibited very little change in the actin cytoskeleton in response to HC

IgG stimulation. There were significant increases in actin area (p=0.002), relative area (p=0.006), and relative perimeter (p=0.01) between aAAV and HC neutrophils following stimulation with HC IgG. A similar effect, although of lower magnitude was seen following MPO-ANCA stimulation, with significant increases in relative area (p=0.008) and relative perimeter (p=0.02) of actin. There were no differences seen in quantified parameters between aAAV and HC neutrophils following PR3-ANCA stimulation, although there were fewer replicate values for these conditions (**Fig 66A-D**). This suggests aAAV neutrophils may have undergone significant priming or activation *in vivo* leaving them more susceptible to stimulation *ex vivo*.

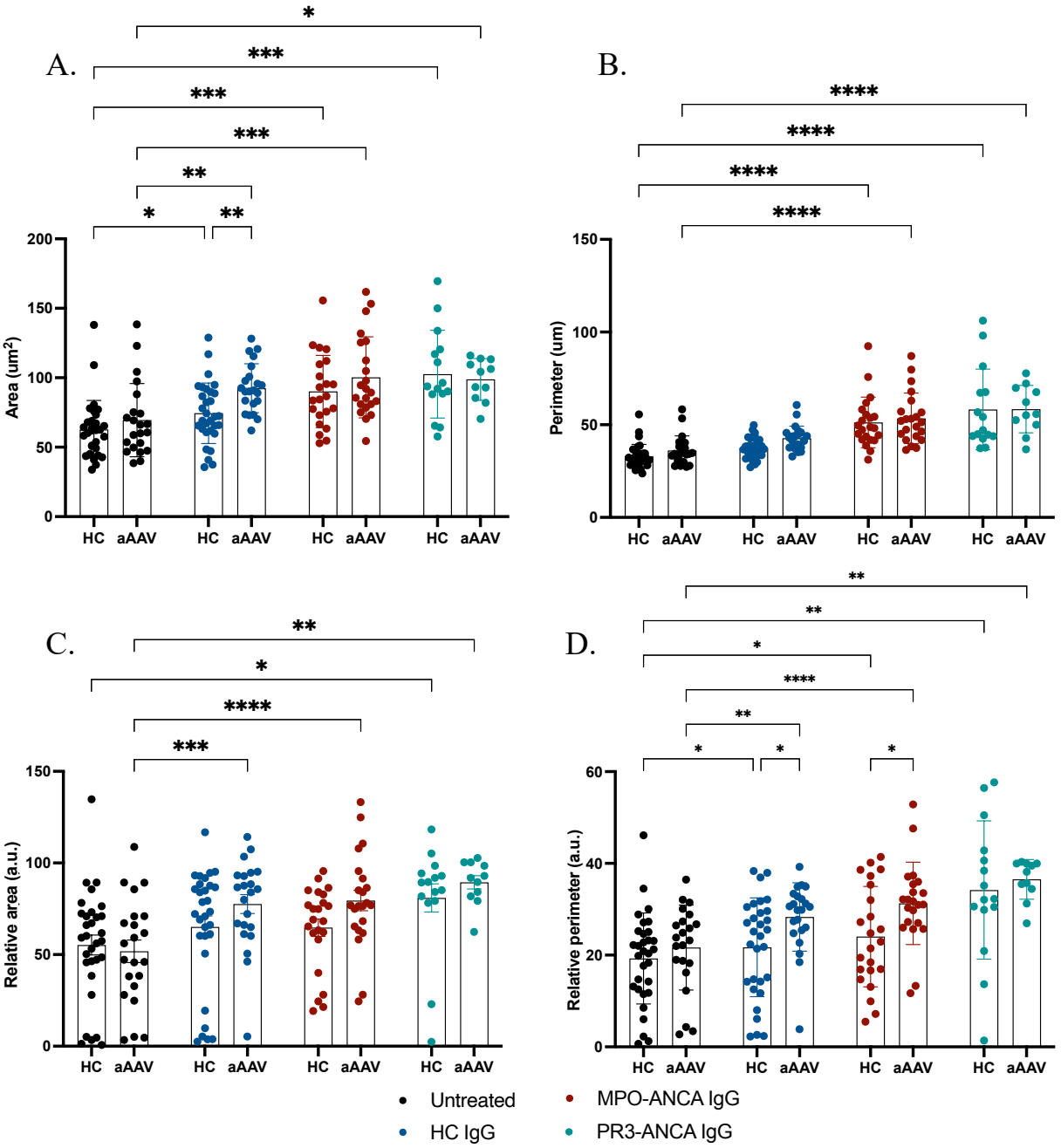


Figure 60. Increase in actin polymerisation in MPO/PR3-ANCA stimulated AAV neutrophils

(A-D) Isolated neutrophils from HC or aAAV were isolated, untreated with media only (neutrophil culture media, 'untreated') or primed with 2 ng/mL TNF (15 minutes) and stimulated with 100 ug/mL HC IgG, MPO-ANCA IgG (HC: n=23, aAAV n=22), PR3-ANCA IgG (HC: n=15, aAAV: n=10) for 1h at 21% O_2. Neutrophils were fixed, stained for Phalloidin (AF488), and mounted with VectaShield[R] Antifade Mounting Medium with DAPI, and imaged at 63x using an inverted Zeiss LSM-780 (A) Area, (B) Perimeter, (C) Relative area, and (D) Relative perimeter. Data was analysed using a macro developed for use with ImageJ to measure area, perimeter, relative area, and relative perimeter. Data are shown as mean +/- SEM, statistical analysis was performed using two-way ANOVA mixed effects model with Geisser-Greenhouse correction, with Tukey's multiple comparisons test.

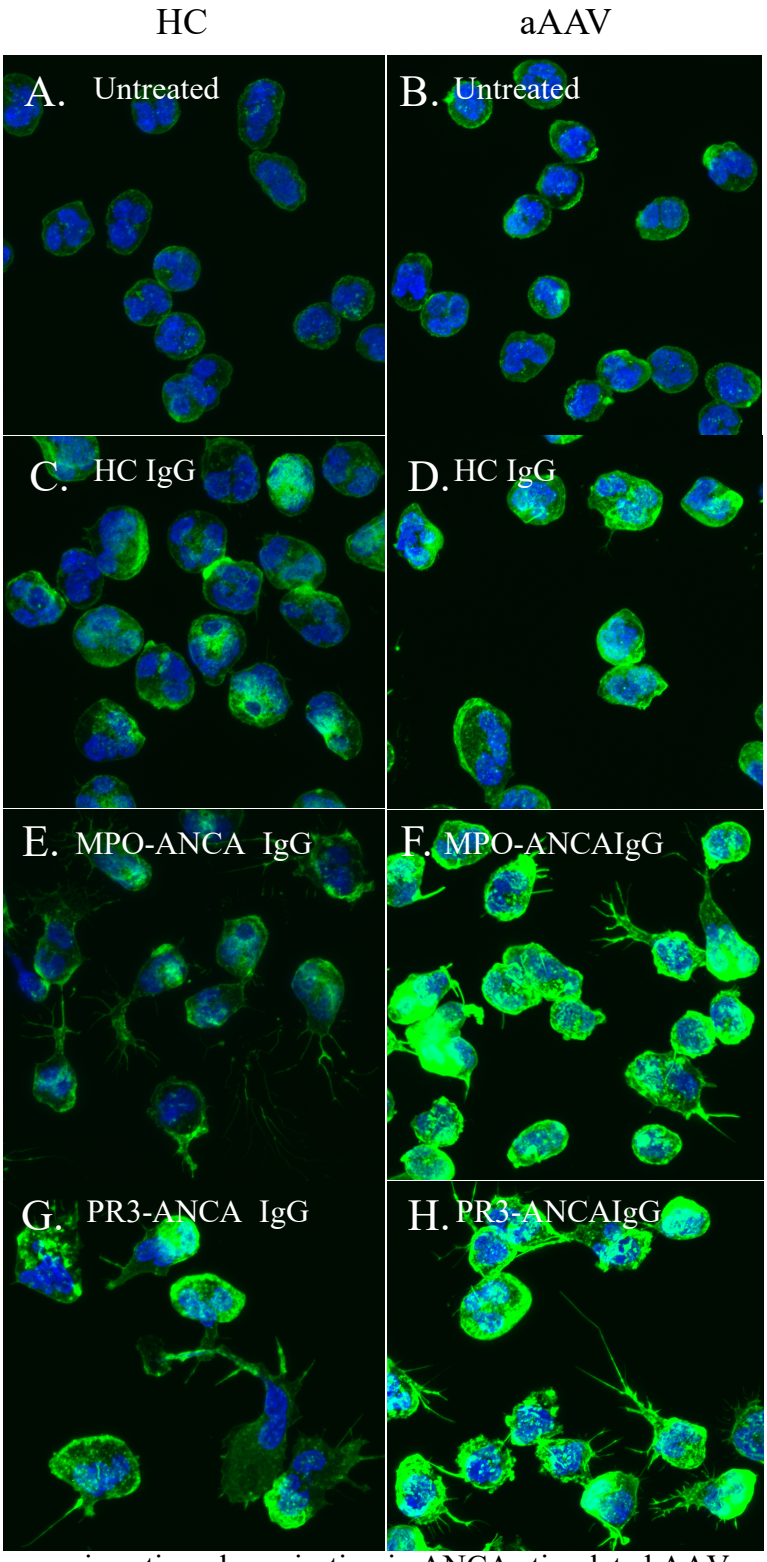


Figure 61. Increase in actin polymerisation in ANCA stimulated AAV neutrophils
Neutrophils in whole blood from HC and aAAV were isolated, untreated with media only (neutrophil culture media, 'untreated') or primed with 2 ng/mL TNF (15 minutes) and stimulated with 100 ug/mL HC IgG, MPO-ANCA IgG, PR3-ANCA IgG for 1h at 21% O_2. Neutrophils were fixed, stained for Phalloidin (green) (AF488), and mounted with VectaShield[R] Antifade Mounting Medium with DAPI (blue), and imaged at 63x using an inverted Zeiss LSM-780 (A/B) Untreated, (C/D) HC IgG, (E/F) MPO-ANCA IgG, and (G/H) PR3-ANCA IgG. Representative images from HC (n=31) and AAV(n=22) experiments are shown.

6.4.3. Hypoxia increases actin polymerisation in AAV neutrophils

Having shown that pathological hypoxia can alter actin polymerisation in untreated HC neutrophils, I next examined the effect of decreased oxygen tension on aAAV neutrophil actin polymerisation. HC or aAAV isolated neutrophils were cultured at 21%, 5%, or 1% O_2 (1h), fixed, and stained for Phalloidin using immunofluorescence to visualise actin polymerisation Experiments were performed comparing 21% v 5% O_2, or 21% v 1% O_2 to examine the effects of venous physiological oxygen or pathological oxygen versus standard atmospheric culture conditions.

Representative images shown in **Figure 62** display a visually brighter stain and increased actin cap formation at 5% and 1% O_2 in both HC and aAAV untreated neutrophils in comparison to 21% O_2. Untreated HC and aAAV neutrophils at 5% and 1% O_2 exhibit a visually brighter stain and blebbing at the cell perimeter in comparison to 21% O_2 untreated. No significant changes were shown in 1% or 5% O_2 untreated aAAV neutrophils in any parameter in comparison to 21% O_2 untreated aAAV neutrophils (**Fig 63**). 1% O_2 promoted actin polymerisation in HC and although not significant, a similar effect was seen in aAAV at 1% O_2. Interestingly, there is also a suggestion that aAAV neutrophils are displaying this increased actin polymerisation at 5% O_2, unlike HC neutrophils.

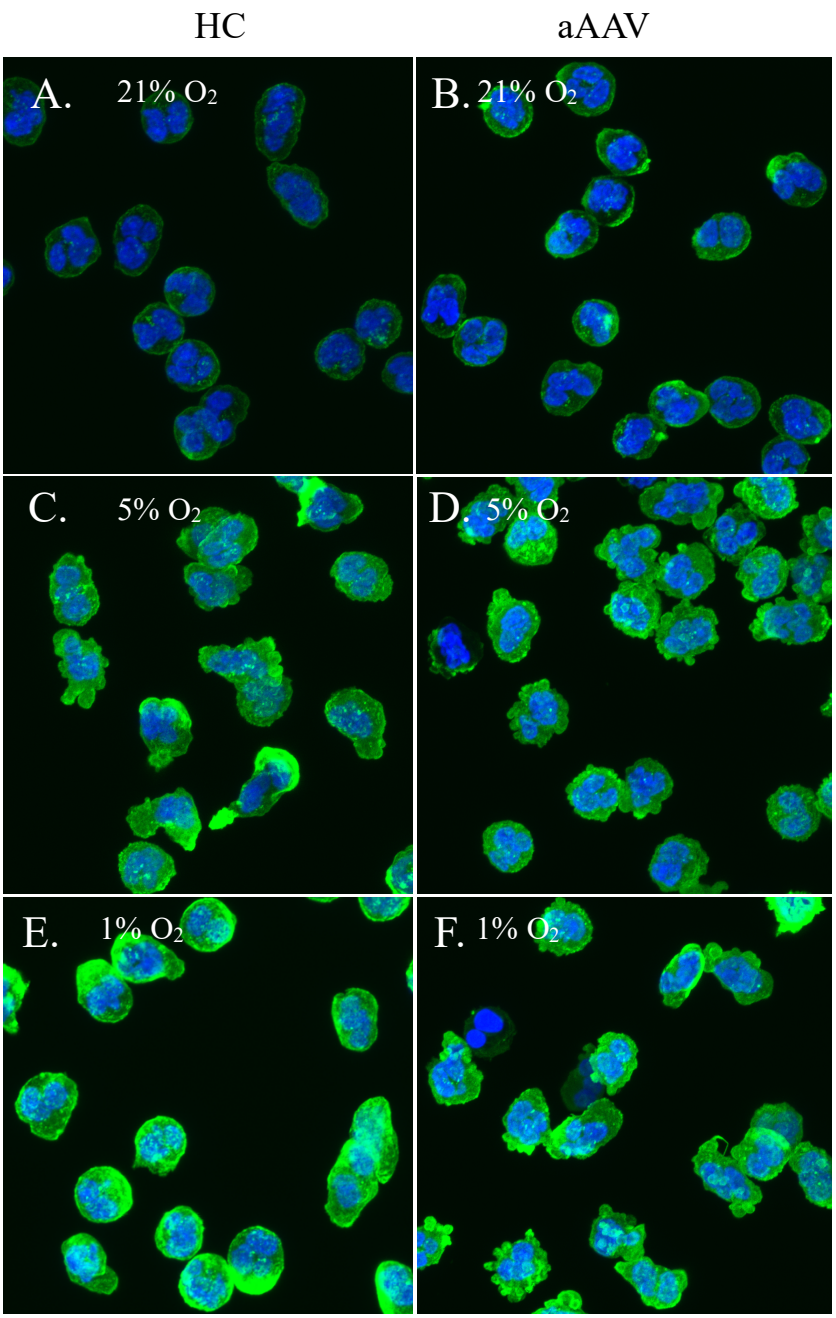


Figure 62. Oxygen tension influences actin polymerisation in HC and AAV neutrophils
Neutrophils from HC (A/C/E) or AAV (B/D/F) were isolated, cultured at 21%, 5%, or 1% O_2 (15 minutes), and incubated in media only (neutrophil culture media, 'untreated') for 1h. Neutrophils were fixed, stained for Phalloidin (green) (AF488), and mounted with VectaShield[R] Antifade Mounting Medium with DAPI (blue), and imaged at 63x using confocal microscopy (A/C/E) HC, (B/D/F) AAV, (A/B) 21% O_2, (C/D) 5% O_2, (E/F) 1% O_2. Representative images from HC: 21% O_2 (n=30), 5% O_2 (n=18), 1% O_2 (n=12), AAV: 21% O_2 (n=22), 5% O_2 (n=5), 1% O_2 (n=9) experiments are shown.

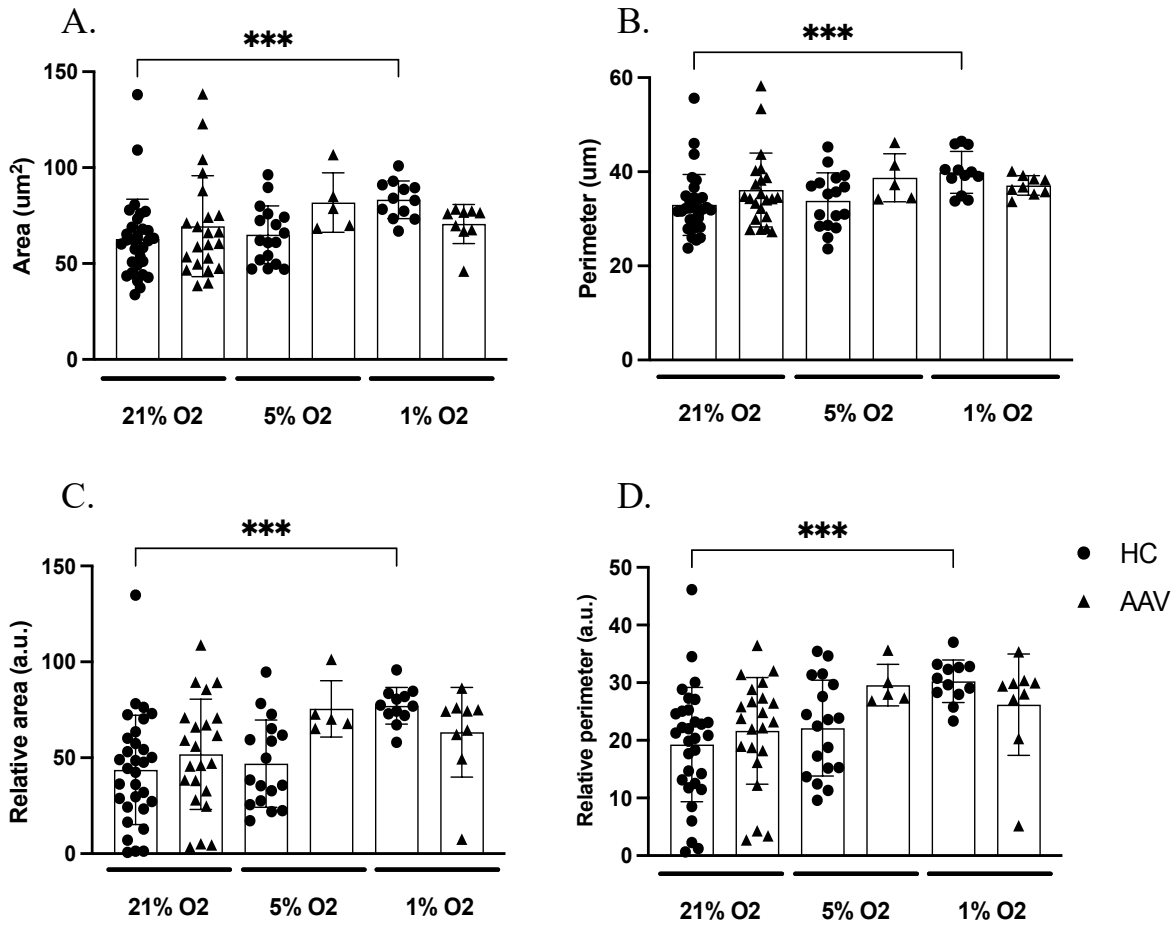


Figure 63. Oxygen tension influences HC and AAV neutrophil actin polymerisation
(A-D) Neutrophils from HC or AAV were isolated and incubated with media only (neutrophil culture media, 'untreated') for 1h (HC: 21% O_2 n=30, 5% O_2 n=18, 1% O_2 n=12, AAV: 21% O_2 n=22, 5% O_2 n=5, 1% O_2 n=9). Neutrophils were fixed, stained for Phalloidin (AF488), and mounted with VectaShield[R] Antifade Mounting Medium with DAPI, and imaged at 63x using an inverted Zeiss LSM-780 (A) Area, (B) Perimeter, (C) Relative area, and (D) Relative perimeter. Data was analysed using a macro developed for use with ImageJ to measure area, perimeter, relative area, and relative perimeter. Data are shown as mean +/- SEM, statistical analysis was performed using two-way ANOVA mixed effects model with Geisser-Greenhouse correction, with Tukey's multiple comparisons test; ***$p<0.001$.

6.4.4. Hypoxia increases actin polymerisation in AAV ANCA stimulated neutrophils

Next, I investigated if the enhanced effect of ANCA on actin polymerisation in aAAV is augmented or diminished by different oxygen tensions. In section 4.6 I identified that in neutrophils, ANCA induced actin changes were inhibited by incubation at 5% O_2 but were equivalent or enhanced at 1% O_2. However, as aAAV neutrophils were more responsive to ANCA stimulation, I hypothesised this may not be the case when experiments were replicated at aAAV cells.

I first assessed the impact of 5% O_2 on ANCA-induced responses in aAAV neutrophils in comparison to HC. Representative images shown in **Figure 66** display a visually brighter stain and increased protrusion formation at 5% in both HC and aAAV MPO-/PR3-ANCA stimulated neutrophils in comparison to untreated and HC IgG. While the increase in area previously seen at 21% O_2 in MPO-ANCA stimulated HC neutrophils (**Fig 60**) is here prevented by 5% O_2, this reduction was not seen in aAAV neutrophils, which exhibited an increase in area upon MPO-ANCA stimulation (**Fig 64**; p=<0.0001 for HC vs aAAV following MPO-ANCA stimulation). There was an increase in perimeter at 5% O_2 in aAAV neutrophils compared to HC in untreated cells and following HC IgG stimulation, but this was not augmented further by ANCA stimulation (**Fig 64B**; MPO ns). There were significant increases in relative area and relative perimeter in MPO-ANCA aAAV stimulated neutrophils at 5% O_2 in comparison to to HC MPO-ANCA stimulated neutrophils at 5% (**Fig 64C and D**; relative area p=<0.0001, relative perimeter p=0.001). AAV neutrophils therefore behave differently from HC neutrophils under 5% O_2 and as seen in the untreated neutrophils, the quiescence signal seen in HC neutrophils following ANCA stimulation at 5% O_2 is lost in aAAV neutrophils. Although PR3 ANCA stimulation is displaying a similar pattern as that identified in 21% O_2, more replicates are required before drawing conclusions on the effect of incubating PR3-

ANCA with aAAV neutrophils at 5% O_2 as I was only able to recruit one patient with PR3 active disease whilst conducting these experiments.

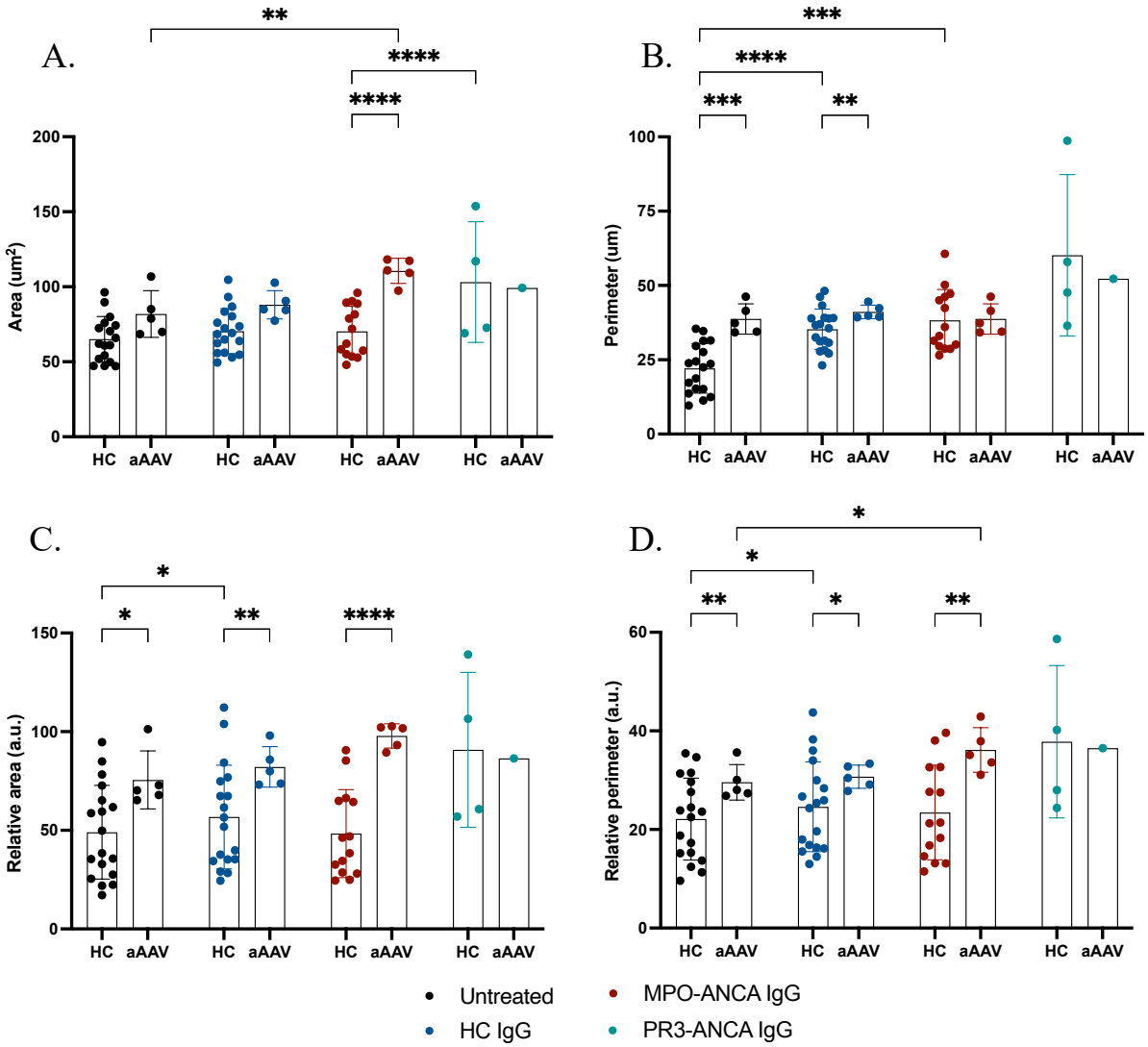


Figure 64. 5% O_2 increases actin polymerisation in AAV ANCA stimulated neutrophils
(A-D) Neutrophils in whole blood from HC or aAAV were isolated, untreated with media only (neutrophil culture media, 'untreated') or primed with 2 ng/mL TNF (15 minutes) and stimulated with 100 ug/mL HC IgG, MPO-ANCA IgG (HC: n=14, aAAV: n=5), PR3-ANCA IgG (HC: n=4, aAAV: n=1) for 1h at 5% O_2. Neutrophils were fixed, stained for Phalloidin (AF488), and mounted with VectaShield[R] Antifade Mounting Medium with DAPI, and imaged at 63x using an inverted Zeiss LSM-780 (A) Area, (B) Perimeter, (C) Relative area, and (D) Relative perimeter. Data was analysed using a macro developed for use with ImageJ to measure area, perimeter, relative area, and relative perimeter. Data are shown as mean +/- SEM, statistical analysis was performed using two-way ANOVA mixed effects model with Geisser-Greenhouse correction, with Tukey's multiple comparisons test.

I next assessed the impact of 1% O_2 on ANCA-induced responses in aAAV neutrophils. Similar to results in HC neutrophils, and in aAAV neutrophils at 5% O_2, decreased oxygen tension induced a visually brighter actin signal in all stimulation conditions (**Fig 67**). In contrast to cells at 5% O_2, the effect of ANCA stimulation on area was similar between aAAV neutrophils and HC neutrophils at 1% O_2 was (**Fig 65A**; ns). Unexpectedly, there was less change in cell perimeter in MPO- and PR3-ANCA stimulated aAAV neutrophils was shown at 1% O_2 in comparison to 1% O_2 MPO- and PR3-ANCA stimulated HC neutrophils (**Fig 65B**; MPO: p=0.001, PR3: p=0.005). Relative area and relative perimeter were both increased following MPO- and PR3-ANCA stimulation in aAAV neutrophils at 1% O_2, but the changes were similar to those seen in HC neutrophils (**Fig 65C and D**; ns).

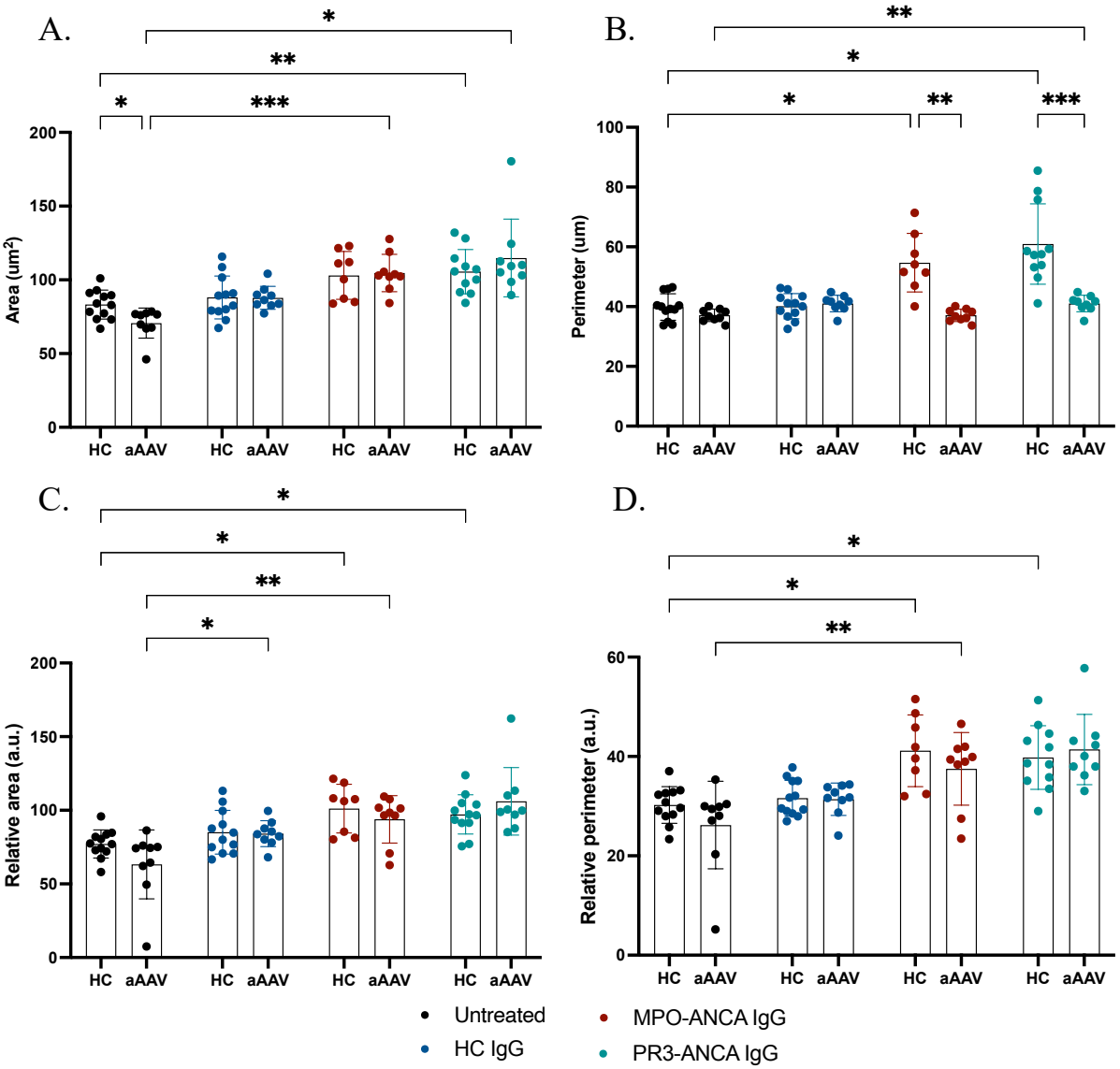


Figure 65. Hypoxia increases actin polymerisation in AAV ANCA stimulated neutrophils
(A-D) Neutrophils in whole blood from HC or aAAV were isolated, untreated with media only (neutrophil culture media, 'untreated') or primed with 2 ng/mL TNF (15 minutes) and stimulated with 100 ug/mL HC IgG, MPO-ANCA IgG (HC: n=8, aAAV: n=9), PR3-ANCA IgG (HC: n=11, aAAV: n=9) for 1h at 1% O_2. Neutrophils were fixed, stained for Phalloidin (AF488), and mounted with VectaShield[R] Antifade Mounting Medium with DAPI, and imaged at 63x using an inverted Zeiss LSM-780 (A) Area, (B) Perimeter, (C) Relative area, and (D) Relative perimeter. Data was analysed using a macro developed for use with ImageJ to measure area, perimeter, relative area, and relative perimeter. Data are shown as mean +/- SEM, statistical analysis was performed using two-way ANOVA mixed effects model with Geisser-Greenhouse correction, with Tukey's multiple comparisons test.

Taking these results together, decreased oxygen tension alters actin polymerisation overall, in comparison to 21% O_2, in untreated, HC IgG, and MPO-/PR3-ANCA stimulated aAAV neutrophils. At 21% O_2, ANCA induces actin polymerisation, with increases in all measured parameters compared to untreated HC neutrophils. In aAAV neutrophils, at 21% O_2, there is enhanced actin polymerisation at baseline, and a greater increase in relative area and relative perimeter following both HC IgG and MPO-ANCA stimulation. In contrast, at 5% O_2 then prevents ANCA responses in HC neutrophils, this was not found in ANCA stimulated aAAV neutrophils. 1% O_2 appears to synergise with ANCA to promote actin polymerisation in HC neutrophils, even starting from an increase at baseline in untreated HC neutrophils. For most parameters, these were similar in aAAV neutrophils, although there was significantly lower ANCA induced cell perimeter at 1% O_2 in aAAV neutrophils compared to in HC neutrophils possibly due to more polymerised actin building up around the cell membrane. Oxygen tension alone had less of an effect on actin polymerisation in untreated aAAV neutrophils, possibly due to the changes that were already present at baseline in these cells. Overall, these experiments indicate pathological hypoxia promotes actin polymerisation in aAAV neutrophils to a similar extent as previously seen with ANCA stimulation in HC neutrophils but the quiescent effect, in contrast to HC neutrophils at 5% O_2 (section 4.6) is not seen in aAAV neutrophils at 5% O_2.

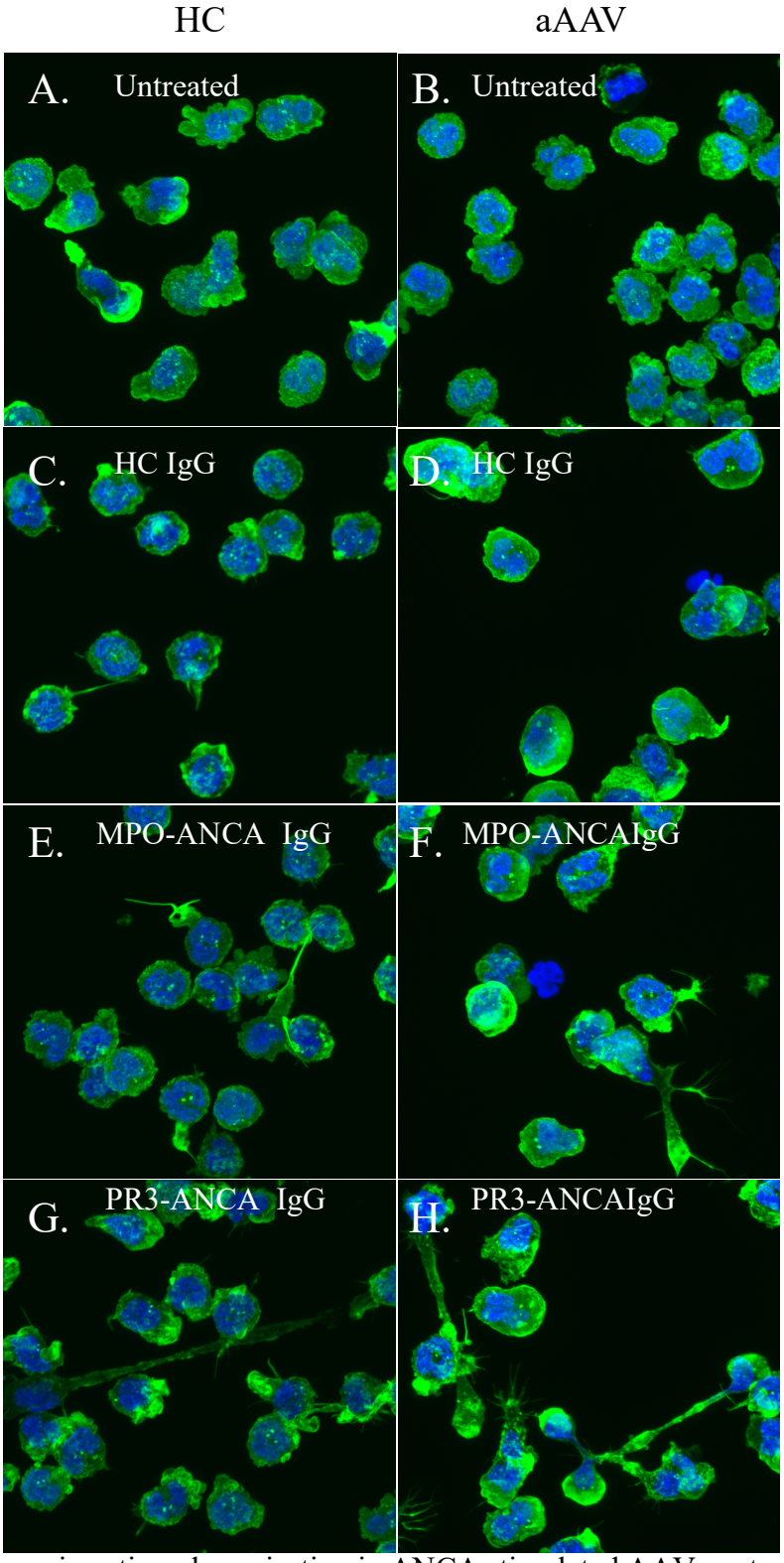


Figure 66. Increase in actin polymerisation in ANCA stimulated AAV neutrophils at 5% O_2 Neutrophils in whole blood from aAAV were isolated, cultured at 5% O_2 (15 minutes), primed with 2 ng/mL TNF (15 minutes) and stimulated with 100 ug/mL HC IgG, MPO-ANCA IgG, PR3-ANCA IgG or media only (neutrophil culture media, 'untreated') for 1h. Neutrophils were fixed, stained for Phalloidin (green) (AF488), and mounted with VectaShield [R] Antifade Mounting Medium with DAPI (blue), and imaged at 63x using confocal microscopy (A/C/E/G) HC, (B/D/F/H) AAV, (A/B) Untreated, (C/D) HC IgG, (E/F) MPO-ANCA, (G/H) PR3-ANCA. Representative images from HC: 5% O_2 (n=18), AAV: 5% O_2 (n=5), experiments are shown.

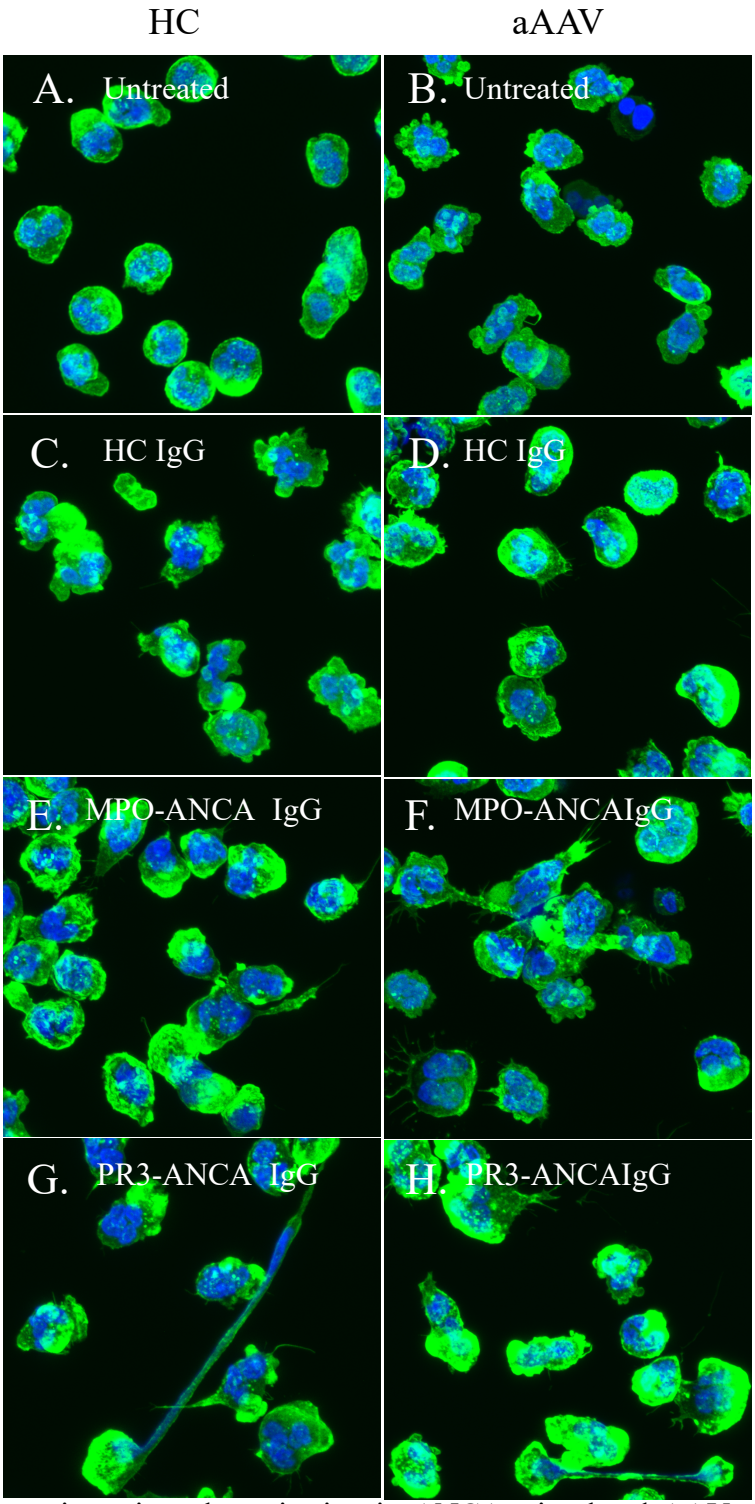


Figure 67. Increase in actin polymerisation in ANCA stimulated AAV neutrophils under hypoxia

Neutrophils in whole blood from aAAV were isolated, cultured at 1% O_2 (15 minutes), untreated with media only (neutrophil culture media, 'untreated') or primed with 2 ng/mL TNF (15 minutes) and stimulated with 100 ug/mL HC IgG, MPO-ANCA IgG, PR3-ANCA IgG for 1h. Neutrophils were fixed, stained for Phalloidin (green) (AF488), and mounted with VectaShield [R] Antifade Mounting Medium with DAPI (blue), and imaged at 63x using confocal microscopy (A/C/E/G) HC, (B/D/F/H) AAV, (A/B) Untreated, (C/D) HC IgG, (E/F) MPO-ANCA, (G/H) PR3-ANCA. Representative images from HC: 1% O_2 (n=12), AAV: 1% O_2 (n=9) experiments are shown.

6.5. Protein secretion levels

6.5.1. Increased IL-8, ICAM-1, and VCAM-1 secretion in aAAV

Previous work has shown increased CAM expression in neutrophils in inflammation (129,564). ANCA stimulates IL-8 secretion from neutrophils (327), therefore I wanted to assess whether untreated aAAV neutrophils differ in IL-8 secretion levels in the absence of additional stimulation. To assess whether neutrophils from patients with AAV have hypersecretory tendencies *ex vivo*, I measured cytokine release from untreated neutrophils isolated from patients with rAAV and aAAV in comparison to age match HCs. Neutrophils were isolated from HC or AAV, incubated at 37°C at 21% O_2 for 1h, and SN was harvested for measurement using ELISA.

There is a significant increase in IL-8 secretion from untreated neutrophils from patients with rAAV and aAAV in comparison to HC (**Fig 68A**; rAAV p=0.0001, aAAV p=0.0001). Neutrophils from patients with aAAV secrete increased VCAM-1 in comparison to HC and rAAV (**Fig 68B**; HC p=0.0186, rAAV p=0.0438), and an even greater increase in ICAM-1 secretion (**Fig 68C**; HC p=0.0875, rAAV p=0.0001). This likely contributes to increases seen in neutrophil recruitment to sites of inflammation and promotion of adhesion at the vascular endothelium.

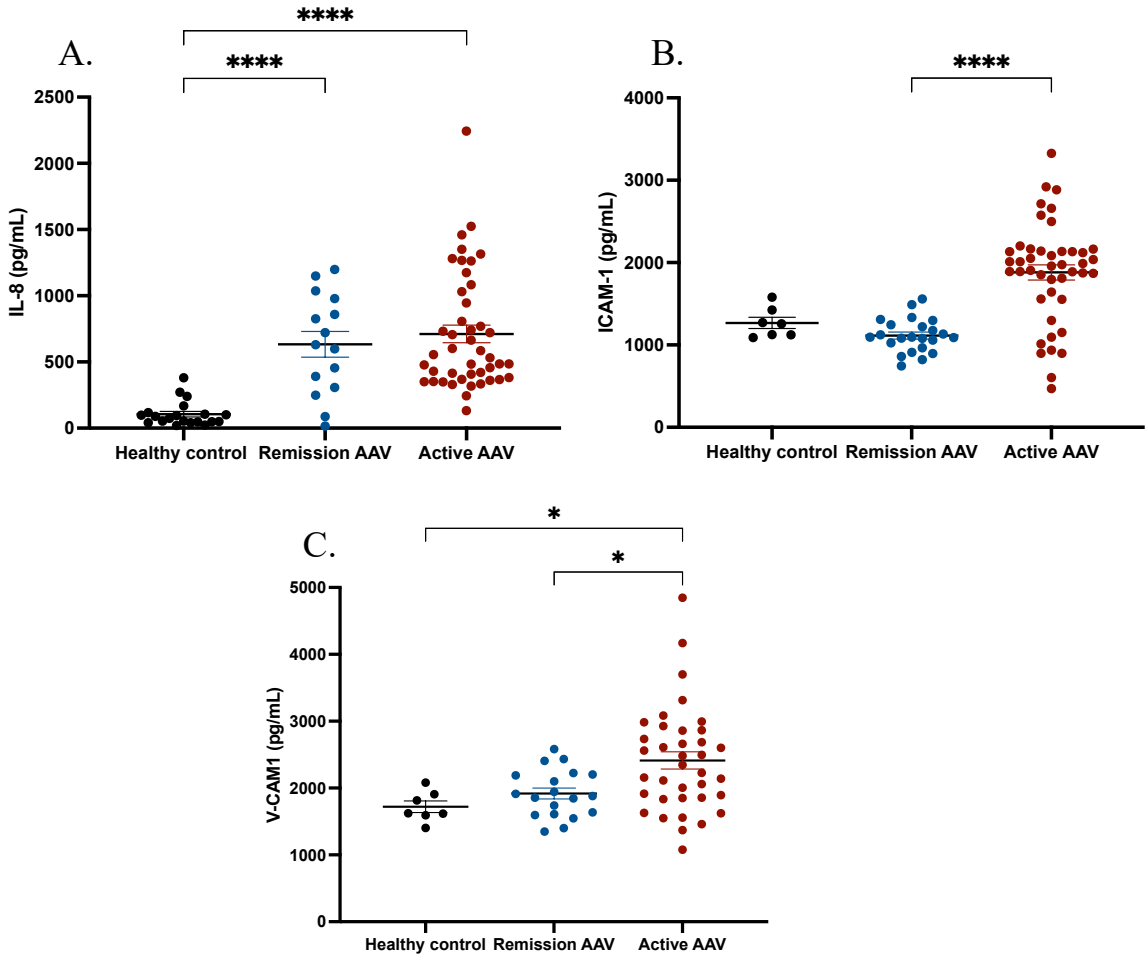


Figure 68. Increased IL-8, ICAM-1, and VCAM-1 secretion in AAV

Isolated neutrophils from HC, rAAV, or aAAV whole blood ($10x10^6$) were incubated for 15 minutes to recover from isolation at 21% O_2, and then incubated for 1h untreated. Neutrophils were pelleted, and cell-free SN was stored. SN IL-8, VCAM-1, and ICAM-1 content was measured by ELISA. Data are shown as mean +/- SEM. Statistical comparison by one-way ANOVA Kruskal-Wallis test, with Dunn's multiple comparisons test. aAAV (n=37), remission (n=19) and HC (IL-8 (HC n=16), VCAM-1 (HC n=7), and ICAM-1 (HC n=7)); A. IL-8, B. VCAM-1, and C. ICAM-1. Data are shown as mean +/- SEM, statistical analysis was performed using one-way ANOVA Kruskal-Wallis test, with Dunn's multiple comparisons test; *p<0.05. ****p<0.0001.

6.5.2. Effect of hypoxia on co-cultured neutrophil and gEC protein secretion

As mentioned in section 6.5.1., neutrophil secretion of cell adhesion and inflammatory molecules potentially increases endothelial activation in AAV. I then investigated whether co-culture with neutrophil supernatant promotes endothelial activation to a greater degree from aAAV neutrophils than HC, and whether this is modulated by oxygen tension

6.5.2.1. Hypoxia influences gEC protein secretion levels when treated with AAV SN

Data from section 5.4.1. showed in the presence of ANCA, hypoxia decreased EC inflammatory cytokine release occurred over time. I therefore investigated whether hypoxia would influence endothelial secretion levels once exposed to secretion products from AAV neutrophils, in a similar manner to that seen with HC neutrophils stimulated with ANCA IgG. To determine if there is a difference in endothelial secretion of IL-8, ICAM-1, and VCAM-1 under hypoxia, gEC incubated at 21%, 5%, or 1% O_2 were treated with supernatant from untreated neutrophils at 21% O_2 isolated from patients with aAAV, rAAV or healthy volunteers.

As expected, there were very low levels of IL8 secretion from gEC. However, by 24 hours there was increased IL-8 production from gEC treated with aAAV neutrophil supernatants, compared to HC at both 21% and 5% O_2 (**Fig 69A**; 21%: p= 0.087, 5%: p=0.0584). Similarly, by 24h there is a significant increase in VCAM-1 secretion from gEC treated with aAAV neutrophil supernatants compared to HC at both 21% and 5% O_2 (**Fig 69B**; 21%: p=0.0027, 5%: p=0.0169). There was no significant difference between any stimulation condition comparing 21% and 5% O_2 for IL-8 or VCAM-1 secretion. Levels of ICAM-1 secretion were low and quite variable, with no significant differences in ICAM-1 release at 6h or 24h between oxygen tensions or stimulation conditions (**Fig 69C**).

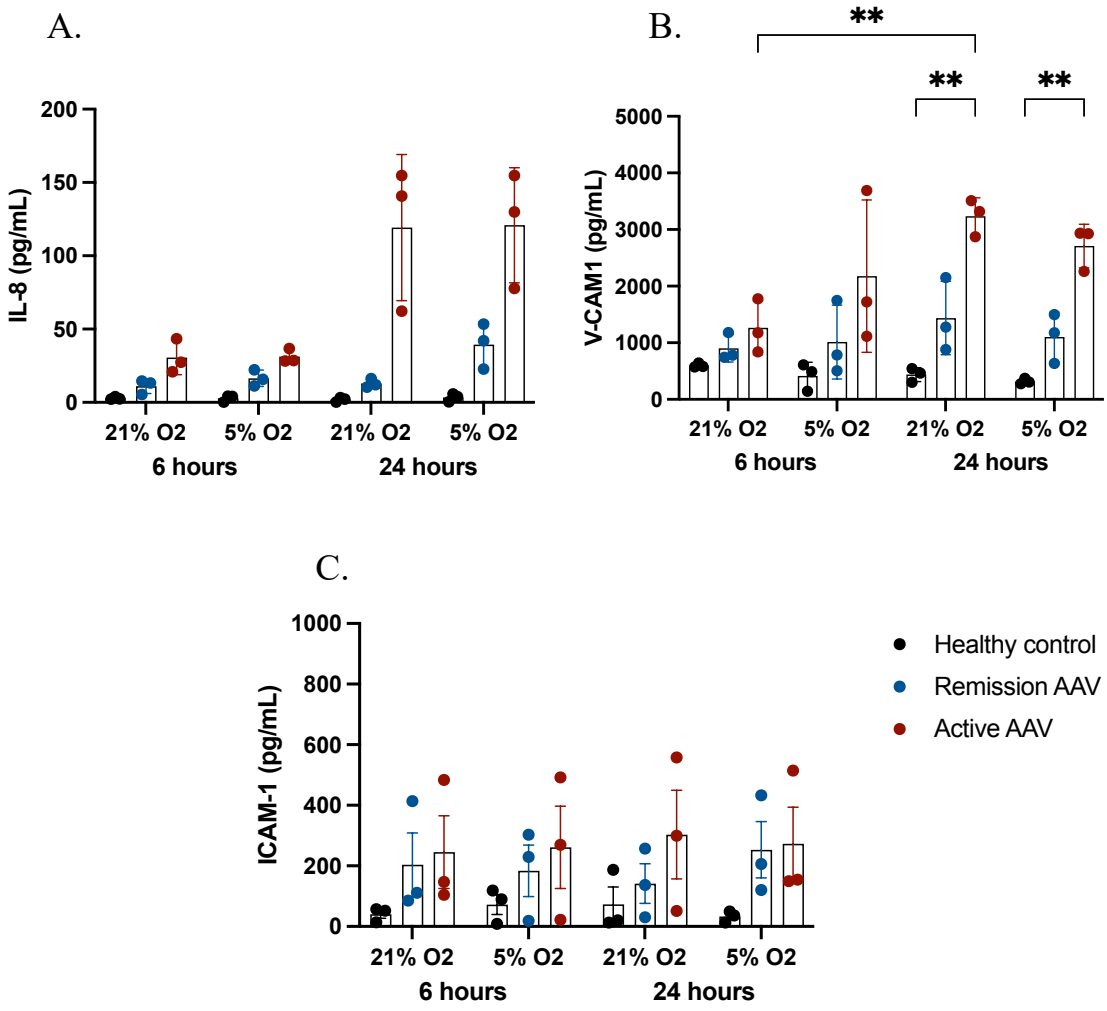


Figure 69. aAAV SN promote gEC secretion of IL-8 and VCAM-1 at 21% and 5% O_2
Untreated HC, rAAV, or aAAV neutrophils ($2x10^5$) were incubated for 1h in neutrophil culture media, and SN (corrected for cytokine amount in the neutrophil SN during quantification) was added to gEC wells for 6h or 24h incubation at 21% or 5% O_2 (n=3). SN IL-8, VCAM-1, and ICAM-1 content was measured by ELISA. SN was corrected for during quantification of the cytokine amount in the added neutrophil SN (A) IL-8, (B) VCAM-1, (C) ICAM-1. Data are shown as mean +/- SEM, statistical analysis was performed using two-way ANOVA with Geisser-Greenhouse correction, with Dunnett's multiple comparisons test. ns, non-significant. *p<0.05. **p<0.01.

There is a significant increase in gEC IL-8 secretion after aAAV neutrophil supernatant treatment compared with HC for both 21% and 1% O_2 at 6h and 24h (**Fig 70A**; 21% 6h: p=0.0190, 1% 6h: p=0.0551, 21% 24h: p=0.0218, 21% 24h: p=0.0051). Secretion levels increase slightly at 24h compared to 6h in both 21% and 1% O_2 aAAV treatment but this was not significant. The increase in ICAM-1 (**Fig 70B**; p=0.0436) and VCAM-1 (**Fig 70C**; ns) secretion levels in aAAV versus HC treated gEC showed a similar overall pattern but were more variable. Secretion profiles in 21% and 1% O_2 were very similar. This suggests it may be the impact of hypoxia on neutrophils which is more important than the impact of hypoxia on gEC as neutrophil SNs were all prepared at 21% O_2.

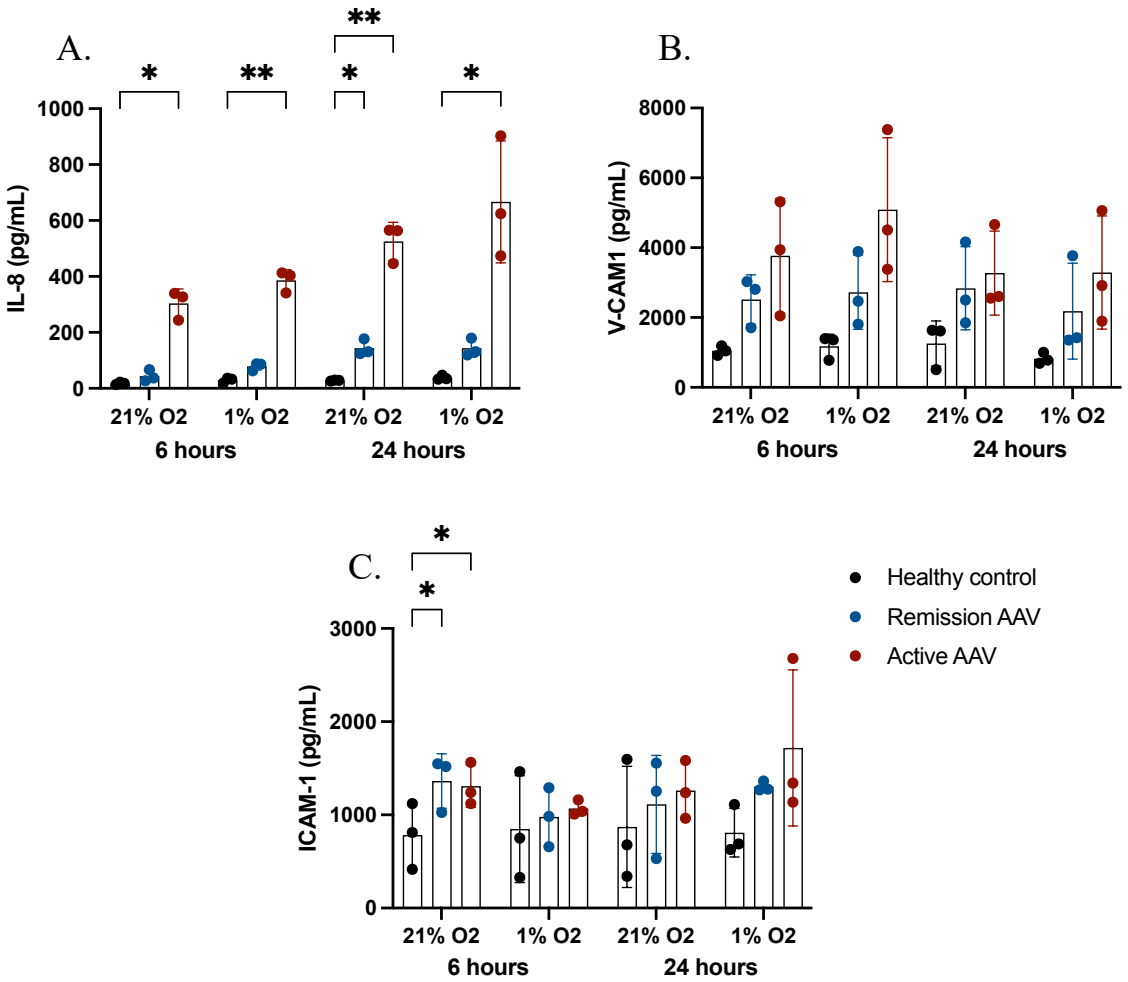


Figure 70. gEC protein secretion levels when treated with aAAV SN are similar in 21% and 1% O_2

Untreated HC, rAAV, or aAAV neutrophils ($2x10^5$) were incubated for 1h in neutrophil culture media, and SN (corrected for cytokine amount in the neutrophil SN before addition) was added to gEC wells for 6h or 24h incubation at 21% or 1% O_2 (n=3). SN IL-8, VCAM-1, and ICAM-1 content was measured by ELISA. SN was corrected for during quantification of the cytokine amount in the added neutrophil SN (A) IL-8, (B) VCAM-1, (C) ICAM-1. Data are shown as mean +/- SEM, statistical analysis was performed using two-way ANOVA with Geisser-Greenhouse correction, with Dunnett's multiple comparisons test. ns, non-significant. *p<0.05. **p<0.01.

6.6. Optimising isolation of RNA isolation and gene expression analysis from aAAV neutrophils

Having identified differences in neutrophil biophysical phenotype and function in patients with aAAV, I next investigated whether transcriptional changes underlie this phenotype. I conducted initial optimisation experiments using a panel of gene targets identified as differentially expressed in MPO-ANCA IgG stimulated neutrophils using the NanoString targeted gene expression platform (311). From results generated using the Nanostring myeloid gene expression panel, I selected the top 30 DE genes and investigated expression in neutrophils from patients with AAV. Fold change was measured using RT-qPCR by performing relative quantification of untreated rAAV and aAAV neutrophils to HC neutrophils (**Fig 71**).

In keeping with the NanoString data, all genes from the panel were upregulated in aAAV neutrophils (**Fig 71**). This included those involved in chemokine and cytokine signalling (*CXCL8, CCL20, CCL3, CC3L1, CCL4, CCRL2, IL1A, IL1B, NLRP3, TNF, TRAF1,* NF-κβ), chemotaxis (*CCL20, CCL3, CCL4, CCL3L1, CXCL8, IL1B*), adhesion (*ITGB2, F11R*), angiogenesis (*PLAU, VEGFA*), and stress response (*NRFA2, GADD45A*). Of these, *CXCL8*, *NFKB1*, *PLAU*, *STAT5A*, *TRAF1*, and *VEGFA* were significantly upregulated in aAAV neutrophils in comparison to rAAV neutrophils (**Fig 71**). A specific target of interest that was upregulated in aAAV is *WAS*, which is a gene involved in signalling for the actin cytoskeleton polymerisation. These results suggest significant differences in neutrophil transcriptional profiles in aAAV versus rAAV neutrophils.

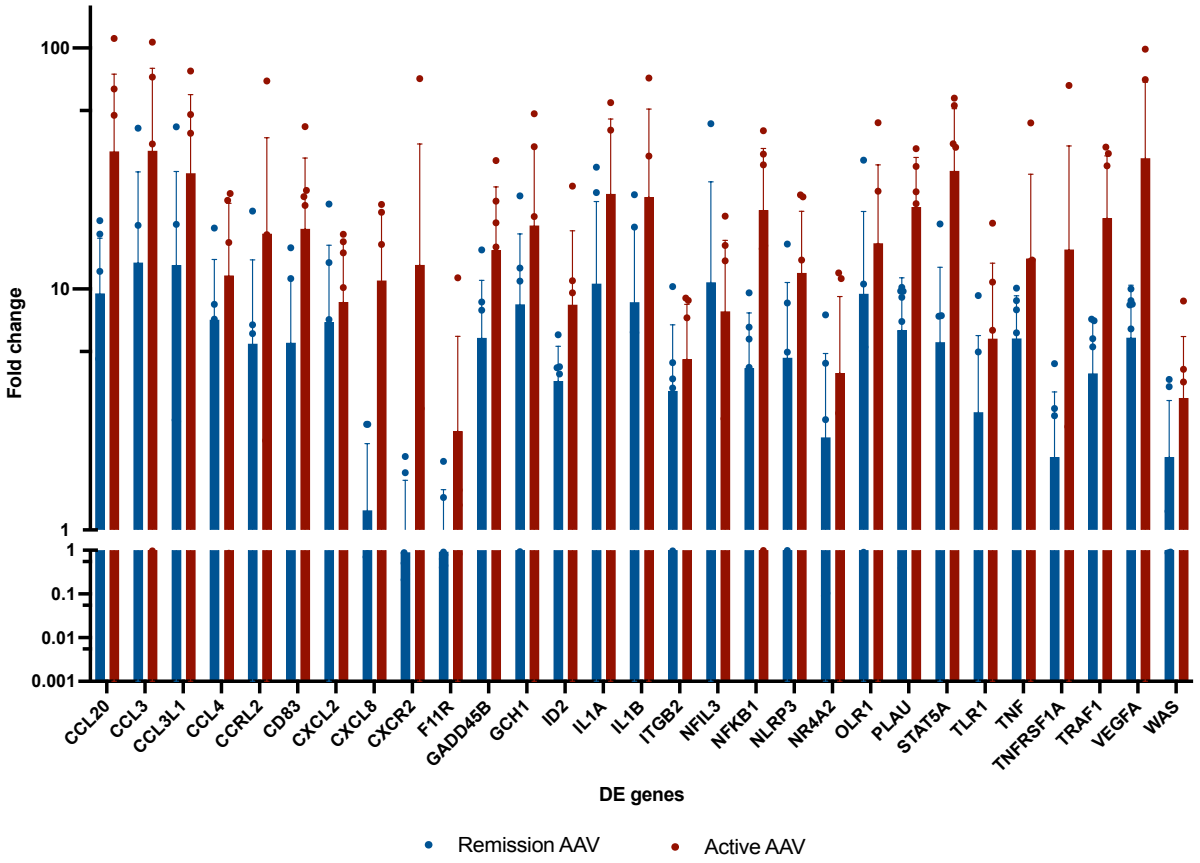


Figure 71. Top DE genes express greatest fold change in aAAV

Neutrophils ($10x10^6$) from untreated HC, rAAV, or aAAV were incubated for 15 minutes to return from their active state, and then 1h with RNAse inhibitor in neutrophil culture media (n=7). Neutrophils were pelleted, and cell-free SN was stored. Cell pellet was lysed in TriZol, homogenised with a 0.3-gauge syringe, and RNA was extracted following Qiagen mini prep. Sample was eluted in TE buffer and cDNA was prepared as 250 ug/ mL. mRNA expression was measured via RT-qPCR. mRNA expression is shown relative to untreated HC; Data are normalised to the housekeeping gene, B2M. Data are shown as mean with SEM, statistical comparison by multiple unpaired t-test, FDR 5%; *p<0.05.

6.7. RNA Sequencing – Age match HC v rAAV v aAAV

Following optimisation of protocols and confirming that I could identify a gene signature of neutrophils from patients with aAAV using RT-PCR, I next carried out poly(A) RNA-seq using untreated neutrophils from patients with aAAV, rAAV and healthy controls.

		Active	**Remission**	**Healthy control**
Characteristic		n=20 (%)	n=10 (%)	n=10
Age	Years (IQR)	58 (42.3-73.9)	72 (44-77)	52(48-63)
Gender	Male	10 (50.0)	4 (40.0)	5 (50.0)
Comorbidities	T2DM Cancer Asthma/COPD CVD HTN	6 (13.0) 1 (2.0) 8 (17.3) 0 13 (28.2)	0 (0) 1 (10.0) 1 (10.0) 1 (10.0) 7 (70.0)	
ANCA specificity	MPO PR3 Negative	22 (37.5) 24 (62.5) 0	4 (40.0) 5 (50.0) 1 (10.0)	
Immunotherapy-induction	Prednisolone/ Methylprednisolone	28 (60.8)	5 (50.0)	
Immunotherapy-maintenance	Prednisolone <5mg Azathioprine Rituximab MMF MTX Nil		6 (60.0) 3 (30.0) 6 (60.0) 0 (0.0) 0 (0.0) 0 (0.0)	
Presentation	First presentation Relapse	38 (82.6) 8 (17.3)		
Haematology/ Biochemistry	CRP (mg/dL) (IQR) Creatinine (µmol/L) (IQR) BVAS (IQR) WCC (x10^9) (IQR) Neutrophil count (x10^9) (IQR)	21 (3.05-180) 176 (67.5-636.8) 15 (8-20) 12 (6.6-16.6) 10 (4.7-13.8)	2.4 (0.5-13.6) 87 (63-239) N/A 8.1 (4.3-13.5) 5.7 (3.0-10.9)	
Organ involvement	Renal ENT Lung Eye Skin Cardiac	37 (80.4) 17 (40.0) 21 (46.0) 6 (13.0) 2 (4.3) 1 (2.0)	1 (10.0) 1(10.0) 1(10.0) N/A 0 1 (10.0)	

Table 28. Characteristics of patients included in RNA-seq
Data are median with IQR. MPO-myeloperoxidase, PR3- Proteinase-3, T2DM- Type 2 diabetes mellitus, CVD- cardiovascular disease, HTN- hypertension, MMF- mycophenolate mofetil, MTX- methotrexate, CRP- C reactive protein, BVAS- Birmingham vasculitis activity score, WCC- white cell count.

6.7.1. Identification of a gene signature comparing aAAV to age matched HC

Comparing the transcriptome of neutrophil from patients with aAAV to healthy controls identified a gene signature of active AAV, with 627 significantly DE genes (**Fig 72A**, **Table 29**). The top 20 upregulated and top 10 downregulated significant DE genes in aAAV compared to HC are presented in Table 29 (healthy control v aAAV). Pathway analysis identified enrichment for genes related to positive regulation of T-helper 1 type immune response, response to bacterium, and defence response were over-represented on gene ontology analysis (**Fig 72B**). Analysis of cellular processes identified over-representation of DEG related to dysregulation of neutrophil specific granules and the condensed chromosome kinetochore, which potentially may link with the effect found of ANCA stimulated increased actin polymerisation (565). There was also DE of many genes which may play a specific role in AAV including *CCL20*, *CD177*, *ELANE*, *CD163*, *MYO1B*, *ANXA1*, OLFM4, *MMP8*, *PRTN3*, *ADAM22*, *CCL3*, *C5*, *MYO10*, *IL18*, *C1R*, *CD93*, and *C4A*. These genes are involved in processes such as apoptosis, the complement pathway, cell protrusion formation, senescence, degranulation, and cell adhesion. The top 20 upregulated and top 10 downregulated significant DE genes are presented in **Table 29** (healthy control v aAAV).

Gene name	P value	FDR	Log2 FC
Upregulated in aAAV			
GRB10	1.21E-15	1.78E-11	3.75462873
OLAH	6.80E-12	4.97E-08	4.85060803
$CORO_2A$	2.18E-10	8.33E-07	1.91500897
SERINC2	2.28E-10	8.33E-07	2.21881467
MAP2K6	2.02E-09	5.92E-06	1.96093767
VWA8	4.56E-09	7.46E-06	3.17679634
DAAM2	4.43E-09	7.46E-06	3.96398633
ZNF608	4.69E-09	7.46E-06	3.37406634
UBE2F	5.02E-09	7.46E-06	1.14869531
FAM183DP	5.10E-09	7.46E-06	4.91261646
CITED4	1.54E-08	2.05E-05	2.41255689
CD177	1.71E-08	2.08E-05	3.74609567
CD163	2.27E-08	2.56E-05	3.94221776
RRAGC	2.67E-08	2.79E-05	1.31735689
TSPAN14	5.00E-08	4.57E-05	1.16572613
FKBP5	6.78E-08	5.83E-05	3.15290936
SNHG16	7.77E-08	6.29E-05	1.13459735
AC020636.1	8.17E-08	6.29E-05	2.798254
TMIGD3	1.07E-07	7.54E-05	3.23220212
SORT1	1.08E-07	7.54E-05	1.63685128
Downregulated in aAAV			
ARRDC4	7.50E-07	0.00035413	-2.2967119
ERI1	1.98E-06	0.00067427	-1.2681231
TSPAN13	5.80E-06	0.00133328	-2.0203268
HLA-DRB6	5.80E-06	0.00133328	-3.7117105
IL18BP	6.51E-06	0.00141263	-1.3852522
PLD2	8.20E-06	0.00168	-1.4104315
SDC2	1.28E-05	0.00217587	-1.8523427
KRT17	2.74E-05	0.00348992	-2.3136877
IL1RL2	3.04E-05	0.00370936	-2.0402206
SIGLEC12	3.39E-05	0.00393933	-1.8475957

Table 29. Top upregulated and downregulated significant DE in HC v aAAV

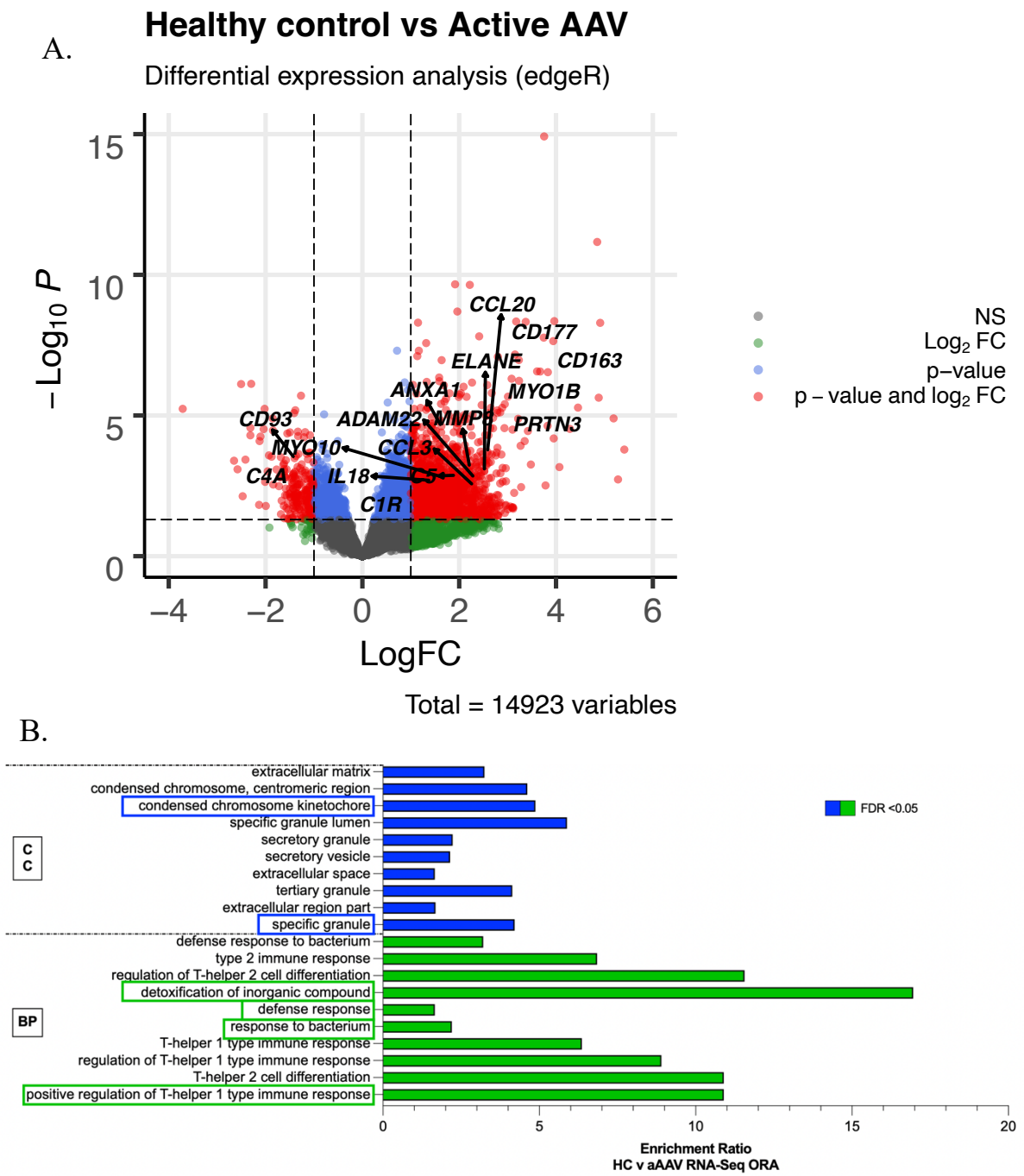


Figure 72. Transcriptomic analysis of healthy control versus active AAV
(A) Volcano plot of 21% O_2 healthy control versus active AAV. One dot signifies each gene. Red dots represent genes meeting p-value and Log_2FC, blue dots represent genes meeting p-value alone, green dots represent genes meeting p-value (<0.05) and Log_2FC (<0.05), blue data points represent genes meeting p-value alone, green data points represent genes meeting Log_2FC alone, and grey data points represent nonsignificant genes. (B) Gene ontology classification of 21% O_2 healthy control v active AAV DEGs (Log_2FC <0.05, p<0.05). ORA was performed on enrichment of cellular component and molecular function pathway dysregulation.

6.7.2. Identification of a gene signature comparing rAAV to age match HC

Comparing the transcriptome of neutrophils from patients with rAAV to healthy controls identified a gene signature of remission AAV, with 7,182 significantly DE genes (**Fig 73A**, **Table 30**). The top 20 upregulated and top 10 downregulated significant DE genes are presented in **Table 30** (healthy control v rAAV). DEGs (**Fig 73B**) related to positive regulation of cell adhesion, cell-cell signalling, cytoskeleton, and cell projection were over-represented on gene ontology analysis. There was also DE of many genes which may play a specific role in AAV including *C3*, *TRAF1*, *VEGFA*, *F3*, *CCL3*, *CCL20*, *RHOU*, *CD48*, *NFKB1*, *RAB21*, *TRAF3*, *ICAM-1*, *SRC*, *CD163*, *TNFRSF12A*, *MMP8*, *ELANE*, and *PRTN3*. These genes are involved in processes such as inflammation, coagulation, cell protrusion formation, autophagy, neutrophil-endothelial adhesion, and immune cell activation.

Gene name	P value	FDR	Log_2FC
Upregulated in rAAV			
NCR3LG1	2.72E-58	4.84E-54	6.86807895
CLIC4	9.12E-53	8.13E-49	5.37591376
VILL	2.39E-51	1.42E-47	5.41545698
C1orf61	3.96E-51	1.76E-47	6.60298846
TRIP10	5.75E-51	2.05E-47	4.72150114
ZC3H12C	9.21E-51	2.74E-47	6.81049832
TPRA1	1.81E-49	4.61E-46	4.78197833
AC124798.1	4.55E-49	1.01E-45	6.89843491
SH2D3A	5.24E-46	1.04E-42	4.52002365
SLC11A2	1.06E-45	1.89E-42	5.79930061
RALGDS	7.22E-45	1.17E-41	5.23792021
MFSD2A	5.21E-43	7.73E-40	5.6795056
AC048341.1	1.41E-42	1.93E-39	2.94171795
AC010980.1	1.57E-41	2.00E-38	7.26745473
MRNIP	2.47E-40	2.94E-37	3.5121808
LINC01093	7.00E-40	7.80E-37	4.27378848
CCRL2	9.85E-40	1.03E-36	4.32772592
HCAR1	1.21E-39	1.19E-36	4.84661546
SLC43A3	1.87E-39	1.75E-36	4.82460752
C3	3.74E-39	3.33E-36	5.03955265
Downregulated in rAAV			
IGHV3-23	9.05E-25	2.09E-22	-8.9898544
NCBP3	6.21E-24	1.30E-21	-1.171362
TOPBP1	8.35E-23	1.43E-20	-1.4906562
PPM1G	2.29E-22	3.79E-20	-1.0819263
LINC00957	2.46E-22	3.98E-20	-1.8122961
FAM214B	1.06E-20	1.43E-18	-2.171427
MS4A1	1.94E-20	2.51E-18	-6.3227291
CD79A	3.19E-20	3.95E-18	-5.3410869
RASAL3	3.93E-20	4.80E-18	-1.2993186
CAMKK1	8.46E-20	9.78E-18	-1.9184505

Table 30. Top upregulated and downregulated significant DE in HC v rAAV

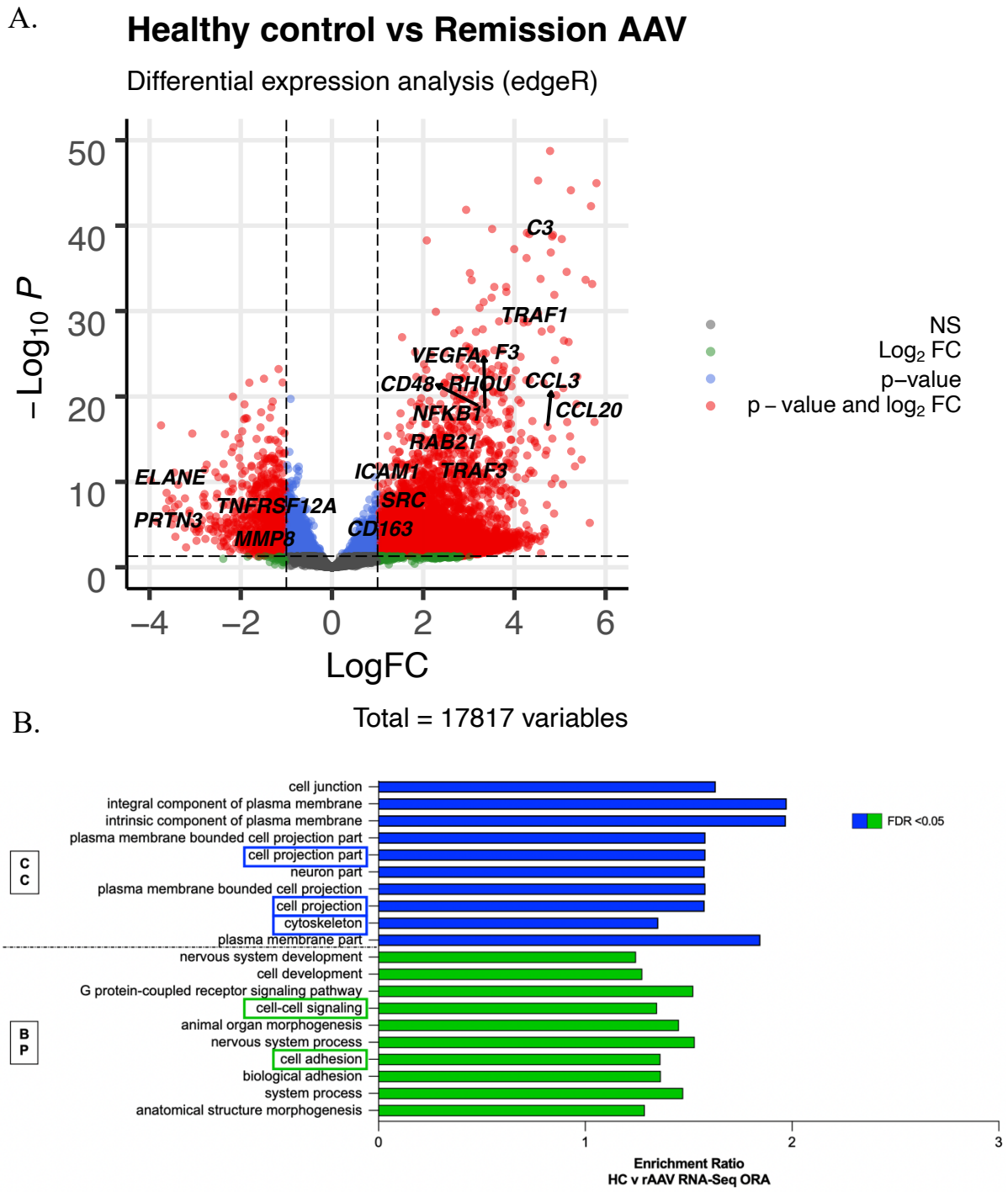


Figure 73. Transcriptomic analysis healthy control versus remission AAV
(A) Volcano plot of 21% O_2 healthy control versus remission AAV. One dot signifies each gene. Red dots represent genes meeting p-value (<0.05) and Log_2FC (<0.05), blue data points represent genes meeting p-value alone, green data points represent genes meeting Log_2FC alone, and grey data points represent nonsignificant genes. Downregulated genes are presented on the left panel from -5 to 0, and upregulated genes are presented on the right panel from 0-10. ns=nonsignificant, $p<0.05$; log_2 FC signifies mean gene expression level of individual genes. (B) Gene ontology classification of 21% O_2 healthy control v remission AAV DEGs (Log_2FC <0.05, $p<0.05$). ORA was performed on enrichment of cellular component and molecular function pathway dysregulation.

6.7.3. Identification of a gene signature comparing aAAV to rAAV

Comparing the transcriptome of neutrophil from patients with aAAV to patients with rAAV identified a gene signature of active AAV, with 2,356 significantly DE genes (**Fig 74A**, **Table 31**). The top 20 upregulated and top 10 downregulated significant DE genes are presented in **Table 31** (rAAV v aAAV). DEGs (**Fig 74B**) related to positive regulation of immune response, response to bacterium, cell activation, and leucocyte activation were over-represented on gene ontology analysis. Analysis of cellular processes identified over-representation of DEG related to dysregulation of neutrophil whole membrane and plasma membrane part, which potentially may also link with the effect found altered neutrophil mechanophenotype in section 5.9.1. There was also DE of many genes which may play a specific role in AAV including *MPO*, *PRTN3*, *MMP8*, *TNFRSF12A*, *CD163*, *ANXA1*, *ERG*, *CCL20*, *CCL3*, *SRC*, *NFKB1*, *VEGFA*, *TRAF3*, *RAB21*, and *RHOU*. These genes are involved in angiogenesis, cell adhesion, chemotaxis, inflammation, degranulation, and immune response.

Gene name	P value	FDR	Log_2FC
Upregulated in aAAV			
MPO	8.56E-19	1.84E-15	5.44517171
RSBN1	3.72E-18	7.12E-15	2.2048865
ELANE	1.28E-17	2.21E-14	6.12318697
IGHG1	2.22E-17	3.47E-14	7.43859116
IGHV3-23	3.20E-17	4.59E-14	8.60925119
IGHGP	2.70E-16	2.45E-13	8.37923888
IGHA1	3.08E-16	2.66E-13	7.91809401
DEFA4	4.00E-16	3.13E-13	6.16098128
ZNF784	6.57E-16	4.72E-13	2.53831126
NKIRAS1	1.36E-12	2.49E-10	-1.9536584
IGHM	5.31E-15	3.13E-12	6.46995447
IGKV1-5	5.45E-15	3.13E-12	8.36805861
IGLC2	1.00E-14	5.23E-12	7.00397412
IGLV1-40	1.92E-14	8.71E-12	7.95568312
CREB5	2.11E-14	9.09E-12	1.59190669
IGKV3-15	2.07E-14	9.09E-12	7.8616977
DRAM1	1.04E-11	1.41E-09	-1.8236157
IGHD	3.78E-14	1.51E-11	6.554752
IGLC3	4.01E-14	1.52E-11	6.83948713
IGKC	6.12E-14	2.07E-11	7.23058923
Downregulated in aAAV			
AGAP3	2.76E-24	4.75E-20	-4.3051453
AC098613.1	1.04E-22	8.95E-19	-3.7568863
LSS	8.81E-22	5.06E-18	-3.851687
TPRA1	3.23E-21	1.39E-17	-3.5352357
TCFL5	1.52E-19	5.23E-16	-2.6773038
UBE2E1	1.97E-19	5.65E-16	-2.7845786
ZC3H12C	2.36E-19	5.81E-16	-5.3769726
ADORA2A	4.06E-17	5.38E-14	-3.0489344
DENND4A	4.55E-17	5.60E-14	-2.3116373
DUSP16	5.58E-17	6.40E-14	-3.3688795

Table 31. Top upregulated and downregulated significant DE in rAAV v aAAV

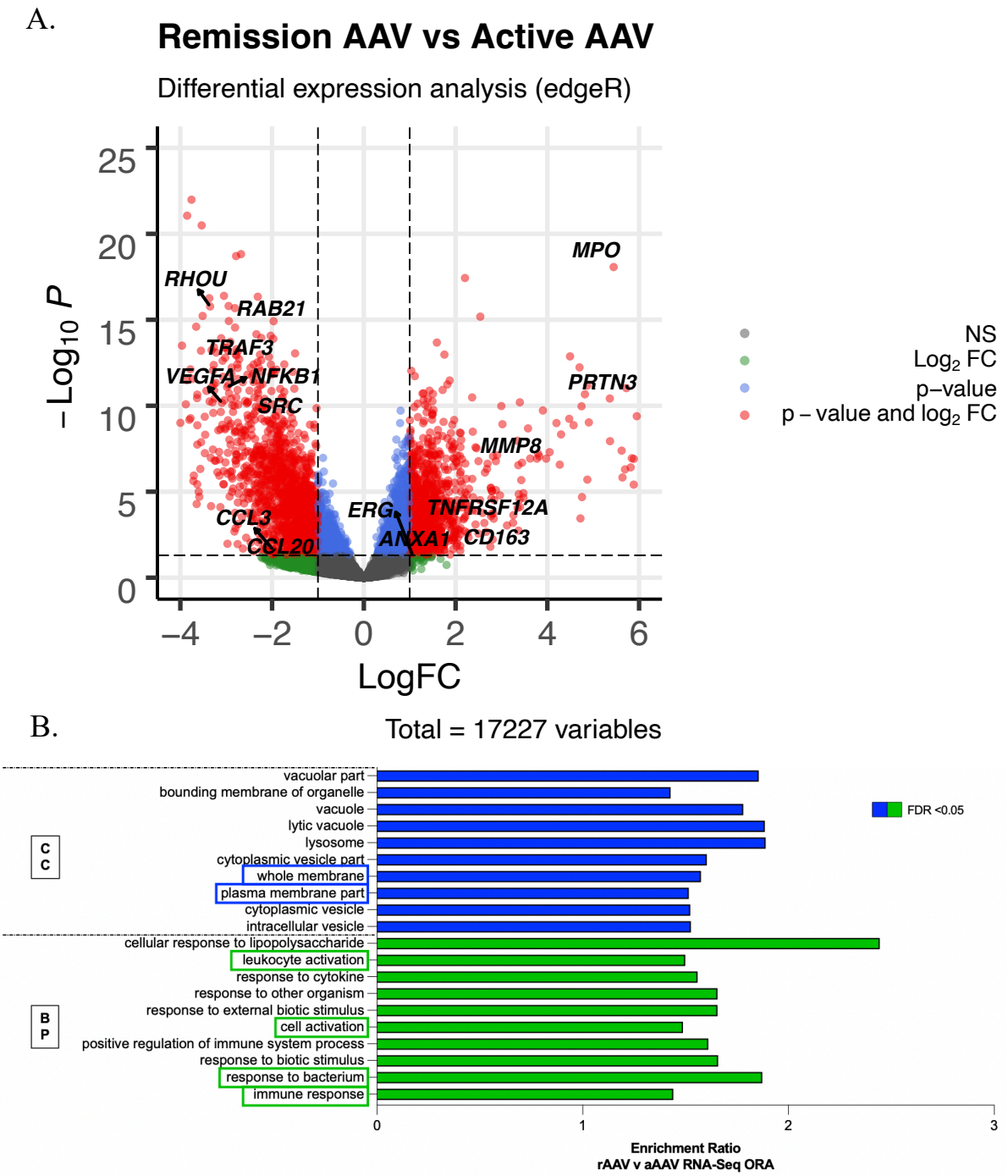


Figure 74. Transcriptomic analysis of remission AAV versus active AAV
(A) Volcano plot of 21% O_2 remission AAV versus active AAV. One dot signifies each gene. Red dots represent genes meeting p-value (<0.05) and Log_2FC (<0.05), blue data points represent genes meeting p-value alone, green data points represent genes meeting Log_2FC alone, and grey data points represent nonsignificant genes. Downregulated genes are presented on the left panel from -5 to 0, and upregulated genes are presented on the right panel from 0-10. ns=nonsignificant, p<0.05; log_2 FC signifies mean gene expression level of individual genes. (B) Gene ontology classification of 21% O_2 untreated v MPO-ANCA DEGs (Log_2FC <0.05, p<0.05). ORA was performed on enrichment of cellular component and molecular function pathway dysregulation.

6.8. Discussion

The main objectives of this chapter were to phenotype neutrophils from patients with aAAV using RT-DC and investigate how neutrophil function and ANCA IgG responses differ from those in neutrophils from healthy volunteers. aAAV whole blood neutrophils exhibited a significant decrease in deformability which correlates with disease activity score, an increase in *ex vivo* cytokine and adhesion molecule (IL-8, ICAM-1, and VCAM-1) secretion without additional stimuli, and increased actin polymerisation, particularly once stimulated with pathogenic ANCA and/or exposed to decreased oxygen tensions.

Mechanophenotyping using RT-DC identified a significant decrease in neutrophil deformability in whole blood samples from patients with aAAV compared to both healthy controls and AAV patients in remission. It is known that stiffer, less deformable neutrophils are more likely to be trapped in the microvasculature (566). In AAV, this phenotype of increased stiffness may lead to retention of neutrophils in microvascular beds such as the lung or the kidney and thus perpetuate neutrophil-endothelium interaction and exacerbate endothelial injury. There was a significant negative correlation between a deformability and disease severity as measured by the BVAS activity score. Therefore, patients with more severe aAAV have stiffer cells. Previous studies have shown glucocorticoids can mediate granulocyte cytoskeleton remodelling and softening (43,567). However, I did not identify any differences between patients with aAAV in my study who had received treatment with steroids (prednisolone) prior to sampling and those who were treatment naïve. These previous studies using HC protocolised timing of sampling after steroid treatment and had a difference in steroid doses. An equivalent of 75 mg of prednisolone was used in Fay et. al, which was greater than the dosage prescribed to most patients in this study, as in this single centre a low steroid approach is used (43). There were also variable time points for sampling post steroid dose.

Additionally, the effect mediated by aAAV may outweigh any potential effect of steroid treatment that was seen when healthy volunteers are treated with steroid.

One potential explanation for decreased neutrophil deformability in patients with aAAV is a direct effect of ANCA on cells *in vivo*, particularly as I identified an effect of ANCA stimulation in vitro on neutrophil biomechanical phenotype. However, I did not identify any difference in deformability between patients with MPO-AAV and PR3-AAV (in contrast to later *in vitro* experiments investigating actin remodelling), and there was no correlation with ANCA titre. This suggests that other factors in vivo, such as the transit of neutrophils through inflamed vasculature or exposure to additional inflammatory mediators, may play a role. Alternatively, the phenotype of neutrophils in patients with AAV may be inherently different. Another possibility regarding the lack of correlation with ANCA suggests that it is the neutrophil response, such as the cell stiffness, that is important for regulating fundamental cell behaviour; therefore, patients whose neutrophils are "more reactive", once activated by ANCA, may develop more severe disease. This association between neutrophil stiffness has also been seen in other inflammatory conditions, although using less sensitive techniques than RT-DC. Using micropipette aspiration, data from Linderkamp et. al suggested neutrophil stiffness correlated with disease severity in septicaemia (568).

There was an association between decreased neutrophil deformability and lung involvement in patients with aAAV. Patients with lung disease may have lower cell deformability due to a failure of the de-priming mechanism (38) in the lung in disease such as has been shown in ARDS. Neutrophils travelling slower within the lungs is a consequence of neutrophil trapping within the lung (46,232) and this trapping within the pulmonary capillaries could be a result of activated neutrophil's decreased deformability due to actin reorganisation (45,229,569).

Worthen et al. identified fMLP stimulated neutrophils, which are larger in size (8 μm) than pulmonary capillaries (5 μm), have decreased deformability, increased actin assembly, and retention in the lung. Interestingly, cytochalasin D also inhibited these effects, suggesting that targeting the actin cytoskeleton in neutrophils with increased stiffness may be of therapeutic potential (569). In AAV, therefore similar mechanisms may occur, with stiffer neutrophils retained in the lungs, exacerbating pulmonary vasculitis. Decreased deformability has also previously been identified in neutrophils from patients with advanced chronic kidney disease (570). and there was a trend of decreased neutrophil deformability (p=0.0710) shown in patients with aAAV kidney involvement in this thesis. In my study, there was a trend to patients with renal involvement having lower neutrophil deformability, although the number of patients without renal disease was small. I did not identify a difference in neutrophil deformability between patients requiring renal replacement therapy and those not, and there was no correlation between eGFR and neutrophil deformability. A key difference between my study and previous results in CKD is that most patients with AAV have acute derangement of their renal function, whereas patients in the published study had been receiving haemodialysis for at least 3 months. This suggests that in CKD, altered deformability may be due to a prolonged effect of e.g. uraemia on the bone marrow.

Monocytes are of a much lower percentage in whole blood, therefore obtaining an adequate number of monocytes for analysis during a whole blood RT-DC run was challenging. Potentially due to patients being on immunotherapies, they may have depleted monocyte populations, again making it challenging to record enough monocyte events for analysis. Therefore, it was only possible to analyse monocyte biophysical properties in a subgroup of the patients as a result. However, a trend to increased cell stiffness was shown in aAAV monocytes in comparison to rAAV or age matched HC monocytes, suggesting a myeloid

phenotype may be present in aAAV. In contrast to my findings in AAV, larger, more deformable neutrophils have been identified in patients with acute COVID-19 (502), and larger, more deformable monocytes were found in patients with SSc (504). No biomechanical difference in lymphocytes or monocytes were found in patients with SLE in comparison to HC, but a small sample set data showed increased deformability in active SLE neutrophils in comparison to HC (218). Therefore, my results suggest that a phenotype of decreased deformability may be specific to AAV, and also identifies how activated neutrophils may present with a different mechanophenotype dependent upon disease processes (218,502).

Prior to any additional stimulus, there were trending differences in actin polymerisation in aAAV neutrophils in comparison to HC neutrophils, and actin capping in aAAV neutrophils upon visual inspection, suggesting a different phenotype of aAAV neutrophils at baseline. As shown in Chapter 3, ANCA stimulation of HC neutrophils promotes increased actin polymerisation, and this same effect was also seen in neutrophils from patients with aAAV. Due to unplanned timing of active patients, access to the hypoxia chamber was not always possible so fewer replicates were performed in low oxygen tension compared to 21% O_2 which may impact on the interpretability of my results. However, I consistently identified that while 5% O_2 decreased the effects of ANCA stimulation on actin cytoskeleton seen at 21% O_2 in HC neutrophils, neutrophils from patients with aAAV still exhibited actin polymerisation in response to ANCA stimulation at 5% O_2. In physiological normoxia, the quiescent response seen in HC neutrophils is lost, and aAAV neutrophil still respond to ANCA. This may suggest that AAV neutrophils may have more capacity to cause vascular damage. 1% O_2 enhances HC neutrophil responses, therefore potentially when hypoxia occurs in inflammation, this perpetuates the damaging phenotype of all neutrophils, whether or not they have encountered ANCA.

The role of hypoxia and HIF role in the actin cytoskeleton potentially involves multiple signalling pathways activated in different tissues by hypoxia, but consistent evidence has shown Rho GTPases are a main contributor in this overall effect (571–574). In other studies, the mechanism of hypoxia increasing actin polymerisation is shown to be dependent upon the environment and degree of hypoxia. In keeping with this, hypoxia has shown to increase cellular protrusion formation by increasing actin polymerisation and therefore cell motility (575,576). This relationship between aAAV neutrophils and actin polymerisation is of interest as patients with actin cytoskeletal or remodelling defects are more prone to autoinflammatory disease, as displayed in patients with WAS, a primary immunodeficiency genetic disorder characterised by thrombocytopaenia (Volpi 2016). Additionally, although Rac and RhoA were found to be upregulated in COPD, proteomic analysis from bronchoalveolar lavage cells from patients with COPD displayed dysregulation of FcyR-mediated phagocytosis; this correlated with decreased Arp 2/3 complex levels and dysregulated actin cytoskeletal processes (577). My results from RNASeq have identified differential expression of some of these pathways, suggesting that there may be transcriptional differences in genes which regulate the actin cytoskeleton in aAAV. Genes related to Cdc42 (*CDC42EP3, CDC42BG30*), Rho GTP binding family proteins (*RHOB, RHOC*), and Rho GTPases (*RHOV, RHOU, RND1*) were differentially expressed in aAAV neutrophils compared to rAAV neutrophils. *HIF1a* was also differentially expressed.

I also identified increased IL-8, VCAM-1, and ICAM-1 secretion from aAAV untreated neutrophils in comparison to rAAV and age matched HC. Increased IL-8 release was also shown in patients with rAAV suggesting that even though these patients are in remission, they still have some increased proinflammatory responses. This result coupled with the effect shown when rAAV supernatant is co-cultured with gEC, where there is a small increase in cytokine

release compared to when gEC are cultured with HC neutrophil SN, suggests these cells are slightly inflammatory and potentially these patients are still experiencing some neutrophil induced EC injury. aAAV neutrophils may display a primed phenotype *ex vivo* due to being more prone to activation *in vivo*, explaining their increase in size, cytokine production, and response to secondary stimuli, therefore effecting their programmed mechanisms like actin polymerisation. Although, there is no secondary stimulus in the untreated aAAV neutrophils, which potentially suggesting there may be a full activation signal shown in these cells. A similar phenotype of gEC treated with aAAV neutrophil SN was displayed in comparison to gEC treated with ANCA IgG stimulated HC neutrophil SN at 1% and 5% O_2 with IL-8, VCAM-1, and ICAM-1 secretion levels at both time points. This showed that secretion products from untreated aAAV neutrophils may exert similar effects on EC as do HC neutrophils stimulated with MPO-ANCA IgG, indicating that aAAV cells display an activated phenotype, without additional stimulation, which can alter EC behaviour even following *ex vivo* isolation.

Results from my RNA sequencing identified the main gene signature of aAAV and rAAV was dysregulation in cell adhesion, cytoskeleton, chromatin, and granule genes in comparison to HC. I identified up-regulation of genes related to the actin cytoskeleton, which may explain the differences I saw in aAAV patients prior to additional stimulation.

Most previously published studies of RNA-Seq data in AAV have focussed on whole blood or PBMC (336,580). There are a small number of studies which have used isolated neutrophil transcriptional analysis. Yamaoka et al compared 26 patients with AAV to 28 HC and identified up-regulation of a NET signature in neutrophils isolated from patients with AAV in comparison to HCs, in addition to IL-6 signalling, which aligned with my results identifying

up-regulation of genes involved in NETosis. However this study has significant differences from my own; the majority (90%) of patients had a clinical diagnosis of GPA, any patient prescribed greater than 10mg of prednisolone was excluded, and the majority of patients were in remission (579). Interestingly, I also identified significant transcriptional differences between neutrophils from patients with rAAV and HC, including up-regulation of many genes related to NETosis (*CYBB, IL1B, IL6, PTAFR, TLR2, HPSE*) suggesting there may be fundamental differences in neutrophil phenotype in AAV which persists in remission and despite immunosuppression treatment. This signature of up-regulation of NETosis genes in AAV has also been identified in the kidney using pooled analysis of five datasets with sequencing data from human kidney tissue. Jones et. al also used sequencing of isolated neutrophils; a key finding from this study was up-regulation of auto-antigen genes in patients with aAAV (589). This was also a feature of my sequencing results, with significant up-regulation of *MPO* and *PRTN3* in aAAV compared to rAAV. In this study, expression of MPO and PRTN3 correlated with ANCA induced activation (ROS production), and it would be interesting to investigate if a similar hypothesis is true for ANCA induced changes in actin cytoskeleton or EC injury.

Using whole blood transcriptional analysis, Banos et. al, identified neutrophil degranulation and IFN signalling were the top dysregulated pathways found in GPA and MPA patients, which also was similar to signatures found in aAAV neutrophils in my study, which identified upregulation of numerous granule protein transcripts including those related to primary granules (*MPO, ELANE, CTSG, PRTN3, AZU1, PRSS57, ARG1* were all significantly upregulated in aAAV compared to rAAV) and secondary granules (*LTF, CAMP, MMP8, CRISP3* were all significantly upregulated in aAAV compared to rAAV), I did not identify a particular interferon related signature in my study, although there were several differences

which may explain this. In particular, the previous study performed whole blood mRNA sequencing as opposed to isolated neutrophils suggesting interferon signatures may be more relevant to other leucocyte populations. There were also significant differences in patient clinical phenotype, the majority of patients had lung involvement (90%) and had BVAS at a maximum of 8.25, whereas patients from my cohort had more severe disease with BVAS up to 27 (580). A granulocyte signature related to disease activity in Grayson et al was determined in deep whole blood large RNA-seq, which also displayed bacterial defence, myeloid differentiation, and neutrophil activation as upregulated pathways, as also found in my preliminary sequencing results. Yet, due to this being measured in whole blood, this signature may not be specific to neutrophils in AAV (336). Taken together, my current sequencing results confirm the reproducibility, and specificity of signatures first found in whole blood panels (336,580) and isolated neutrophil sequencing (579) in AAV.

Overall, aAAV neutrophils display a different phenotype than rAAV and age match HC, potentially reflecting increased priming and/or activation. This is displayed through mechanophenotyping, neutrophil programmed processes, and response to different oxygen tensions, and correlates with clinical parameters in patients with AAV.

Key findings:

1. Neutrophils from patients with aAAV have decreased deformability that correlates with disease activity, and potentially pulmonary/renal involvement
2. ANCA stimulation induces greater neutrophil actin polymerisation in aAAV than HC
3. Physiological 5% O_2 appears to reduce ANCA actin responses in HC neutrophils but not aAAV, whereas pathological 1% O_2 promotes ANCA responses

4. aAAV neutrophils have increased cytokine and adhesion molecule production at baseline in comparison to HC neutrophils
5. Neutrophils from patients with aAAV display a distinct gene signature in comparison to rAAV and HC with implications for the actin cytoskeleton, NETosis and degranulation

7. Chapter 7 – Concluding remarks

7.1. Discussion and Future work

In this project I aimed to define a biomechanical phenotype of neutrophils in AAV, in response to ANCA IgG stimulation, and to investigate the role hypoxia plays in this and in other functional neutrophil readouts. Using the novel technique of RT-DC, I studied neutrophil deformability using AAV patient samples and in response to *in vitro* stimulation. I defined neutrophil actin cytoskeletal changes to identify how this relates to cell stiffness and used a range of neutrophil functional readouts including cytokine production, NETosis, and EC injury to investigate how hypoxia may modulate ANCA induced neutrophil responses.

My key findings include:

1. Neutrophils from patients with active AAV have altered biophysical phenotype
2. ANCA stimulation alters HC and AAV neutrophil actin polymerisation
3. Oxygen tension alters actin polymerisation and NET formation
4. Hypoxia and ANCA increase neutrophil migration though endothelial cell monolayers
5. Cell protrusion formation is transcriptionally dysregulated in AAV neutrophils

7.1.1. Active AAV neutrophils have altered biophysical phenotype

One of the goals of this thesis was to determine whether there is an individual phenotype of neutrophils specific to patients with AAV, and how this may contribute to neutrophil retention in the microvasculature, promoting neutrophil-mediated tissue injury in the disease state. To measure this, untreated HC neutrophils were mechanophenotyped in comparison to ANCA stimulated HC neutrophils or AAV neutrophils. A significant decrease in deformability was exhibited by aAAV neutrophils without any priming or secondary stimulus (Chapter 6). Thus, the focus of this work was based upon the finding of increased stiffness in neutrophils from patients with aAAV.

There is evidence that neutrophil priming can become dysregulated in inflammatory disease in autoimmunity (581) and idiopathic inflammatory myopathies (582). Accumulation of primed neutrophils in the pulmonary vessels hinders neutrophil transport through blood vessels, resulting in inflammation and increased vascular damage (38,583). While this mechanism has so far only been demonstrated during cell trafficking through the lung microvasculature *in vivo* (584), similar mechanism may also be relevant in the glomerular capillary bed. These capillary beds vary in size as the pulmonary capillary bed has the largest surface area of any capillary bed in the body at 125 m^2, in comparison to the glomerular capillary bed which is only 0.6 m^2 (585,586). This means that an *in vivo* retention signal may be more difficult to detect in the kidney. In addition to the lung having to filter the blood, the kidney only receives a portion of this blood, so a lung signal may be more obvious or occur sooner. In keeping with neutrophil microvascular trapping, my results indicated that those patients with the stiffest cells were more likely to have pulmonary or renal involvement.

I propose RT-DC would aid phenotyping of whole blood samples in experimental medicine studies. RT-DC can be used for mechanophenotyping isolated cells; however, isolation techniques may alter their biomechanics due to activating the cells, and readouts are not as robust in comparison to whole blood measurements. For other experiments, using isolated cells was unavoidable, but in terms of RT-DC, the results are less reliable and the alternative of using whole blood is preferred as a result. Therefore, whole blood mechanophenotyping is a more accurate method due to being more physiologically relevant and cells are less manipulated.

7.1.2. ANCA stimulation leads to altered biophysical phenotype and changes in actin, which associates with EC injury

To investigate the effect of ANCA IgG on neutrophil deformability, untreated HC neutrophils were mechanophenotyped in comparison to ANCA IgG stimulated HC neutrophils. ANCA IgG stimulation in neutrophils induced decreased deformability significantly in whole blood and in isolated cells (Chapter 3), similar to results in aAAV neutrophils. In keeping with decreased deformability, both HC and aAAV neutrophils displayed increased actin polymerisation following stimulation with ANCA IgG. I identified a greater increase in aAAV neutrophils suggesting they are more responsive to the effect of ANCA IgG stimulation. The effect of increased ANCA induced actin polymerisation and protrusion formation was able to be inhibited by the cytochalasins, either at 1% or 21% O_2, suggesting there was a reduction in the F-actin polymerisation effect as a result of cytochalasin treatment. Although further replicates are required, the cytochalasins did not enhance ANCA induced decreased deformability in HC neutrophils either. This was in contrast to a previous study using HL-60 cells, in which cytochalasin D increased HL-60 deformability in a dose dependent manner (496). Therefore, I expected to see an increase in deformability was expected when ANCA stimulated neutrophils were treated with the cytochalasins, but this was not seen. Technical aspects, such a timing of stimulation, or differences between primary cells and cell line responses, could potentially explain differences between my study in neutrophils and the previous one using HL60 cells. The seeming divergence of my results between actin cytoskeletal changes and deformability could be due to comparing static versus flow conditions. Alternatively, there may also be other factors which are influencing cell deformability following ANCA stimulation such as cell cytoplasm osmolality. Changes in neutrophil cytoskeletal integrity contributes to alteration in neutrophil properties, such as actin cytoskeletal rearrangement contributing to NE release, ROS generation, and NET formation (108,553). Although the cytochalasins and other inhibitors I used had no impact on ANCA

induced cytokine release, it may be that they would be more effective in inhibiting other functional readouts such as NETosis.

Taken together, I suggest neutrophil biophysical properties, including area, deformation, elasticity, are altered because of increased actin polymerisation present in aAAV neutrophil phenotype and promoted by ANCA stimulation thereafter. My data suggests that altered neutrophil phenotype from ANCA IgG and/or additional stimuli in aAAV neutrophils promotes the alteration of neutrophil programmed mechanisms, in turn promoting an amplified inflammatory disease state in patients with aAAV.

7.1.3. Oxygen tension alters NET formation and actin polymerisation

Following stimulation of neutrophils with ANCA IgG, increased proinflammatory (IL-8) cytokine release and NET formation are well defined functional readouts. While decreased oxygen tension (5% or 1% O_2) did not alter IL-8 secretion in isolated neutrophils, 5% and 1% O_2 did alter NET formation.

Increased NET formation and actin polymerisation were displayed in neutrophils stimulated with ANCA at 21% and 1% O_2, but both functions were profoundly diminished at 5% O_2 despite ANCA treatment. Furthermore, untreated neutrophils displayed increased deformation in whole blood at 5% O_2, likely reflecting these differences in actin polymerisation, whereas neutrophil deformability was comparable at 21% and 1% O_2. Whilst this difference in neutrophil phenotype observed for several functional parameters measured at 5% O_2 was unexpected, it indicates that oxygen tension alone alters neutrophil homeostasis. Given that the pathogenic mechanism of NETosis (which is promoted by ANCA at other oxygen tensions) could in fact be diminished due to incubation at 5% O_2, these findings suggest that 5% O_2

(representative of normal venous oxygen tension) exerts a "quiescent" homeostatic effect. aAAV neutrophils were still displaying an active phenotype at 5% O_2, therefore an additional factor may be regulating this effect that cannot be reverted by oxygen homeostasis. While I anticipated changes in oxygen tension would alter neutrophil function and mechanisms, I had not predicted to see such changes at 5% O_2, in comparison to other oxygen tensions measured. Neutrophils are not exposed to 21% O_2 physiologically and it likely alters their responses to do so. 21% O_2 may potentially increase cell stress, therefore explaining why neutrophils may be more likely to have a pathogenic reaction in this oxygen tension. Additionally, I am curious to continue investigating this homeostatic difference at 5% O_2 and the mechanisms by which this alters neutrophil responses and effector mechanisms as a result.

Overall, my data supports the importance of oxygen tension in modulating cells programmed mechanisms, behaviours, and interactions within their physiological environment to measure accurate readouts in experiments. Now that neutrophil phenotype has been further characterised mechanically and functionally under hypoxia, and in the context of ANCA, more representative *ex vivo* modelling of what occurs *in vivo* may produce more accurate results. Due to limitations of measuring neutrophils *ex vivo*, such as their being terminally differentiated and a shortened life span, determining their optimal environment for responses *ex vivo* is essential for measuring their roles in health and disease models, particularly AAV. I suggest that there needs to be greater consideration of the impact of oxygen tension in *in vitro* studies which are carried out to model an *in vivo* environment. As I have shown that more physiological oxygen tensions can alter neutrophil responses, it may be important to perform cell isolations under physiological oxygen tensions to eliminate exposure to supra-physiological oxygen tensions, which may alter subsequent responses to other stimuli.

7.1.4. Hypoxia and ANCA alters neutrophil TEM

I identified that oxygen tension alters neutrophil biomechanics, NET production, and actin polymerisation in neutrophils alone, and in the context of ANCA stimulation. Increased NET production, and actin polymerisation were displayed in neutrophils incubated at 1% O_2 in comparison to 21% O_2, and an additional enhancement of these effects were shown once neutrophils were stimulated with ANCA. These results display collectively how hypoxia and ANCA can synergistically alter neutrophil mechanisms involved in pathogenic defence, motility, and cytoskeletal rearrangement.

Considering the structural and locomotive effects of neutrophils are altered by hypoxia and ANCA, I then wanted to also investigate how this influenced cell-to-cell interaction in a co-culture setting. ANCA stimulated HC neutrophil SN and untreated aAAV SN promoted comparable effects of cytokine release in gEC that was not further influenced by oxygen tension However, in a co-culture setting with neutrophils and gEC there was increased TEM and cytokine release (IL-8, VCAM-1, ICAM-1) in the presence of ANCA IgG, and TEM was further enhanced by exposure to pathological hypoxia (1% O_2), this may reflect changes in the neutrophil cytoskeleton enabling migration.

7.1.5. Cell protrusion formation is transcriptionally dysregulated in AAV neutrophils

Multiple known pathways are involved in actin polymerisation and cytoskeletal rearrangement but have not been investigated in the context of ANCA stimulation or in AAV. Nor is it known how these processes are dysregulated in the context of ANCA stimulation or AAV neutrophils. Therefore, I wanted to determine whether the effect I found of ANCA promoted neutrophil actin polymerisation in neutrophils was transcriptionally regulated. Pathways involved in neutrophil cell surface and whole membrane were dysregulated in aAAV in comparison to

rAAV, and in MPO-ANCA stimulated neutrophils and PR3-ANCA stimulated neutrophils in comparison to untreated neutrophils at both 21% and 1% O_2. This therefore may link why there is increased neutrophil stiffness and actin polymerisation in the presence of ANCA.

I also wanted to determine whether aAAV neutrophils had transcriptionally regulated differences in membrane reorganisation and protrusion formation. This could provide rationale for the increased neutrophil stiffness mechanophenotype I found in untreated aAAV neutrophils, and the difference in aAAV neutrophil actin polymerisation response to ANCA stimulation. Certain cytoskeletal proteins were upregulated in aAAV neutrophils in addition to cell protrusion pathways being one of the top dysregulated pathways in GO analysis. Whether the effect of increased neutrophil stiffening, protrusion formation, and NET formation in aAAV neutrophils and resultant of ANCA stimulation is linked, is a planned focus of further analysis.

7.1.6. Future work

To complete this project, I plan to measure the effect of ANCA induced actin polymerisation of neutrophils in a co-culture setting with gEC under flow, to determine the difference in effect as found under static conditions. Considering that many patients recruited within this study had lung involvement and that this likely correlated with neutrophil stiffness, I also plan to perform the same co-culture experiments with pulmonary microvascular endothelial cells, as I conducted with gEC. Lastly, I will conduct further covariate analysis on my RNA-seq from patient samples to determine whether other variables such as sex, steroid treatment, and lung or kidney involvement may correlate with transcriptional dysregulation.

There are then several aspects of my results which would be potential avenues for future studies. For example, it is known the neutrophil cytoskeleton contributes to programmed

mechanisms and my study has shown altered biophysical phenotype of aAAV neutrophils, suggesting this may also contribute to altered neutrophil function in disease. As increased pro-inflammatory and adhesion molecule secretion levels were shown in untreated aAAV neutrophil SN, it would be interesting to investigate alteration of other cytokine levels and compare this with levels in serum or plasma. As part of this project, I have developed a biobank of stored neutrophil supernatants, serum, and plasma from patients and HC, and plan to use this with either a multiplex cytokine panel, or potentially proteomic analysis. This data would couple with RNA-seq results to determine whether identified proinflammatory or adhesion molecule expression are dysregulated at both the gene and protein expression level, which could potentially inform development of a disease biomarker.

Additionally, future work in determining how to alter the neutrophil cytoskeleton in aAAV as a mode of therapeutic targeting, would be desirable as a novel method to prevent neutrophilic inflammation and damage in AAV, perhaps without causing unintentional additional immunosuppression. This could be investigated through *in vitro* usage of additional inhibitors not included in this study, targeting cytoskeletal remodelling, in addition to determining how inhibitors alter neutrophil effector functions in aAAV neutrophils. While actin polymerisation inhibitors were proven effective on ANCA stimulated HC neutrophils, future work would therefore involve experimentation with aAAV neutrophils and replicating experiments performed *in vitro* with HC neutrophils.

While I would measure how these inhibitors alter degranulation, phagocytosis, and NETosis in HC and aAAV neutrophils, I consider NETosis the main effector function of interest warranting further investigation. As shown in this thesis, ANCA induce increased NET production, and patients with aAAV are prone to thrombotic events, perhaps because of NET

induced vascular damage. Additionally, tissue factor (F3) was a top upregulated significant DE gene in my RNA-seq results comparing ANCA stimulated neutrophils to untreated neutrophils. This may be another contributor to increased coagulation, potentially coupling with increased tissue damage induced by NETs. These effector mechanisms, specifically NETosis, would be most interesting to measure in a co-culture model with venous and capillary EC. I also have access to paraffin-embedded tissue slices (FFPE) from sites of active vasculitis; and it would be interesting to perform IHC to investigate the presence of tissue factor and NETs in the tissue, not only in circulation (587). It is difficult to confirm tissue hypoxia in human samples but potentially also using IHC for HIF1alpha as a surrogate may show evidence of hypoxia at sites of active vasculitis in aAAV.

I would also perform endothelial damage and integrity assays, measuring vascular permeability and angiogenesis. This would particularly be of interest under hypoxia due to the role of hypoxia in wound repair and whether ANCA alters this. A standard scratch assay could be performed to measure cell migration and angiogenesis, particularly considering *VEGFA*, a HIIF regulated gene, was a top significantly upregulated DE gene in MPO-ANCA stimulated neutrophils in the RNA-seq. RNA and protein lysates from gEC experiments were collected and stored; therefore, future work would include measurement of top DE gene expression from RNA-seq results and protein expression levels in these samples. While this study did not focus on elucidating the molecular effects of EC, how these cells are regulated is of interest for future work, as neutrophil EC interactions are what drive disease pathogenesis. Results displaying increased proinflammatory cytokine and adhesion molecule release would promote neutrophil recruitment, adhesion, and inflammation in co-culture. Future work is necessary to assess whether further endothelial damage occurs due to exposure of these conditions through

measurement of oxidative and shear stress, senescence, angiogenesis capacity, and cell viability assays.

While this study did not focus on EC pathways, as the focus of my thesis was on neutrophil function, how these cells are regulated is of interest for future work, as neutrophil EC interactions are what drive disease pathogenesis in AAV. EC are also exposed to the same oxygen tensions as circulating leucocytes *in vivo* and it would be interesting to further study the impact of hypoxia on EC activation and injury in the context of AAV. For example, I could perform endothelial damage and integrity assays, measuring vascular permeability and angiogenesis. This would particularly be of interest under hypoxia due to the role of hypoxia in wound repair and whether ANCA alters this. A standard scratch assay could be performed to measure cell migration and angiogenesis. I have stored RNA and protein lysates from gEC experiments, some of which were carried out under hypoxia and following incubation with aAAV supernatants; therefore, future work would include initial analysis of protein and gene expression in these samples to guide future studies.

Another potential future direction for this study is to expand my analysis to investigate neutrophil subsets. There is increasing evidence that neutrophils are not a homogenous population and LDGs have been identified AAV and studied more extensively in SLE. Increased NETosis and alterations in other functional readouts have been shown to occur LDGs have displayed in SLE (331,588). Future work could investigate differences in mechanophenotype, actin cytoskeleton, and NET production in LDGs. It would also be interesting to investigate potential pathways for the development of LDG such as senescence as the stage of LDG maturation and phenotype is still speculated in AAV.

Lastly, as the focus of this thesis was neutrophils, further future work in mechanophenotyping could include further assessment of monocytes due to their contribution to disease pathogenesis in aAAV. Optimisation of an improved gating strategy for separating neutrophils from the monocyte population may be necessary first in whole blood. Isolated monocytes have been mechanophenotyped using real time deformability fluorescence cytometry (504), but due to the limitation I found when using RT-DC for isolated cells, optimising an approach for whole blood analysis is preferred. Monocytes and neutrophils fall within the same gating strategy of area between 50-100mM^2 and overlap in the brightness average within contour (a.u.) between 65-70 a.u., whereby I employed a polygon gate to separate populations during ShapeOut analysis. Due to the abundancy of neutrophils in whole blood, events recorded in ShapeIn reach the number necessary for neutrophil analysis within 10 minutes, whereas recording the equivalent number of monocyte events may take up to 30 minutes which is not technically feasible. Therefore, for future work, optimising a more efficient and accurate gating strategy for monocyte measurement in whole blood would be necessary and of interest to mechanophenotyping in aAAV and other immune-mediated diseases.

7.2. Conclusions

The focus of my thesis was to evaluate how neutrophil biophysical phenotype is altered in response to ANCA stimulation and in patients with aAAV, and whether hypoxia exacerbates this effect, contributing to EC injury. My results identify that neutrophil trapping in the microvasculature in disease may be a result of altered neutrophil mechanophenotype in patients with aAAV or in the presence of ANCA IgG. I present a novel pathogenic effect of ANCA IgG on neutrophil actin polymerisation and demonstrate how reduced oxygen tension to pathological levels alters neutrophil and EC functional responses in the presence of ANCA, thus increasing the potential for neutrophil-mediated vascular injury. Targeting ANCA

promoted neutrophil stiffening in AAV may be a potential option for treatment to reduce neutrophil trapping in the microvasculature, therefore decreasing inflammation and dampening pathogenic mechanisms.

References:

1. Dancey JT, Deubelbeiss KA, Harker LA, Finch CA. Neutrophil Kinetics in Man. 1976; 58(3):705-15.
2. Bainton Dorothy Ford , Ullyot JL, Farquhar MG. In Human Bone Marrow Origin and Context of Azurophil and Specific Granules. Vol. 134, The Journal of Experimental Medicine. 1971; 134(4): 907-34.
3. Pillay J, Den Braber I, Vrisekoop N, Kwast LM, De Boer RJ, Borghans JAM, et al. In vivo labeling with 2H2O reveals a human neutrophil lifespan of 5.4 days. Blood. 2010;116(4):625–7.
4. Tofts PS, Chevassut T, Cutajar M, Dowell NG, Peters AM. Doubts concerning the recently reported human neutrophil lifespan of 5.4 days. Vol. 117, Blood. 2011;117(22):6050-2.
5. Lahoz-Beneytez J, Elemans M, Zhang Y, Ahmed R, Salam A, Block M, et al. Human neutrophil kinetics: Modeling of stable isotope labeling data supports short blood neutrophil half-lives. Blood. 2016;127(26).
6. Athens JW, Haab OP, Raab SO, Mauer AM, Ashenbrucker H, Cartwright GE, et al. Leukokinetic studies. IV. The total blood, circulating and marginal granulocyte pools and the granulocyte turnover rate in normal subjects. J Clin Invest. 1961;40 (6):989-95.
7. West BC, Rosenthal AS, Gelb NA, Kimball HR. Separation and Characterization of Human Neutrophil Granules Address reprint requests to. National Institutes of Health. 1974; 77(1):41-66.
8. Garcia RC, Peterson CGB, Segal AW, Venge P. Elastase in the different primary granules of the human neutrophil. Biochem Biophys Res Commun. 1985;132(3):1130–6.
9. Egesten A, Breton-Gorius J, Guichard J, Gullberg U, Olsson I. The Heterogeneity of Azurophil Granules in Neutrophil Promyelocytes: Immunogold Localization of Myeloperoxidase, Cathepsin G, Elastase, Proteinase 3, and Bactericidal/Permeability Increasing Protein. Blood. 1994;83(10):2985–94.
10. O'Shea JJ, Brown EJ, Seligmann BE, Metcalf JA, Frank MM, Gallin JI. Evidence for distinct intracellular pools of receptors for C3b and C3bi in human neutrophils. J Immunol. 1985;134(4).
11. Stevenson KB, Nauseef WM, Clark RA. The neutrophil glycoprotein Mo1 is an integral membrane protein of plasma membranes and specific granules. J Immunol. 1987;139(11).
12. Suchard SJ, Burton MJ, Stoehr SJ. Thrombospondin receptor expression in human neutrophils coincides with the release of a subpopulation of specific granules. Biochem J. 1992;284(2).
13. Mollinedo F, Pulido R, Lacal PM, Sanchez-Madrid F. Mobilization of Gelatinase-Rich Granules as a Regulatory Mechanism of Early Functional Responses in Human Neutrophils. Scand J Immunol. 1991;34(1).
14. Mollinedo F, Nakajima M, Llorens A, Barbosa E, Callejo S, Gajate C, et al. Major co-localization of the extracellular-matrix degradative enzymes heparanase and gelatinase

in tertiary granules of human neutrophils. Vol. 327, Biochem. J. 1997; 327(Pt 3):917-23.
15. Olins AL, Zwerger M, Herrmann H, Zentgraf H, Simon AJ, Monestier M, et al. The human granulocyte nucleus: Unusual nuclear envelope and heterochromatin composition. Eur J Cell Biol. 2008;87(5):279–90.
16. Segal AW. How neutrophils kill microbes. Vol. 23, Annual Review of Immunology. 2005; 23:197–223.
17. Savill JS, Wyllie AH, Henson JE, Walport MJ, Henson PM, Haslett C. Macrophage Phagocytosis of Aging Neutrophils in Inflammation Programmed Cell Death in the Neutrophil Leads to its Recognition by Macrophages. J Clin Invest. 1989; 83(3):865-75.
18. Pryzwansky KB, MacRae EK, Spitznagel JK, Cooney MH. Early degranulation of human neutrophils: Immunocytochemical studies of surface and intracellular phagocytic events. Cell. 1979;18(4).
19. Bainton DF. Sequential degranulation of the two types of polymorphonuclear leukocyte granules during phagocytosis of microorganisms. J Cell Biol. 1973;58(2).
20. Nathan CF. Neutrophil activation on biological surfaces. Massive secretion of hydrogen peroxide in response to products of macrophages and lymphocytes. J Clin Invest. 1987;80(6).
21. Guthrie LA, Mcphail LC, Henson PM, Johnston RB. Priming of Neutrophils for Enhanced Release of Oxygen Metabolites by Bacterial Lipopolysaccharide. Evidence for Increased Activity of the Superoxide-producing Enzyme. J Exp Med. 1984;160(6):1656-71.
22. Hallett MB, Lloyds D. Neutrophil priming: the cellular signals that say ‘amber’ but not ‘green.’ Immunol Today. 1995;16(6):264–8.
23. Koenderman L, Kanters D, Maesen B, Raaijmakers J, Lammers J-WJ, de Kruif J, et al. Monitoring of neutrophil priming in whole blood by antibodies isolated from a synthetic phage antibody library. J Leukoc Biol. 2000;68(1).
24. Condliffe AM, Chilvers ER. Priming differentially regulates neutrophil adhesion molecule expression/function. Vol. 89, Immunology. 1996.
25. Silvestre-Roig C, Hidalgo A, Soehnlein O. Neutrophil heterogeneity: Implications for homeostasis and pathogenesis. Blood. 2016;127(18):2173–81.
26. Hallett MB, Dewitt S. Ironing out the wrinkles of neutrophil phagocytosis. Trends Cell Biol. 2007;17(5).
27. Herster F, Bittner Z, Codrea MC, Archer NK, Heister M, Löffler MW, et al. Platelets aggregate with neutrophils and promote skin pathology in psoriasis. Front Immunol. 2019;10:1867.
28. Li T, Wang C, Liu Y, Li B, Zhang W, Wang L, et al. Neutrophil Extracellular Traps Induce Intestinal Damage and Thrombotic Tendency in Inflammatory Bowel Disease. J Crohn’s Colitis. 2020;14(2).
29. Liang X, Xiu C, Liu M, Lin C, Chen H, Bao R, et al. Platelet-neutrophil interaction aggravates vascular inflammation and promotes the progression of atherosclerosis by activating the TLR4/NF-κB pathway. J Cell Biochem. 2019;120(4).
30. Filep JG, Ariel A. Neutrophil heterogeneity and fate in inflamed tissues: implications for the resolution of inflammation. Am J Physiol - Cell Physiol. 2020;319(3):C510–32.

31. Fleischmann J, Golde DW, Weisbart RH, Gasson JC. Granulocyte-Macrophage Colony-Stimulating Factor Enhances Phagocytosis of Bacteria by Human Neutrophils. Blood. 1986;68(3):708–11.
32. Forehand JR, Pabst MJ, Phillips WA, Johnston RB. Lipopolysaccharide Priming of Human Neutrophils for an Enhanced Respiratory Burst Role of Intracellular Free Calcium. J Clin Invest. 1989; 83(1):74-83.
33. Berkow RL, Wang D, Larrick JW, Dodson RW, Howard TH. Enhancement of neutrophil superoxide production by preincubation with recombinant human tumor necrosis factor. J Immunol. 1987;139(11).
34. Futosi K, Fodor S, Mócsai A. Neutrophil cell surface receptors and their intracellular signal transduction pathways. Int Immunopharmacol [Internet]. 2013;17(3):638–50.
35. Corey S, Eguino A, Puyana-Theaii K, Bolen JB, Cantley L, Mollinedo F, et al. Granulocyte macrophage-colony stimulating factor stimulates both association and activation of phosphoinositide 30H-kinase and src-related tyrosine kinase(s) in human myeloid derived cells. Vol. 1, The EMBO Journal. 1993; 12(7): 2681-2690.
36. Vogt KL, Summers C, Chilvers ER, Condliffe AM. Priming and de-priming of neutrophil responses in vitro and in vivo. Eur J Clin Invest. 2018;48:0–2.
37. Hafezi-Moghadam A, Thomas KL, Prorock AJ, Huo Y, Ley K. L-selectin shedding regulates leukocyte recruitment. J Exp Med. 2001;193(7).
38. Summers C, Singh NR, White JF, Mackenzie IM, Johnston A, Solanki C, et al. Pulmonary retention of primed neutrophils: A novel protective host response, which is impaired in the acute respiratory distress syndrome. Thorax. 2014;69(7).
39. Singh P, Hu P, Hoggatt J, Moh A, Pelus LM. Expansion of bone marrow neutrophils following G-CSF administration in mice results in osteolineage cell apoptosis and mobilization of hematopoietic stem and progenitor cells. Leukemia. 2012;26(11).
40. Sapey E, Stockley RA. Red, amber and green: The role of the lung in de-priming active systemic neutrophils. Thorax. 2014;69(7):606–8.
41. Bashant KR, Vassallo A, Herold C, Berner R, Menschner L, Subburayalu J, et al. Real-time deformability cytometry reveals sequential contraction and expansion during neutrophil priming. J Leukoc Biol. 2019;105(6):1143–53.
42. Toepfner N, Herold C, Otto O, Rosendahl P, Jacobi A, Kräter M, et al. Detection of human disease conditions by single-cell morpho-rheological phenotyping of whole blood. bioRxiv. 2017;1–22.
43. Fay ME, Myers DR, Kumar A, Turbyfield CT, Byler R, Crawford K, et al. Cellular softening mediates leukocyte demargination and trafficking, thereby increasing clinical blood counts. Proc Natl Acad Sci U S A. 2016;113(8).
44. Tregay N, Begg M, Cahn A, Farahi N, Povey K, Madhavan S, et al. Use of autologous 99m Technetium-labelled neutrophils to quantify lung neutrophil clearance in COPD. Thorax. 2019 Jul 1;74(7):659–66.
45. Yoshida K, Kondo R, Wang Q, Doerschuk CM. Neutrophil cytoskeletal rearrangements during capillary sequestration in bacterial pneumonia in rats. Am J Respir Crit Care Med. 2006;174(6).
46. Ekpenyong AE, Toepfner N, Fiddler C, Herbig M, Li W, Cojoc G, et al. Mechanical deformation induces depolarization of neutrophils. Sci Adv. 2017;3(6):1–11.

47. Zhang F, Liu AL, Gao S, Ma S, Guo S Bin. Neutrophil dysfunction in sepsis. Chin Med J (Engl). 2016;129(22).
48. Finlay LDB, Conway Morris A, Deane AM, Wood AJT. Neutrophil kinetics and function after major trauma: A systematic review. World J Crit Care Med. 2021;10(5).
49. Bruserud Ø, Mosevoll KA, Bruserud Ø, Reikvam H, Wendelbo Ø. The Regulation of Neutrophil Migration in Patients with Sepsis: The Complexity of the Molecular Mechanisms and Their Modulation in Sepsis and the Heterogeneity of Sepsis Patients. Vol. 12, Cells. 2023; 12(7): 1003.
50. Mortaz E, Zadian SS, Shahir M, Folkerts G, Garssen J, Mumby S, et al. Does Neutrophil Phenotype Predict the Survival of Trauma Patients? Vol. 10, Frontiers in Immunology. 2019; 10: 2122.
51. Faurschou M, Sørensen OE, Johnsen AH, Askaa J, Borregaard N. Defensin-rich granules of human neutrophils: characterization of secretory properties. 2002; 1591(1-3): 29-35.
52. Verma RS, Antony AC, Kjeldsen L, Bjerrum W, Askaa J, Borregaard N, et al. Immunoreactive folate-binding proteins from human saliva Subcellular localization and release of human neutrophil gelatinase, confirming the existence of separate gelatinase-containing granules Evaluation of hydrogen-bonding and enantiomeric P. Vol. 289, Biochem. J. 1993; 286(Pt 3): 707-715.
53. Huizinga TWJ, Roos D, Von Dem Borne AEGK. Neutrophil Fc-γ receptors: A two-way bridge in the immune system. Vol. 75, Blood. 1990; 75(6):1211-4.
54. Sengeløv H, Follin P, Kjeldsen L, Lollike K, Dahlgren C, Borregaard N. Mobilization of granules and secretory vesicles during in vivo exudation of human neutrophils. J Immunol. 1995;154(8).
55. Jog NR, Rane MJ, Lominadze G, Luerman GC, Ward RA, McLeish KR. The actin cytoskeleton regulates exocytosis of all neutrophil granule subsets. Am J Physiol - Cell Physiol [Internet]. 2007;292(5).
56. Berton G, Lowell CA. Integrin signalling in neutrophils and macrophages. Vol. 11, Cellular Signalling. 1999; 11(9):621-35.
57. Suchard SJ, Boxer LA. Exocytosis of a subpopulation of specific granules coincides with $H2O_2$ production in adherent human neutrophils. J Immunol. 1994;152(1).
58. Bruns S, Kniemeyer O, Hasenberg M, Aimanianda V, Nietzsche S, Thywien A, et al. Production of extracellular traps against aspergillus fumigatus in vitro and in infected lung tissue is dependent on invading neutrophils and influenced by hydrophobin roda. PLoS Pathog. 2010;6(4).
59. Branzk N, Lubojemska A, Hardison SE, Wang Q, Gutierrez MG, Brown GD, et al. Neutrophils sense microbe size and selectively release neutrophil extracellular traps in response to large pathogens. Nat Immunol. 2014;15(11).
60. Charles LA, Caldas MLR, Falk RJ, Terrell RS, Jennette JC. Antibodies against granule proteins activate neutrophils in vitro. J Leukoc Biol. 1991;50(6).
61. Chapman ALP, Mocatta TJ, Shiva S, Seidel A, Chen B, Khalilova I, et al. Ceruloplasmin is an endogenous inhibitor of myeloperoxidase. J Biol Chem. 2013;288(9).
62. Duranton J, Bieth JG. Inhibition of proteinase 3 by α1-antitrypsin in vitro predicts very fast inhibition in vivo. Am J Respir Cell Mol Biol. 2003;29(1).

63. Csernok E, Ernst M, Schmitt W, Bainton DF, Gross WL. Activated neutrophils express proteinase 3 on their plasma membrane in vitro and in vivo. Clin Exp Immunol. 1994;95(2):244–50.
64. Metzler KD, Goosmann C, Lubojemska A, Zychlinsky A, Papayannopoulos V. Myeloperoxidase-containing complex regulates neutrophil elastase release and actin dynamics during NETosis. Cell Rep [Internet]. 2014;8(3):883–96.
65. Chollet-Martin S, Montravers P, Gibert C, Elbim C, Desmonts JM, Fagon JY, et al. Subpopulation of hyperresponsive polymorphonuclear neutrophils in patients with adult respiratory distress syndrome: Role of cytokine production. Am Rev Respir Dis. 1992;146(4).
66. Li XJ, Tian W, Stull ND, Grinstein S, Atkinson S, Dinauer MC, et al. A Fluorescently Tagged C-Terminal Fragment of p47 phox Detects NADPH Oxidase Dynamics during Phagocytosis. Mol Biol Cell. 2009;20:1520–32.
67. Blanter M, Gouwy M, Struyf S. Studying neutrophil function in vitro: Cell models and environmental factors. J Inflamm Res. 2021;14:141–62.
68. Steinberg BE, Grinstein S. Unconventional roles of the NADPH oxidase: signaling, ion homeostasis, and cell death. Sci STKE. 2007;2007(379).
69. Glennon-Alty L, Hackett AP, Chapman EA, Wright HL. Neutrophils and redox stress in the pathogenesis of autoimmune disease. Free Radic Biol Med [Internet]. 2018;125(March):25–35.
70. Meegan JE, Yang X, Coleman DC, Jannaway M, Yuan SY. Neutrophil-mediated vascular barrier injury: Role of neutrophil extracellular traps. Vol. 24, Microcirculation. Wiley Blackwell; 2017: 24(3):10.
71. Urban CF, Ermert D, Schmid M, Abu-Abed U, Goosmann C, Nacken W, et al. Neutrophil extracellular traps contain calprotectin, a cytosolic protein complex involved in host defense against Candida albicans. PLoS Pathog. 2009;5(10).
72. Hakkim A, Fuchs TA, Martinez NE, Hess S, Prinz H, Zychlinsky A, et al. Activation of the Raf-MEK-ERK pathway is required for neutrophil extracellular trap formation. Nat Chem Biol. 2011;7(2).
73. Behnen M, Leschczyk C, Möller S, Batel T, Klinger M, Solbach W, et al. Immobilized Immune Complexes Induce Neutrophil Extracellular Trap Release by Human Neutrophil Granulocytes via FcγRIIIB and Mac-1. J Immunol. 2014;193(4).
74. Fuchs TA, Abed U, Goosmann C, Hurwitz R, Schulze I, Wahn V, et al. Novel cell death program leads to neutrophil extracellular traps. J Cell Biol. 2007;176(2):231–41.
75. Papayannopoulos V, Metzler KD, Hakkim A, Zychlinsky A. Neutrophil elastase and myeloperoxidase regulate the formation of neutrophil extracellular traps. J Cell Biol. 2010;191(3).
76. Wolfson M, McPhail LC, Nasrallah VN, Snyderman R. Phorbol myristate acetate mediates redistribution of protein kinase C in human neutrophils: potential role in the activation of the respiratory burst enzyme. J Immunol. 1985;135(3).
77. Brinkmann V, Reichard U, Goosmann C, Fauler B, Uhlemann Y, Weiss DS, et al. Neutrophil Extracellular Traps Kill Bacteria. Science (80-). 2004;303(5663).
78. Brinkmann V, Zychlinsky A. Beneficial suicide: Why neutrophils die to make NETs. Nat Rev Microbiol. 2007;5(8).

79. Pilsczek FH, Salina D, Poon KKH, Fahey C, Yipp BG, Sibley CD, et al. A Novel Mechanism of Rapid Nuclear Neutrophil Extracellular Trap Formation in Response to Staphylococcus aureus . J Immunol. 2010;185(12).
80. Yousefi S, Mihalache C, Kozlowski E, Schmid I, Simon HU. Viable neutrophils release mitochondrial DNA to form neutrophil extracellular traps. Cell Death Differ. 2009;16(11):1438–44.
81. Wang H, Li T, Chen S, Gu Y, Ye S. Neutrophil extracellular trap mitochondrial DNA and its autoantibody in systemic lupus erythematosus and a proof-of-concept trial of metformin. Arthritis Rheumatol. 2015;67(12).
82. Ingelsson B, Söderberg D, Strid T, Söderberg A, Bergh AC, Loitto V, et al. Lymphocytes eject interferogenic mitochondrial DNA webs in response to CpG and non-CpG oligodeoxynucleotides of class C. Proc Natl Acad Sci U S A. 2018;115(3).
83. Mitroulis I, Kambas K, Chrysanthopoulou A, Skendros P, Apostolidou E, Kourtzelis I, et al. Neutrophil extracellular trap formation is associated with IL-1β and autophagy-related signaling in gout. PLoS One. 2011;6(12).
84. Remijsen Q, Berghe T Vanden, Wirawan E, Asselbergh B, Parthoens E, De Rycke R, et al. Neutrophil extracellular trap cell death requires both autophagy and superoxide generation. Cell Res. 2011;21(2).
85. Germic N, Stojkov D, Oberson K, Yousefi S, Simon HU. Neither eosinophils nor neutrophils require ATG5-dependent autophagy for extracellular DNA trap formation. Immunology. 2017;152(3).
86. Douda DN, Khan MA, Grasemann H, Palaniyar N. SK3 channel and mitochondrial ROS mediate NADPH oxidase-independent NETosis induced by calcium influx. Proc Natl Acad Sci U S A. 2015;112(9).
87. Fossati G, Moulding DA, Spiller DG, Moots RJ, White MRH, Edwards SW. The Mitochondrial Network of Human Neutrophils: Role in Chemotaxis, Phagocytosis, Respiratory Burst Activation, and Commitment to Apoptosis. J Immunol. 2003;170(4).
88. Maianski NA, Geissler J, Srinivasula SM, Alnemri ES, Roos D, Kuijpers TW. Functional characterization of mitochondria in neutrophils: A role restricted to apoptosis. Cell Death Differ. 2004;11(2).
89. Scherz-Shouval R, Elazar Z. Regulation of autophagy by ROS: Physiology and pathology. Vol. 36, Trends in Biochemical Sciences. 2011; 36(1):30-8.
90. Brill A, Fuchs TA, Savchenko AS, Thomas GM, Martinod K, de Meyer SF, et al. Neutrophil extracellular traps promote deep vein thrombosis in mice. J Thromb Haemost. 2012;10(1).
91. Chargui A, El May MV. Autophagy mediates neutrophil responses to bacterial infection. Vol. 122, APMIS. 2014; 122(11):1047-58.
92. Chen KW, Monteleone M, Boucher D, Sollberger G, Ramnath D, Condon ND, et al. Noncanonical inflammasome signaling elicits gasdermin D–dependent neutrophil extracellular traps. Sci Immunol. 2018;3(26).
93. Gupta AK, Giaglis S, Hasler P, Hahn S. Efficient neutrophil extracellular trap induction requires mobilization of both intracellular and extracellular calcium pools and is modulated by cyclosporine A. PLoS One. 2014;9(5):19–21.
94. Sollberger G, Choidas A, Burn GL, Habenberger P, Lucrezia R Di, Kordes S, et al.

Gasdermin D plays a vital role in the generation of neutrophil extracellular traps. Sci Immunol. 2018;3(26).
95. Stojkov D, Claus MJ, Kozlowski E, Oberson K, Schären OP, Benarafa C, et al. NET formation is independent of gasdermin D and pyroptotic cell death. Sci Signal. 2023;16(769).
96. Slack JL, Jones LE, Bhatia MM, Thompson PR. Autodeimination of protein arginine deiminase 4 alters protein-protein interactions but not activity. Biochemistry. 2011;50(19).
97. Takahara H, Okamoto H, Sugawara K. Affinity chromatography of peptidylarginine deiminase from rabbit skeletal muscle on a column of soybean trypsin inhibitor (kunitz)-sepharose. J Biochem. 1986;99(5).
98. Nakashima K, Hagiwara T, Yamada M. Nuclear localization of peptidylarginine deiminase V and histone deimination in granulocytes. J Biol Chem. 2002;277(51).
99. Wang Y, Wysocka J, Sayegh J, Lee YH, Pertin JR, Leonelli L, et al. Human PAD4 regulates histone arginine methylation levels via demethylimination. Science (80-). 2004;306(5694).
100. Konig MF, Andrade F. A critical reappraisal of neutrophil extracellular traps and NETosis mimics based on differential requirements for protein citrullination. Front Immunol. 2016;7(11).
101. Liu X, Arfman T, Wichapong K, Reutelingsperger CPM, Voorberg J, Nicolaes GAF. PAD4 takes charge during neutrophil activation: Impact of PAD4 mediated NET formation on immune-mediated disease. Vol. 19, Journal of Thrombosis and Haemostasis. 2021; 19(7):1607-1617
102. Janmey PA. Phosphoinositides and calcium as regulators of cellular actin assembly and disassembly. Vol. 56, Annual Review of Physiology. 1994.
103. Gupta S, Chan DW, Zaal KJ, Kaplan MJ. A high throughput real-time imaging technique to quantify NETosis and distinguish mechanisms of cell death in human neutrophils. Physiol Behav. 2018;176(3):139–48.
104. Thiama HR, Wong SL, Qiu R, Kittisopikul M, Vahabikashi A, Goldman AE, et al. NETosis proceeds by cytoskeleton and endomembrane disassembly and PAD4-mediated chromatin decondensation and nuclear envelope rupture. Proc Natl Acad Sci U S A. 2020;117(13):7326–37.
105. Neeli I, Dwivedi N, Khan S, Radic M. Regulation of extracellular chromatin release from neutrophils. J Innate Immun. 2009;1(3).
106. Neubert P, Homann A, Wendelborn D, Bär AL, Krampert L, Trum M, et al. NCX1 represents an ionic Na+ sensing mechanism in macrophages. PLoS Biol. 2020;18(6).
107. Stojkov D, Amini P, Oberson K, Sokollik C, Duppenthaler A, Simon HU, et al. ROS and glutathionylation balance cytoskeletal dynamics in neutrophil extracellular trap formation. J Cell Biol. 2017;216(12).
108. Sprenkeler EGG, Tool ATJ, Henriet SS V, van Bruggen R, Kuijpers TW. Formation of neutrophil extracellular traps requires actin cytoskeleton rearrangements. Blood. 2022;139(21).
109. Kasperkiewicz P, Hempel A, Janiszewski T, Kołt S, Snipas SJ, Drag M, et al. NETosis occurs independently of neutrophil serine proteases. J Biol Chem. 2020;295(51).

110. Van Der Linden M, Westerlaken GHA, Van Der Vlist M, Van Montfrans J, Meyaard L. Differential Signalling and Kinetics of Neutrophil Extracellular Trap Release Revealed by Quantitative Live Imaging. Sci Rep. 2017;7(1).
111. Li P, Li M, Lindberg MR, Kennett MJ, Xiong N, Wang Y. PAD4 is essential for antibacterial innate immunity mediated by neutrophil extracellular traps. J Exp Med. 2010;207(9):1853–62.
112. Palmer LJ, Damgaard C, Holmstrup P, Nielsen CH. Influence of complement on neutrophil extracellular trap release induced by bacteria. J Periodontal Res. 2016;51(1):70–6.
113. Nauseef WM. Human neutrophils ≠ murine neutrophils: Does it matter? Vol. 314, Immunological Reviews. John Wiley and Sons Inc; 2023; 314(1): 442-456.
114. Benabid R, Wartelle J, Malleret L, Guyot N, Gangloff S, Lebargy F, et al. Neutrophil elastase modulates cytokine expression: Contribution to host defense against pseudomonas aeruginosa-induced pneumonia. J Biol Chem. 2012;287(42):34883–94.
115. Metzemaekers M, Gouwy M, Proost P. Neutrophil chemoattractant receptors in health and disease: double-edged swords. Cell Mol Immunol [Internet]. 2020;17(5):433–50.
116. Németh T, Sperandio M, Mócsai A. Neutrophils as emerging therapeutic targets. Nat Rev Drug Discov [Internet]. 2020;19(4):253–75.
117. Scapini P, Calzetti F, Cassatella MA. On the detection of neutrophil-derived vascular endothelial growth factor VEGF. Vol. 232, Journal of Immunological Methods. Elsevier; 1999; 232(1-2): 121-9.
118. Apostolidou E, Skendros P, Kambas K, Mitroulis I, Konstantinidis T, Chrysanthopoulou A, et al. Neutrophil extracellular traps regulate IL-1β-mediated inflammation in familial Mediterranean fever. Ann Rheum Dis. 2016;75(1).
119. Schnabel A, Csernok E, Isenberg DA, Mrowka C, Gross WL. Antineutrophil cytoplasmic antibodies in systemic lupus erythematosus. Prevalence, specificities, and clinical significance. Arthritis Rheum. 1995;38(5).
120. Nässberger L, Jonsson H, Sjoholm AG, Sturfelt G, Heubner A. Circulating Anti-Elastase in Systemic Lupus Erythematosus. Vol. 333, The Lancet. 1989; 1(8636):509.
121. Christensen SR, Kashgarian M, Alexopoulou L, Flavell RA, Akira S, Shlomchik MJ. Toll-like receptor 9 controls anti-DNA autoantibody production in murine lupus. J Exp Med. 2005;202(2).
122. Means TK, Latz E, Hayashi F, Murali MR, Golenbock DT, Luster AD. Human lupus autoantibody-DNA complexes activate DCs through cooperation of CD32 and TLR9. J Clin Invest. 2005;115(2).
123. Lande R, Ganguly D, Facchinetti V, Frasca L, Conrad C, Gregorio J, et al. Neutrophils activate plasmacytoid dendritic cells by releasing self-DNA-peptide complexes in systemic lupus erythematosus. Sci Transl Med. 2011;3(73).
124. von Brühl ML, Stark K, Steinhart A, Chandraratne S, Konrad I, Lorenz M, et al. Monocytes, neutrophils, and platelets cooperate to initiate and propagate venous thrombosis in mice in vivo. J Exp Med. 2012;209(4).
125. Darbousset R, Thomas GM, Mezouar S, Frère C, Bonier R, Mackman N, et al. Tissue factor-positive neutrophils bind to injured endothelial wall and initiate thrombus formation. Blood. 2012;120(10).

126. Kambas K, Chrysanthopoulou A, Vassilopoulos D, Apostolidou E, Skendros P, Girod A, et al. Tissue factor expression in neutrophil extracellular traps and neutrophil derived microparticles in antineutrophil cytoplasmic antibody associated vasculitis may promote thromboinflammation and the thrombophilic state associated with the disease. Ann Rheum Dis. 2014;73(10).
127. Altstaedt J, Kirchner H, Rink L. Cytokine production of neutrophils is limited to interleukin-8. Immunology. 1996;89(4).
128. Smedman C, Gårdlund B, Nihlmark K, Gille-Johnson P, Andersson J, Paulie S. ELISpot analysis of LPS-stimulated leukocytes: Human granulocytes selectively secrete IL-8, MIP-1β and TNF-α. J Immunol Methods. 2009;346(1–2):1–8.
129. Wright HL, Moots RJ, Bucknall RC, Edwards SW. Neutrophil function in inflammation and inflammatory diseases. Rheumatology. 2010;49(9):1618–31.
130. McCourt M, Wang JH, Sookhai S, Redmond HP. Proinflammatory mediators stimulate neutrophil-directed angiogenesis. Arch Surg. 1999;134(12).
131. Tecchio C, Cassatella MA. Neutrophil-derived chemokines on the road to immunity. Vol. 28, Seminars in Immunology. 2016; 28(2):119-28.
132. Scapini P, Lapinet-Vera JA, Gasperini S, Calzetti F, Bazzoni F, Cassatella MA. The neutrophil as a cellular source of chemokines. Vol. 177, Immunological Reviews. 2000; 177:195-203.
133. Altan-Bonnet G, Mukherjee R. Cytokine-mediated communication: a quantitative appraisal of immune complexity. Vol. 19, Nature Reviews Immunology. 2019; 19: 205-217.
134. Walsh DE, Greene CM, Carroll TP, Taggart CC, Gallagher PM, O'Neill SJ, et al. Interleukin-8 Up-regulation by Neutrophil Elastase is Mediated by MyD88/IRAK/TRAF-6 in Human Bronchial Epithelium. J Biol Chem. 2001;276(38).
135. Hayashi F, Means TK, Luster AD. Toll-like receptors stimulate human neutrophil function. Blood. 2003;102(7).
136. Zhou Y, Doerschuk CM, Anderson JM, Marchant RE. Biomaterial surface-dependent neutrophil mobility. J Biomed Mater Res - Part A. 2004;69(4).
137. Soler-Rodriguez AM, Zhang H, Lichenstein HS, Qureshi N, Niesel DW, Crowe SE, et al. Neutrophil Activation by Bacterial Lipoprotein Versus Lipopolysaccharide: Differential Requirements for Serum and CD14. J Immunol. 2000;164(5).
138. Kaiser R, Leunig A, Pekayvaz K, Popp O, Joppich M, Polewka V, et al. Self-sustaining IL-8 loops drive a prothrombotic neutrophil phenotype in severe COVID-19. JCI Insight. 2021;6(18).
139. Azevedo MLV, Zanchettin AC, Vaz de Paula CB, Motta Júnior J da S, Malaquias MAS, Raboni SM, et al. Lung Neutrophilic Recruitment and IL-8/IL-17A Tissue Expression in COVID-19. Front Immunol. 2021;12.
140. de Oliveira S, Reyes-Aldasoro CC, Candel S, Renshaw SA, Mulero V, Calado Â. Cxcl8 (IL-8) Mediates Neutrophil Recruitment and Behavior in the Zebrafish Inflammatory Response. J Immunol. 2013;190(8).
141. Fujishima S, Hoffman AR, Vu T, Kim KJ, Zheng H, Daniel D, et al. Regulation of neutrophil interleukin 8 gene expression and protein secretion by LPS, TNF-α, and IL-1β. J Cell Physiol. 1993;154(3):478–85.

142. Hammond ME, Lapointe GR, Feucht PH, Hilt S, Gallegos CA, Gordon CA, et al. IL-8 induces neutrophil chemotaxis predominantly via type I IL-8 receptors. J Immunol. 1995;155(3).
143. Casanova-Acebes M, Nicolás-Ávila JA, Yao Li JL, García-Silva S, Balachander A, Rubio-Ponce A, et al. Neutrophils instruct homeostatic and pathological states in naive tissues. J Exp Med. 2018;215(11).
144. Wang J, Hossain M, Thanabalasuriar A, Gunzer M, Meininger C, Kubes P. Visualizing the function and fate of neutrophils in sterile injury and repair. Science (80-). 2017;358(6359).
145. Foxman EF, Campbell JJ, Butcher EC. Multistep Navigation and the Combinatorial Control of Leukocyte Chemotaxis [Internet]. Vol. 139, The Journal of Cell Biology. 1997; 139(5): 1349-60.
146. Nourshargh S, Renshaw SA, Imhof BA. Reverse Migration of Neutrophils: Where, When, How, and Why? Vol. 37, Trends in Immunology. 2016; 37(5): 273-286.
147. Gallatin WM, Weissman IL, Butcher EC. A cell-surface molecule involved in organ-specific homing of lymphocytes. Nature. 1983;304(5921).
148. Bevilacqua MP, Stengelin S, Gimbrone MA, Seed B. Endothelial Leukocyte Adhesion Molecule 1: An Inducible Receptor for Neutrophils Related to Complement Reglatory Proteins and Lectins. Science (80-) [Internet]. 1989;243(4895).
149. Hsu-Lin SC, Berman CL, Furie BC. A platelet membrane protein expressed during platelet activation and secretion. Studies using a monoclonal antibody specific for thrombin-activated platelets. J Biol Chem. 1984;259(14):9121–6.
150. Stadtmann A, Germena G, Block H, Boras M, Rossaint J, Sundd P, et al. The PSGL-1-L-selectin signaling complex regulates neutrophil adhesion under flow. J Exp Med. 2013;210(11).
151. Shaw SK, Ma S, Kim MB, Rao RM, Hartman CU, Froio RM, et al. Coordinated redistribution of leukocyte LFA-1 and endothelial cell ICAM-1 accompany neutrophil transmigration. J Exp Med. 2004;200(12):1571–80.
152. Sumagin R, Prizant H, Lomakina E, Waugh RE, Sarelius IH. LFA-1 and Mac-1 Define Characteristically Different Intralumenal Crawling and Emigration Patterns for Monocytes and Neutrophils In Situ. J Immunol. 2010;185(11).
153. Barreiro O, Yáñez-Mó M, Serrador JM, Montoya MC, Vicente-Manzanares M, Tejedor R, et al. Dynamic interaction of VCAM-1 and ICAM-1 with moesin and ezrin in a novel endothelial docking structure for adherent leukocytes. J Cell Biol. 2002;157(7):1233–45.
154. Carman C V, Springer TA. A transmigratory cup in leukocyte diapedesis both through individual vascular endothelial cells and between them. J Cell Biol. 2004;167(2):377–88.
155. Braverman IM. The cutaneous microcirculation: Ultrastructure and microanatomical organization. Vol. 4, Microcirculation. 1997; (3): 329-40.
156. Pober JS. Cytokine-Mediated Activation of Vascular Endothelium Physiology and Pathology. Vol. 133, American Journal ofPathology. 1988; 133(3): 426-433.
157. Mulligan MS, Vaporciyan AA, Miyasaka M, Tamatani T, Ward PA. Tumor Necrosis Factor a Regulates in Vivo Intrapulmonary Expression of ICAM-1. Vol. 142, American

Journal of Pathology. 1993; 142(6):1739-49.
158. Stark K, Eckart A, Haidari S, Tirniceriu A, Lorenz M, Von Brühl ML, et al. Capillary and arteriolar pericytes attract innate leukocytes exiting through venules and “instruct” them with pattern-recognition and motility programs. Nat Immunol. 2013;14(1):41–51.
159. Doerschuk CM. The role of CD18-mediated adhesion in neutrophil sequestration induced by infusion of activated plasma in rabbits. Am J Respir Cell Mol Biol. 1992;7(2).
160. Doerschuk CM. Mechanisms of leukocyte sequestration in inflamed lungs. Vol. 8, Microcirculation. 2001; (2):71-88.
161. Patterson AM, Schmutz C, Davis S, Gardner L, Ashton BA, Middleton J, et al. Differential binding of chemokines to macrophages and neutrophils in the human inflamed synovium [Internet]. 2002; 4(3): 209-214.
162. Serhan CN, Brain SD, Buckley CD, Gilroy DW, Haslett C, O’Neill LAJ, et al. Resolution of in flammation: state of the art, definitions and terms. FASEB J. 2007;21(2):325–32.
163. Cowburn AS, Cadwallader KA, Reed BJ, Farahi N, Chilvers ER. Role of PI3-kinase-dependent Bad phosphorylation and altered transcription in cytokine-mediated neutrophil survival. Blood. 2002;100(7):2607–16.
164. Khreiss T, József L, Chan JSD, Filep JG. Activation of extracellular signal-regulated kinase couples platelet-activating factor-induced adhesion and delayed apoptosis of human neutrophils. Cell Signal. 2004;16(7):801–10.
165. Fox S, Leitch AE, Duffin R, Haslett C, Rossi AG. Neutrophil apoptosis: Relevance to the innate immune response and inflammatory disease. J Innate Immun. 2010;2(3):216–27.
166. Kennedy AD, Deleo FR. Neutrophil apoptosis and the resolution of infection. Immunol Res. 2009;43(1–3):25–61.
167. Pérez-Figueroa E, Álvarez-Carrasco P, Ortega E, Maldonado-Bernal C. Neutrophils: Many Ways to Die. Front Immunol. 2021;12(March):1–19.
168. Rossi AG, Sawatzky DA, Walker A, Ward C, Sheldrake TA, Riley NA, et al. Cyclin-dependent kinase inhibitors enhance the resolution of inflammation by promoting inflammatory cell apoptosis. Nat Med. 2006;12(9):1056–64.
169. El Kebir D, József L, Pan W, Filep JG. Myeloperoxidase delays neutrophil apoptosis through CD11b/CD18 integrins and prolongs inflammation. Circ Res. 2008;103(4):352–9.
170. Jerke U, Rolle S, Purfürst B, Luft FC, Nauseef WM, Kettritz R. B2 Integrin-Mediated Cell-Cell Contact Transfers Active Myeloperoxidase From Neutrophils To Endothelial Cells. J Biol Chem. 2013;288(18):12910–9.
171. Everts-Graber J, Martin KR, Thieblemont N, Mocek J, Roccabianca A, Chafey P, et al. Proteomic analysis of neutrophils in ANCA-associated vasculitis reveals a dysregulation in proteinase 3-associated proteins such as annexin-A1 involved in apoptotic cell clearance. Kidney Int. 2019;96(2):397–408.
172. Yang JJ, Preston GA, Pendergraft WF, Segelmark M, Heeringa P, Hogan SL, et al. Internalization of proteinase 3 is concomitant with endothelial cell apoptosis and internalization of myeloperoxidase with generation of intracellular oxidants. Am J

Pathol. 2001;158(2):581–92.
173. Oleinika K, Mauri C, Salama AD. Effector and regulatory B cells in immune-mediated kidney disease. Nat Rev Nephrol [Internet]. 2019;15(1):11–26.
174. Murray J, Barbara JAJ, Dunkley SA, Lopez AF, Van Ostade X, Condliffe AM, et al. Regulation of Neutrophil Apoptosis by Tumor Necrosis Factor-α: Requirement for TNFR55 and TNFR75 for Induction of Apoptosis In Vitro. Blood. 1997;90(7):2772–83.
175. Colotta F, Re F, Polentarutti N, Sozzani S, Mantovani A. Modulation of Granulocyte Survival and Programmed Cell Death by Cytokines and Bacterial Products. Blood. 1992;80(8):2012–20.
176. Lee NK, Lee SY. Modulation of Life and Death by the Tumor Necrosis Factor Receptor-Associated Factors (TRAFs). Vol. 35, Journal of Biochemistry and Molecular Biology. 2002.
177. Herrmann H, Aebi U. Intermediate filaments: Structure and assembly. Cold Spring Harb Perspect Biol. 2016;8(11).
178. Holmes KC, Kabsch W, Mannherz HG, Suck D, Pai EF. Atomic structure of the actin:DNase I complex. Nature. 1990;347.
179. Slauterback DB. Cytoplasmic Microtubulues. I. Hydra. J Cell Biol. 1963;18.
180. Hatano S, Oosawa F. Extraction of an actin-like protein from the plasmodium of a myxomycete and its interaction with myosin a from rabbit striated muscle. J Cell Physiol. 1966;68(2).
181. Oosterheert W, Klink BU, Belyy A, Pospich S, Raunser S. Structural basis of actin filament assembly and aging. Nature. 2022;611(7935).
182. Vitriol EA, McMillen LM, Kapustina M, Gomez SM, Vavylonis D, Zheng JQ. Two functionally distinct sources of actin monomers supply the leading edge of lamellipodia. Cell Rep. 2015;11(3).
183. Feuer G, Molnar F. Studies on the composition and polymerization of actin. Hung Acta Physiol. 1948;1(4–5).
184. Bugyi B, Kellermayer M. The discovery of actin: “to see what everyone else has seen, and to think what nobody has thought”. J Muscle Res Cell Motil. 2020;41(1).
185. Darling EM, Topel M, Zauscher S, Vail TP, Guilak F. Viscoelastic properties of human mesenchymally-derived stem cells and primary osteoblasts, chondrocytes, and adipocytes. J Biomech. 2008;41(2):454–64.
186. Yu H, Tay CY, Leong WS, Tan SCW, Liao K, Tan LP. Mechanical behavior of human mesenchymal stem cells during adipogenic and osteogenic differentiation. Biochem Biophys Res Commun. 2010;393(1):150–5.
187. Tsai MA, Waugh RE, Keng PC. Changes in HL-60 cell deformability during differentiation induced by DMSO. Biorheology. 1996;33(1):1–15.
188. Lautenschläger F, Paschke S, Schinkinger S, Bruel A, Beil M, Guck J, et al. The regulatory role of cell mechanics for migration of differentiating myeloid cells [Internet]. Vol. 106, Proceedings of the National Academy of Sciences of the United States of America. 2009; 106(37):15696-701.
189. Moisan E, Girard D. Cell surface expression of intermediate filament proteins vimentin and lamin B1 in human neutrophil spontaneous apoptosis. J Leukoc Biol. 2005;79(3):489–98.

190. Ekpenyong AE, Toepfner N, Chilvers ER, Guck J. Mechanotransduction in neutrophil activation and deactivation. Biochim Biophys Acta - Mol Cell Res [Internet]. 2015;1853(11):3105–16.
191. Nozawa H, Chiu C, Hanahan D. Infiltrating neutrophils mediate the initial angiogenic switch in a mouse model of multistage carcinogenesis [Internet]. Vol. 15, PNAS August. 2006; 103(33): 12493-8.
192. Lichtman MA, Kearney E. Cellular Deformability during Maturation of the Myeloblast: Possible Role in Marrow Egress. N Engl J Med. 1970;283(18).
193. Olins AL, Hoang T V, Zwerger M, Herrmann H, Zentgraf H, Noegel AA, et al. The LINC-less granulocyte nucleus. Eur J Cell Biol. 2009;88(4):203–14.
194. Hawkins RJ, Piel M, Faure-Andre G, Lennon-Dumenil AM, Joanny JF, Prost J, et al. Pushing off the walls: A mechanism of cell motility in confinement. Phys Rev Lett. 2009;102(5).
195. Renkawitz J, Sixt M. Mechanisms of force generation and force transmission during interstitial leukocyte migration. Vol. 11, EMBO Reports. 2010.
196. Rocheleau AD, Wang W, King MR. Effect of Pseudopod Extensions on Neutrophil Hemodynamic Transport Near a Wall. Cell Mol Bioeng. 2016;9(1).
197. Phillipson M, Heit B, Colarusso P, Liu L, Ballantyne CM, Kubes P. Intraluminal crawling of neutrophils to emigration sites: A molecularly distinct process from adhesion in the recruitment cascade. J Exp Med. 2006;203(12):2569–75.
198. Sixt M, Fritz-Laylin LK, Riel-Mehan M, Chen B-C, Lord SJ, Goddard TD, et al. Actin-based protrusions of migrating neutrophils are intrinsically lamellar and facilitate direction changes. 2017; 6:e26990.
199. Chodniewicz D, Zhelev D V. Novel pathways of F-actin polymerization in the human neutrophil. Blood. 2003;102(6).
200. Machesky LM, Atkinson SJ, Ampe C, Vandekerckhove J, Pollard TD. Purification of a cortical complex containing two unconventional actins from Acanthamoeba by affinity chromatography on profilin-agarose. J Cell Biol. 1994;127(1).
201. Robinson RC, Turbedsky K, Kaiser DA, Marchand JB, Higgs HN, Choe S, et al. Crystal structure of Arp2/3 complex. Science (80-). 2001;294(5547).
202. Litschko C, Linkner J, Brühmann S, Stradal TEB, Reinl T, Jänsch L, et al. Differential functions of WAVE regulatory complex subunits in the regulation of actin-driven processes. Eur J Cell Biol. 2017;96(8).
203. Whitelaw JA, Swaminathan K, Kage F, Machesky LM. The WAVE Regulatory Complex Is Required to Balance Protrusion and Adhesion in Migration. Cells. 2020;9(7).
204. Prendergast GC, Gibbs JB. Pathways of Ras Function: Connections to the Actin Cytoskeleton. Adv Cancer Res. 1993;62(C).
205. Etienne-Manneville S, Hall A. Rho GTPases in cell biology. Vol. 420, Nature. 2002.
206. Tackenberg H, Möller S, Filippi MD, Laskay T. The Small GTPase Cdc42 Is a Major Regulator of Neutrophil Effector Functions. Front Immunol. 2020;11(June).
207. Ridley AJ, Hall A. The small GTP-binding protein rho regulates the assembly of focal adhesions and actin stress fibers in response to growth factors. Cell. 1992;70(3).
208. Mullins RD, Heuser JA, Pollard TD. The interaction of Arp2/3 complex with actin:

Nucleation, high affinity pointed end capping, and formation of branching networks of filaments. Proc Natl Acad Sci U S A. 1998;95(11).
209. Salvermoser M, Begandt D, Alon R, Walzog B. Nuclear deformation during neutrophil migration at sites of inflammation. Front Immunol. 2018;9(NOV):1–9.
210. Voisin MB, Woodfin A, Nourshargh S. Monocytes and neutrophils exhibit both distinct and common mechanisms in penetrating the vascular basement membrane in vivo. Arterioscler Thromb Vasc Biol. 2009;29(8):1193–9.
211. Condliffe AM, Kitchen E, Chilvers ER. Editorial Review Neutrophil priming: pathophysiological consequences and underlying mechanisms [Internet]. Vol. 94, Clinical Science. 1998; 94(5):461-71.
212. Denk S, Taylor RP, Wiegner R, Cook EM, Lindorfer MA, Pfeiffer K, et al. Complement C5a-Induced Changes in Neutrophil Morphology During Inflammation. Scand J Immunol. 2017;86(3):143–55.
213. Dewitt S, Francis RJ, Hallett MB. Ca2+ and calpain control membrane expansion during the rapid cell spreading of neutrophils. J Cell Sci. 2013;126(20):4627–35.
214. Schnipper N, Stassen HH, Kallinich T, Sperling K, Hoffmann K. Image analysis of neutrophil nuclear morphology: Learning about phenotypic range and its reliable analysis from patients with pelger-Huët-anomaly and treated with colchicine. Cytom Part B - Clin Cytom. 2017;92(6).
215. Rowat AC, Jaalouk DE, Zwerger M, Ung WL, Eydelnant IA, Olins DE, et al. Nuclear envelope composition determines the ability of neutrophil-type cells to passage through micron-scale constrictions. J Biol Chem. 2013;288(12).
216. Wu T, Feng JJ. Modeling the Mechanosensitivity of Neutrophils Passing through a Narrow Channel. Biophys J. 2015;109(11):2235–45.
217. Skallberg A, Bunnfors K, Brommesson C, Uvdal K. New Tools for Imaging Neutrophils: Work Function Mapping and Element-Specific, Label-Free Imaging of Cellular Structures. Nano Lett. 2021;21(1).
218. Bashant KR, Aponte AM, Randazzo D, Rezvan Sangsari P, Wood AJT, Bibby JA, et al. Proteomic, biomechanical and functional analyses define neutrophil heterogeneity in systemic lupus erythematosus. Ann Rheum Dis. 2021;80(2):209–18.
219. Riddle RB, Jennbacken K, Hansson KM, Harper MT. Endothelial inflammation and neutrophil transmigration are modulated by extracellular matrix composition in an inflammation-on-a-chip model. Sci Rep [Internet]. 2022;12(1):1–14.
220. Jones HR, Robb CT, Perretti M, Rossi AG. The role of neutrophils in inflammation resolution. Vol. 28, Seminars in Immunology. 2016; 28(2):137-45.
221. Irimia D, Ellett F. Big insights from small volumes: deciphering complex leukocyte behaviors using microfluidics. J Leukoc Biol. 2016;100(2).
222. Meyer-Bahlburg A, Becker-Herman S, Humblet-Baron S, Khim S, Weber M, Bouma G, et al. Wiskott-Aldrich syndrome protein deficiency in B cells results in impaired peripheral homeostasis. Blood. 2008;112(10).
223. Papa R, Penco F, Volpi S, Gattorno M. Actin Remodeling Defects Leading to Autoinflammation and Immune Dysregulation. Front Immunol. 2021;11(January):1–11.
224. Ebrahimzadeh PR, Braide M. The initiation of the neutrophil chemotactic response in filters. J Leukoc Biol. 1999;66(1).

225. Farahi N, Gillett D, Southwood M, Rassl D, Tregay N, Hill U, et al. Lesson of the month: Novel method to quantify neutrophil uptake in early lung cancer using SPECT-CT. Thorax. 2020;75(11).
226. Ruef P, Böhler T, Linderkamp O. Deformability and volume of neonatal and adult leukocytes. Pediatr Res. 1991;29(2).
227. Ruef P, Zilow EP, Linderkamp O. Deformability of peripheral immature and mature neutrophils. Clin Hemorheol Microcirc. 1994;14(2).
228. Yap B, Kamm RD. Cytoskeletal remodeling and cellular activation during deformation of neutrophils into narrow channels. J Appl Physiol. 2005;99(6).
229. Drost EM, Kassabian G, Meiselman HJ, Gelmont D, Fisher TC. Increased rigidity and priming of polymorphonuclear leukocytes in sepsis. Am J Respir Crit Care Med. 1999;159(6).
230. Van Eeden SF, Kitagawa Y, Klut ME, Lawrence E, Hogg JC. Polymorphonuclear leukocytes released from the bone marrow preferentially sequester in-lung micro vessels. Vol. 4, Microcirculation. 1997; 4(3): 369-80.
231. Martin TR, Raugi G, Merritt TL, Henderson WR. Relative contribution of leukotriene B4 to the neutrophil chemotactic activity produced by the resident human alveolar macrophage. J Clin Invest. 1987;80(4).
232. MacNee W, Wiggs B, Belzberg AS, Hogg JC. The Effect of Cigarette Smoking on Neutrophil Kinetics in Human Lungs. N Engl J Med. 1989;321(14).
233. Shalit M, Dabiri GA, Southwick FS. Platelet-activating factor both stimulates and "primes" human polymorphonuclear leukocyte actin filament assembly. Blood. 1987;70(6).
234. Weiner OD, Servant G, Welch MD, Mitchison TJ, Sedat JW, Bourne HR. Spatial control of actin polymerization during neutrophil chemotaxis. Nat Cell Biol. 1999;1(2).
235. Frasch SC, Berry KZ, Fernandez-Boyanapalli R, Jin HS, Leslie C, Henson PM, et al. NADPH oxidase-dependent generation of lysophosphatidylserine enhances clearance of activated and dying neutrophils via G2A. J Biol Chem. 2008;283(48).
236. Bengtsson T, Jaconi MEE, Gustafson M, Magnusson KE, Theler JM, Lew DP, et al. Actin dynamics in human neutrophils during adhesion and phagocytosis is controlled by changes in intracellular free calcium. Eur J Cell Biol. 1993;62(1).
237. Botelho RJ, Teruel M, Dierckman R, Anderson R, Wells A, York JD, et al. Localized Biphasic Changes in Phosphatidylinositol-4,5-Bisphosphate at Sites of Phagocytosis [Internet]. Vol. 151, The Journal of Cell Biology. 2000; 151(7):1353-68.
238. Lè Ne Defacque H, Egeberg M, Habermann A, Diakonova M, Roy C, Mangeat P, et al. Involvement of ezrin/moesin in de novo actin assembly on phagosomal membranes. Vol. 19, The EMBO Journal. 2000; 19(2): 199-212.
239. Immler R, Simon SI, Sperandio M. Calcium signalling and related ion channels in neutrophil recruitment and function. Eur J Clin Invest. 2018;48(June):1–11.
240. Richter J, Ng-Sikorskit J, Olsson I, Anderssont T. Tumor necrosis factor-induced degranulation in adherent human neutrophils is dependent on CD1lb/CD18-integrin-triggered oscillations of cytosolic free Ca2+. Vol. 87, Proc. Naid. Acad. Sci. USA. 1990; 87(23): 9472-6.
241. Nauclér C, Grinstein S, Sundler R, Tapper H. Signaling to localized degranulation in

neutrophils adherent to immune complexes. J Leukoc Biol. 2002;71(4).
242. MacLean-Fletcher S, Pollard TD. Mechanism of action of cytochalasin B on actin. Cell. 1980;20(2).
243. Casella JF, Flanagan MD, Lin S. Cytochalasin D inhibits actin polymerization and induces depolymerization of actin filaments formed during platelet shape change. Nature. 1981;293(5830).
244. Martens JC, Radmacher M. Softening of the actin cytoskeleton by inhibition of myosin II. Pflugers Arch Eur J Physiol. 2008;456(1).
245. Steinmetz MO, Goldie KN, Aebi U. A correlative analysis of actin filament assembly, structure, and dynamics. J Cell Biol. 1997;138(3).
246. Machesky LM, Mullins RD, Higgs HN, Kaiser DA, Blanchoin L, May RC, et al. Scar, a WASp-related protein, activates nucleation of actin filaments by the Arp2/3 complex. Proc Natl Acad Sci U S A. 1999;96(7).
247. Aldridge DC, Armstrong JJ, Speake RN, Turner WB. The cytochalasins, a new class of biologically active mould metabolites. Chem Commun. 1967;(1).
248. Carter SB. Effects of cytochalasins on mammalian cells. Nature. 1967;213(5073).
249. Brown SS, Spudich JA. Mechanism of action of cytochalasin: evidence that it binds to actin filament ends. J Cell Biol. 1981;88(3).
250. Spudich JA, Lin S. Cytochalasin B, its interaction with actin and actomyosin from muscle (cell movement-microfilaments-rabbit striated muscle). Proc Natl Acad Sci U S A. 1972;69(2).
251. Theodoropoulos PA, Gravanis A, Tsapara A, Margioris AN, Papadogiorgaki E, Galanopoulos V, et al. Cytochalasin B may shorten actin filaments by a mechanism independent of barbed end capping. Biochem Pharmacol. 1994;47(10).
252. Goddette DW, Frieden C. Actin polymerization. The mechanism of action of cytochalasin D. J Biol Chem. 1986;261(34).
253. Silveira AAA, Dominical VM, Almeida CB, Chweih H, Ferreira WA, Vicente CP, et al. TNF induces neutrophil adhesion via formin-dependent cytoskeletal reorganization and activation of β-integrin function. J Leukoc Biol. 103(1).
254. Honeycutt PJ, Niedel JE. Cytochalasin B enhancement of the diacylglycerol response in formyl peptide-stimulated neutrophils. J Biol Chem. 1986;261(34):15900–5.
255. Kovács M, Tóth J, Hetényi C, Málnási-Csizmadia A, Seller JR. Mechanism of blebbistatin inhibition of myosin II. J Biol Chem. 2004;279(34).
256. Várkuti BH, Képiró M, Horváth IÁ, Végner L, Ráti S, Zsigmond Á, et al. A highly soluble, non-phototoxic, non-fluorescent blebbistatin derivative. Sci Rep. 2016;6.
257. Li Y, Wang D, Ge H, Güngör C, Gong X, Chen Y. Cytoskeletal and Cytoskeleton-Associated Proteins: Key Regulators of Cancer Stem Cell Properties. Vol. 15, Pharmaceuticals. 2022; 15(11): 1369.
258. Wiles ME, Dykens JA, Wright CD. Human Neutrophil (PMN) Oxygen Radical Production and the Cytoskeleton. Vol. 57, Life Sciences. 1995; (Suppl 3): 40.
259. Chiewchengchol D, Wright HL, Thomas HB, Lam CW, Roberts KJ, Hirankarn N, et al. Differential changes in gene expression in human neutrophils following TNF-α stimulation: Up-regulation of anti-apoptotic proteins and down-regulation of proteins involved in death receptor signaling. Immunity, Inflamm Dis. 2016;4(1):35–44.

260. Lamprecht P, Kerstein A, Klapa S, Schinke S, Karsten CM, Yu X, et al. Pathogenetic and clinical aspects of anti-neutrophil cytoplasmic autoantibody-associated vasculitides. Front Immunol. 2018;9(APR):1–10.
261. Mattila PE, Green CE, Schaff U, Simon SI, Walcheck B. Cytoskeletal interactions regulate inducible L-selectin clustering. Am J Physiol Cell Physiol [Internet]. 2005;289:323–32.
262. Müller-Deile J, Jaremenko C, Haller H, Schiffer M, Haubitz M, Christiansen S, et al. Chemokine/cytokine levels correlate with organ involvement in pr3-anca-associated vasculitis. J Clin Med. 2021;10(12).
263. Leech S. Molecular mimicry in autoimmune disease. Vol. 79, Archives of Disease in Childhood. 1998.
264. Andrews AG, Dysko RC, Spilman SC, Kunkel RG, Brammer DW, Johnson KJ. Immune Complex Vasculitis with Secondary Ulcerative Dermatitis in Aged C57BL/6NNia Mice. Vet Pathol. 1994;31(3).
265. Book Review: The Collected Papers of Paul Ehrlich. Proc R Soc Med. 1957;50(3).
266. Jennette JC. Overview of the 2012 revised International Chapel Hill Consensus Conference nomenclature of vasculitides. Vol. 17, Clinical and Experimental Nephrology. 2013; 17(5): 603-606.
267. Lu X, Garfield A, Rainger GE, Savage COS, Nash GB. Mediation of endothelial cell damage by serine proteases, but not superoxide, released from antineutrophil cytoplasmic antibody-stimulated neutrophils. Arthritis Rheum. 2006;54(5).
268. Holl-Ulrich K. Histopathologie systemischer Vaskulitiden. Pathologe. 2010;31(1):67–76.
269. Rahmattulla C, Mooyaart AL, Van Hooven D, Schoones JW, Bruijn JA, Dekkers OM, et al. Genetic variants in ANCA-associated vasculitis: A meta-analysis. Ann Rheum Dis. 2016;75(9):1687–92.
270. Hirahashi J, Mekala D, Van Ziffle J, Xiao L, Saffaripour S, Wagner DD, et al. Mac-1 Signaling via Src-Family and Syk Kinases Results in Elastase-Dependent Thrombohemorrhagic Vasculopathy. Immunity. 2006;25(2).
271. Tomasson G, Grayson PC, Mahr AD, LaValley M, Merkel PA. Value of ANCA measurements during remission to predict a relapse of ANCA-associated vasculitis-a meta-analysis. Rheumatology. 2012;51(1):100–9.
272. Lyons PA, Rayner TF, Trivedi S, Holle JU, Watts RA, Jayne DRW, et al. Genetically Distinct Subsets within ANCA-Associated Vasculitis. N Engl J Med. 2012;367(3):214–23.
273. Merkel PA, Xie G, Monach PA, Ji X, Ciavatta DJ, Byun J, et al. Identification of Functional and Expression Polymorphisms Associated With Risk for Antineutrophil Cytoplasmic Autoantibody–Associated Vasculitis. Arthritis Rheumatol. 2017;69(5):1054–66.
274. Fussner LA, Hummel AM, Schroeder DR, Silva F, Cartin-Ceba R, Snyder MR, et al. Factors Determining the Clinical Utility of Serial Measurements of Antineutrophil Cytoplasmic Antibodies Targeting Proteinase 3. Arthritis Rheumatol. 2016;68(7):1700–10.
275. Popa ER, Stegeman CA, Abdulahad WH, van der Meer B, Arends J, Manson WM, et

al. Staphylococcal toxic-shock-syndrome-toxin-1 as a risk factor for disease relapse in Wegener's granulomatosis. Rheumatology. 2007 Jun;46(6):1029–33.
276. Kain R, Exner M, Brandes R, Ziebermayr R, Cunningham D, Alderson CA, et al. Molecular mimicry in pauci-immune focal necrotizing glomerulonephritis. Nat Med. 2008;14(10).
277. Roth AJ, Brown MC, Smith RN, Badhwar AK, Parente O, Chung HC, et al. Anti-LAMP-2 antibodies are not prevalent in patients with antineutrophil cytoplasmic autoantibody glomerulonephritis. J Am Soc Nephrol. 2012;23(3).
278. Pendergraft WF, Preston GA, Shah RR, Tropsha A, Carter CW, Jennette JC, et al. Autoimmunity is triggered by cPR-3(105-201), a protein complementary to human autoantigen proteinase-3. Nat Med. 2004;10(1).
279. Yu F, Chen M, Wang SX, Zou WZ, Zhao MH, Wang HY. Clinical and pathological characteristics and outcomes of Chinese patients with primary anti-neutrophil cytoplasmic antibodies-associated systemic vasculitis with immune complex deposition in kidney. Nephrology. 2007;12(1).
280. Pendergraft WF, Cortazar FB, Wenger J, Murphy AP, Rhee EP, Laliberte KA, et al. Long-term maintenance therapy using rituximab-induced continuous B-cell depletion in patients with anca vasculitis. Clin J Am Soc Nephrol. 2014;9(4).
281. van Wijngaarden RAF d. L, van Rijn L, Hagen EC, Watts RA, Gregorini G, Tervaert JWC, et al. Hypotheses on the etiology of antineutrophil cytoplasmic autoantibody-associated vasculitis: The cause is hidden, but the result is known. Vol. 3, Clinical Journal of the American Society of Nephrology. 2008; 3(1):237-52.
282. Scott J, Hartnett J, Mockler D, Little MA. Environmental risk factors associated with ANCA associated vasculitis: A systematic mapping review. Vol. 19, Autoimmunity Reviews. 2020; 19(11):102660.
283. Bossuyt X, Cohen Tervaert JW, Arimura Y, Blockmans D, Flores-Suáez LF, Guillevin L, et al. Revised 2017 international consensus on testing of ANCAs in granulomatosis with polyangiitis and microscopic polyangiitis. Nat Rev Rheumatol. 2017;13(11).
284. Knütter I, Hiemann R, Brumma T, Büttner T, Großmann K, Cusini M, et al. Automated interpretation of ANCA patterns - a new approach in the serology of ANCA-associated vasculitis. Arthritis Res Ther. 2012;14(6).
285. Mukhtyar C, Lee R, Brown D, Carruthers D, Dasgupta B, Dubey S, et al. Modification and validation of the Birmingham vasculitis activity score (version 3). Ann Rheum Dis. 2009;68(12).
286. Hellmich B, Sanchez-Alamo B, Schirmer JH, Berti A, Blockmans D, Cid MC, et al. EULAR recommendations for the management of ANCA-associated vasculitis: 2022 update. Ann Rheum Dis. 2023.
287. Halbwachs-Mecarelli L, Bessou G, Lesavre P, Lopez S, Witko-Sarsat V. Bimodal distribution of proteinase 3 (PR3) surface expression reflects a constitutive heterogeneity in the polymorphonuclear neutrophil pool. FEBS Lett. 1995;374(1):29–33.
288. Lee DKH, Faunce D, Henry D, Sturm RJ, Rimele T. Neutrophil-derived relaxing factor relaxes vascular smooth muscle through a cGMP-mediated mechanism. Life Sci. 1990;46(21):1531–8.

289. Falk RJ, Terrell RS, Charlest LA, Jennettet JC. Anti-neutrophil cytoplasmic autoantibodies induce neutrophils to degranulate and produce oxygen radicals in vitro. Vol. 87, Proc. Natl. Acad. Sci. USA. 1990; 87(11):4115-9.
290. Kettritz R, Jennette JC, Falk RJ. Crosslinking of ANCA-Antigens Stimulates Superoxide Release by Human Neutrophils [Internet]. JASN. 1997; 8(3): 386-94.
291. Schreiber A, Xiao H, Jennette JC, Schneider W, Luft FC, Kettritz R. C5a receptor mediates neutrophil activation and ANCA-induced glomerulonephritis. J Am Soc Nephrol. 2009;20(2):289–98.
292. Ewert BH, Jennette JC, Falk RJ. Anti-myeloperoxidase antibodies stimulate neutrophils to damage human endothelial cells. Vol. 41, Kidney International. 1992; 41(2): 375-83.
293. Ewert BH, Becker ME, Jennette JC, Falk RJ. Antimyeloperoxidase antibodies induce neutrophil adherence to cultured human endothelial cells. Ren Fail. 1995;17(2):125–33.
294. Xiao H, Heeringa P, Hu P, Liu Z, Zhao M, Aratani Y, et al. Antineutrophil cytoplasmic autoantibodies specific for myeloperoxidase cause glomerulonephritis and vasculitis in mice. J Clin Invest. 2002;110(7):955–63.
295. Jennette JC, Xiao H, Falk R, Gasim AMH. Experimental models of vasculitis and glomerulonephritis induced by antineutrophil cytoplasmic autoantibodies. Contrib Nephrol. 2011;169:211–20.
296. Little MA, Smyth CL, Yadav R, Ambrose L, Cook HT, Nourshargh S, et al. Antineutrophil cytoplasm antibodies directed against myeloperoxidase augment leukocyte-microvascular interactions in vivo. Blood. 2005;106(6):2050–8.
297. Little MA, Hassan B, Jacques S, Game D, Salisbury E, Courtney AE, et al. Renal transplantation in systemic vasculitis: When is it safe. Nephrol Dial Transplant. 2009;24(10):3219–25.
298. Eisenberger U, Fakhouri F, Vanhille P, Beaufils H, Mahr A, Guillevin L, et al. ANCA-negative pauci-immune renal vasculitis: Histology and outcome. Nephrol Dial Transplant. 2005;20(7):1392–9.
299. Jayne DRW, Gaskin G, Rasmussen N, Abramowicz D, Ferrario F, Guillevin L, et al. Randomized trial of plasma exchange or high-dosage methylprednisolone as adjunctive therapy for severe renal vasculitis. J Am Soc Nephrol. 2007;18(7):2180–8.
300. Roth AJ, Ooi JD, Hess JJ, Van Timmeren MM, Berg EA, Poulton CE, et al. Epitope specificity determines pathogenicity and detectability in anca-associated vasculitis. J Clin Invest. 2013;123(4):1773–83.
301. Muller Kobold AC, Kallenberg CGM, Cohen Tervaert JW. Monocyte activation in patients with Wegener's granulomatosis. Ann Rheum Dis. 1999;58(4).
302. Freeley SJ, Coughlan AM, Popat RJ, Dunn-Walters DK, Robson MG. Granulocyte colony stimulating factor exacerbates antineutrophil cytoplasmic antibody vasculitis. Ann Rheum Dis. 2013;72(6):1053–8.
303. Schreiber A, Xiao H, Falk RJ, Jennette JC. Bone marrow-derived cells are sufficient and necessary targets to mediate glomerulonephritis and vasculitis induced by anti-myeloperoxidase antibodies. J Am Soc Nephrol. 2006;17(12).
304. Primo VC, Marusic S, Franklin CC, Goldmann WH, Achaval CG, Smith RN, et al. Anti-PR3 immune responses induce segmental and necrotizing glomerulonephritis. Clin Exp Immunol. 2010;159(3):327–37.

305. Yumura W, Itabashi M, Ishida-Okawara A, Tomizawa K, Yamashita J, Kaneshiro Y, et al. A novel mouse model for MPO-ANCA-associated glomerulonephritis. Microbiol Immunol. 2006;50(2):149–57.
306. Chen Y-X, Zhang W, Chen X-N, Shen P-Y, Shi H, Xu Y-W, et al. Application of RIFLE criteria in Chinese patients with ANCA-associated renal vasculitis. 2011; 29(6):951-7.
307. Nowack R, Grab I, Áz L-FF-S, Schnu P, Yard B, Van Der Woude FJ. ANCA titres, even of IgG subclasses, and soluble CD14 fail to predict relapses in patients with ANCA-associated vasculitis . Vol. 16, NDT, 2001; 16(8): 1631-7.
308. Mulder AHL, Heeringa P, Brouwer E, Limburg PC, Kallenberg CGM. Activation of granulocytes by anti-neutrophil cytoplasmic antibodies (ANCA): a Fc-yRII-dependent process. Vol. 98, Clin Exp Immunol. 1994; 98(2):270-8.
309. Pankhurst T, Nash G, Williams J, Colman R, Hussain A, Savage C. Immunoglobulin subclass determines ability of immunoglobulin (Ig)G to capture and activate neutrophils presented as normal human IgG or disease-associated anti-neutrophil cytoplasm antibody (ANCA)-IgG. Clin Exp Immunol. 2011;164(2):218–26.
310. Radford DJ, Savage COS, Nash GB. Treatment of rolling neutrophils with antineutrophil cytoplasmic antibodies causes conversion to firm integrin-mediated adhesion. Arthritis Rheum. 2000;43(6):1337–45.
311. Prendecki M, Gulati K, Pisacano N, Pinheiro D, Bhatt T, Mawhin MA, et al. Syk Activation in Circulating and Tissue Innate Immune Cells in Antineutrophil Cytoplasmic Antibody–Associated Vasculitis. Arthritis Rheumatol. 2023;75(1):84–97.
312. Weidner S, Neupert W, Goppelt-Struebe M, Rupprecht HD. Antineutrophil cytoplasmic antibodies induce human monocytes to produce oxygen radicals in vitro. Arthritis Rheum. 2001;44(7):1698–706.
313. Porges AJ, Redecha PB, Kimberly WT, Csernok E, Gross WL, Kimberly RP. Anti-neutrophil cytoplasmic antibodies engage and activate human neutrophils via Fc gamma RIIa. J Immunol. 1994;153(3):1271–80.
314. Miralda I, Uriarte SM, McLeish KR. Multiple phenotypic changes define neutrophil priming. Vol. 7, Frontiers in Cellular and Infection Microbiology. 2017.
315. Hewins P, Williams JM, Wakelam MJO, Savage COS. Activation of Syk in Neutrophils by Antineutrophil Cytoplasm Antibodies Occurs via Fcγ Receptors and CD18. J Am Soc Nephrol. 2004;15(3).
316. Hao J, Meng LQ, Xu PC, Chen M, Zhao MH. P38MAPK, ERK and PI3K signaling pathways are involved in C5a-Primed neutrophils for ANCA-Mediated activation. PLoS One. 2012;7(5):1–10.
317. Kessenbrock K, Krumbholz M, Schönermarck U, Back W, Gross WL, Werb Z, et al. Netting neutrophils in autoimmune small-vessel vasculitis. Nat Med. 2009;15(6):623–5.
318. Wang H, Wang C, Zhao MH, Chen M. Neutrophil extracellular traps can activate alternative complement pathways. Clin Exp Immunol. 2015;181(3).
319. Lewis HD, Liddle J, Coote JE, Atkinson SJ, Barker MD, Bax BD, et al. Inhibition of PAD4 activity is sufficient to disrupt mouse and human NET formation. Nat Chem Biol. 2015;11(3):189–91.
320. O'Sullivan KM, Lo CY, Summers SA, Elgass KD, McMillan PJ, Longano A, et al.

Renal participation of myeloperoxidase in antineutrophil cytoplasmic antibody (ANCA)-associated glomerulonephritis. Kidney Int. 2015;88(5):1030–46.
321. Sangaletti S, Tripodo C, Chiodoni C, Guarnotta C, Cappetti B, Casalini P, et al. Neutrophil extracellular traps mediate transfer of cytoplasmic neutrophil antigens to myeloid dendritic cells toward ANCA induction and associated autoimmunity. Blood. 2012;120(15):3007–18.
322. Croker BA, Metcalf D, Robb L, Wei W, Mifsud S, DiRago L, et al. SOCS3 Is a Critical Physiological Negative Regulator of G-CSF Signaling and Emergency Granulopoiesis. Immunity. 2004;20(2).
323. Rosales C. Neutrophil: A cell with many roles in inflammation or several cell types? Front Physiol. 2018;9(FEB):1–17.
324. Jerke U, Hernandez DP, Beaudette P, Korkmaz B, Dittmar G, Kettritz R. Neutrophil serine proteases exert proteolytic activity on endothelial cells. Kidney Int [Internet]. 2015;88(4):764–75.
325. Schreiber A, Pham CTN, Hu Y, Schneider W, Luft FC, Kettritz R. Neutrophil serine proteases promote IL-1β generation and injury in necrotizing crescentic glomerulonephritis. J Am Soc Nephrol. 2012;23(3).
326. Meyer D, Telele S, Zelená A, Gillen AJ, Antonucci A, Neubert E, et al. Transport and programmed release of nanoscale cargo from cells by using NETosis. Nanoscale. 2020;12(16).
327. Cockwell P, Brooks CJ, Adu D, Savage COS. Interleukin-8: A pathogenetic role in antineutrophil cytoplasmic autoantibody-associated glomerulonephritis. Kidney Int. 1999;55(3):852–63.
328. Casselman BL, Kilgore KS, Miller BF, Warren JS. Antibodies to neutrophil cytoplasmic antigens induce monocyte chemoattractant protein-1 secretion from human monocytes. J Lab Clin Med. 1995;126(5).
329. Denny MF, Yalavarthi S, Zhao W, Thacker SG, Anderson M, Sandy AR, et al. A Distinct Subset of Proinflammatory Neutrophils Isolated from Patients with Systemic Lupus Erythematosus Induces Vascular Damage and Synthesizes Type I IFNs. J Immunol. 2010;184(6):3284–97.
330. Ge S, Zhu X, Xu Q, Wang J, An C, Hu Y, et al. Neutrophils in ANCA-associated vasculitis: Mechanisms and implications for management. Front Pharmacol. 2022;13(September):1–15.
331. Carmona-Rivera C, Kaplan MJ. Low-density granulocytes: A distinct class of neutrophils in systemic autoimmunity. Vol. 35, Seminars in Immunopathology. 2013.
332. Ning X, Wang WM, Jin HZ, Fang W. Low-Density Granulocytes in Immune-Mediated Inflammatory Diseases. Vol. 2022, Journal of Immunology Research. 2022; 31:2022:1622160.
333. Carmona-Rivera C, Zhao W, Yalavarthi S, Kaplan MJ. Neutrophil extracellular traps induce endothelial dysfunction in systemic lupus erythematosus through the activation of matrix metalloproteinase-2. Ann Rheum Dis. 2015;74(7).
334. Carlucci PM, Purmalek MM, Dey AK, Temesgen-Oyelakin Y, Sakhardande S, Joshi AA, et al. Neutrophil subsets and their gene signature associate with vascular inflammation and coronary atherosclerosis in lupus. JCI insight. 2018;3(8).

335. Mistry P, Nakabo S, O'Neil L, Goel RR, Jiang K, Carmona-Rivera C, et al. Transcriptomic, epigenetic, and functional analyses implicate neutrophil diversity in the pathogenesis of systemic lupus erythematosus. Proc Natl Acad Sci U S A. 2019;116(50).
336. Grayson PC, Carmona-Rivera C, Xu L, Lim N, Gao Z, Asare AL, et al. Neutrophil-related gene expression and low-density granulocytes associated with disease activity and response to treatment in antineutrophil cytoplasmic antibody-associated vasculitis. Arthritis Rheumatol. 2015;67(7).
337. Ui Mhaonaigh A, Coughlan AM, Dwivedi A, Hartnett J, Cabral J, Moran B, et al. Low Density Granulocytes in ANCA Vasculitis Are Heterogenous and Hypo-Responsive to Anti-Myeloperoxidase Antibodies. Front Immunol. 2019;10(11).
338. Sagiv JY, Michaeli J, Assi S, Mishalian I, Kisos H, Levy L, et al. Phenotypic diversity and plasticity in circulating neutrophil subpopulations in cancer. Cell Rep. 2015;10(4).
339. Halbwachs L, Lesavre P. Endothelium-neutrophil interactions in ANCA-Associated Diseases. J Am Soc Nephrol. 2012;23(9):1449–61.
340. Calderwood JW, Williams JM, Morgan MD, Nash GB, Savage COS. ANCA induces β2 integrin and CXC chemokine-dependent neutrophil-endothelial cell interactions that mimic those of highly cytokine-activated endothelium. J Leukoc Biol. 2004 Sep 30;77(1):33–43.
341. Abdgawad M, Gunnarsson L, Bengtsson AA, Geborek P, Nilsson L, Segelmark M, et al. Elevated neutrophil membrane expression of proteinase 3 is dependent upon CD177 expression. Clin Exp Immunol. 2010;161(1).
342. Tse WY, Nash GB, Hewins P, Savage COS, Adu D. ANCA-induced neutrophil F-actin polymerization: Implications for microvascular inflammation. Kidney Int. 2005;67(1):130–9.
343. Jerke U, Marino SF, Daumke O, Kettritz R. Characterization of the CD177 interaction with the ANCA antigen proteinase 3. Sci Rep. 2017;7.
344. Koyner JL, Murray PT. Mechanical ventilation and lung-kidney interactions. Clin J Am Soc Nephrol. 2008;3(2).
345. Nolan SL, Kalia N, Nash GB, Kamel D, Heeringa P, Savage COS. Mechanisms of ANCA-mediated leukocyte-endothelial cell interactions in vivo. J Am Soc Nephrol. 2008;19(5):973–84.
346. Yang L, Froio RM, Sciuto TE, Dvorak AM, Alon R, Luscinskas FW. ICAM-1 regulates neutrophil adhesion and transcellular migration of TNF-α-activated vascular endothelium under flow. Blood. 2005;106(2):584–92.
347. Bautz DJ, Preston GA, Lionaki S, Hewins P, Wolberg AS, Jia JY, et al. Antibodies with dual reactivity to plasminogen and complementary PR3 in PR3-ANCA vasculitis. J Am Soc Nephrol. 2008;19(12).
348. Berden AE, Nolan SL, Morris HL, Bertina RM, Erasmus DD, Hagen EC, et al. Anti-plasminogen antibodies compromise fibrinolysis and associate with renal histology in ANCA-associated vasculitis. J Am Soc Nephrol. 2010;21(12).
349. Kang A, Antonelou M, Wong NL, Tanna A, Arulkumaran N, Tam FWK, et al. High incidence of arterial and venous thrombosis in antineutrophil cytoplasmic antibody-associated vasculitis. J Rheumatol. 2019;46(3):285–93.
350. Söderberg D, Segelmark M. Neutrophil extracellular traps in ANCA-associated

vasculitis. Front Immunol. 2016;7(6):1–9.
351. Dick J, Gan PY, Ford SL, Odobasic D, Alikhan MA, Loosen SH, et al. C5a receptor 1 promotes autoimmunity, neutrophil dysfunction and injury in experimental anti-myeloperoxidase glomerulonephritis. Kidney Int [Internet]. 2018;93(3):615–25.
352. Brill A, Fuchs TA, Chauhan AK, Yang JJ, De Meyer SF, Köllnberger M, et al. Von Willebrand factor-mediated platelet adhesion is critical for deep vein thrombosis in mouse models. Blood. 2011;117(4).
353. Ju L, Chen Y, Zhou F, Lu H, Cruz MA, Zhu C. Von Willebrand factor-A1 domain binds platelet glycoprotein Ibα in multiple states with distinctive force-dependent dissociation kinetics. Thromb Res. 2015;136(3).
354. Fuchs TA, Brill A, Duerschmied D, Schatzberg D, Monestier M, Myers DD, et al. Extracellular DNA traps promote thrombosis. Proc Natl Acad Sci U S A. 2010;107(36).
355. Ammollo CT, Semeraro F, Xu J, Esmon NL, Esmon CT. Extracellular histones increase plasma thrombin generation by impairing thrombomodulin-dependent protein C activation. J Thromb Haemost. 2011;9(9).
356. Noubouossie DF, Whelihan MF, Yu Y Bin, Sparkenbaugh E, Pawlinski R, Monroe DM, et al. In vitro activation of coagulation by human neutrophil DNA and histone proteins but not neutrophil extracellular traps. Blood. 2017;129(8).
357. Diaz JA, Fuchs TA, Jackson TO, Hovinga JAK, Lämmle B, Henke PK, et al. Plasma DNA is elevated in patients with deep vein thrombosis. J Vasc Surg Venous Lymphat Disord. 2013;1(4).
358. Van Montfoort ML, Stephan F, Lauw MN, Hutten BA, Van Mierlo GJ, Solati S, et al. Circulating nucleosomes and neutrophil activation as risk factors for deep vein thrombosis. Arterioscler Thromb Vasc Biol. 2013;33(1).
359. Fuchs TA, Brill A, Wagner DD. Neutrophil extracellular trap (NET) impact on deep vein thrombosis. Vol. 32, Arteriosclerosis, Thrombosis, and Vascular Biology. 2012.
360. Jiménez-Alcázar M, Rangaswamy C, Panda R, Bitterling J, Simsek YJ, Long AT, et al. Host DNases prevent vascular occlusion by neutrophil extracellular traps. Science (80-). 2017;358(6367).
361. Carminita E, Crescence L, Brouilly N, Altié A, Panicot-Dubois L, Dubois C. DNAse-dependent, NET-independent pathway of thrombus formation in vivo. Proc Natl Acad Sci U S A. 2021;118(28).
362. Martinod K, Demers M, Fuchs TA, Wong SL, Brill A, Gallant M, et al. Neutrophil histone modification by peptidylarginine deiminase 4 is critical for deep vein thrombosis in mice. Proc Natl Acad Sci U S A. 2013;110(21).
363. Yuen J, Pluthero FG, Douda DN, Riedl M, Cherry A, Ulanova M, et al. NETosing neutrophils activate complement both on their own NETs and bacteria via alternative and non-alternative pathways. Front Immunol. 2016;7(4).
364. Al-Hussain T, Hussein MH, Conca W, Mana H Al, Akhtar M. Pathophysiology of ANCA-associated Vasculitis. Vol. 24, Advances in Anatomic Pathology. 2017.
365. Brilland B, Garnier AS, Chevailler A, Jeannin P, Subra JF, Augusto JF. Complement alternative pathway in ANCA-associated vasculitis: Two decades from bench to bedside. Vol. 19, Autoimmunity Reviews. 2020; 19(1): 102424.
366. Filer AD, Bacon PA, Gardner-Medwin JM, Thambyrajah J, Raza K, Carruthers DM, et

al. Diffuse endothelial dysfunction is common to ANCA associated systemic vasculitis and polyarteritis nodosa. Ann Rheum Dis. 2003;62(2).
367. Ballieux BEPB, Zondervan KT, Kievit P, Hagen EC, Van Es LA, Van Der Woude FJ, et al. Binding of proteinase 3 and myeloperoxidase to endothelial cells: ANCA-mediated endothelial damage through ADCC? Clin Exp Immunol. 1994;97(1).
368. Savage COS, Gaskin G, Pusey CD, Pearson JD. Myeloperoxidase binds to vascular endothelial cells, is recognized by ANCA and can enhance complement dependent cytotoxicity. Adv Exp Med Biol. 1993;336.
369. Ohlsson SMS, Holm L, Hansson C, Ohlsson SMS, Gunnarsson L, Pettersson Å, et al. Neutrophils from ANCA-associated vasculitis patients show an increased capacity to activate the complement system via the alternative pathway after ANCA stimulation. PLoS One. 2019;14(6):1–16.
370. Xiao H, Schreiber A, Heeringa P, Falk RJ, Jennette JC. Alternative complement pathway in the pathogenesis of disease mediated by anti-neutrophil cytoplasmic autoantibodies. Am J Pathol. 2007;170(1):52–64.
371. Gou SJ, Yuan J, Chen M, Yu F, Zhao MH. Circulating complement activation in patients with anti-neutrophil cytoplasmic antibody-associated vasculitis. Kidney Int [Internet]. 2013;83(1):129–37.
372. Dick J, Gan PY, Richard Kitching A, Holdsworth SR. The c3ar promotes macrophage infiltration and regulates anca production but does not affect glomerular injury in experimental antimyeloperoxidase glomerulonephritis. PLoS One. 2018;13(1):1–15.
373. Jayne DRW, Merkel PA, Schall TJ, Bekker P. Avacopan for the Treatment of ANCA-Associated Vasculitis. N Engl J Med. 2021;384(7):599–609.
374. Kronbichler A, Lee KH, Denicol S, Choi D, Lee HH, Ahn D, et al. Immunopathogenesis of ANCA-Associated Vasculitis. 2020; 21(19):7319.
375. Berti A, Hillion S, Konig MF, Moura MC, Hummel AM, Carmona E, et al. Autoreactive Plasmablasts After B Cell Depletion With Rituximab and Relapses in Antineutrophil Cytoplasmic Antibody–Associated Vasculitis. Arthritis Rheumatol. 2023;75(5).
376. Berti A, Hillion S, Hummel AM, Son YM, Chriti N, Peikert T, et al. Circulating autoreactive proteinase 3+ B cells and tolerance checkpoints in ANCA-associated vasculitis. JCI Insight. 2021;6(22).
377. Dumoitier N, Terrier B, London J, Lofek S, Mouthon L. Implication of B lymphocytes in the pathogenesis of ANCA-associated vasculitides. Vol. 14, Autoimmunity Reviews. Elsevier B.V.; 2015. 14(11):996-1004.
378. Alberici F, Smith RM, Jones RB, Roberts DM, Willcocks LC, Chaudhry A, et al. Long-term follow-up of patients who received repeat-dose rituximab as maintenance therapy for ANCA-associated vasculitis. Rheumatol (United Kingdom). 2015;54(7):1153–60.
379. Todd SK, Pepper RJ, Draibe J, Tanna A, Pusey CD, Mauri C, et al. Regulatory B cells are numerically but not functionally deficient in anti-neutrophil cytoplasm antibody-associated vasculitis. Rheumatol (United Kingdom). 2014;53(9):1693–703.
380. Wilde B, Thewissen M, Damoiseaux J, Knippenberg S, Hilhorst M, Van Paassen P, et al. Regulatory B cells in ANCA-associated vasculitis. Ann Rheum Dis. 2013;72(8):1416–9.
381. Holden NJ, Williams JM, Morgan MD, Challa A, Gordon J, Pepper RJ, et al. ANCA-

stimulated neutrophils release BLyS and promote B cell survival: A clinically relevant cellular process. Ann Rheum Dis. 2011;70(12):2229–33.
382. Krumbholz M, Specks U, Wick M, Kalled SL, Jenne D, Meinl E. BAFF is elevated in serum of patients with Wegener's granulomatosis. J Autoimmun. 2005;25(4):298–302.
383. Pollard RPE, Abdulahad WH, Vissink A, Hamza N, Burgerhof JGM, Meijer JM, et al. Serum levels of BAFF, but not APRIL, are increased after rituximab treatment in patients with primary Sjögren's syndrome: Data from a placebo-controlled clinical trial. Vol. 72, Annals of the Rheumatic Diseases. 2013. 71(1):146-8.
384. Shimojima Y, Kishida D, Ichikawa T, Takamatsu R, Nomura S, Sekijima Y. Features of BAFF and APRIL receptors on circulating B cells in antineutrophil cytoplasmic antibody-associated vasculitis. Clin Exp Immunol. 2023;213(1):125–37.
385. Alberici F, Smith RM, Fonseca M, Willcocks LC, Jones RB, Holle JU, et al. Association of a TNFSF13B (BAFF) regulatory region single nucleotide polymorphism with response to rituximab in antineutrophil cytoplasmic antibody–associated vasculitis. J Allergy Clin Immunol. 2017;139(5).
386. Zhang T, Wang M, Zhang J, Feng X, Liu Z, Cheng Z. Association between tubulointerstitial CD8+T cells and renal prognosis in lupus nephritis. Int Immunopharmacol. 2021;99.
387. Marinaki S, Kälsch AI, Grimminger P, Breedijk A, Birck R, Schmitt WH, et al. Persistent T-cell activation and clinical correlations in patients with ANCA-associated systemic vasculitis. Nephrol Dial Transplant. 2006;21(7):1825–32.
388. Masutani K, Tokumoto M, Nakashima H, Tsuruya K, Kashiwagi M, Kudoh Y, et al. Strong polarization toward th1 immune response in ANCA-associated glomerulonephritis. Clin Nephrol. 2003;59(6).
389. Szczeklik W, Jakieła B, Wawrzycka-Adamczyk K, Sanak M, Hubalewska-Mazgaj M, Padjas A, et al. Skewing toward Treg and Th2 responses is a characteristic feature of sustained remission in ANCA-positive granulomatosis with polyangiitis. Eur J Immunol. 2017;47(4):724–33.
390. Morgan MD, Day CJ, Piper KP, Khan N, Harper L, Moss PA, et al. Patients with Wegener's granulomatosis demonstrate a relative deficiency and functional impairment of T-regulatory cells. Immunology. 2010;130(1):64–73.
391. Martinez Valenzuela L, Bordignon Draibe J, Fulladosa Oliveras X, Bestard Matamoros O, Cruzado Garrit JM, Torras Ambrós J. T-lymphocyte in ANCA-associated vasculitis: What do we know? A pathophysiological and therapeutic approach. Clin Kidney J. 2019;12(4):503–11.
392. Shochet L, Holdsworth S, Kitching AR. Animal Models of ANCA Associated Vasculitis. Vol. 11, Frontiers in Immunology. Frontiers Media S.A. 2020; 9:11:525.
393. Hoshino A, Nagao T, Nagi-Miura N, Ohno N, Yasuhara M, Yamamoto K, et al. MPO-ANCA induces IL-17 production by activated neutrophils in vitro via its Fc region- and complement-dependent manner. J Autoimmun. 2008;31(1):79–89.
394. Nogueira E, Hamour S, Sawant D, Henderson S, Mansfield N, Chavele KM, et al. Serum IL-17 and IL-23 levels and autoantigen-specific Th17 cells are elevated in patients with ANCA-associated vasculitis. Nephrol Dial Transplant. 2010;25(7):2209–17.
395. Dolff S, Witzke O, Wilde B. Th17 cells in renal inflammation and autoimmunity.

Autoimmun Rev. 2019;18(2):129–36.
396. Velden J, Paust HJ, Hoxha E, Turner JE, Steinmetz OM, Wolf G, et al. Renal IL-17 expression in human ANCA-associated glomerulonephritis. Am J Physiol - Ren Physiol. 2012;302(12).
397. Mah KK, Cheng HM. Diffusion, Blood O_2, CO_2 Content and Transport. In 2015.
398. Carreau A, Hafny-Rahbi B El, Matejuk A, Grillon C, Kieda C. Why is the partial oxygen pressure of human tissues a crucial parameter? Small molecules and hypoxia. J Cell Mol Med. 2011;15(6).
399. Leichtweiss HP, Lübbers DW, Weiss C, Baumgärtl H, Reschke W. The oxygen supply of the rat kidney: Measurements of intrarenal pO_2. Pflügers Arch Eur J Physiol. 1969;309(4).
400. Aukland K, Krog J. Renal oxygen tension. Nature. 1960;188(4751).
401. McCollum ED, King C, Ahmed S, Hanif AAM, Roy AD, Islam AA, et al. Defining hypoxaemia from pulse oximeter measurements of oxygen saturation in well children at low altitude in Bangladesh: An observational study. BMJ Open Respir Res. 2021;8(1).
402. Zaidi M, Fu F, Cojocari D, McKee TD, Wouters BG. Quantitative Visualization of Hypoxia and Proliferation Gradients Within Histological Tissue Sections. Front Bioeng Biotechnol. 2019;7.
403. Giatromanolaki A, Sivridis E, Kouskoukis C, Gatter KC, Harris AL, Koukourakis MI. Hypoxia-inducible factors 1α and 2α are related to vascular endothelial growth factor expression and a poorer prognosis in nodular malignant melanomas of the skin. Melanoma Res. 2003;13(5).
404. Kempf VAJ, Lebiedziejewski M, Alitalo K, Wälzlein JH, Ehehalt U, Fiebig J, et al. Activation of hypoxia-inducible factor-1 in bacillary angiomatosis: Evidence for a role of hypoxia-inducible factor-1 in bacterial infections. Circulation. 2005;111(8).
405. Ninivaggi M, De Laat M, Lancé MMD, Kicken CH, Pelkmans L, Bloemen S, et al. Hypoxia induces a prothrombotic state independently of the physical activity. PLoS One. 2015;10(10).
406. Fernandes IA, Rocha MP, Campos MO, Mattos JD, Mansur DE, Rocha HNM, et al. Reduced arterial vasodilatation in response to hypoxia impairs cerebral and peripheral oxygen delivery in hypertensive men. J Physiol. 2018;596(7).
407. Walmsley SR, Print C, Farahi N, Peyssonnaux C, Johnson RS, Cramer T, et al. Hypoxia-induced neutrophil survival is mediated by HIF-1α-dependent NF-κB activity. J Exp Med. 2005;201(1):105–15.
408. Metzen E, Berchner-Pfannschmidt U, Stengel P, Marxsen JH, Stolze I, Klinger M, et al. Intracellular localisation of human HIF-1α hydroxylases: Implications for oxygen sensing. Vol. 116, Journal of Cell Science. 2003.
409. Kotch LE, Iyer N V., Laughner E, Semenza GL. Defective vascularization of HIF-1α-null embryos is not associated with VEGF deficiency but with mesenchymal cell death. Dev Biol. 1999;209(2).
410. Ivan M, Kondo K, Yang H, Kim W, Valiando J, Ohh M, et al. HIFα targeted for VHL-mediated destruction by proline hydroxylation: Implications for O_2 sensing. Science (80-). 2001;292(5516).
411. Jaakkola P, Mole DR, Tian YM, Wilson MI, Gielbert J, Gaskell SJ, et al. Targeting of

HIF-α to the von Hippel-Lindau ubiquitylation complex by O_2-regulated prolyl hydroxylation. Science (80-). 2001;292(5516).
412. Masson N, Willam C, Maxwell PH, Pugh CW, Ratcliffe PJ. Independent function of two destruction domains in hypoxia-inducible factor-α chains activated by prolyl hydroxylation. EMBO J. 2001;20(18).
413. Yu F, White SB, Zhao Q, Lee FS. HIF-1α binding to VHL is regulated by stimulus-sensitive proline hydroxylation. Proc Natl Acad Sci U S A. 2001;98(17).
414. Mahon PC, Hirota K, Semenza GL. FIH-1: A novel protein that interacts with HIF-1α and VHL to mediate repression of HIF-1 transcriptional activity. Genes Dev. 2001;15(20).
415. Thompson AAR, Elks PM, Marriott HM, Eamsamarng S, Higgins KR, Lewis A, et al. Hypoxia-inducible factor 2a regulates key neutrophil functions in humans, mice, and zebrafish. Blood. 2014;123(3).
416. K. Bruegge, W. Jelkmann, E. Metzen. Hydroxylation of Hypoxia-Inducible Transcription Factors and Chemical Compounds Targeting the HIF-α Hydroxylases. Curr Med Chem. 2007;14(17).
417. Zhang N, Fu Z, Linke S, Chicher J, Gorman JJ, Visk D, et al. The asparaginyl hydroxylase factor inhibiting HIF-1α is an essential regulator of metabolism. Cell Metab. 2010;11(5).
418. Sim J, Cowburn AS, Palazon A, Madhu B, Tyrakis PA, Macías D, et al. The Factor Inhibiting HIF Asparaginyl Hydroxylase Regulates Oxidative Metabolism and Accelerates Metabolic Adaptation to Hypoxia. Cell Metab. 2018;27(4).
419. Lando D, Peet DJ, Whelan DA, Gorman JJ, Whitelaw ML. Asparagine hydroxylation of the HIF transactivation domain: A hypoxic switch. Science (80-). 2002;295(5556).
420. Marxsen JH, Stengel P, Doege K, Heikkinen P, Jokilehto T, Wagner T, et al. Hypoxia-inducible factor-1 (HIF-1) promotes its degradation by induction of HIF-α-prolyl-4-hydroxylases. Biochem J. 2004;381(3).
421. Ema M, Taya S, Yokotani N, Sogawa K, Matsuda Y, Fujii-Kuriyama Y. A novel bHLH-PAS factor with close sequence similarity to hypoxia-inducible factor 1α regulates the VEGF expression and is potentially involved in lung and vascular development. Proc Natl Acad Sci U S A. 1997;94(9).
422. Flamme I, Fröhlich T, Von Reutern M, Kappel A, Damert A, Risau W. HRF, a putative basic helix-loop-helix-PAS-domain transcription factor is closely related to hypoxia-inducible factor-lot and developmentally expressed in blood vessels. Mech Dev. 1997;63(1).
423. Tian H, McKnight SL, Russell DW. Endothelial PAS domain protein 1 (EPAS1), a transcription factor selectively expressed in endothelial cells. Genes Dev. 1997;11(1).
424. Makino Y, Kanopka A, Wilson WJ, Tanaka H, Poellinger L. Inhibitory PAS domain protein (IPAS) is a hypoxia-inducible splicing variant of the hypoxia-inducible factor-3α locus. J Biol Chem. 2002;277(36).
425. Chan MC, Ilott NE, Schödel J, Sims D, Tumber A, Lippl K, et al. Tuning the transcriptional response to hypoxia by inhibiting Hypoxia-inducible Factor (HIF) prolyl and asparaginyl hydroxylases. J Biol Chem. 2016;291(39).
426. Greijer AE, van der Groep P, Kemming D, Shvarts A, Semenza GL, Meijer GA, et al.

Up-regualtion of gene expression by hypoxia is mediated predominantly by hypoxia-inducible factor I (HIF-I). J Pathol. 2005;206(3).
427. Ceradini DJ, Kulkarni AR, Callaghan MJ, Tepper OM, Bastidas N, Kleinman ME, et al. Progenitor cell trafficking is regulated by hypoxic gradients through HIF-1 induction of SDF-1. Nat Med. 2004;10(8).
428. Carmeliet P, Dor Y, Herbert JM, Fukumura D, Brusselmans K, Dewerchin M, et al. Role of HIF-1alpha in hypoxia-mediated apoptosis, cell proliferation and tumour angiogenesis. Nature. 1998;394(6692).
429. Papandreou I, Cairns RA, Fontana L, Lim AL, Denko NC. HIF-1 mediates adaptation to hypoxia by actively downregulating mitochondrial oxygen consumption. Cell Metab. 2006;3(3).
430. Talla U, Bozonet SM, Parker HA, Hampton MB, Vissers MCM. Prolonged exposure to hypoxia induces an autophagy-like cell survival program in human neutrophils. J Leukoc Biol. 2019;106(6):1367–79.
431. Mecklenburgh KI, Walmsley SR, Cowburn AS, Wiesener M, Reed BJ, Upton PD, et al. Involvement of a ferroprotein sensor in hypoxia-mediated inhibition of neutrophil apoptosis. Blood. 2002;100(8):3008–16.
432. Cramer T, Yamanishi Y, Clausen BE, Förster I, Pawlinski R, Mackman N, et al. HIF-1α is essential for myeloid cell-mediated inflammation. Cell. 2003;112(5).
433. Ziello JE, Jovin IS, Huang Y. Hypoxia-Inducible Factor (HIF)-1 regulatory pathway and its potential for therapeutic intervention in malignancy and ischemia. Vol. 80, Yale Journal of Biology and Medicine. 2007.
434. Parmar K, Mauch P, Vergilio JA, Sackstein R, Down JD. Distribution of hematopoietic stem cells in the bone marrow according to regional hypoxia. Proc Natl Acad Sci U S A. 2007;104(13).
435. Kubota Y, Takubo K, Suda T. Bone marrow long label-retaining cells reside in the sinusoidal hypoxic niche. Biochem Biophys Res Commun. 2008;366(2).
436. Lo Celso C, Fleming HE, Wu JW, Zhao CX, Miake-Lye S, Fujisaki J, et al. Live-animal tracking of individual haematopoietic stem/progenitor cells in their niche. Nature. 2009;457(7225).
437. Lodge KM, Cowburn AS, Li W, Condliffe AM. The impact of hypoxia on neutrophil degranulation and consequences for the host. Int J Mol Sci. 2020;21(4).
438. Williams AE, Chambers RC. Neutrophils and tissue damage: Is hypoxia the key to excessive degranulation? Thorax. 2016;71(11):977–8.
439. McGovern NN, Cowburn AS, Porter L, Walmsley SR, Summers C, Thompson AAR, et al. Hypoxia Selectively Inhibits Respiratory Burst Activity and Killing of Staphylococcus aureus in Human Neutrophils . J Immunol. 2011;186(1):453–63.
440. Imtiyaz HZ, Williams EP, Hickey MM, Patel SA, Durham AC, Yuan LJ, et al. Hypoxia-inducible factor 2α regulates macrophage function in mouse models of acute and tumor inflammation. J Clin Invest. 2010;120(8).
441. Elks PM, Van Eeden FJ, Dixon G, Wang X, Reyes-Aldasoro CC, Ingham PW, et al. Activation of hypoxia-inducible factor-1α (hif-1α) delays inflammation resolution by reducing neutrophil apoptosis and reverse migration in a zebrafish inflammation model. Blood. 2011;118(3).

442. Karakurum M, Shreeniwas R, Chen J, Pinsky D, Yan SD, Anderson M, et al. Hypoxic induction of interleukin-8 gene expression in human endothelial cells. J Clin Invest. 1994;93(4).
443. Grutkoski PS, Graeber CT, D'Amico R, Keeping H, Simms HH. Regulation of IL-8RA (CXCR1) expression in polymorphonuclear leukocytes by hypoxia/reoxygenation. J Leukoc Biol. 1999;65(2).
444. Baudry N, Danialou G, Boczkowski J, Vicaut E. In vivo study of the effect of systemic hypoxia on leukocyte- endothelium interactions. Am J Respir Crit Care Med. 1998;158(2).
445. Wood JG, Johnson JS, Mattioli LF, Gonzalez NC. Systemic hypoxia promotes leukocyte-endothelial adherence via reactive oxidant generation. J Appl Physiol. 1999;87(5).
446. Wood JG, Mattioli LF, Gonzalez NC. Hypoxia causes leukocyte adherence to mesenteric venules in nonacclimatized, but not in acclimatized, rats. J Appl Physiol. 1999;87(3).
447. Rainger GE, Fisher A, Shearman C, Nash GB. Adhesion of flowing neutrophils to cultured endothelial cells after hypoxia and reoxygenation in vitro. Am J Physiol - Hear Circ Physiol. 1995;269(4 38-4).
448. Beck-Schimmer B, Schimmer RC, Madjdpour C, Bonvini JM, Pasch T, Ward PA. Hypoxia mediates increased neutrophil and macrophage adhesiveness to alveolar epithelial cells. Am J Respir Cell Mol Biol. 2001;25(6).
449. Arnould T, Michiels C, Remacle J. Increased PMN adherence on endothelial cells after hypoxia: involvement of PAF, CDlt3/CDIlb, and ICAM. 1993; 264 (Pt 1):C1102-10.
450. Milhoan KA, Lane TA, Bloor CM. Hypoxia induces endothelial cells to increase their adherence for neutrophils: Role of PAF. Am J Physiol - Hear Circ Physiol. 1992;263(3 32-3).
451. da Silva-Ferreira S, Duarte-Oliveira C, Antunes D, Barbosa-Matos C, Mendes-Frias A, Torrado E, et al. Hypoxia inducible-factor 1 alpha regulates neutrophil recruitment during fungal-elicited granulomatous inflammation. Front Cell Infect Microbiol. 2022;12.
452. Sormendi S, Deygas M, Sinha A, Bernard M, Krüger A, Kourtzelis I, et al. HIF2α is a direct regulator of neutrophil motility. Blood [Internet]. 2021;137(24):3416–27.
453. Scannell G, Waxman K, Vaziri ND, Zhang J, Kaupke CJ, Jalali M, et al. Hypoxia-induced alterations of neutrophil membrane receptors. J Surg Res. 1995;59(1).
454. Ginis I, Mentzer SJ, Faller D V. Hypoxia induces lymphocyte adhesion to human mesenchymal cells via an LFA- 1-dependent mechanism. Am J Physiol - Cell Physiol. 1993;264(3 33-3).
455. Rainger GE, Fisher AC, Nash GB. Endothelial-borne platelet-activating factor and interleukin-8 rapidly immobilize rolling neutrophils. Am J Physiol - Hear Circ Physiol. 1997;272(1 41-1).
456. Lodge KM, Vassallo A, Liu B, Long M, Tong Z, Newby PR, et al. Hypoxia Increases the Potential for Neutrophil-mediated Endothelial Damage in Chronic Obstructive Pulmonary Disease. Am J Respir Crit Care Med. 2022;205(8).
457. Madeddu P, Kraenkel N, Barcelos LS, Siragusa M, Campagnolo P, Oikawa A, et al.

Phosphoinositide 3-kinase γ gene knockout impairs postischemic neovascularization and endothelial progenitor cell functions. Arterioscler Thromb Vasc Biol. 2008;28(1).
458. Ferguson GJ, Milne L, Kulkarni S, Sasaki T, Walker S, Andrews S, et al. PI(3)Kγ has an important context-dependent role in neutrophil chemokinesis. Nat Cell Biol. 2007;9(1).
459. Hoenderdos K, Lodge KM, Hirst RA, Chen C, Palazzo SGC, Emerenciana A, et al. Hypoxia upregulates neutrophil degranulation and potential for tissue injury. Thorax. 2016;71(11):1030–8.
460. Glasner C, Van Timmeren MM, Stobernack T, Omansen TF, Raangs EC, Rossen JW, et al. Low anti-staphylococcal IgG responses in granulomatosis with polyangiitis patients despite long-term Staphylococcus aureus exposure. Sci Rep. 2015;5.
461. Egners A, Erdem M, Cramer T. The response of macrophages and neutrophils to hypoxia in the context of cancer and other inflammatory diseases. Mediators Inflamm. 2016;2016:2053646.
462. Eckle T, Faigle M, Grenz A, Laucher S, Thompson LF, Eltzschig HK. A2B adenosine receptor dampens hypoxia-induced vascular leak. Blood. 2008;111(4):2024–35.
463. Rahat MA, Bitterman H, Lahat N. Molecular mechanisms regulating macrophage response to hypoxia. Vol. 2, Frontiers in Immunology. 2011; 2:45.
464. Semba H, Takeda N, Isagawa T, Sugiura Y, Honda K, Wake M, et al. HIF-1α-PDK1 axis-induced active glycolysis plays an essential role in macrophage migratory capacity. Nat Commun. 2016;7.
465. Choi HJ, Sanders TA, Tormos K V, Ameri K, Tsai JD, Park AM, et al. ECM-Dependent HIF Induction Directs Trophoblast Stem Cell Fate via LIMK1-Mediated Cytoskeletal Rearrangement. PLoS One. 2013;8(2).
466. Huang C, Qian SL, Sun LY, Cheng B. Light-Emitting Diode Irradiation (640 nm) Regulates Keratinocyte Migration and Cytoskeletal Reorganization Via Hypoxia-Inducible Factor-1α. Photomed Laser Surg. 2016;34(8).
467. Tamura DY, Moore EE, Partrick DA, Johnson JL, Offner PJ, Silliman CC. Acute hypoxemia in humans enhances the neutrophil inflammatory response. Shock. 2002;17(4).
468. Rademakers SE, Lok J, van der Kogel AJ, Bussink J, Kaanders JHAM. Metabolic markers in relation to hypoxia; staining patterns and colocalization of pimonidazole, HIF-1α, CAIX, LDH-5, GLUT-1, MCT1 and MCT4. BMC Cancer. 2011;11.
469. Liles W, Dale D, Klebanoff S. Glucocorticoids inhibit apoptosis of human neutrophils. Blood. 1995;86(8).
470. Marwick JA, Dorward DA, Lucas CD, Jones KO, Sheldrake TA, Fox S, et al. Oxygen levels determine the ability of glucocorticoids to influence neutrophil survival in inflammatory environments. J Leukoc Biol. 2013;94(6).
471. Kilburn KH, Dowell AR. Renal Function in Respiratory Failure: Effects of Hypoxia, Hyperoxia, and Hypercapnia. Arch Intern Med. 1971;127(4).
472. Walmsley S, Harris A, Thompson AAR, Whyte MKB. HIF-mediated innate immune responses: cell signaling and therapeutic implications. Hypoxia. 2014;
473. Grahl N, Puttikamonkul S, Macdonald JM, Gamcsik MP, Ngo LY, Hohl TM, et al. In vivo hypoxia and a fungal alcohol dehydrogenase influence the pathogenesis of invasive

pulmonary aspergillosis. PLoS Pathog. 2011;7(7).
474. Foy RA, Shimizu S, Paul RJ. The effects of hypoxia on pH(i) in porcine coronary artery endothelium and smooth muscle: A novel method for measurements in endothelial cells in situ. Circ Res. 1997;80(1).
475. Frøbert O, Mikkelsen EO, Bagger JP, Gravholt CH. Measurement of interstitial lactate during hypoxia-induced dilatation in isolated pressurised porcine coronary arteries. J Physiol. 2002;539(1).
476. Hedegaard ER, Nielsen BD, Kun A, Hughes AD, Krøigaard C, Mogensen S, et al. KV7 channels are involved in hypoxia-induced vasodilatation of porcine coronary arteries. Br J Pharmacol. 2014;171(1).
477. Westbury CB, Pearson A, Nerurkar A, Reis-Filho JS, Steele D, Peckitt C, et al. Hypoxia can be detected in irradiated normal human tissue: A study using the hypoxic marker pimonidazole hydrochloride. Br J Radiol. 2007;80(959).
478. Joshi FR, Manavaki R, Fryer TD, Figg NL, Sluimer JC, Aigbirhio FI, et al. Vascular Imaging With 18F-Fluorodeoxyglucose Positron Emission Tomography Is Influenced by Hypoxia. Vol. 69, Journal of the American College of Cardiology. 2017; 69(14): 1873-1874.
479. Akhavani MA, Madden L, Buysschaert I, Sivakumar B, Kang N, Paleolog EM. Hypoxia upregulates angiogenesis and synovial cell migration in rheumatoid arthritis. Arthritis Res Ther. 2009;11(3).
480. Sorriento D, Iaccarino G. Inflammation and cardiovascular diseases: The most recent findings. Vol. 20, International Journal of Molecular Sciences. MDPI AG; 2019; 20(16).
481. Pelling AE, Horton MA. An historical perspective on cell mechanics. Vol. 456, Pflugers Archiv European Journal of Physiology. 2008; 456: 3-12.
482. González-Cruz RD, Fonseca VC, Darling EM. Cellular mechanical properties reflect the differentiation potential of adipose-derived mesenchymal stem cells. Proc Natl Acad Sci U S A. 2012;109(24).
483. Binnig G, Quate CF, Gerber C. Atomic force microscope. Phys Rev Lett. 1986;56(9).
484. Müller DJ, Dufrêne YF. Atomic force microscopy: A nanoscopic window on the cell surface. Vol. 21, Trends in Cell Biology. 2011; 21(8): 461-9.
485. Horton M, Charras G, Lehenkari P. Analysis of ligand-receptor interactions in cells by atomic force microscopy. In: Journal of Receptors and Signal Transduction. 2002; 22(1-4):169-90.
486. Sattin BD, Pelling AE, Goh MC. DNA base pair resolution by single molecule force spectroscopy. Nucleic Acids Res. 2004;32(16).
487. Roduit C, Longo G, Dietler G, Kasas S. Measuring cytoskeleton and cellular membrane mechanical properties by atomic force microscopy. Methods Mol Biol. 2015;1232.
488. Roca-Cusachs P, Almendros I, Sunyer R, Gavara N, Farré R, Navajas D. Rheology of passive and adhesion-activated neutrophils probed by atomic force microscopy. Biophys J. 2006;91(9).
489. Ashkin A, Dziedzic JM, Chu S. Observation of a single-beam gradient-force optical trap for dielectric particles in air. Opt Lett. 1986;22(11).
490. Guck J, Ananthakrishnan R, Mahmood H, Moon TJ, Cunningham C Casey, Käs J. The Optical Stretcher: A Novel Laser Tool to Micromanipulate Cells. 2001; 81(2): 767-784.

491. Guck J, Schinkinger S, Lincoln B, Wottawah F, Ebert S, Romeyke M, et al. Optical deformability as an inherent cell marker for testing malignant transformation and metastatic competence. Biophys J. 2005;88(5).
492. Ashkin A, Dziedzic JM, Bjorkholm JE, Chu S. Observation of a single-beam gradient force optical trap for dielectric particles. In: Optical Angular Momentum. 2016.
493. Gossett DR, Tse HTK, Lee SA, Ying Y, Lindgren AG, Yang OO, et al. Hydrodynamic stretching of single cells for large population mechanical phenotyping. Proc Natl Acad Sci U S A. 2012;109(20).
494. Ekpenyong AE, Whyte G, Chalut K, Pagliara S, Lautenschläger F, Fiddler C, et al. Viscoelastic Properties of Differentiating Blood Cells Are Fate- and Function-Dependent. PLoS One. 2012;7(9).
495. Guck J, Chilvers ER. Mechanics meets medicine. Sci Transl Med. 2013;5(212):3–6.
496. Otto O, Rosendahl P, Mietke A, Golfier S, Herold C, Klaue D, et al. Real-time deformability cytometry: On-the-fly cell mechanical phenotyping. Nat Methods. 2015;12(3):199–202.
497. Herold C. Mapping of deformation to apparent Young's modulus in real-time deformability cytometry. arXiv. 2017.
498. Lin J, Kim D, Tse HT, Tseng P, Peng L, Dhar M, et al. High-throughput physical phenotyping of cell differentiation. Microsystems Nanoeng. 2017;3.
499. Nawaz AA, Urbanska M, Herbig M, Nötzel M, Kräter M, Rosendahl P, et al. Using real-time fluorescence and deformability cytometry and deep learning to transfer molecular specificity to label-free sorting. bioRxiv. 2019;1–21.
500. Herbig M, Mietke A, Müller P, Otto O. Statistics for real-time deformability cytometry: Clustering, dimensionality reduction, and significance testing. Biomicrofluidics [Internet]. 2018;12(4).
501. Porter L, Toepfner N, Bashant KR, Guck J, Ashcroft M, Farahi N, et al. Metabolic profiling of human eosinophils. Front Immunol. 2018;9(JUN).
502. Kubánková M, Hohberger B, Hoffmanns J, Fürst J, Herrmann M, Guck J, et al. Physical phenotype of blood cells is altered in COVID-19. Biophys J [Internet]. 2021;120(14):2838–47.
503. Herbig M, Jacobi A, Wobus M, Weidner H, Mies A, Kräter M, et al. Machine learning assisted real-time deformability cytometry of CD34+ cells allows to identify patients with myelodysplastic syndromes. Sci Rep. 2022;12(1).
504. Matei AE, Kubánková M, Xu L, Györfi AH, Boxberger E, Soteriou D, et al. Identification of a Distinct Monocyte-Driven Signature in Systemic Sclerosis Using Biophysical Phenotyping of Circulating Immune Cells. Arthritis Rheumatol. 2023;75(5).
505. Blighe K, Rana S, Lewis M. EnhancedVolcano version 1.10.0: Publication-ready volcano plots with enhanced colouring and labeling. R-Package. 2021.
506. Blighe K, Rana S, Lewis M. Publication-ready volcano plots with enhanced colouring and labeling. Bioconductor. 2022.
507. Zhang B, Kirov S, Snoddy J. WebGestalt: An integrated system for exploring gene sets in various biological contexts. Nucleic Acids Res. 2005;33(SUPPL. 2).
508. Wang J, Duncan D, Shi Z, Zhang B. WEB-based GEne SeT AnaLysis Toolkit

(WebGestalt): update 2013. Nucleic Acids Res. 2013;41.
509. Wang J, Vasaikar S, Shi Z, Greer M, Zhang B. WebGestalt 2017: A more comprehensive, powerful, flexible and interactive gene set enrichment analysis toolkit. Nucleic Acids Res. 2017;45(W1).
510. Liao Y, Wang J, Jaehnig EJ, Shi Z, Zhang B. WebGestalt 2019: gene set analysis toolkit with revamped UIs and APIs. Nucleic Acids Res. 2019;47(W1).
511. Cockwell P, Savage COS, Cockwell P. Role of Leukocytes in the Immunopathogenesis of ANCA-Associated Glomerulonephritis [Internet]. Vol. 85, Nephron. 2000.
512. Hussain A, Pankhurst T, Goodall M, Colman R, Jefferis R, Savage COS, et al. Chimeric IgG4 PR3-ANCA induces selective inflammatory responses from neutrophils through engagement of Fcγ receptors. Immunology. 2009;128(2).
513. Yap B, Kamm RD. Mechanical deformation of neutrophils into narrow channels induces pseudopod projection and changes in biomechanical properties. J Appl Physiol. 2005;98(5).
514. Spillmann CM, Lomakina E, Waugh RE. Neutrophil adhesive contact dependence on impingement force. Biophys J. 2004;87(6).
515. Sachs L, Wesche J, Lenkeit L, Greinacher A, Bender M, Palankar R. Ex vivo anticoagulants affect human blood platelet biomechanics with implications for high-throughput functional mechanophenotyping . 2021;1–28.
516. Banfi G, Salvagno GL, Lippi G. The role of ethylenediamine tetraacetic acid (EDTA) as in vitro anticoagulant for diagnostic purposes. Vol. 45, Clinical Chemistry and Laboratory Medicine. 2007; 45(5): 565-76.
517. Quach A, Ferrante A. The Application of Dextran Sedimentation as an Initial Step in Neutrophil Purification Promotes Their Stimulation, due to the Presence of Monocytes. J Immunol Res. 2017;2017.
518. Krabbe J, Beilmann V, Alamzad-Krabbe H, Böll S, Seifert A, Ruske N, et al. Blood collection technique, anticoagulants and storing temperature have minor effects on the isolation of polymorphonuclear neutrophils. Sci Rep [Internet]. 2020;10(1):1–10.
519. Hong Y, Eleftheriou D, Hussain AAK, Price-Kuehne FE, Savage CO, Jayne D, et al. Anti-neutrophil cytoplasmic antibodies stimulate release of neutrophil microparticles. J Am Soc Nephrol. 2012;23(1):49–62.
520. Kettritz R, Schreiber A, Luft FC, Haller H. Role of Mitogen-Activated Protein Kinases in Activation of Human Neutrophils by Antineutrophil Cytoplasmic Antibodies [Internet]. 2001; 12(1):37-46.
521. Hattar K, Oppermann S, Ankele C, Weissmann N, Schermuly RT, Bohle RM, et al. c-ANCA-induced neutrophil-mediated lung injury: A model of acute Wegener's granulomatosis. Eur Respir J. 2010;36(1).
522. Leshner M, Wang S, Lewis C, Zheng H, Chen XA, Santy L, et al. PAD4 mediated histone hypercitrullination induces heterochromatin decondensation and chromatin unfolding to form neutrophil extracellular trap-like structures. Front Immunol. 2012;3(19).
523. Neubert E, Senger-Sander SN, Manzke VS, Busse J, Polo E, Scheidmann SEF, et al. Serum and serum albumin inhibit in vitro formation of Neutrophil Extracellular Traps (NETs). Front Immunol. 2019;10(1).

524. Hilhorst M, Van Paassen P, Tervaert JWC. Proteinase 3-ANCA vasculitis versus myeloperoxidase- ANCA vasculitis. Vol. 26, Journal of the American Society of Nephrology. 2015; 26(1): 2314-27.
525. Ting-Beall HP, Lee AS, Hochmuth RM. Effect of cytochalasin D on the mechanical properties and morphology of passive human neutrophils. Ann Biomed Eng. 1995;23(5).
526. Shen X, Hu L, Li Z, Wang L, Pang X, Wen CY, et al. Extracellular calcium ion concentration regulates chondrocyte elastic modulus and adhesion behavior. Int J Mol Sci. 2021;22(18).
527. Clinical Methods: The History, Physical, and Laboratory Examinations. Ann Intern Med. 1990;113(7).
528. Popat RJ, Robson MG. Neutrophils are not consistently activated by antineutrophil cytoplasmic antibodies in vitro. Vol. 78, Annals of the Rheumatic Diseases. 2019; 78(5): 701-711.
529. Harper L, Savage COS. Leukocyte-endothelial interactions in antineutrophil cytoplasmic antibody-associated systemic vasculitis. Rheum Dis Clin North Am. 2001;27(4):887–903.
530. Franssen CFM, Huitema MG, Muller Kobold AC, Oost-Kort WW, Limburg PC, Tiebosch A, et al. In vitro neutrophil activation by antibodies to proteinase 3 and myeloperoxidase from patients with crescentic glomerulonephritis. J Am Soc Nephrol. 1999;10(7).
531. Tsai MA, Frank RS, Waugh RE. Passive mechanical behavior of human neutrophils: effect of cytochalasin B. Biophys J. 1994;66(6).
532. Sengupta K, Aranda-Espinoza H, Smith L, Janmey P, Hammery D. Spreading of neutrophils: From activation to migration. Biophys J. 2006;91(12).
533. Zhang JL, Morrell G, Rusinek H, Warner L, Vivier PH, Cheung AK, et al. Measurement of renal tissue oxygenation with blood oxygen level-dependent MRI and oxygen transit modeling. Am J Physiol - Ren Physiol. 2014;306(6).
534. Aguilera K, Brekken R. Hypoxia Studies with Pimonidazole in vivo. Bio-Protocol. 2014;4(19).
535. Branitzki-Heinemann K, Möllerherm H, Völlger L, Husein DM, de Buhr N, Blodkamp S, et al. Formation of neutrophil extracellular traps under low oxygen level. Front Immunol. 2016;7(NOV):1–9.
536. Kellum JA. Determinants of blood pH in health and disease. Vol. 4, Critical Care. 2000.
537. Klock J, Boyles J, Bainton D, Stossel T. Nylon-fiber-induced neutrophil fragmentation. Blood. 1979;54(6).
538. Bignold LP, Ferrante A. Effects of cytochalasin B, N-formyl peptide and plasma on polarisation, zeiosis (blebbing) and degranulation of polymorphonuclear leukocytes in suspension. Cell Biol Int Rep. 1988;12(3).
539. Zieseniss A. Hypoxia and the modulation of the actin cytoskeleton – emerging interrelations. Hypoxia. 2014; 25:2:11-21.
540. Tardif M, Huang S, Redmond T, Safer D, Pring M, Zigmond SH. Actin polymerization induced by GTPγS in permeabilized neutrophils is induced and maintained by free barbed ends. J Biol Chem. 1995;270(47).
541. Rizoli SB, Rotstein OD, Parodo J, Phillips MJ, Kapus A. Hypertonic inhibition of

exocytosis in neutrophils: Central role for osmotic actin skeleton remodeling. Am J Physiol - Cell Physiol. 2000;279(3 48-3).
542. Mitchell T, Lo A, Logan MR, Lacy P, Eitzen G. Primary granule exocytosis in human neutrophils is regulated by Rac-dependent actin remodeling. Am J Physiol - Cell Physiol. 2008;295(5).
543. Derevianko A, D'Amico R, Simms H. Polymorphonuclear leucocyte (PMN)-derived inflammatory cytokines-regulation by oxygen tension and extracellular matrix. Clin Exp Immunol. 1996;106(3).
544. McInturff AM, Cody MJ, Elliott EA, Glenn JW, Rowley JW, Rondina MT, et al. Mammalian target of rapamycin regulates neutrophil extracellular trap formation via induction of hypoxia-inducible factor 1 α. Blood. 2012;120(15).
545. Henneck T, Mergani A, Clever S, Seidler AE, Brogden G, Runft S, et al. Formation of Neutrophil Extracellular Traps by Reduction of Cellular Cholesterol Is Independent of Oxygen and HIF-1α. Int J Mol Sci. 2022;23(6).
546. Pearlstein DP, Ali MH, Mungai PT, Hynes KL, Gewertz BL, Schumacker PT. Role of mitochondrial oxidant generation in endothelial cell responses to hypoxia. Arterioscler Thromb Vasc Biol. 2002;22(4).
547. Mendes RT, Nguyen D, Stephens D, Pamuk F, Fernandes D, Hasturk H, et al. Hypoxia-induced endothelial cell responses – possible roles during periodontal disease. Clin Exp Dent Res. 2018;4(6).
548. Ong CWM, Fox K, Ettorre A, Elkington PT, Friedland JS. Hypoxia increases neutrophil-driven matrix destruction after exposure to Mycobacterium tuberculosis. Sci Rep [Internet]. 2018;8(1):1–11.
549. Chemin K, Bohineust A, Dogniaux S, Tourret M, Guégan S, Miro F, et al. Cytokine Secretion by CD4+ T Cells at the Immunological Synapse Requires Cdc42-Dependent Local Actin Remodeling but Not Microtubule Organizing Center Polarity. J Immunol. 2012;189(5).
550. Schalper KA, Carleton M, Zhou M, Chen T, Feng Y, Huang SP, et al. Elevated serum interleukin-8 is associated with enhanced intratumor neutrophils and reduced clinical benefit of immune-checkpoint inhibitors. Nat Med. 2020;26(5).
551. Hayes-Bradley C. Hypoxia from vasculitic pulmonary haemorrhage improved by prone position ventilation. Br J Anaesth. 2004;92(5).
552. Sourla E, Bagalas V, Tsioulis H, Paspala A, Akritidou S, Pataka A, et al. Acute Respiratory Failure as Primary Manifestation of Antineutrophil Cytoplasmic Antibodies-Associated Vasculitis. Clin Pract. 2014;4(2).
553. Liu ML. Functional actin cytoskeleton is required in early stage of NETosis induction. Proc Natl Acad Sci U S A. 2020;117(37):22653–4.
554. Millar TM, Phan V, Tibbles LA. ROS generation in endothelial hypoxia and reoxygenation stimulates MAP kinase signaling and kinase-dependent neutrophil recruitment. Free Radic Biol Med. 2007;42(8):1165–77.
555. Figura M, Chilton L, Liacini A, Viskovic MM, Phan V, Knight D, et al. Blockade of KATP channels reduces endothelial hyperpolarization and leukocyte recruitment upon reperfusion after hypoxia. Am J Transplant. 2009;9(4).
556. Tang J, Liao Z, Luo L, Deng S, Jiang Y, Wang F, et al. CX3CL1-induced CD16+

monocytes extravasation in myeloperoxidase-ANCA-associated vasculitis correlates with renal damage. Front Immunol. 2022;13.
557. Brooks CJ, King WJ, Radford DJ, Adu D, McGrath M, Savage COS. IL-1β production by human polymorphonuclear leucocytes stimulated by anti-neutrophil cytoplasmic autoantibodies: Relevance to systemic vasculitis. Clin Exp Immunol. 1996;106(2):273–9.
558. Nagao T, Suzuki KK, Utsunomiya K, Matsumura M, Saiga K, Wang PC, et al. Direct activation of glomerular endothelial cells by anti-moesin activity of anti-myeloperoxidase antibody. Nephrol Dial Transplant. 2011;26(9):2752–60.
559. Morote-Garcia JC, Napiwotzky D, Köhler D, Rosenberger P. Endothelial Semaphorin 7A promotes neutrophil migration during hypoxia. Proc Natl Acad Sci U S A. 2012;109(35).
560. Kalra VK, Shen Y, Sultana C, Rattan V. Hypoxia induces PECAM-1 phosphorylation and transendothelial migration of monocytes. Am J Physiol - Hear Circ Physiol. 1996;271(5 40-5).
561. Hevehan DL, Papoutsakis ET, Miller WM. Physiologically significant effects of pH and oxygen tension on granulopoiesis. Exp Hematol. 2000;28(3).
562. Matsumoto K, Kurasawa T, Yoshimoto K, Suzuki K, Takeuchi T. Identification of neutrophil β2-integrin LFA-1 as a potential mechanistic biomarker in ANCA-associated vasculitis via microarray and validation analyses. Arthritis Res Ther. 2021;23(1).
563. Michailidou D, Mustelin T, Lood C. Role of Neutrophils in Systemic Vasculitides. Front Immunol. 2020;11(December):1–11.
564. Woodfin A, Beyrau M, Nourshargh S. ICAM-1 expressing neutrophils exhibit enhanced effector functions in murine models of endotoxemia. 1377;68–70.
565. Harasimov K, Uraji J, Mönnich EU, Holubcová Z, Elder K, Blayney M, et al. Actin-driven chromosome clustering facilitates fast and complete chromosome capture in mammalian oocytes. Nat Cell Biol. 2023;25(3).
566. Phillipson M, Kubes P. The neutrophil in vascular inflammation. Vol. 17, Nature Medicine. 2011.
567. Nakagawa M, Terashima T, D'yachkova Y, Bondy GP, Hogg JC, van Eeden SF. Glucocorticoid-Induced Granulocytosis. Circulation. 1998;98(21).
568. Linderkamp O, Ruef P, Brenner B, Gulbins E, Lang F. Passive deformability of mature, immature, and active neutrophils in healthy and septicemic neonates. Pediatr Res. 1998;44(6).
569. Worthen GS, Schwab B, Elson EL, Downey GP. Mechanics of stimulated neutrophils: Cell stiffening induces retention in capillaries. Science (80-). 1989;245(4914):183–6.
570. Skoutelis AT, Kaleridis VE, Goumenos DS, Athanassiou GM, Missirlis YF, Vlachojannis JG, et al. Polymorphonuclear leukocyte rigidity is defective in patients with chronic renal failure. Nephrol Dial Transplant. 2000;15(11).
571. Turcotte S, Desrosiers RR, Béliveau R. HIF-1α mRNA and protein upregulation involves Rho GTPase expression during hypoxia in renal cell carcinoma. Vol. 116, Journal of Cell Science. 2003.
572. Bailly K, Ridley AJ, Hall SM, Haworth SG. RhoA activation by hypoxia in pulmonary arterial smooth muscle cells is age and site specific. Circ Res. 2004;94(10).

573. Wojciak-Stothard B, Tsang LYF, Haworth SG. Rac and Rho play opposing roles in the regulation of hypoxia/reoxygenation- induced permeability changes in pulmonary artery endothelial cells. Am J Physiol - Lung Cell Mol Physiol. 2005;288(4 32-4).
574. Vogler M, Vogel S, Krull S, Farhat K, Leisering P, Lutz S, et al. Hypoxia Modulates Fibroblastic Architecture, Adhesion and Migration: A Role for HIF-1α in Cofilin Regulation and Cytoplasmic Actin Distribution. PLoS One. 2013;8(7).
575. Eul B, Rose F, Krick S, Savai R, Goyal P, Klepetko W, et al. Impact of HIF-1α and HIF-2α on proliferation and migration of human pulmonary artery fibroblasts in hypoxia. FASEB J. 2006;20(1).
576. Li L, Lu Y. Inhibition of hypoxia-induced cell motility by p16 in MDA-MB-231 breast cancer cells. J Cancer. 2010;1(1).
577. Yang M, Kohler M, Heyder T, Forsslund H, Garberg HK, Karimi R, et al. Proteomic profiling of lung immune cells reveals dysregulation of phagocytotic pathways in female-dominated molecular COPD phenotype. Respir Res. 2018;19(1).
578. Ronzier E, Laurenson AJ, Manickam R, Liu S, Saintilma IM, Schrock DC, et al. The Actin Cytoskeleton Responds to Inflammatory Cues and Alters Macrophage Activation. Cells. 2022;11(11).
579. Yanaoka H, Nagafuchi Y, Hanata N, Takeshima Y, Ota M, Suwa Y, et al. Identifying the most influential gene expression profile in distinguishing ANCA-associated vasculitis from healthy controls. J Autoimmun. 2021;119.
580. Banos A, Thomas K, Garantziotis P, Filia A, Malissovas N, Pieta A, et al. The genomic landscape of ANCA-associated vasculitis: Distinct transcriptional signatures, molecular endotypes and comparison with systemic lupus erythematosus. Front Immunol. 2023;14.
581. Nakabo S, Romo-Tena J, Kaplan MJ. Neutrophils as Drivers of Immune Dysregulation in Autoimmune Diseases with Skin Manifestations. Vol. 142, Journal of Investigative Dermatology. 2022; 142(3): 823-822.
582. Seto N, Torres-Ruiz JJ, Carmona-Rivera C, Pinal-Fernandez I, Pak K, Purmalek MM, et al. Neutrophil dysregulation is pathogenic in idiopathic inflammatory myopathies. JCI Insight. 2020;5(3).
583. Balamayooran G, Batra S, Fessler MB, Happel KI, Jeyaseelan S. Mechanisms of neutrophil accumulation in the lungs against bacteria. Vol. 43, American Journal of Respiratory Cell and Molecular Biology. 2010; 43(1): 5-16).
584. Selby C, Drost E, Wraith PK, MacNee W. In vivo neutrophil sequestration within lungs of humans is determined by in vitro "filterability." J Appl Physiol. 1991;71(5).
585. Pollak MR, Quaggin SE, Hoenig MP, Dworkin LD. The glomerulus: The sphere of influence. Clin J Am Soc Nephrol. 2014;9(8).
586. Townsley MI. Structure and composition of pulmonary arteries, capillaries, and veins. Compr Physiol. 2012;2(1).
587. Jonasdottir AD, Manojlovic M, Vojinovic J, Nordin A, Bruchfeld A, Gunnarsson I, et al. Augmented thrombin formation is related to circulating levels of extracellular vesicles exposing tissue factor and citrullinated histone-3 in anti-neutrophil cytoplasmic antibody-associated vasculitides. Front Med. 2023;10.
588. Tay SH, Celhar T, Fairhurst AM. Low-Density Neutrophils in Systemic Lupus

Erythematosus. Vol. 72, Arthritis and Rheumatology. 2020.
589. Jones BE, Herrera CA, Agosto-Burgos C, Starmer J, Bass WA, et al. ANCA autoantigen gene expression highlights neutrophil heterogeneity where expression in normal-density neutrophils correlates with ANCA-induced activation. Kidney Int. 2020; 98(3):744-757.
590. Sachs UJH, Andrei-Selmer CL, Maniar A, Weiss T, Paddock C, et al. The neutrophil-specific antigen CD177 is a counter-receptor for platelet endothelial cell adhesion molecule-1 (CD31). J Biol Chem. 2007; 282(32):23603-12.